
# Characterizing insecticide resistance mechanisms in mosquitoes using genetic modification and a rapid, automated larval resistance detection assay

---

Thesis submitted in accordance with the requirements of the Liverpool School of Tropical Medicine for the Degree of Doctor in Philosophy by

Beth Crawford Poulton

1st October 2021

Supervised by Dr. Gareth J. Lycett and Prof. David B. Sattelle

“The more we know, the more we realize there is to know”

Prof. Jennifer Doudna

*Nobel Prize in Chemistry 2020*

# Acknowledgements

My first thanks must go to my supervisor Gareth. If it were not for him I would not be the scientist I am today and I will be forever grateful for that. His support from the very beginning has been exactly what I needed and I am grateful to have had a supervisor who understands what I need better than I do myself at times. He allowed me to grow and learn from my mistakes while always being around for advice and support. His guidance and detailed feedback have been invaluable and I could not have completed this project or my thesis without it. Thank you for everything from Friday lunches troubleshooting over pizza to celebratory drinks after getting positive transgenics and most of all the huge amount of time you have invested in me for the past 4 years.

Thank you also to my supervisor at University College London David Sattelle. He along with Freddie Partridge and Steve Buckingham were excellent collaborators and I am grateful for their support and encouragement as I got to grips with new techniques and coding languages. I thoroughly enjoyed my time working at UCL and was grateful to the whole group for how they welcomed and included me while I was there. I am only sorry I was unable to spend more time with you.

My lab group have been brilliant. It may have been small but they all were endlessly supportive. Without the weekend rota for mosquito rearing it would have been far harder for me throughout my PhD. Amalia Anthousi taught me almost everything I know about mosquito rearing and supported me constantly both as a colleague and a friend. I will always be grateful for her patience in the early days while I learnt to rear mosquitoes and asked endless questions. I also owe huge thanks to Fraser Colman without whom I could not have completed my final year. From the time he joined the lab Fraser was friendly helpful and supportive and always offered to take some of the weight off my shoulders when he could. I was lucky to have such great co-workers to share the workload with.

My gratitude goes out to all those in the vector department who supported me during my project, particularly Linda Grigoraki, Amy Lynd, Jessica Lingley and James Maas. Also to all those I spent time with at socials or playing football – you made my time here great fun.

Thank you to James LaCourse for his support and the opportunities he found for me to progress in teaching. James and the Dagnal team gave me so many opportunities and advice to improve and for that I owe them many thanks.

I was lucky to have met some great friends while here. Eleri Ashworth, Emily Martin, Charlotte Quinn, Dan McDermott, Annabel Murphy and Frank Mechan are only a few of those who have been so supportive through the highs and the lows and made my PhD something I have enjoyed overall.

My biggest supporters to whom I owe so much are my family, particularly my Mum and Dad without whom I wouldn't have the drive to have gotten this far. Their unwavering support and encouragement even from a distance have motivated me and driven me to do the best I can. Thank you also to my brother William and sister Amy for your constant love and support.

Last but in no way least, I want to thank my partner, Jack, who has been caring and encouraging throughout and I am grateful for his unending support through the long hours and for always pushing me to do the best I possibly can. His reassurance and understanding have kept me going in the hard times and the good and I will always be grateful for that.

# Abstract

Insecticide resistance is a threat to malaria and arbovirus control programmes targeting mosquito vectors. Integrated control programmes which include control of larval stages are becoming more important for *Anopheles* control as urbanisation in malaria endemic areas increases and remain crucial in *Aedes* control. However, the success of control programmes is threatened by the evolution of molecular mechanisms which confer insecticide resistance. Potential resistance mechanisms are identified by screening the genome, transcriptome and proteome for mutations or gene upregulation that correlate with resistance phenotypes. Once candidate mechanisms have been identified they need to be functionally characterised in isolation to determine their role, as in field and lab insecticide-selected mosquitoes many mutations may co-occur which complicate the analysis. This functional characterisation is best conducted using genetically modified mosquitoes, which has been realised for members of several gene families thought to be involved in adulticide resistance. However, very little has been conducted in relation to larvicide resistance.

One reason for the lack of research on larval resistance is that the existing WHO recommended mortality-based larval resistance assay is low-throughput and subject to investigator bias. To address these issues, a novel assay was developed in collaboration with the Sattelle group at UCL using the Invertebrate Automated Phenotyping Platform (INVAPP) and analysis algorithm (Vectorgon). The INVAPP assay provides automated quantification of larval motility after insecticide exposure. In this project, three statistical methods, based in R and python, were trialled to analyse a complex data set collected by exposing a set of transgenic *Anopheles gambiae* larvae to a range of insecticides. The transgenic larvae each ubiquitously overexpressed a single gene, which had previously demonstrated roles in adult resistance. The drc package showed some promise in defining larval resistance status, but ultimately more data is needed draw conclusions with confidence. Further data collection and optimisation is required before this assay can be reliably used for such relative resistance analysis.

A second project aimed to functionally characterise the carboxylesterase, CCEae3A, which has been implicated in temephos resistance in *Aedes aegypti* and *Aedes albopictus* larvae, using a GAL4-UAS expression system in *An. gambiae*. Insecticide resistance profiling in larvae indicated significant increases in resistance ratio compared to a strain which does not express CCEae3A, for three organophosphate insecticides, temephos (5.98), chloropyrifos (6.64) and fenthion (3.18). Cross resistance to adulticides from four insecticide classes: malathion and fenitrothion (organophosphates), bendiocarb and propoxur (carbamates), pirimiphos methyl (phosphorothioate) and alpha-cypermethrin (pyrethroid) was also detected. Pirimiphos methyl and alphacypermethrin resistance had not previously been associated with CCEae3A, despite previously occurring in strains where this gene was upregulated. This highlights the importance of characterising mechanisms in isolation to ensure accurate information is used for guiding vector control strategies.

The final project aimed to localise transcription of *ace1* (the neuronal target for organophosphate and carbamate insecticides) and characterise the insecticide resistance and fitness cost profiles associated with the ACE1-G280S single nucleotide polymorphism. These aims were approached by genome modification using CRISPR-Cas9 based homology directed repair. An F2A protospacer-fluorescent protein was used to tag the *ace1* gene in *An. gambiae* and confirmed that *ace1* transcription is highest in larval and adult nerve cord and ganglia but failed to detect embryonic expression. *An. gambiae* carrying the G280S mutation in an otherwise insecticide susceptible background were also created with high efficiency. Mosquitoes homozygous for 280S displayed decreased susceptibility to propoxur, fenitrothion and malathion, but surprisingly not to temephos, the most common organophosphate larvicide. However, the significant reductions in longevity and fecundity observed in the 280S transgenics may explain the absence of single copy *ace1* mutant homozygotes in field mosquitoes. This project reports the first use of genetically modified *An. gambiae* to study mosquito larval resistance mechanisms and the first use of a 2A protospacer to tag an endogenous gene in mosquitoes.

# Contents

# Table of Figures

# Table of Tables

# Table of Equations



# TABLE OF APPENDICES

# List of Abbreviations

3A – CCEae3A

ABC – ATP-binding cassette

*ace1*/ACE1(AChE) – Acetylcholine esterase 1

ACh – Acetylcholine

AChR – Acetylcholine receptor

*Ae. - Aedes*

*An. – Anopheles*

ANOVA – Analysis of variance

ATSBs – Attractive targeted sugar baits

Cas9 – Caspase 9

CCE - Carboxylesterase

CDC – Centres of Disease Control

CHCs – Cuticular hydrocarbons

CHS – Chitin synthase

CI – Confidence intervals

CNS – Central nervous system

CNVs – Copy number variants

CRISPR – Clustered Regularly Interspaced Palindromic Repeats

CSP – Chemosensory protein

CYPs – Cytochrome P450s

DDT – Dichloro-Diphenyl-Trichloroethane

DEF - S,S,S-tributyl phosphorotrithioate

DEM – Diethyl maleate

df – Degrees of freedom

DNA – Deoxyribonucleic acid

dsDNA – doble stranded DNA

dsRed – *Discosoma sp.* Red fluorescent protein

dsRNA – double stranded RNA

EC50 – Effective concentration 50%

EIP – Extrinsic incubation period

eCFP – enhanced Cyan fluorescent protein

eYFP – enhanced Yellow fluorescent protein

GABA – Gamma-Aminobutyric acid

GFP – Green fluorescent protein

GOI – Gene of interest

gRNA – Guide RNA

GST – Glutathione-S-Transferase

GWAS – Genome-wide association studies

HDR – Homology directed repair

IC50 – Inhibitory concentration 50%

IGRs – Insect growth regulators

INVAPP – Invertebrate automated phenotyping platform

IRS – Indoor residual spraying

ITNs – Insecticide treated nets

IVM – Integrated vector management

*kdr* – Knock down resistance

LC50 – Lethal concentration 50%

LED – Light emitting diode

LF – Lymphatic filariasis

LITE – Liverpool insect testing establishment

LL.(x) – Log Logistic (x) parameter function

LLINs – Long lasting insecticidal mosquito nets

LMIC – Low- and middle-income countries

LNA – Locked nucleic acid

LSM – Larval source management

LT50 – Lethal time 50%

MI – Movement index

mRNA – Messenger RNA

nAChR – Nicotinic acetylcholine receptor

nMI – Normalised movement index

NTD(s) – Neglected tropical disease(s)

OP – Organophosphate

PAM – Protospacer adjacent motif

PBO – Piperonyl butoxide

PBS – Phosphate buffered saline

PCR – Polymerase chain reaction

pIC50 – $-\log_{10}$IC50

PVC – Polyvinyl chloride

qPCR – quantitative PCR

QTL – Quantitative trait locus

RFLP – Restriction fragment length polymorphism

RMCE – Recombinase mediated cassette exchange

RNA – Ribonucleic acid

RNAi – RNA interference

RR – Resistance ratio

SAP – Sensory Appendage Protein

SDS – Sodium dodecyl sulphate

sgRNA – Synthetic guide RNA

shRNA – Short hairpin RNA

siRNA – Short interfering RNA

SNP – Single nucleotide polymorphism

UAS – Upstream activation sequence

UCL – University College London

*vgsc*/VGSC – Voltage gated sodium channel

WHO – World Health Organization

WHOPES – WHO Pesticide evaluation scheme

WT – Welcome Trust

*zpg* – zero population growth (promoter and terminator)

# Introduction

## 1.1 MOSQUITO LIFE CYCLE AND BIOLOGY

Mosquitoes are insects (part of the family Culicidae) that are responsible for the transmission of pathogens which infect hundreds of millions of people and cause several hundred thousand human deaths every year (WHO *et al.*, 2017). The burden of mosquito borne diseases disproportionately affects the poorest countries and people in the world, entrenching them in and driving poverty.

Mosquitoes transition through four distinct life stages: egg, larva, pupa and adult. Adult female mosquitoes tend to mate only once, typically in the first few days of adulthood, and store sperm in a spermatheca for fertilization during deposition, for multiple batches of eggs. Both male and female adult mosquitoes feed on natural sugar secretions for nutrition. The adult females of most species of mosquito, including all those relevant to disease spread, must take a blood-meal to acquire proteins required for egg development. After blood feeding, adult females 'rest' (location varies between species) while they digest the blood and eggs mature. As only female mosquitoes blood feed, it is only female mosquitoes which are vectors of pathogenic viruses and parasites.

Depending on species preferences, eggs are oviposited in or near water and larvae either hatch into the water and only hatch when submerged in water (and sometimes additional environmental stimuli). For some species (e.g. *Anopheles*) hatching occurs within a few days (though this timing varies with temperature) and their eggs are not viable if they do not remain wet. In other species (e.g. *Aedes*) whose eggs withstand desiccation when they dry out, hatching may not occur for months or years following oviposition until they are submerged in water. Mosquito larvae must remain in water for development through four instar stages or desiccation will occur, though the type of water sources varies greatly between different mosquito genera. Most mosquito larvae must reach the water surface to breathe, though some species are able to obtain oxygen from plant roots and stems. The time spent at each larval stage is dependent on species, environment, and climate (particularly temperature). Following the final larval instar stage mosquitoes transform into comma-shaped pupae which do not

eat and undergo metamorphosis into the adult. Again, the length of the pupal stage varies depending on species and temperature. It ends when metamorphosis is complete and eclosion of the adult occurs.

Mosquito life history traits are affected by the conditions encountered during early developmental stages, particularly larval stages, the only immature stage which feeds, which must accumulate sufficient nutrients for development through pupal to adult stages. Larvae feed on microorganisms, plant and animal matter in the water they live in, and some species are cannibalistic or carnivorous (Service, 2012). One important consequence of this interaction is that adult body size is determined by the density, nutrition and temperature during larval development. As larger adults have been shown to live longer (Reiskind and Lounibos, 2009; Owusu, Chitnis and Müller, 2017), larval breeding conditions can impact their potential to transmit diseases and resist insecticides (Takken, Klowden and Chambers, 1998; Okech *et al.*, 2007; Araújo, Gil and e-Silva, 2012; Moller-Jacobs, Murdock and Thomas, 2014). Decreasing larval density and increasing nutrition leads to faster development and improved survival rates (Owusu, Chitnis and Müller, 2017).

In addition to environmental factors, several mosquito behaviours and biological characteristics impact the likelihood of pathogen transmission in humans. Host preference for humans (anthropophily) increases the likelihood of human pathogen spread, though some zoophilic species do contribute to spread of human pathogens in areas of high-density human population (Service, 2012; Wolff and Riffell, 2018). Mosquitoes may blood feed primarily at night (e.g. *Anopheles* mosquitoes) or during the day (e.g. *Aedes aegypti*) and often have a preference to feed inside human habitation (endophagy) or outdoors (exophagy) (WHO, 2019b). These preferences are important to transmission in how they correspond to typical human behaviours of sleeping indoors at night and spending time outdoors during the day. Different mosquito species also have different vector capabilities and importance in pathogen transmission (Kramer and Ciota, 2015).

## 1.2 ANOPHELES MOSQUITOES AND DISEASE

Malaria is an infectious disease caused by a single-celled eukaryotic parasite of the *Plasmodium* group which are transmitted to humans primarily by mosquitoes of the *Anopheles* genus. It is estimated that there are over two hundred million cases of human malaria and hundreds of thousands of deaths annually, with both concentrated in Africa and other low and middle income countries (LMIC) outside this region (WHO, 2020). Additionally *Anopheles* mosquitoes are the main vector of lymphatic filariasis in West Africa (de Souza *et al.*, 2012) and transmit the alphavirus o'nyong-nyong (Rezza, Chen and Weaver, 2017; Nanfack Minkeu and Vernick, 2018).

### 1.2.1 MALARIA

Four species of *Plasmodium* parasite (*Plasmodium falciparum, Plasmodium vivax, Plasmodium ovale* and *Plasmodium malariae*) plus a fifth zoonotic species (*Plasmodium knowlesi* – which primarily infects primates but has been shown to cause very small numbers of human infections cause human malaria. The majority of malaria deaths are in children under 5 years old and attributed to *P. falciparum* which is the most common species found in Africa (Ashley and Poespoprodjo, 2020). *P. vivax* is prevalent in Latin America and South East Asia, whereas *P. ovale* is present in west-Africa, and *P. malariae* is widespread but they only cause a small minority of infections (Bradley and Warrell, 2003).

All *Plasmodium* parasites go through a complex life cycle with asexual replication in both the human and mosquito hosts and sexual reproduction in the mosquito host. Sporozoites transferred in the saliva of mosquitoes during blood feeding on a mammalian host travel to and invade hepatocytes where they undergo asexual replication. Merozoites are released from liver cells into the bloodstream where they invade erythrocytes. Cyclical replication resulting in lysis of red blood cells and release of blood stage forms causes the clinical manifestations (fever and neurological symptoms) of disease. Differentiation into sexual stage gametocytes, that are ingested when a mosquito takes a bloodmeal, occurs in some parasites. In the mosquito gut the male gametes penetrate female gametes and develop into zygotes

then ookinetes. Ookinetes invade the mosquito midgut wall and form oocysts which develop and multiply into sporozoites which are released and travel to the salivary glands to complete the life cycle (CDC, 2020a).

Unlike some arboviruses, *Plasmodium* parasites are exclusively transmitted by mosquitoes which bite an infected host, as the parasite must develop through several stages in different mosquito tissues before reaching a stage which is infectious to humans in the salivary glands. As a result, *Plasmodium* parasites are not passed from mosquito parent to progeny or between mating pairs (as occurs in some arbo-viruses). The time from ingestion of gametocytes by the mosquito to sporozoite colonisation of salivary glands is the extrinsic incubation period (EIP) (Ohm *et al.*, 2018). The EIP varies as widely as 7-30 days and is influenced by *Plasmodium* and mosquito species (CDC, 2019) and many environmental factors (particularly temperature) affecting mosquito biology (Araújo, Gil and e-Silva, 2012). This has a crucial impact on geographical distribution and magnitude of malaria transmission (Ohm *et al.*, 2018).

For many other infectious diseases control programmes are effective using chemotherapy, chemoprophylaxis and/or vaccines, but this is not the case for malaria. Several drugs are available to cure malaria infection and several promising compounds with novel modes of action are in development (Tse, Korsik and Todd, 2019). The contribution of chemotherapy to malaria control is diminished by: increasingly widespread resistance that results in treatment failure; weak regulation resulting in poor drug quality; and political barriers to funding, treatment programme implementation and resistance management (Hanboonkunupakarn and White, 2020). Chemoprophylaxis is available and effective for short term (e.g., for non-immune travellers) *P. falciparum* protection but adverse effects and cost associated with long term use (> 6 months) mean that prophylactic treatment is not used in endemic areas (Schwartz, 2012; Ahmad *et al.*, 2021). There is not currently a widely distributable vaccine for malaria. Although several vaccines (including RTS,S/AS01e (Bell *et al.*, 2021)) are in the late stages of clinical trials (Pance, 2020; Bell *et al.*, 2021). These methods of control are not sufficiently effective in their current form, so funding for malaria control has been focused on the control of the *Anopheles* mosquito vector which has historically been more effective at providing

community protection (WHO, 2020) and has the added benefit of targeting several mosquito borne diseases at once (e.g. lymphatic filariasis).

### 1.2.2 LYMPHATIC FILARIASIS

859 million people are threatened by lymphatic filariasis (LF) (WHO, 2021). LF is caused by infection with filarial roundworms which are transmitted to humans by mosquitoes of several different species (WHO, 2021) and often co-occurs with endemic malaria transmission (de Souza *et al.*, 2012). LF infection presents as asymptomatic, acute and chronic conditions and patients often acquire infection as children and experience all three conditions (deteriorating gradually) as the disease progresses. Chronic symptoms occur when adult worms block lymphatic vessels causing tissue swelling and hydrocele. Meanwhile microfilariae circulate in the blood and are picked up by mosquitoes where they develop into mature parasite larvae which are deposited onto the skin of a new host. More acute episodes often occur because of an immune response to the parasite or secondary infections which are more likely due to lymphatic system damage.

Around 90% of human LF cases are caused by *Wuchereria bancrofti*, and the rest are caused by *Brugia malayi* and *Brugia timori*. LF spread in urban and semi urban areas is normally by *Culex*, in rural areas is mainly by *Anopheles* and on islands in the Pacific by *Aedes* mosquitoes (WHO, 2021). Mass drug administration is the main strategy for targeted LF control (Lupenza, Gasarasi and Minzi, 2021) and as LF often co-occurs with malaria transmission, vector control programmes which target malaria are often also effective in reducing LF transmission (de Souza *et al.*, 2012). Control of LF resulted in a 74% reduction in cases between 2000 and 2018 but 51 million people were still infected in 2018, so intervention is still required (WHO, 2021).

### 1.2.3 ANOPHELINE VECTORS

Only mosquitoes of the *Anopheles* genus transmit human malaria but not all members of the genus have this capacity. There are over 500 named or provisionally designated *Anopheles* species though only around 70 of these are confirmed as competent human malaria vectors and only around 40 are

thought to be of importance (Gilles and Warrell, 2002). *Anopheles* mosquitoes are found worldwide and the distribution of those species which can successfully transmit human malaria parasites has been predicted using expert opinion maps and boosted regression tree modelling (Figure 1.2.1) (Sinka *et al.*, 2012). Members of the *An. gambiae* subgroup (*An. gambiae s.s*, *An. coluzzii*, *An. melas*, *An. arabiensis* and *An. merus*), *An. funestus s.s*, *An. nili* and *An. mouchetti* are the most dominant vectors of *Plasmodium* parasites in the WHO African region (WHO, 2019b) where 93% of cases occur, almost all of which are caused by *P. falciparum* (WHO, 2019c). *An. gambiae s.l* is regarded as the most effective and efficient vector of human malaria (Sinka *et al.*, 2010) though in some areas *An. funestus s.s* contributes more to malaria transmission (Coetzee and Fontenille, 2004). It is difficult to determine the most important species in the Asian-Pacific region as 19 dominant vector species are recognised (including *An. minimus*, *An. stephensi*, *An sinensis* and *An, dirus*) which often co-exist (Sinka *et al.*, 2011) and as *P. falciparum* and *P. vivax* each account for approximately half of the regions cases (WHO, 2019c). *An. albimanus*, *An. darlingi* and *An. freeborni* are the most commonly found malaria vectors in the WHO American region (Sinka *et al.*, 2010). Malaria transmission is minimal in Europe and the Middle East, despite presence of six vector species which are classed as dominant in other areas (Sinka *et al.*, 2010).

The distribution of different *Plasmodium* species is impacted by the distribution of the vector (Figure 1.2.1) as some *Anopheles* species are more efficient malaria vectors than others or are more likely to transmit a particular *Plasmodium* species. For example, *P. falciparum* (which is the most commonly found species on the African continent) is transmitted primarily by mosquitoes of the *An. gambiae* complex. However, variability in vector competence varies even within the *An.* gambiae complex. An inversion polymorphism (2La) in *An. gambiae* and *An. coluzzii* which is widespread in Africa is predicted to increase *P. falciparum* spread by these vectors compared to other members of the *An. gambiae* complex (Riehle *et al.*, 2017). Meanwhile, the burden of *P. vivax* is concentrated in South East Asia and the Americas with 47% of cases of *P. vivax* in India alone (WHO, 2019c) where *An. stephensi* is the major malaria vector in urban areas (Mohanty *et al.*, 2018). Additionally, the urban

form of *An. stephensi* (type) is a more efficient vector of *P. vivax* than the rural form (mysorensis) as the rural form is highly zoophilic (Gholizadeh, Zakeri and Djadid, 2013).

The *Anopheles* mosquito species that are most crucial for human malaria transmission tend to share the behavioural traits of biting indoors at night then resting on the internal walls of houses which has massive impacts on malaria transmission as humans are usually the primary source of a bloodmeal for these species. This has provided opportunities for strategies for vector control by exploiting these behavioural traits to specifically target malaria spreading mosquito species (WHO, 2019b). However, this trend is not absolute and can vary between species, subpopulation or even within species depending on environmental factors (WHO, 2019b) such as host availability and insecticide pressures (Niang *et al.*, 2019).

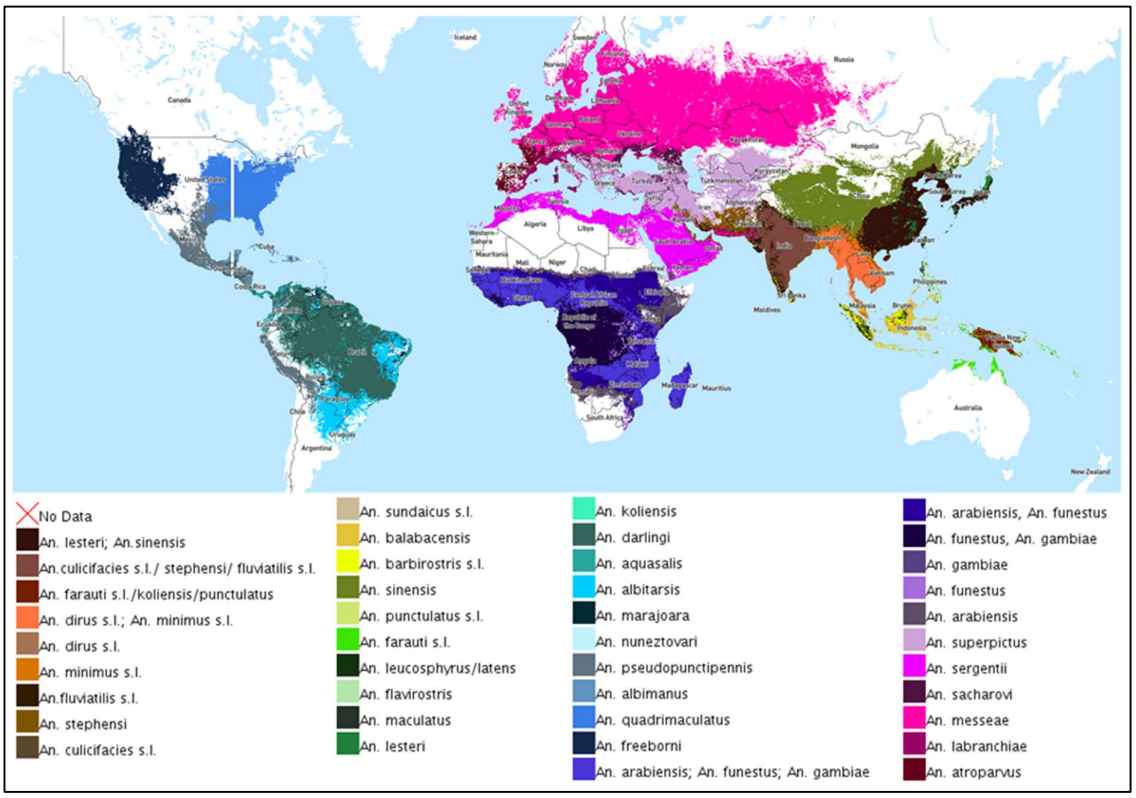


Figure 1.2.1: Predicted global distribution of dominant malaria vector species 2010 – adapted from (Sinka et al., 2012).

If many species are predicted to be present in a country, only the species of major importance as a malaria vector are shown.

Another important trait which varies between species is the preference for different larval habitat types. Larval habitat preference has an impact on the potential distribution of a species and thus the potential spread of malaria. Mosquitoes in the *An. gambiae* complex display a preference for natural, often temporary or dynamic water sources (e.g. footprints, puddles, rice fields, pits) whereas *An. funestus* larval habitats are typically more permanent and have vegetation which provides shade (e.g. marshes, the edge of rivers and streams, ricefields) (Service, 2012). Urban *An. stephensi* display a preference for manmade water sources (e.g. cisterns, gutters, containers) reflecting the difference in environment to which they have adapted (Service, 2012).

## 1.3 CULICIDAE MOSQUITOES AND ARBOVIRUSES

### 1.3.1 ARBOVIRUSES

Mosquito borne arboviruses have a massive impact on human and animal health. Those that have the greatest impact – dengue, chikungunya, zika and yellow fever viruses – have been recognised as neglected tropical diseases (NTDs) by the WHO for the last few decades (Velayudhan, 2019). Despite reductions in case numbers of other vector-borne diseases, arboviruses are geographically spreading and case numbers increasing (WHO *et al.*, 2017). 3.6 billion people in over 100 countries are at risk of infection with mosquito borne viruses but although overall case numbers are increasing, the case fatality rate is declining globally. (WHO *et al.*, 2017).

Dengue fever is caused by the dengue flaviviridae virus which in the last century has adapted to human hosts. Dengue virus is transmitted by *Aedes* mosquitoes – primarily *Ae. aegypti* (and possibly *Ae. albopictus*) and far more rarely in blood transfusions, blood exposure and mother-to-child transmission during pregnancy (Basurko *et al.*, 2018). Also unlike malaria transmission, dengue virus transmits vertically from mother to progeny in both the human (Basurko *et al.*, 2018) and the mosquito vector (Shroyer, 1990; Ferreira-de-Lima *et al.*, 2020). Infection with dengue virus results in either mild symptoms (e.g., fever, myalgia, vomiting) which tend to resolve fully without intervention or severe symptoms (dengue haemorrhagic fever). There are four key serotypes of dengue virus and

severe symptoms tend to occur when patients become infected for a second time with a different serotype to the first infection (Aguas *et al.*, 2019). Dengue is spreading rapidly, driven by *Ae. aegypti* expansion into new habitats and increasing urbanisation resulting in increased human to mosquito contact (Brady and Hay, 2020).

Zika virus is also a flaviviridae virus transmitted by *Aedes* mosquitoes and similar to other arboviruses most infections result in asymptomatic or mild symptoms (rash, fever, conjunctivitis and/or headache). More severe cases result in Guillain-Barre syndrome, acute myelitis or meningoencephalitis. If zika virus is contracted during pregnancy severe birth defects, such as microcephaly and other brain defects, can occur (Wolford and Schaefer, 2021).

Chikungunya is caused by a togaviridae virus which is transmitted to humans by *Aedes* mosquitoes. Similar to dengue virus, Chikungunya virus can be transmitted vertically from female mosquitoes to their progeny (Vega-Rúa *et al.*, 2014). Typically symptoms are mild, rarely progresses to be life threatening and normally recovery happens within 7-10 days (Lakshmi *et al.*, 2008).

As these most common arboviral infections tend to be short lived and relatively mild, usually no treatment is required, and any treatment given will not directly target the virus but instead treat the symptoms. An efficient vaccine is available for yellow fever (CDC, 2021c), whereas the dengue vaccine is only licenced for those aged 9 – 45 years old and is only recommended for those who have previously been infected with dengue virus (CDC, 2021a). There are no vaccines available for the other arboviruses. Therefore, the focus of arbovirus control has been to control the mosquito vector. This has the added benefit of impacting transmission of several arbo-viruses at the same time.

### 1.3.2 *AEDES* VECTORS

The global spread of *Ae. aegypti* (native to forests in Africa) coincided with behavioural change shifting from zoophilic biting to biting humans and adaption to new larval habitats which are more prevalent in domestic environments and this geographical spreading is expected to continue (Kraemer *et al.*, 2019). The widespread distribution of *Ae. aegypti* is in part due to exogenously controlled

quiescence in eggs which temporarily delays larval hatching until conditions are favorable for survival. *Ae. albopictus*, the Asian tiger mosquito, is an invasive species now found on every continent (Paupy *et al.*, 2009). Its spread from forests in Asia to Europe, the United States and Brazil (Kraemer *et al.*, 2015), has been facilitated by increases in worldwide ship transport since the 1980s (Lounibos, 2003) with air travel further driving its spread worldwide (Findlater and Bogoch, 2018). *Ae. albopictus* eggs upregulate yolk lipid production and enter a state of dormancy (diapause) to adapt to cold temperatures enabling the spread of *Ae. albopictus* further North than *Ae. aegypti*. *Ae. albopictus* serves as a vector to a wide range of arbo-viruses, for example: dengue virus, West Nile virus, alphavirus and chikungunya virus (Paupy et al., 2009).

Although *Ae. albopictus* exhibits anthropophilic behaviour, it usually feeds opportunistically on both humans and animals outdoors, thus its potential distribution is less restricted by absence of human populations than that of *Ae. aegypti* (Kraemer *et al.*, 2015) increasing its capability to spread arbo-viruses from animal hosts to humans. Diapause and feeding behaviour, in addition to its strong ecological plasticity and broader range of larval breeding grounds, contributes to the variation in the distribution (Figure 1.3.1 and Figure 1.3.2) of *Ae. albopictus* compared to *Ae. aegypti* (Paupy et al., 2009). Figure 1.3.1 and Figure 1.3.2 depict the predicted distribution of *Ae. aegypti* and *Ae. albopictus* respectively although it is important to note that some occurrence points are predicted where the species has not yet been reported (e.g. in South East Europe and the Balkans) and that sparse reporting in Africa means it is unknown in many areas whether the predicted population is accurate (Kraemer *et al.*, 2015).

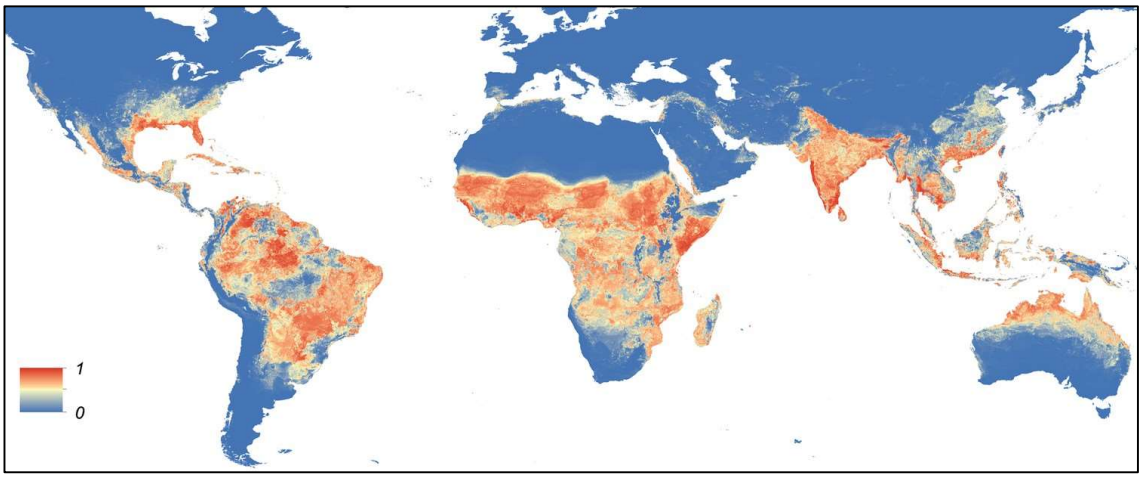


Figure 1.3.1: Predicted distribution of *Aedes aegypti* globally (Kraemer et al., 2015).

From 0 (blue) to 1 (red) the map depicts the probability of *Aedes aegypti* being present at a 5 km x 5 km spatial resolution.

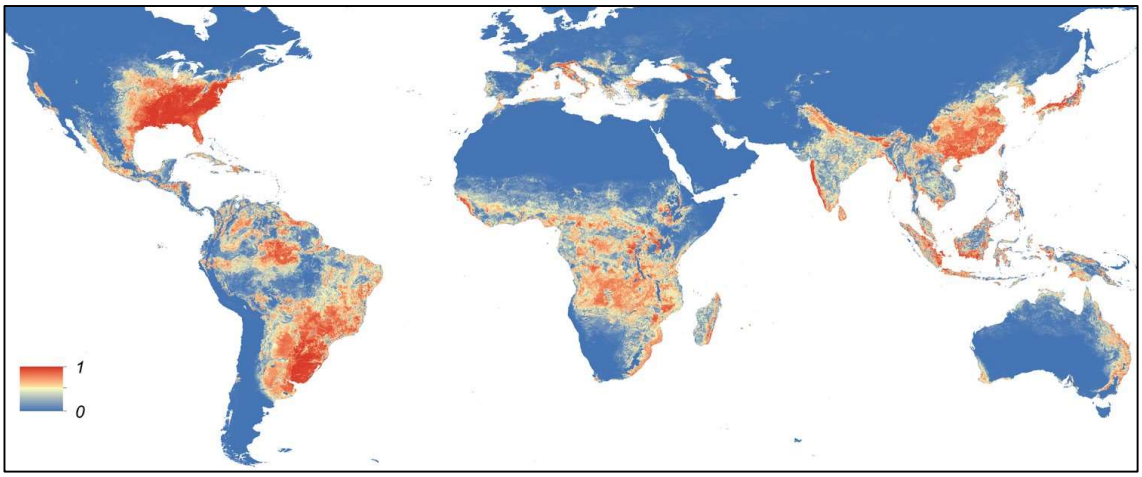


Figure 1.3.2: Predicted distribution of *Aedes albopictus* globally (Kraemer et al., 2015).

From 0 (blue) to 1 (red) the map depicts the probability of *Aedes albopictus* being present at a 5 km x 5 km spatial resolution.

## 1.4 METHODS OF VECTOR CONTROL

A crucial method of controlling vector-borne diseases is to employ measures that limit the ability of a vector to transmit the pathogen (Tizifa *et al.*, 2018). Prior to the second world war, mosquito control programmes used environmental modification or manipulation (WHO, 2012a) but since then mosquito control has been achieved primarily through killing of mosquito adults and larvae using insecticidal compounds, toxins or removal of larval habitats (Tizifa *et al.*, 2018). Other non-lethal compounds which mimic insect hormones are employed that block reproduction, egg hatching and/or larval development (Kamal and Khater, 2010; Suman *et al.*, 2013; Suman, Wang and Gaugler, 2015; Lawler, 2017). More recently methods have been developed and are employed which also block transmission of arbo-pathogens - e.g., release of *Wolbachia* infected mosquitoes (Crawford *et al.*, 2020). Complete eradication of the vector is not believed to be necessary to eradicate vector-borne pathogens (Bates *et al.*, 2016) as transmission will decrease if the number of mosquitoes in an area is brought below a critical threshold (Ferguson, 2018). It is essential, for the success of any vector control programme, that regular epidemiological and entomological surveillance is conducted alongside any of the methods described below to measure the success and detect any potential resistance or control failures early. Regular monitoring is also a vital tool for understanding and learning about the vector and its interactions with the environment, hosts and our control measures (WHO, 2012a).

The success of each control measure is dependent on a wide range of factors including; vector biology, vector and human behaviour and local ecology (Tizifa *et al.*, 2018). Due to variations in behaviour of *Aedes* and *Anopheles* mosquitoes different control methods are utilised for arbo-virus and malaria control (Barrozo *et al.*, 2004; Pates and Curtis, 2005). *Anopheles* mosquitoes are typically endophilic, endophagic and bite primarily at night so sleeping under insecticide treated bed nets is effective in reducing biting and indoor residual spraying of insecticides kills adults which rest on internal walls after biting (Service, 2012). Conversely, most *Aedes* mosquitoes bite at dawn and dusk and so are unlikely to interact with a bed net or internal walls of dwellings so adults are targeted by

outdoor fogging (Service, 2012; Captain-Esoah *et al.*, 2020). Important differences between species also exists when targeting the larval stage. *Anopheles* larvae tend to reside in natural transient pools of water which are often difficult to reach, cover or drain and so larval control measures are often difficult to implement but *Aedes* larvae reside more commonly in artificial containers which can be emptied or treated efficiently, even by members of the public (Pates and Curtis, 2005).

### 1.4.1 NON-INSECTICIDE BASED CONTROL MEASURES

#### 1.4.1.1 Larval Source Management

Larval Source Management (LSM) is a group of methods used to control mosquitoes by targeting larvae and pupae in mosquito breeding sites with the aim of reducing the number of mosquitoes which emerge as adults (Tusting *et al.*, 2013). LSM has benefits for both indoor and outdoor biting mosquitoes as immature forms in aquatic habitats are killed (or stop developing correctly) prior to adult emergence but it is not commonly used for control of *Anopheles* mosquitoes, particularly in rural areas, as it is usually too laborious (Ferguson, 2018). LSM was the primary method used for malaria control until the discovery of chemical insecticides in the 1950s after which its use declined (Fillinger and Lindsay, 2011). The WHO has formally encouraged use of combined interventions for malaria control since 2012 (WHO, 2012b) and recognition was given for LSM in reducing the contribution of outdoor biting to malaria transmission (Tizifa *et al.*, 2018).

There are four broad components of LSM (Rozendaal, 1997). 1. Modification of habitats: making permanent changes to land and water sources (e.g., draining marshland, filling pits or ditches, removing artificial containers). 2. Habitat Manipulation: making temporary changes to land and water sources (e.g., covering water tanks, regular emptying of artificial containers, use of oil to coat the surface of the water). 3. Biological control: introducing natural larvae predators or other organisms to water sources (e.g., larvivorous fish). 4. Larviciding: application of biological or chemical insecticides to water sources. Within LSM, as with all vector control, the method chosen should match the vector habitat, behaviours, resources and ability to achieve effective coverage. Larviciding is currently the

most commonly used LSM method (Tizifa *et al.*, 2018) and is discussed individually in detail in 'Section 1.4.3.4'.

LSM is commonly used as a key component in the control of *Aedes* mosquito vectors. *Aedes* vectors primarily live in artificial containers which can be emptied, covered or treated with insecticides. Crucially, these habitats are generally easily identifiable and accessible and campaigns often involve significant community engagement to conduct LSM (Roiz *et al.*, 2018). A communication for behavioural impact (COMBI) approach and a toolkit for effective outbreak response that are recommended by the WHO are being used in many countries for encouraging community participation in dengue control (WHO and UNICEF, 2012). In the early 20$^{th}$ century, LSM was a crucial component in the elimination of *Ae. aegypti* mosquitoes responsible for yellow fever transmission (and reducing malaria transmission) and permitting the completion of the Panama canal shortly after the connection between *Aedes* mosquitoes and yellow fever transmission was understood (Dominguez and Schrock, 2019). Unfortunately, this success led to continent wide complacency and lack of political support for vector control and monitoring programmes resulting in gradual return of *Ae. aegypti* from areas which had not achieved complete elimination (Wilson *et al.*, 2020) permitting the return of yellow fever and spread of other arboviruses in decades to come (Achee *et al.*, 2015).

Two Cochrane reviews on LSM for malaria control indicated that LSM can have substantial impacts on malaria incidence in areas where larval habitats can be identified readily but also highlighted situations where LSM appears to have no effect (Tusting *et al.*, 2013; Choi, Majambere and Wilson, 2019). One of the most important factors in the success (and cost effectiveness (Worrall and Fillinger, 2011)) of LSM was reported to be that a sufficient proportion of larval habitats could be targeted which relies on them being identifiable, accessible and discrete (Tusting *et al.*, 2013; Choi, Majambere and Wilson, 2019). Both reviews also highlight the low quality of evidence available despite inclusion of randomised cluster trials (Tusting *et al.*, 2013; Choi, Majambere and Wilson, 2019). As the WHO recommend the use of LSM for malaria control as a complementary tool to methods targeting adult mosquitoes meaning that more countries will use the method so it is important to understand the most effective implementation approaches. It is equally (if not more) important

given the limited funding available for control programmes to determine the ecological settings and levels of transmission which may be too difficult to target or where LSM will not be cost effective (Keiser, Singer and Utzinger, 2005; Worrall and Fillinger, 2011).

Despite reporting of use of LSM measures in Africa (Sierra Leone) as early as 1812 it is important to recognise that despite LSM not being typically used for control of African malaria mosquitoes it has contributed to all successful eradication efforts, and vector control programmes worldwide (Fillinger and Lindsay, 2011). This includes control of *An. gambiae* in Upper Egypt (Shousha, 1948) and Brazil (Killeen *et al.*, 2002), *An. gambiae* and *An. funestus* Zambia (Utzinger, Tozan and Singer, 2001) and several species of *Anopheles* in Italy, Palestine/Israel and the Tennessee river valley (South United States) (Kitron and Spielman, 1989) and thus, in combination with existing tools, LSM could be an important measure against malarial mosquitoes (Fillinger and Lindsay, 2011). It should be noted however that all these programmes combined LSM with other control methods, vector surveillance/monitoring and/or recruitment of local men to implement the measures and some also involved military assistance. Although it may not have been defined as such when these programmes were conducted, integrated vector management (IVM) using a combination of vector control tools was likely crucial to the success of these programmes and this must be considered when planning control programmes now (Fillinger and Lindsay, 2011).

It also should be noted that, although the larval habitats and climate resembled that of malaria endemic areas in Africa, the successful rapid eradication of *An. gambiae* from Brazil in the 1930s occurred following accidental introduction of the vector to the country (Fillinger and Lindsay, 2011). There are some crucial differences between this success story and the current situation in Africa and other areas of endemic malaria transmission. Firstly, *An. gambiae* was introduced to Brazil and control started and was completed shortly after, thus the likelihood of reintroduction from surrounding areas was very low (Killeen *et al.*, 2002). This is not the case in almost all endemic areas, particularly those in sub Saharan Africa where the likelihood of reintroduction following local elimination is very high (Shretta *et al.*, 2017). Secondly, the control programme in Brazil was conducted in a coordinated manner with “military precision” to prevent this reintroduction into areas which had achieved

elimination (Killeen *et al.*, 2002). This is far more difficult to achieve in the complicated political landscape of sub Saharan Africa where many different countries and stakeholders need to cooperate effectively while working across many language, religious, cultural and funding barriers which add to the complexity of attempting a coordinated approach, though some countries have formed networks to facilitate collaboration (Shretta *et al.*, 2017). Finally, despite success in the 1930s, Brazil was unable to sustain malaria elimination beyond the 1960s. This has been attributed to increased national and international travel, industrialisation and the resulting growth of urban areas and population density (Martens and Hall, 2000). Similar changes are in progress in sub-Saharan Africa currently which suggests that mosquito control is potentially becoming more difficult and will rely on understanding the link between human movements and mosquito environments (Hay *et al.*, 2005).

Non-insecticide based LSM methods have not changed much since the commercialisation of chemical insecticides, except for the discovery and commercialization of the first microbial pesticide targeting mosquitoes, *Bacillus thuringiensis* subsp, *israeliensis* (*bti*), in the 1970s (Laird, 1985).

#### 1.4.1.2 Building Improvement

In the late 19$^{th}$ and early 20$^{th}$ century, following the understanding of the connection between mosquito bites and disease, personal protective wear (gloves, veiled hats etc.), mosquito nets for cradles and wire gauze for blocking windows became widely available (Tusting *et al.*, 2015; Gachelin *et al.*, 2018). Additionally people began to paint the internal walls of homes white to aid in spotting and killing resting mosquitoes (Grancaric, Botteri and Ghaffari, 2019). Improving housing quality not only reduces mosquito bites and thus the likelihood of disease transmission but also can have a broader effect beyond mosquito-borne diseases (e.g. improvement of chronic conditions and reduced risk of chagas disease) (Thomson *et al.*, 2013). Housing improvements now tend to focus on presence of a ceiling and closing eaves as this prevents entry of the mosquitoes into homes (Lindsay *et al.*, 2003).

#### 1.4.1.3 Wolbachia

The microbiome of mosquitoes affects many physiological factors. *Wolbachia pipientis* is an obligate endosymbiotic bacteria (present in two-thirds of insect species) which was first identified in *Culex pipiens* mosquitoes in 1923 (Inácio da Silva *et al.*, 2021). Release of artificially *Wolbachia* infected mosquitoes is a control measure which is being used in field releases and randomised control trials for control of *Aedes* and *Culex* mosquitoes but not for *Anopheles* mosquitoes currently (Ross, 2021; Utarini *et al.*, 2021). There are two phenotypes which occur in *Aedes* mosquitoes depending on whether females are infected with *Wolbachia* that impact disease transmission. The first occurs when non-*Wolbachia* infected females mate with infected males resulting in cytoplasmic incompatibility between gametes and no viable offspring, favouring the spread of *Wolbachia* through populations in via infected females. The second occurs in *Wolbachia* infected females, since the presence of the bacterium reduces the replication of several arboviruses in the mosquito preventing transmission (Inácio da Silva *et al.*, 2021).

### 1.4.2 INSECTICIDES USED FOR MOSQUITO CONTROL

Insecticides have been used for over a century for mosquito control, since the connection between mosquitoes and disease was discovered, first through burning or spraying of pyrethrum powder indoors and the use of Paris Green which is (arsenic based and no is longer used due to human toxicology and ecological concerns) as a larvicide (Wilson *et al.*, 2020). These approaches were replaced by extensive use of dichlorodiphenyltrichloroethane (DDT) for indoor residual spraying (IRS) from 1943 (Gachelin *et al.*, 2018). Ecological considerations resulted in a ban on the use of DDT in 1972 but the WHO has since recommended that the compound can be used in areas when mosquitoes are still susceptible and other options are not reasonable (WHO, 2006a).

Currently, compounds from four key classes of insecticide are fully approved for vector control (organochlorines, organophosphates, carbamates and pyrethroids), plus compounds from two other

broader groups - insect growth regulators (IGRs) which mimic insect hormones and impact development (WHO, 2017) and an insecticide synergist, piperonyl butoxide (PBO), which acts alongside pyrethroid compounds to improve their efficacy (Global Malaria Programme, 2017). Compounds which belong to another class of compound, neonicotinoids, are effective against mosquitoes but not widely used yet, due to controversy surrounding the toxicology profile of the compounds to wildlife and other insects (particularly bumblebees) (Thompson *et al.*, 2020).

#### 1.4.2.1 Organochlorine (Chlorinated Hydrocarbon) Insecticides

One of the first chemicals to be widely utilized for insect control was DDT, an organochlorine insecticide, which was the first synthetic organic insecticide to be used for mosquito control (Raghavendra *et al.*, 2011). In 1942, DDT became commercially available, following discovery of its insecticidal properties by Swiss chemist Paul Hermann Müller. The use of DDT was successful in controlling malaria and typhus during World War I and it and similar synthetic compounds were used widely for agricultural purposes (Blus, 2003). However, evidence was gathered with regards to negative characteristics - persistence and toxicity to non-target organisms and to the environment - which resulted in the banning of DDT for all uses except for malaria control by WHO (Blus, 2003).

Members of the organochlorine class, previously the most widely used insecticides, including DDT, dieldrin and toxaphene, are toxic due to hyperexcitation of the nervous system. All organochlorine insecticides have chlorinated hydrocarbon structures, low water solubility, high lipid solubility and are therefore resistant to degradation.

There are two major groups of organochlorine pesticides – the DDT-types and the chlorinated alicyclics – which are defined based on the site and mechanism of toxic action and the resulting symptoms (Coats, 1990). DDT type insecticides act on receptor site-7 voltage gated sodium channels (*vgsc*) (Suppiramaniam *et al.*, 2010) at axons in the peripheral nervous system, preventing the deactivation of the gate, and causing hyperexcitability of the nerve resulting in trains of repetitive discharge within the neuron (Blus, 2003). The chlorinated alicyclic insecticides (e.g., aldrin, dieldrin and toxaphene) are a more diverse group of compounds within which chlorination patterns differ in

the number of chloro-substituents and position. These insecticides bind to the ϒ- aminobutyric acid (GABA) chloride ionophore complex inhibiting $Cl^-$ passage into the nerve causing hyperexcitation and repetitive discharges in nerves (Coats, 1990).

#### 1.4.2.2 Organophosphate Insecticides

Organophosphorus insecticides (OPs), for example malathion and temephos are derivatives of phosphonic ($H_3PO_3$) or phosphoric ($H_3PO_4$) acid. Organic moieties replace all hydrogen atoms and one or more of the oxygen atoms are replaced by nitrogen and/or sulphur (Chambers, Meek and Chambers, 2010a). As a result these insecticides display substantial chemical diversity (Chambers, Meek and Chambers, 2010b).

OPs (or the metabolites of OPs) phosphorylate the serine hydroxyl moiety within the active site of serine esterases – primarily acetylcholinesterase (ACE1) in mosquitoes - causing enzyme inhibition (Chambers, Meek and Chambers, 2010b). In cholinergic synaptic and neuromuscular junctions, ACE1 regulates transmission of nerve impulses to effector cells, through catalysed hydrolysis of acetylcholine to choline and acetic acid (Fukuto, 1990). Phosphorylation of ACE1 results in accumulation of acetylcholine (a neurotransmitter which drives action potentials across the synapse at neuromuscular junctions) in cholinergic synapses and neuromuscular/glandular junctions resulting in toxic hypercholinergic activity (Chambers, Meek and Chambers, 2010b) leading to convulsions and death (O'Brien, 1967).

The potential toxicity of OPs was recognised in the 1930s and by 1940 Gerhard Schrader and B. C. Saunders and their respective teams had utilized this toxicity for chemical warfare agents (e.g., sarin gas) and the first commercial OP insecticides. The early OP insecticides although effective were very toxic to mammals but in 1950, the American Cyanamid Company developed malathion which is still one of the safest OPs available (Chambers, Meek and Chambers, 2010a). It is a pro-insecticide which must be broken down to malaoxon, by oxidative sulphuration. Malaoxon binds irreversibly to several serine residues within the binding site of acetylcholinesterase (Bigley and Plapp Jr, 1962; Aker *et al.*, 2008). Mammals have higher levels of carboxylesterase activity than insects which means they

degrade malathion quicker than malaoxon is formed through oxidation which makes it safer than other insecticides (Gervais *et al.*, 2009). Malathion is commonly used as an adulticide for indoor residual spraying (WHO, 2015). Fenthion is a contact and stomach effective organothiophosphate compound which although toxic itself, is activated through enzymatic oxidation to multiple more active anti-cholinesterase compounds (e.g. phosphor atom containing unhydrolyzed fenthion metabolites) (FAO and WHO, 1972). Fenthion was used as a larvicide for malaria control in India for 30 years but has since been banned (Ashwani, 2016). Chlorpyriphos is a non-systemic insecticide, effective through inhalation, ingestion, and direct contact, which must be bioactivated to exert cholinesterase inhibition through substitution of a sulphur group with oxygen. Cytochrome P450s have been associated with this activation in human liver (Christensen *et al.*, 2009). Temephos is a WHO recommended organothiophosphate larvicide, which must be metabolised to its toxic oxon form *in vivo* (Grigoraki *et al.*, 2016). The recommended dosage for temephos in potable water is 1 mg/L of active substance (WHO, 2009).

#### 1.4.2.3 Carbamate Insecticides

Carbamate insecticides are derivatives of carbamic acid and the mechanism of action is virtually identical to that of the OPs as they also inhibit ACE1 (Costa *et al.*, 2008), however, carbamate inhibition is transient due to rapid reactivation of carbamylated AChE (Fukuto, 1990).

#### 1.4.2.4 Pyrethroid Insecticides

Pyrethroid insecticides are axonal excitocins (Rahnama-Moghadam, Hillis and Lange, 2015), based on an extract of *Chrysanthemum cinerariaefolium* consisting of six esters that are all highly toxic to insects, though compared to organochlorines show reduced toxicity to mammals and birds. Based on this pyrethrum extract, synthetic analogues have been developed through chemical alteration to reduce photo lability, while retaining or enhancing insecticidal activity (Coats, 1990). Like DDT, all pyrethroids primarily act through interference of sodium channels in nerve membranes resulting in neurotoxic effects (Soderlund, 2010). Most pyrethroid compounds belong to one of two classes –

Type 1 and Type 2. Increased afterpotential means that Type 1 pyrethroids that lack a cyano group (e.g. permethrin) produce bursts of repetitive discharges (Suppiramaniam *et al.*, 2010). Whereas depolarization of the membrane by Type 2 pyrethroids (e.g. deltamethrin), that have an α-cyano group present in the phenyl benzyl alcohol position, causes a reduction in amplitude of the action potentials eventually completely blocking neural activity (Suppiramaniam *et al.*, 2010). Some pyrethroids (e.g. cyphenothrin) produce a combination of the two syndromes and therefore are not assigned into either of the classifications (Costa, 2015). In mosquitoes, rapid paralysis is caused by prolonged activation of VGSCs which is described as 'knockdown' which increases the risk of mortality in the field due to extra predation while paralysed on the ground (Dong *et al.*, 2014).

Pyrethroids are typically utilized to target adult mosquitoes during host-seeking behaviour (Dattani, Prajapati and Raval, 2009). Natural pyrethrum has been used since the late 19$^{th}$ century for mosquito control either burnt or sprayed as a powder then post World War One the compound was extracted using alcohol or kerosene and used in liquid form. (Gachelin *et al.*, 2018) They are commonly used to impregnate ITNs as the main method of malaria prevention in several African Countries (N'Guessan *et al.*, 2007) as they are relatively harmless to mammals under normal circumstances so are safe to be used in close proximity to humans. They have also been used extensively for indoor residual spraying. Permethrin is a type 1 pyrethroid composed of two stereoisomers, both of which act on sodium channels disrupting neuronal function, causing muscle spasms, paralysis, and death. It is effective by ingestion or contact. Deltamethrin, unlike other pyrethroids, consists of one pure compound. It is a synthetic type II pyrethroid ester which is effective via ingestion and direct contact (Ray, 2005).

#### 1.4.2.5 Neonicotinoid Insecticides

Neonicotinoid insecticides are selective agonists of insect nicotinic acetylcholine receptors (nAChR) in the central nervous system inducing nervous stimulation at low concentrations and at high concentrations receptor blockage, paralysis and death (Han, Tian and Shen, 2018). In both vertebrates and invertebrates, nAChR is a pentameric cys-loop ligand-gated ion channel (Bass *et al.*, 2015), that functions as a major excitatory neurotransmitter receptor. Several potent agonists and antagonists of

nAChR that target insects have been isolated from plants (Millar and Denholm, 2007). Both natural and synthetic chemicals of this class are selectively toxic in insects as they bind more strongly to insect nAChRs than to that of vertebrates (Han, Tian and Shen, 2018). They were initially believed to be favourable to other insecticide classes, as the $LD_{50}$ for some neonicotinoids, imidacloprid and clothiandin, is $1/10000^{th}$ of that of DDT (Goulson, 2013). Neonicotinoids have been predominantly used in agriculture. 60% of neonicotinoids used worldwide and 91% of neonicotinoids used in the UK are used in seed dressings for long term prophylactic protection of crops (Goulson, 2013). Neonicotinoids however were partially banned by the European Union in May 2013 as a result of the high risk to bees and since this ban evidence has accumulated that demonstrates the negative effects on a wide range of organisms by low level persistence of the insecticides in the environment (Wood and Goulson, 2017). Despite this clothianidin is a neonicotinoid insecticide which is recommended by the WHO (WHO, 2018c) and Fludora Fusion (clothianidin and deltamethrin) by Bayer S.A.S. has been prequalified as a product for Indoor residual spraying (IRS) (WHO, 2018a).

#### 1.4.2.6 Insect Growth Regulators / Hormone Mimics

Insect growth regulators (IGRs) are an alternative to directly lethal chemical insecticides which are believed to pose a comparably reduced risk to non-target species (Mian, Dhillon and Dodson, 2017) and are used to target both *Anopheles* and *Aedes* mosquitoes. There are three IGRs which are commonly used for mosquito control. Pyriproxyfen is a juvenile hormone analogue that is an inhibitor of embryogenesis and metamorphosis in several insects which is used in larval habitats to inhibit egg hatching (Suman *et al.*, 2013; Suman, Wang and Gaugler, 2015) and adult emergence or in combination with pyrethroid insecticides on bed nets (Ohashi *et al.*, 2012; Kawada *et al.*, 2014; Aiku, Yates and Rowland, 2006). Methoprene is another juvenile hormone analogue that interferes with midgut remodelling in mosquito pupae following exposure as larvae and prevents adult moulting (Wu *et al.*, 2006) and has similar effects on adults exposed but is not regularly used as an adulticide for mosquito control (Brabant and Dobson, 2013). The final IGR used for mosquito control, diflubenzuron – a benzoyl(phenyl)urea compound, that is only used to target larvae, inhibits chitin

synthase 1 preventing moulting (Douris *et al.*, 2016; Fotakis *et al.*, 2020). Diflubenzuron is primarily a stomach poison in larvae which inhibits chitin production affecting the formation of the exoskeleton, triggering early moulting prior to formation of a complete exoskeleton resulting in larval death. Tolerance typically increases with instar age (Grosscurt, 1978). Juvenile hormone analogue dissemination stations dust adult female mosquitoes with a highly potent larval IGR. These females then 'deliver' the IGR to oviposition sites, resulting in dosing of larval habitats depending on the frequency of visits so targeting the most important breeding sites (Devine *et al.*, 2009). IGRs have great potential but are more expensive to synthesise and poor environmental stability (Singh, Pandher and Sharma, 2013).

### 1.4.3 INSECTICIDE-BASED METHODS FOR MOSQUITO CONTROL

Bed nets treated with insecticide have been used since the mid-20$^{th}$ century but a rapid increase in their distribution of in the early 21$^{st}$ century and development of new and improved generations of nets saw them responsible for over half of the 663 million malaria cases that are predicted to have been averted between 2000 and 2015 (Bhatt *et al.*, 2015). IRS has been used consistently with pyrethrum powder, DDT and now a variety of insecticides from five different insecticide classes which are recommended by the WHO, but at lower distribution levels than has been achieved with bed nets (Oxborough, 2016; WHO, 2018d). So, IRS is only estimated to be responsible for over 10% of those averted cases (Bhatt *et al.*, 2015). Control of *Aedes* mosquitoes tend to centre around community action removing stagnant water sources and treating those that cannot be removed with insecticides and/or space spraying of insecticides targeting swarms in the areas around habitats that cannot be moved (WHO *et al.*, 2017). The use of bed nets and IRS is less effective against *Aedes* mosquitoes due to their tendency to both bite and rest outdoors. Larviciding and outdoor space spraying are commonly used for *Aedes* control as they are most effective given their exophilic and exophagic behaviours (Roiz *et al.*, 2018).

#### 1.4.3.1 Long-Lasting Insecticide Treated Bed Nets (LLINs)

The use of bed nets (fine netting which hangs around the bed to prevent mosquitoes reaching the person sleeping beneath to reduce successful biting) specifically for malaria protection was recommended as early as 1910 by Sir Ronald Ross (Wilson *et al.*, 2020). In the 1970s addition of insecticides to nets (ITNs) was possible as safe synthetic pyrethroids had been developed (Elliott, 1976). From 2000, coverage of ITNs increased dramatically, then in 2007 widespread distribution of a generation of long lasting insecticide treated nets (LLINs) began (Wilson *et al.*, 2020). LLINs are recommended as having a serviceable lifespan of three years, and thus most distribution programmes distribute new nets in three-year cycles. However, substantial loss of fabric integrity (hole formation) of nets has repeatedly been shown to occur within two years in some areas (Kilian *et al.*, 2008; Gnanguenon *et al.*, 2014; Hakizimana *et al.*, 2014; Solomon *et al.*, 2018). Loss of bio efficacy (loss of compound from the net to a level where mosquitoes are no longer readily killed) in less than three years has been observed in some field assessments but not in others (Kilian *et al.*, 2008; Solomon *et al.*, 2018) suggesting that other factors in addition to time and brand of net are having an impact. This has led the WHO to develop guidelines for the assessment of bednet durability in the field (WHO, 2011).

Both ITNs and LLINs provide community protection beyond those individuals sleeping directly underneath a net increasing their effectiveness (Binka, Indome and Smith, 1998; Howard *et al.*, 2000; Hawley *et al.*, 2003). It is estimated that 69% (uncertainty: +4%, -6%) of the 663 million (uncertainty: +4%, -6%) malaria cases averted between 2001 and 2015 (uncertainty interval: 542–753 million) were due to ITNs/LLINs (Cibulskis *et al.*, 2016). However, it has been suggested that the effectiveness of LLINs could be limited by the emergence of insecticide resistance leading to the development of a third generation of bed nets which are impregnated with a long-lasting pyrethroid formation and a second compound, piperonyl butoxide (PBO). PBO is a pesticide synergist which has no direct insecticidal activity but instead increases the effectiveness of pyrethroid compounds through inhibition of the mosquitoes defence mechanisms. Inhibition of cytochrome-P450 enzymes by PBO reduces the detoxification of pyrethroid insecticides (Dadzie *et al.*, 2017). These LLIN-PBO bed nets

have been shown to be more effective than second generation LLINs in areas with mosquito populations that are very resistant to the pyrethroid compounds (Gleave *et al.*, 2021).

#### 1.4.3.2 Indoor Residual Spraying (IRS)

Following blood feeding, mosquitoes need to find a surface to rest upon to digest the blood and permit egg development. IRS targets blood fed mosquitoes by spraying internal walls of buildings (typically homes) with an insecticide formulation to kill resting mosquitoes. *Aedes* mosquitoes typically rest outdoors and so IRS is not widely used for arbovirus control as it is usually ineffectual. Although it has been tested and shown to be effective - but this was a single study (Paredes-Esquivel *et al.*, 2016; Samuel *et al.*, 2017). *Anopheles* mosquitoes (particularly the African malaria vector *An. gambiae*) conversely rest indoors and so IRS is a front-line tool for malaria control and has contributed to the reduction in cases observed this century (Bhatt *et al.*, 2015). Detailed instructions on conducting IRS is published by the WHO along with recommendations of insecticides to use, including at least one compound from each of the four key insecticide classes recommended with minimum residual periods ranging from 2-6 months (WHO, 2015). It has been suggested that use of a non-pyrethroid insecticide (e.g. pirimephos-methyl or chlorfenapyr) for IRS may best complement LLINs use, assuming the population is susceptible to the IRS insecticide, as development of resistance is likely to be slower when using two very different insecticides (Syme *et al.*, 2021). This is because when mosquitoes develop resistance to one of the insecticides there is a good chance that they will be killed by the other insecticide before they have an opportunity to reproduce and pass the resistance phenotype onto the next generation.

#### 1.4.3.3 Outdoor Space Spraying/Fogging

Space spraying or fogging is used primarily in emergency situations for malaria control with high intensity for a short period of time as it is costly to maintain and must be conducted at the peak time of adult activity (dusk for most *Aedes* mosquito vectors) for maximum effect (CDC, 2020b). The process generates fine droplets of insecticide through rapid heating of liquid insecticide that resemble

smoke or fog so temporarily hang in the air and encounter adult mosquitoes. Natural pyrethrum extract, synthetic pyrethroids and malathion are the most commonly used compounds for outdoor spraying for mosquito control (Raghavendra *et al.*, 2011; CDC, 2020c).

#### 1.4.3.4 Larviciding

Larvicides are compounds that are added to water sources that are likely to contain mosquito larvae. Many larvicides typically belong to the organophosphate class and the most employed chemical larvicide is temephos (George *et al.*, 2015) but recently IGR compounds such as pyriproxyfen and diflubenzuron have been employed more often. Control of *Aedes* mosquitoes was conducted historically using Paris Green which was replaced by DDT (McGregor and Connelly, 2021). Organophosphate insecticides were employed following development of DDT resistance (and because of their safety for use in potable water) but their use has declined due to concerns about their impact on non-target organisms (Milam, Farris and Wilhide, 2000) and the emergence of resistance (Bisset *et al.*, 2014).

Larviciding can be effective against malarial mosquitoes if larval habitats can be effectively identified but it is not often used due to the same difficulties identified in the section above on LSM (Antonio-Nkondjio *et al.*, 2018). The effectiveness of larviciding for malaria control could be improved through use of geographic information systems and mapping techniques to identify larval habitats for targeting (Martin *et al.*, 2002; Govoetchan *et al.*, 2014; Stanton *et al.*, 2021). This is important as the WHO have recommended the use of LSM and larviciding as alternative control measures when insecticide resistance is affecting other control measures (WHO, 2012b; WHO, 2013; WHO, 2020).

#### 1.4.3.5 Methods in development/trials

Several other control measures are in the late stages of development and are being prepared for commercialization. Insecticide treated attractive targeted sugar baits (ATSBs) are designed to be more specific than other control measures at targeting mosquitoes only (Fiorenzano, Koehler and Xue, 2017). Mosquitoes must feed on sugar as adults in order to survive (Foster, 1995), ATSBs exploit this

necessity for mosquito control with a lure and kill approach. Insecticides of many different classes have been incorporated into ATSBs alongside attractants and a sugar source and this mix has been added to hanging baits and sprayed on vegetation (Diarra *et al.*, 2021).

Many houses in Africa have open eaves (where the roof meets the house walls). As discussed earlier closing these gaps can reduce the number of mosquitoes found indoors (Ondiba *et al.*, 2018) however, this reduces ventilation which can be uncomfortable in a hot and humid environment. One solution to this is to embed eave tubes with a removable section of electrostatically charged netting which is coated in insecticide formulations (Knols *et al.*, 2016). Eave tubes also work by a lure and kill approach as the heat and odour cues are concentrated to the outdoor end of the tube. As the eave tubes are not interacted with by humans or non-target organisms in the same way LLINs, IRS or larval habitats are, so higher insecticide concentrations and different classes can be incorporated to overcome certain resistance mechanisms in local mosquitoes (Andriessen *et al.*, 2015). Despite evidence of effectiveness, this method has not yet been widely implemented (Sternberg *et al.*, 2021).

## 1.5 CHALLENGES TO VECTOR CONTROL

When organisms face stressful situations, they must adapt or they risk population decline or in extreme situations becoming extinct. Mosquitoes have been shown to have remarkable adaptation abilities which enable their survival in hugely variable environments (Sokhna, Ndiath and Rogier, 2013). This evolution can have severe negative impacts on our ability to control mosquitoes as they respond to the control measures that are implemented, particularly insecticides, and a changing environment influenced by climate change and urbanisation. The large population size and short generation time in sexual insect populations results in high levels of genetic variation which facilitates rapid adaption to stresses (e.g. insecticides and climate variations) (Hoffmann, 2017).

### 1.5.1 INSECTICIDE RESISTANCE

Insecticide resistance represents a measurable reduction in susceptibility of a population resulting from a heritable genetic change (Zalucki and Furlong, 2017). Resistance is acquired through changes to the genome sequence (e.g. point mutations, copy number variation) which affect the activity or binding of related proteins or in altered expression of the target-site or detoxifying enzymes which changes the efficiency of target-site binding, metabolism, sequestering of the insecticide or physiological changes which restrict access to the target-site (Fouet, Atkinson and Kamdem, 2018). It has also been suggested that behavioural changes may be associated with resistance however a hereditary association between behaviour and resistance has not yet been established (Zalucki and Furlong, 2017).

It had been thought that removal of an insecticide would decrease the resistance in the population as the fitness cost of resistance would negatively select against resistance but although it is well understood that repeated selection of laboratory mosquitoes is required to retain resistance mechanisms, the same clear phenotype has not been well characterised in the field (Ffrench-Constant and Bass, 2017). This could be due to cross-resistance between insecticidal compounds, the fact that insecticides are based on natural compounds which may still be present in the environment or that cross-resistance can occur between insecticides and thermal stress (Hoffmann, 2017) all of which may maintain the mechanism in the environment. It is rare for insect pests to resist a single compound as resistance mechanisms commonly provide protection against chemicals of the same class or with similar modes of action and can also – though with less predictability – affect other classes, for example through detoxifying enzyme action (Bass *et al.*, 2015). This is particularly concerning as only a limited number of insecticides are approved for use for vector control (Hemingway *et al.*, 2006).

#### 1.5.1.1 Metabolic Resistance Mechanisms

Detoxification enzymes that metabolise or sequester toxic compounds can confer resistance when up regulated (or duplicated) or if mutations are present which increase their activity against the compound. There are three key superfamilies of detoxification enzymes that are thought to contribute to metabolic resistance: cytochrome P450s (CYPs), glutathione-S-transferases (GSTs) and carboxylesterases (CCEs) (Ranson *et al.*, 2002). Although, there are other proteins which are implicated in resistance that do not belong to these families (e.g. SAP2) (Ingham *et al.*, 2020).

CYPs are a very large enzyme super family present in a wide range of tissues in many organisms playing an important role in many biosynthetic pathways, but CYPs in the subfamilies CYP4, CYP6 and CYP9 families are thought to be of particular importance to *Aedes* and *Anopheles* pyrethroid and carbamate resistance (David *et al.*, 2013). Resistance is believed to occur primarily as a result of increased mRNA production from these genes through transcriptional regulation and/or copy number variation (CNV) increasing the level of ring hydroxylation and/or excretion of insecticides (Ranson *et al.*, 2002). In mosquitoes CYPs have been most strongly and consistently linked with pyrethroid resistance though also in some cases to carbamate and DDT resistance (Vontas, Katsavou and Mavridis, 2020). *Ag*CYP6P3, *Ag*CYP6M2 and *Ag*CYP9K1 are the most widely detected CYPs in *An. gambiae* to be upregulated in resistant populations and *Af*CYP6P9 and *Af*CYP6P4 are the orthologues/paralogue in *An. funestus* (Vontas, Katsavou and Mavridis, 2020). Detection of CYPs believed to impact resistance in *Ae. aegypti* has been more variable but *Aaeg*CYP9J28 and *Aaeg*CYP6BB2 were the most consistently identified (Moyes *et al.*, 2017). Additionally, CYPs are thought to confer negative cross resistance through activation of some pro-insecticides such as organophosphates increasing the susceptibility to these compounds which could be very important in an integrated management programme involving insecticide rotation (Vontas, Katsavou and Mavridis, 2020).

GSTs which have been implicated in pyrethroid and DDT resistance in *Ae. aegypti, An. gambiae* and *An. funestus* mosquitoes, tend to belong to subfamilies delta (d) and epsilon (e) (Ranson *et al.*, 2002;

Ayres *et al.*, 2011). Most work thus far has been conducted on GSTe2 (Daborn *et al.*, 2012; Riveron *et al.*, 2017; Adolfi *et al.*, 2019; Menze *et al.*, 2020) which is considered to have a key role in DDT (Mitchell *et al.*, 2014), pyrethroid (Menze *et al.*, 2020) and more recently temephos (Helvecio *et al.*, 2020) resistance. But as GSTe2 is often duplicated as part of a large GST cluster several other GST genes are co-upregulated and may also be contributing to resistance phenotypes (Kouamo *et al.*, 2021). There are two key SNPs found in both *An. funestus* (L119F and I114T) and *An. gambiae* (L120F and I114T) species which increase activity against DDT increasing resistance (Riveron *et al.*, 2014).

OPs are tertiary esters and thus are susceptible to hydrolytic degradation mediated by a range of esterases and therefore OPs do not persist in the environment (Fukuto, 1990). Carboxylesterases (CCE) hydrolyse carboxylic esters and are grouped into α and β esterases depending on if they are not or are inhibited by paraoxon respectively (Hemingway and Karunaratne, 1998). CCEae3A and CCEae6A have been identified as overexpressed (including through CNV) in temephos resistant *Ae. aegypti* and *Ae. albopictus* (Poupardin *et al.*, 2014; Grigoraki *et al.*, 2015; Grigoraki *et al.*, 2016; Grigoraki *et al.*, 2017a; Seixas *et al.*, 2017; Marcombe *et al.*, 2019). CCE involvement has been implicated in *An. sinensis* that were resistant to DDT, deltamethrin and malathion but no individual CCE genes have been identified as candidates for resistance yet (Chen *et al.*, 2019).

Apart from the metabolic enzymes, sensory appendage proteins (SAPs) have also recently been indentified as having a role in conferring pyrethroid resistance. SAPs are a group of small (10 - 30 kDa) soluble chemosensory proteins (CSP) only found in arthropods (Vieira and Rozas, 2011) which have been found to be overexpressed in pyrethroid resistant *An. gambiae* populations (with low PBO synergism) from Côte d'Ivoire and Burkina Faso (Edi *et al.*, 2014; Toe *et al.*, 2018). Four of *An. gambiae*'s eight CSP genes can bind aromatic compounds *in vitro* (Iovinella *et al.*, 2013), including sensory appendage protein 2 (SAP2) (AGAP008052) which has been shown to bind to three pyrethroids (permethrin, deltamethrin and α-cypermethrin) but not to pirimiphos methyl or bendiocarb (Ingham *et al.*, 2020). Upregulation of SAP2 by transgenic overexpression in adult *An. gambiae*

mosquitoes has been shown to confer pyrethroid resistance but is believed to act in combination with other mechanisms (Ingham *et al.*, 2020).

#### 1.5.1.2 Target-site Resistance Mechanisms

Mutations in a gene, encoding a protein that is ordinarily bound by the insecticide, which reduce the binding affinity of insecticides are called target site mutations. Target site mutations can confer resistance alone or in combination with CNV of the target site gene. Resistance gene and DNA marker discovery has been dominated by quantitative trait locus (QTL) and candidate gene studies of laboratory strains, however as the availability of genome sequence data increases and the cost of genome wide association studies (GWAS) decreases, the ability to examine field strains improves (Donnelly, Isaacs and Weetman, 2016; Weetman *et al.*, 2018; Weedall *et al.*, 2020).

As mentioned above, *vgsc* are the target for pyrethroid and carbamate insecticides. Several different amino acid substitutions have been identified as conferring resistance including these in: *An. gambiae* - L1014F, L1014S and N1575Y (Silva, Santos and Martins, 2014); and *Ae. aegypti* – V1016G, V1016I and F1534C (Du *et al.*, 2016). These mutations are described as conferring knockdown resistance (*kdr*) as they prevent the rapid paralysis causing knockdown and regularly co-occur resulting in stronger resistance phenotypes. The *Ag*L1014F mutation has been validated as conferring resistance and has demonstrated a combined effect on resistance with GSTe2 (Grigoraki *et al.*, 2021).

Diflubenzuron, which targets chitin synthase 1 (CHS1), is an important larvicide in the control of the West Nile virus vector, *Culex* mosquitoes in Europe but high levels of resistance have been detected which threatens to impact mosquito control (Grigoraki *et al.*, 2017b). Resistance to diflubenzuron, first detected in 2015 in Italy, has been associated with two target site mutations (I1042M and I1043L) in the chitin synthase 1 gene which have been confirmed to confer resistance using CRISPR-Cas9 engineered *D. melanogaster* (Fotakis *et al.*, 2020).

In mosquitoes, ACE1, the target-site for the OP and carbamate classes of insecticides, is encoded by the *ace1* gene. There are two key mechanisms of resistance involving a*ce1* that are found in

*Anopheles* mosquitoes: a single nucleotide polymorphism (SNP) near the active site of ACE1 which alters the shape of the binding pocket (Essandoh, Yawson and Weetman, 2013); and CNV which often co-segregate with the SNP (Weetman *et al.*, 2015). The mutation which is most common in *Anopheles* mosquitoes is a serine substitution for a glycine at codon 280 (G280S) (Cheung *et al.*, 2018). The G280S mutation is also referred to as G119S as when the mutation was identified in *Anopheles* it was named based on the electric ray *Torpedo californica* partial crystal structure (Greenblatt *et al.*, 2004). In this thesis it will be referred to as G280S. *Aedes* mosquitoes have only been found to possess a mutation in *ace1* that confer insecticide resistance once previously (Muthusamy and Shivakumar, 2015).

The second mechanism, CNV, often co-occurs with the G280S point mutation as it is thought to increase the resistance conferred (Assogba *et al.*, 2016) or reduce the fitness cost of the mutation (Assogba *et al.*, 2015). An analysis of the *Anopheles* 1000 genomes (Ag1000) data indicated presence of up to 10 copies of *ace1* in an individual and that there was a significant correlation of large copy number and homozygote 280S individuals. Individuals were not detected as 280S homozygotes with fewer than 7 copies (Grau-Bové *et al.*, 2021) which indicates that a fitness cost is present that is counteracted by the increase in the number of copies.

#### 1.5.1.3 Physiological Resistance Mechanisms

##### *1.5.1.3.1 Cuticular Thickening/Composition*

A mechanism of resistance that often circumvents drug action is reduced access to the target site due to changes in the physiology of the target organism, although there has only been a handful of examples of physiological changes conferring insecticide resistance (Bass and Jones, 2016). These changes have been associated with thickening and altered composition of the insect cuticle through increased deposition of cuticular hydrocarbons (CHCs) (Balabanidou, Grigoraki and Vontas, 2018).

The cuticle is the first protective barrier that protects the insect from external compounds and changes can occur which confer increased resistance to insecticide (Balabanidou, Grigoraki and Vontas, 2018).

These changes reduce penetration of insecticide through the cuticle and allow more time for detoxification enzymes and transporters to act thus reducing the number of molecules which reach their targets (Balabanidou, Grigoraki and Vontas, 2018). The role of ATP-binding-cassette (ABC) transporters in resistance is not yet clear though they have been shown to directly efflux insecticides (Gott *et al.*, 2017) and upregulation of ABC transporters has been implicated in cuticular resistance through increased transport of CHCs through the epidermis potentially impacting not only thickness but also composition of the cuticle (Balabanidou, Grigoraki and Vontas, 2018).

#### *1.5.1.3.2 Microbiome*

A further physiological change which has been proposed to impact insecticide resistance is variations in the mosquito microbiota (Dada *et al.*, 2018; Barnard *et al.*, 2019; Arévalo-Cortés *et al.*, 2020; Muturi *et al.*, 2021; Wang *et al.*, 2021). The mosquito microbiome is diverse and highly variable between species, subpopulations, sex, stages and tissues and is affected by location and both larval and adult environments (Minard, Mavingui and Moro, 2013). The approaches depending on culturing bacterial isolates, which had been relied upon to study mosquito microbiota until this decade, struggle to reflect the environment of the insect body and thus limits the detection of and makes accurate quantification of different species presence difficult (Dillon and Dillon, 2004). Methods which do not require microbiota culture (e.g., 16S ribosomal RNA gene and genome sequencing), have been adopted more recently which has improved our ability to study the role of the microbiota in insecticide resistance. Our understanding is still very limited as these methods, although improved, do not fully represent the complex interactions of insect microbiota (Minard, Mavingui and Moro, 2013; Berg *et al.*, 2020). Initial findings from whole genome sequencing studies in *An. albimanus* suggest that there is an association between insecticide resistance and variations in the composition of adult microbiota, including increased detection of bacterial species that are capable of xenobiotic degradation of organophosphates (Dada *et al.*, 2018). It has also been found using 16S ribosomal RNA gene sequencing that exposure to pyrethroids can alter surface microbiomes in *An. albimanus,* potentially selecting for bacteria which metabolize insecticides (Dada *et al.*, 2019). 16S ribosomal

RNA gene sequencing of *An. gambiae* adults from Western Kenya provided further evidence of a role of increased quantity of certain bacteria in pyrethroid resistance that are known to degrade pyrethroids (Omoke *et al.*, 2021).

#### 1.5.1.4 Behavioural Resistance Mechanisms

Behavioural resistance was defined by Sparks in 1989, as an evolved behaviour that reduces the insects exposure to toxic compounds or allow it to survive in what would otherwise be a fatal environment (Sparks *et al.*, 1989). However, in 2017, Zalucki and Furlong suggest that people conflate behavioural avoidance, sub-lethal effects and effects on learning and neurophysiology post insecticide exposure with true behavioural resistance, which they argue must involve a heritable change which decreases an insect's susceptibility (Zalucki and Furlong, 2017). For a number of *Anopheles* species, changing behavioural traits have been observed in response to significant implementation of insecticide treated bed nets (Sokhna, Ndiath and Rogier, 2013). *An. gambiae* have been shown to exhibit new exophilic behaviour (Githeko *et al.*, 1996) and a trophic deviation from humans to other animals (Lefèvre *et al.*, 2009; Kreppel *et al.*, 2020) both predicted to be as a result of LLIN implementation reducing their ability to bite humans while they sleep. Also changes in biting time result in transmission in early evening before people move inside and are protected by a bed net (Thomsen *et al.*, 2017). As a result of this adaption, malaria transmission has continued despite net distribution in these areas (Sokhna, Ndiath and Rogier, 2013) and there is a need to develop new control measures to address these behavioural changes (Sougoufara, Ottih and Tripet, 2020).

### 1.5.2 URBANIZATION AND THE NEED FOR VECTOR CONTROL

Urbanization brings multidimensional challenges and is an important factor to consider when tackling vector borne diseases as migration from rural areas (initially people seeking education and employment opportunities) has resulted in unplanned and uncontrollable growth of slums which outpaces city infrastructure development (sanitation and urban planning) (Costa *et al.*, 2017). While urbanization provides improved opportunity to reduce the burden of most infectious diseases through

vaccination programs and interventions, there has been no reduction in the burden of vector-borne and zoonotic diseases, with slum populations disproportionately afflicted (Costa *et al.*, 2017).

Expansion of slums often enhances degradation of the environment resulting in establishment of conditions favoring expansion of *Ae. aegypti* populations resulting in increased transmission of arboviruses. This is exacerbated since concomitant human overcrowding and high density of mosquitoes increases human-mosquito contact thus facilitating viral-transmission (Costa *et al.*, 2017). Behavioural changes as a result of increased levels of artificial light has been shown to increase nocturnal blood feeding in *Ae. aegypti* which is thought to have implications for arbovirus transmission (Rund *et al.*, 2020).

In Africa, urban agriculture has developed, to increase food supplies for growing cities, which is irrigated to sustain production year-round. These simple, informal irrigation systems can create 'rural spots' of breeding sites for malaria vectors in urban areas that cause an increase in the entomological inoculation rate (number of infective bites per person per unit time) compared to similar urban areas without irrigated agriculture thus increasing malaria incidence (Afrane *et al.*, 2004). For many years, pyrethroids were not commonly used in agriculture due to their instability in the environment (Elliott, 2006) however because they are cheap and are lethal to a broad range of insect pests, pyrethroids are now the dominant insecticide used in the agriculture industry (Sereda and Meinhardt, 2005; Dewar, 2016; Philbert, Lyantagaye and Nkwengulila, 2019). The cost of pyrethroids has been driven down by the competitiveness of the market, thus decreasing the price of food (Dewar, 2016). However, this has led to vast over usage in agriculture resulting in spill over into mosquito habitats where sublethal exposures are thought to exert strong selection pressures on and ultimately drive resistance spread in mosquito populations (Dewar, 2016; Matowo *et al.*, 2020).

### 1.5.3 CLIMATE CHANGE

The geographical range of mosquitoes and the associated pathogens are restricted by temperature thresholds limiting the life span of the mosquito vector, the rate of viral replication and parasite maturation all of which increase with rising temperatures up to a certain limit. The faster the

development of the pathogen the greater the probability that it will reach a transmissible stage while the vector is still alive and able to bite a new host (Epstein, 2001b). Increasing temperatures in areas previously unsuitable for mosquito survival or for disease transmission favours their spread north (Epstein, 2001a). The 10°C winter isotherm restricts the range of *Ae. aegypti* and thus the geographical distribution of yellow and dengue fever viruses as *Aedes* eggs larvae and adults are susceptible to freezing. *P. falciparum* malaria transmission only occurs where temperatures exceed 16°C as below these temperatures Anopheline mosquitoes do not live long enough to permit maturation of parasites and subsequent transmission.

### 1.5.4 DETECTING INSECTICIDE RESISTANCE

To improve our understanding of insecticide resistance in mosquitoes we must first identify mosquitoes that we believe to have reduced susceptibility for further analysis. Insecticide resistance is currently detected though exposure of adults or larvae to a diagnostic dose or range of concentrations of the insecticide in question and manual counting of mortality rate.

#### 1.5.4.1 Adult Insecticide Susceptibility Assays

The most commonly used assay currently for assessing adult insecticide sensitivity is the WHO Tube assay, which is typically conducted using a diagnostic dose of insecticide applied to paper lining a plastic tube in which the mosquitoes are exposed (WHO and Global Malaria Programme, 2018). CDC bottle assays (CDC, 2021b) or tarsal assays (Lees *et al.*, 2019) are usually used to conduct dose-response assays on adults mosquitoes and involve coating glass bottles or plates respectively with insecticides dissolved in a solvent which can then be allowed to evaporate leaving the compound behind. Another assay which is used to assess adult resistance are 'cone tests', which use a polyvinyl chloride (PVC) cone pressed against a treated surface - usually a wall or a section of insecticide treated bed net (WHO, 2006b; Allossogbe *et al.*, 2017).

In all of these assays (except for the CDC bottle assay), adult mosquitoes are exposed to insecticide for a set exposure time, after which the number of adults knocked down (unable to stand or take off)

is noted immediately post-exposure and mortality is counted after 24 or more hours recovery with an available sugar source (Alout *et al.*, 2017). In the CDC bottle assay mosquitoes are exposed continuously for 24 hours at the end of which mortality is recorded (CDC, 2021b). Additionally in all of the above assays, synergists such as piperonyl butoxide (PBO), S,S,S-tributyl phosphorotrithioate (DEF) and diethyl maleate (DEM), which inhibit detoxification enzymes (cytochrome p450s, esterase's and glutathione-S-transferases respectively), can be added to gain some insight into the possible gene superfamilies responsible for resistance (Pasay *et al.*, 2009; Nwane *et al.*, 2013).

#### 1.5.4.2 WHO Larval Assay

Until recently the main method of assessing larval resistance to insecticides was the WHO larval assay (WHO, 2005). In this traditional assay, larvae are added into ~200 mL water containing insecticide (with several pots containing different insecticide concentrations) then after 24 h exposure, the binary outcome variable, mortality, is assessed. Conducting larval assays like this have the disadvantages of being labour intensive, low-throughput and subject to investigator bias. Thus, a novel assay has recently been developed which aims to tackle these shortcomings, which should enhance our ability to study larval insecticide resistance.

#### 1.5.4.3 The Invertebrate Automated Phenotyping Platform (INVAPP)

The Invertebrate Automated Phenotyping Platform (INVAPP) depicted in Figure 1.5.1 from Partridge *et al*., 2018, captures movies of moving larvae or worms and using an algorithm measures motility. The apparatus consists of an Andor Neo camera and LED array and acrylic diffuser illumination (Figure 1.5.1). INVAPP has been used with a 'Paragon' algorithm to examine parasitic nematode susceptibility to known anthelmintics and to screen nematodes against a 'Pathogen Box Library' using motility measurements, calculated based on pixel variation in movies, to identify compounds which killed nematodes. The platform was integral in the identification of 14 previously undescribed anthelmintics (Partridge *et al.*, 2018). Although mosquito larvae are larger than the nematodes tested previously, it is reasonable to think that this system could be optimised to measure larval motility and

subsequently used to study insecticide susceptibility. In this thesis, the capability of the INVAPP system, and more particularly the software for statistical analysis of INVAPP outputs, was examined during high-throughput analysis of insecticide resistance.

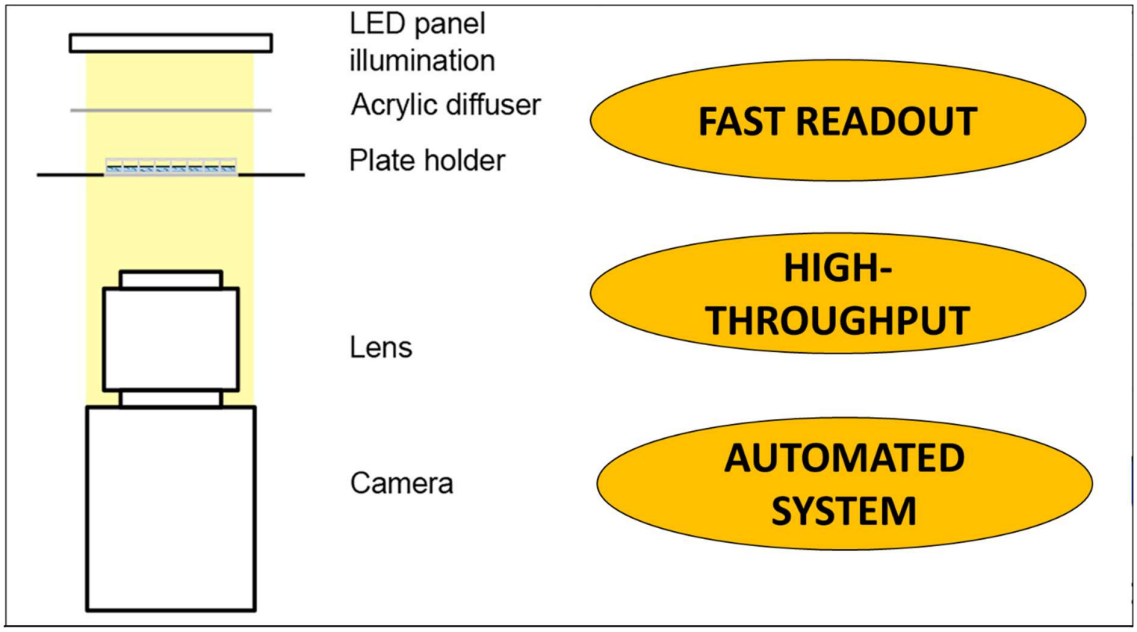


Figure 1.5.1: A schematic representation of the Invertebrate Automated Phenotyping Platform (INVAPP) and the expected benefits of the system (Partridge et al., 2018).

### 1.5.5 Validating Molecular Markers of Insecticide Resistance

Understanding the molecular mechanisms conferring insecticide resistance and identifying cross resistance is important to inform new strategies for combatting the spread of resistance genes and future insecticide development (Donnelly, Isaacs and Weetman, 2016). Insecticide resistance is not exclusively determined by the genome sequence of an individual mosquito. It is influenced by a range of factors including: larval habitat conditions; temperature; humidity and age (Ranson and Lissenden, 2016). Sensitivity to insecticides typically increases with age in adults (Alout *et al.*, 2017; Mbepera *et al.*, 2017). This has implications on malaria transmission, as older females are responsible for infections (as sporogony, *Plasmodium* development in the mosquito, takes around 10-days and the mosquito requires 3 days to mature and mate prior to finding its first bloodmeal) (Alout *et al.*, 2017). Thus although resistant mosquitoes often die later in life (when natural tolerance has declined), if this

is prior to successful development and transmission of the parasite, it is possible that in this population malaria transmission will reduce (Alout *et al.*, 2017). This variability must be considered - and controlled for as much as possible - when assessing the susceptibility of mosquitoes using bioassays. High variability resulting from differences in the age, rearing conditions (e.g. larval density, larval nutrition (Owusu, Chitnis and Müller, 2017), microbiome (Dada *et al.*, 2018; Barnard *et al.*, 2019; Arévalo-Cortés *et al.*, 2020; Wang *et al.*, 2021)) and experimental conditions (e.g. assay selection (Owusu *et al.*, 2015), density of mosquitoes in tube/pot, time of day) can make significant trends difficult to detect (Ranson and Lissenden, 2016). Most of these factors can be controlled for through inclusion of appropriate controls that have been reared in parallel with mosquitoes being tested taking care to treat all groups the same.

Confounding factors are more difficult to address when selection of appropriate control strains is not possible. This problem arises particularly during assessment of field mosquitoes in areas where insecticide resistance has been present for a long time and a susceptible strain of the same species from the same or a similar location is not available or has been reared in the laboratory for a long time. The choice of different susceptible laboratory strains as controls for field mosquitoes can result in different estimations of resistance and also in inaccurate identification of potential resistance markers (Owusu *et al.*, 2015).

One approach to identify potential resistance markers in resistant field populations is to use a variety of genomic, transcriptomic, proteomic or metabolomic analyses (using the best control strains available), then investigate and validate those potential candidates using back-crossing or laboratory selection . Back-crossing (mating resistance mosquitoes to a susceptible strain and examining changes in phenotype/genotype) and laboratory selections (exposing each generation to a sub-lethal dose of insecticide and maintaining the strain using the individuals which survive and looking at changes in phenotypes and genotypes) are useful techniques and can provide some insight into the mechanisms driving resistance.

A major drawback to these approaches is that the genomic or transcriptomic data can be difficult to interpret correctly as often many changes occur which are large, coincidental, do not directly confer

resistance or work in combination to confer meaningful resistance. Additionally, when assessing gene expression data the reliance on quantification of up or downregulation of genes is likely causing the scientific field to neglect very small changes in expression of very important genes or genes expressed at low levels (Feder and Walser, 2005; Evans, 2015). Back crossing and laboratory selections can add supporting evidence to the role of a protein in insecticide resistance but investigating the modification in isolation using transgenic methods is the best method to directly assess the physiological function as it is possible to make a single change in an otherwise susceptible background without the coinheritance of other potential mechanisms. Validation of mechanisms in isolation using transgenic methods is commonly achieved through silencing, mutating or overexpressing the gene of interest *in vivo* and observation of resulting phenotypes (Donnelly, Isaacs and Weetman, 2016).

#### 1.5.5.1 Genetic Modification methods

##### *1.5.5.1.1 RNA interference (RNAi)*

RNAi is a natural control mechanism in most eukaryotic cells and some bacteria, to control gene activity, which has been developed into a versatile method for loss of function analysis in many organisms including mosquitoes (Lycett *et al.*, 2006). Cells produce double stranded RNAs (dsRNA) which are cleaved by the enzyme Dicer to short interfering RNAs (siRNA), or microRNAs with sequences of ~21 bp that are complementary to the mRNA of the gene to be downregulated. siRNAs and microRNAs are recognized by the RNA-induced silencing complex (RISC) and then bind to the mRNA to which they have complementarity directing the Argonaute enzyme within the RISC to cleave the mRNA prior to its processing into protein. This mechanism can be hijacked to reduce the expression of genes of interest through introduction (through injection or forced expression by genetic modification of the genome) of dsRNAs or short hairpin RNAs (shRNA) which are processed by the RNAi machinery.

RNAi analysis of mosquitoes is possible through injection of individuals with dsRNA or siRNA into the mosquito without generation of a genetically modified strain. Doing this is particularly useful for

preliminary experiments, assessment of genes with severe fitness costs or lethal phenotypes, or knockdown of multiple genes simultaneously. However, injections must be conducted for every experimental individual and the level of knockdown can vary depending on the skill of the injector and the site of endogenous gene expression. In spite of this, the approach is regularly used in adult mosquitoes and has been used successfully in embryos (Krzywinska *et al.*, 2016) and pupae (Du *et al.*, 2017) but it is not very successful in larval stages as they do not recover well following injection (Adolfi and Lycett, 2019). An alternative approach using RNAi that permits loss of function analysis in larvae is the generation of transgenic mosquitoes which express mRNA that form short hairpin RNAs with sequences complementary to the gene of interest. This can be used in a bipartite GAL4-UAS system, particularly for knockdown of essential genes (Lynd *et al.*, 2019; Grigoraki *et al.*, 2020; Poulton *et al.*, 2021).

#### *1.5.5.1.2 GAL4-UAS*

The GAL4-UAS system has been used routinely in *Drosophila* with great success proving a powerful functional genomics tool for study of phenotypes through mis- or over-expression and can also be used for stable gene knockdown (when combined with RNAi) and enhancer detection (Lynd and Lycett, 2012; Poulton *et al.*, 2021). Two transgenic lines are generated for the bi-partite GAL4-UAS approach, a driver line and a responder line carrying the yeast transactivator, GAL4, under the control of a specific regulatory region and a candidate gene transcriptionally controlled by GAL4 binding sites, known as upstream activation sequences (UAS) respectively (Figure 1.5.2). As a GAL4 equivalent is not present in most species, the candidate gene or RNAi construct is not expressed in the responder line. The GAL4 and UAS lines are crossed and only the progeny of these crosses where GAL4 and UAS transgenes are brought together in the same genome express the candidate gene or RNAi construct in the temporal and spatial pattern dictated by the promotor which drives GAL4 expression. Each cassette contains a fluorescent marker (typically a variant of GFP) which is used to identify organisms containing the cassette(s). The GAL4 and UAS cassettes typically are produced with different markers to allow the differentiation of organisms containing both cassettes.

One of the benefits of the GAL4-UAS system is the ability to generate banks of driver and UAS lines which can be crossed to investigate different genes expressed in different locations without having to make a new genetically modified line for each combination. Driver lines expressing GAL4 controlled by different promoters are available in the Lycett group: Gareth – Oenocyte_enhancer-GAL4 (Lynd and Lycett, 2012); hml – hemocyte_specific_promoter-GAL4 (Pondeville *et al.*, 2020); F and Dgl – carboxylpeptidase_promoter-GFY-GAL4 (Lycett, Amenya and Lynd, 2011). These lines were generated by *piggybac* integration, in which a mobile genetic element, the *piggybac* transposon, and transposase facilitate integration of fragments of DNA sequence, which are flanked by inverted terminal repeats, at TTAA sites which are dispersed at random throughout the genome. Docking lines are used with ϕC31 integrase to generate new UAS lines. A docking line (A11) and a docking-driver line (Ubi-GAL4) have been generated with attP sites for ϕC31 integration using *piggybac* to insert the cassettes. Using ϕC31 integration the cassettes of these docking lines were exchanged to create UAS transgenic lines capable of overexpressing or with RNAi hairpin constructs for knockdown of candidate metabolic resistance genes (Adolfi *et al.*, 2019; Lees *et al.*, 2020; Ingham *et al.*, 2020; Lynd *et al.*, 2019) (Lynd *et al.*, 2019) have been generated by the Lycett group and adult insecticide susceptibility assessed. Many of these overexpressing lines have been utilised in this PhD project to analyse the INVAPP approach in order to determine to what extent the same enzymes could confer insecticide resistance to larvae, as described in Chapter 3.

When conducting ϕC31 mediated cassette exchange, the new cassette usually replaces the existing cassette, however on rare occasions the new cassette instead integrates beside the existing cassette. When this occurs in the Ubi-GAL4 driver/docking line, new strains which constantly express the UAS transgene are generated as the UAS and GAL4 cassettes are present on the same chromosome. This is sometimes a problem if expression of the transgene results in severe fitness costs, however, if this is not the case these lines can be very useful. For example, these lines can be crossed with other lines (Grigoraki *et al.*, 2021) or other UAS lines to achieve dual gene expression or permit (though limited) analysis of different levels of expression through comparison of homozygote and heterozygote strains.

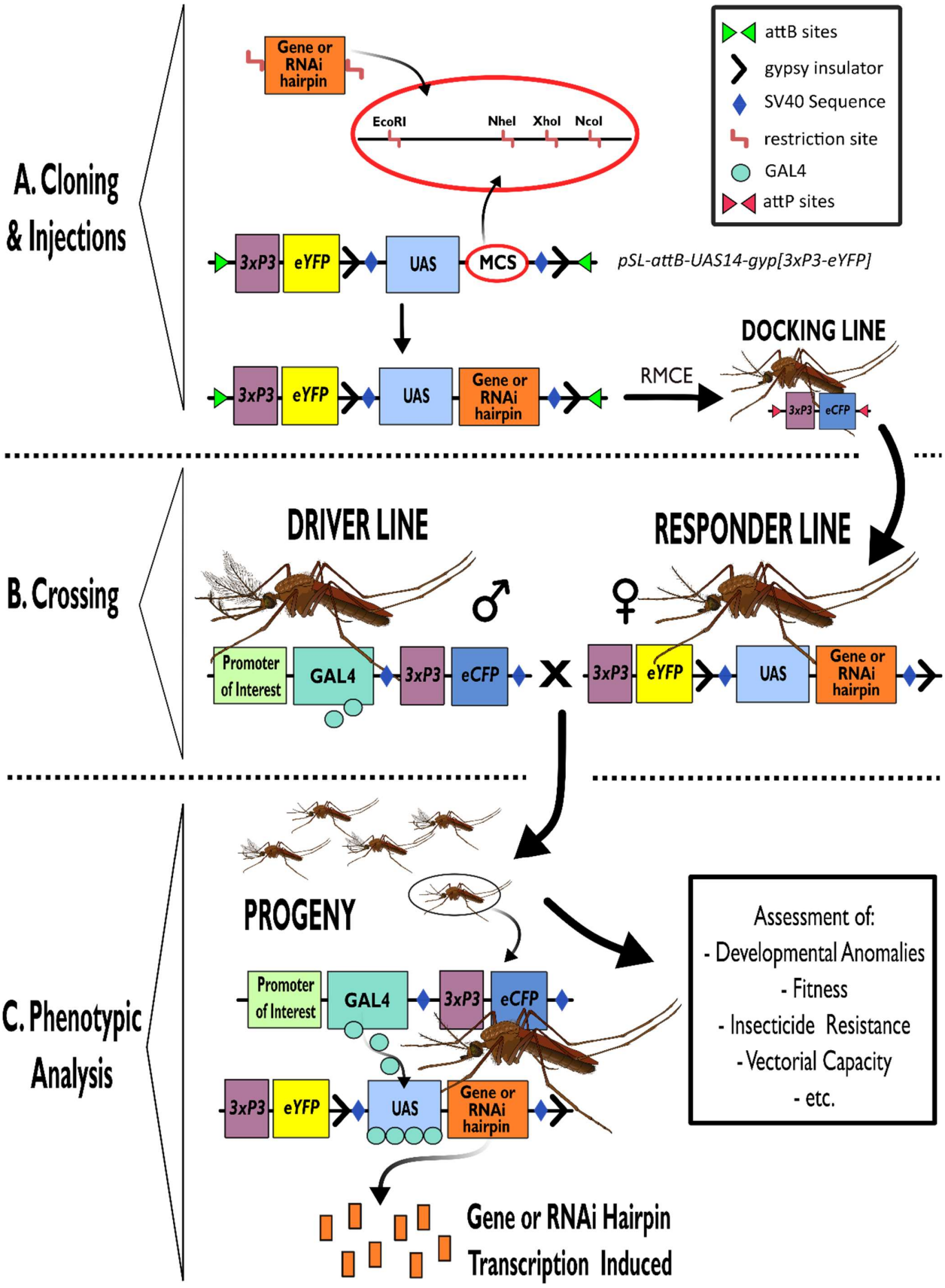
A. Cloning & Injections
Gene or RNAi hairpin
EcoRI
NheI
XhoI
NcoI
attB sites
gypsy insulator
SV40 Sequence
restriction site
GAL4
attP sites
3xP3
eYFP
UAS
MCS
pSL-attB-UAS14-gyp[3xP3-eYFP]
Gene or RNAi hairpin
RMCE
DOCKING LINE
3xP3
eCFP
B. Crossing
DRIVER LINE
RESPONDER LINE
♂
♀
Promoter of Interest
GAL4
3xP3
eCFP
X
3xP3
eYFP
UAS
Gene or RNAi hairpin
C. Phenotypic Analysis
PROGENY
Promoter of Interest
GAL4
3xP3
eCFP
3xP3
eYFP
UAS
Gene or RNAi hairpin
Assessment of:
- Developmental Anomalies
- Fitness
- Insecticide Resistance
- Vectorial Capacity
- etc.
Gene or RNAi Hairpin
Transcription Induced

Figure 1.5.2: Diagrammatic representation of the GAL4-UAS system generation, crossing strategy and phenotypic analysis from (Poulton et al., 2021)

#### 1.5.5.2 Delivery Methods

All transgenic approaches require delivery of plasmid, protein, ribonucleo-protein or viral components into germline cells. This can be achieved via traditional embryonic microinjection (Jasinskiene, Juhn and James, 2007) or the newer strategy of adult ovary injection, ReMOT Control (Receptor-Mediated Ovary Transduction of Cargo), which has been optimised for some CRISPR-Cas9 based indel production, but could also be applicable for other strategies in the future (Chaverra-Rodriguez *et al.*, 2018).

#### 1.5.5.3 Genome editing technology

Historically, transposon-based methods (e.g., *piggyBac*) were used to modify the mosquito genome though their random insertion at TTAA sites (predicted frequency ~ 1 in 256 bp) is problematic due to the position effect (variable expression depending on location of insertion) and potential undesired coding sequence disruption (Ding *et al.*, 2005; Wilson, Coates and George, 2007; Ivics and Izsvák, 2010). This was addressed to some extent by combining transposon-based insertion of target sites for site-directed nucleases (e.g., ϕC31). For example, *piggyBac* has been used to insert a cassette with a marker gene flanked by recombinase docking (attP) sites, in several different genomic locations then each site was evaluated for marker expression and to confirm that the insertion does not disrupt genes of importance or cause significant fitness costs (Adolfi *et al.*, 2018; Lynd *et al.*, 2019). New lines can then be created with insertions at the same genomic locus by injecting a source of ϕC31 enzyme (for catalysis) and a donor plasmid carrying the desired insertion flanked by donor (attB) sites into a stable attP docking strain. The new DNA construct inserts in place of (or beside) the original transgene (Adolfi and Lycett, 2019; Adolfi *et al.*, 2021). This approach permits the generation of many lines with fixed position effect but is limited if the genomic locus of insertion has to be generated randomly (Adolfi *et al.*, 2021).

The field of genetic modification is developing rapidly with major discoveries, such as the use of CRISPR-Cas9 for gene editing, having only been made in the last 10 years (Jinek *et al.*, 2012). This method has permitted such huge strides in the field that its creators were awarded the 2021 Nobel Prize in Chemistry (NobelPrize.org, 2021). CRISPR-Cas9 is derived from a natural bacterial defence mechanism for protection against bacteriophage that has been adapted as a genetic modification tool. The development and rapid expansion of CRISPR-Cas9 gene editing combined with increased availability of whole genome sequences for the major mosquito vectors of human diseases as well as established delivery methods have reduced reliance on model organisms such as *D. melanogaster* when characterising mosquito genes using transgenic approaches (Daborn *et al.*, 2012; Mitchell *et al.*, 2012; Riveron *et al.*, 2013; Riveron *et al.*, 2014; Yunta *et al.*, 2019; Matthews and Vosshall, 2020).

These advances permitted publication of CRISPR-Cas9 gene knockout in *Ae. aegypti* (Kistler, Vosshall and Matthews, 2015) within only two years of that in *D. melanogaster* (Bassett *et al.*, 2013) compared to a difference of 18 years (2011 and 1993 respectively) for use of the GAL4-UAS system (Brand and Perimon, 1993; Kokoza and Raikhel, 2011) which meant that many GAL4-UAS experiments had to be conducted in *D. melanogaster* as a model organism. This is important as recent work has highlighted that phenotypes observed in *D. melanogaster* are not always reflected in the mosquito (e.g. DDT resistance was conferred by CYP6M2 overexpression in *D. melanogaster* but not in *An. gambiae*) (Adolfi *et al.*, 2019). Where possible it is best to conduct phenotypic characterisation in the organism of interest.

The transgenic approach used will depend greatly on the aims of the experiment but some of the possible approaches include loss of function analysis: through generation of indels and more drastic disruption of exons or RNAi; gain of function analysis (usually involves inserting DNA cassettes into the genome); and finer mutational analysis - through creation of a SNP without 'adding' further DNA to the genome).

### 1.5.6 AIMS AND OBJECTIVES

In this PhD three separate projects were approached on the theme of insecticide resistance characterisation in mosquitoes.

In brief, the first project was instigated to use the INVAPP system to examine the resistance conferred to larvae through overexpression of a number of transgenes that have previously been shown to produce resistance to different insecticides in adults.

The second project was carried out to functionally characterise CCEae3A *in vivo*. This enzyme has been previously associated with temephos resistance in *Ae. aegypti* larvae. Through transgenic overexpression with the GAL4-UAS system, we aimed to validate a role for CCEae3A in conferring temephos resistance in larvae and to define the resistance profile conferred against other insecticide classes. In addition, the fitness costs of CCEae3A upregulation were also examined in these transgenic mosquitoes (Chapter 3).

Thirdly, a CRISPR-Cas9 approach was taken to functionally characterise the ACE1-G280 substitution in terms of the extent and breadth of insecticide resistance conferred solely by this mutation in an otherwise susceptible genetic background. In addition, CRISPR-Cas9 has been used to fluorescently tag the site/s of *ace1* expression in order to define the extent and tissue distribution of *ace1* expression in the mosquito (Chapter 5).

# Approaches to the assessment of data generated from the invertebrate automated phenotyping platform (INVAPP) for insecticide resistance testing

## 2.1 INTRODUCTION

Insecticide resistance is a looming threat to malaria control programmes targeting the *Anopheles gambiae* mosquito vector (South and Hastings, 2018). Upregulation of several genes has been implicated in adult stage resistance (Liu, 2015). However, their impact on larval susceptibility is largely unexplored. This understanding is vital as larviciding may be an important supplementary element in a multipronged approach to reduce adult mosquito populations (WHO, 2013; WHO, 2019a).

In traditional assays for the assessment of insecticide susceptibility in larvae, it is necessary to immerse larvae in varying concentrations of insecticide, then, after 24 h exposure, the binary outcome variable, mortality, is assessed. The assays for this are labour intensive, low-throughput and subject to investigator bias (WHO, 2005). A novel assay has been developed aiming to address these issues to enhance our ability to study larval insecticide susceptibility.

The invertebrate automated phenotyping platform (INVAPP) was developed for assessment of nematode motility to rapidly assess and screen potential toxic compounds (Partridge *et al.*, 2018), and has been modified for measurement of larval motility (Buckingham *et al.*, 2021). INVAPP was previously used with a 'Paragon' algorithm to examine parasitic nematode susceptibility to known anthelmintics and to screen a 'Pathogen Box Library', to identify compounds which killed nematodes. The platform was integral in the identification of several members of two novel chemical classes, the dihydrobenz[e][1,4]oxazepin-2(3H)-ones and the 2,4-Diaminothieno[3,2-d]pyrimidines, neither of which were previously shown to have anthelmintic activity (Partridge *et al.*, 2018). INVAPP has also been combined with inducible RNAi knockdown of $\beta_2$-m to study the variants proteotoxicity in *C. elegans* in studying D6N $\beta_2$-microglobulin related amyloidosis (Faravelli *et al.*, 2019). In this thesis it

was investigated whether the INVAPP assay can be used to detect resistance in mosquito larvae which have been genetically modified to upregulate genes known to confer insecticide resistance in adults. To do this, compounds from each of the common classes of insecticides were tested and the results compared to a susceptible control strain to identify resistance.

Transcriptomic and proteomic analysis has identified several candidate genes from field mosquitoes, which when upregulated are implicated in insecticide resistance, including; cytochromes P450s, CYP6P3 (Muller *et al.*, 2008) and CYP6M2 (Stevenson *et al.*, 2011); glutathione-S-transferase: GSTe2 (Ranson *et al.*, 2000; Mitchell *et al.*, 2014; Riveron *et al.*, 2014); and sensory appendage protein 2, SAP2 (Ingham *et al.*, 2020).

Cytochromes P450s (particularly CYP6P3 and CYP6M2 in *An. gambiae*) are associated strongly with resistance to pyrethroids as they have been repeatedly found to be elevated in pyrethroid resistant populations of mosquitoes and other arthropods (Muller *et al.*, 2008; Djouaka *et al.*, 2008; David *et al.*, 2013; Paine and Brooke, 2016). Cross resistance and metabolism of other compound classes has also been predicted (Yunta *et al.*, 2019), including CYP6M2 causing DDT resistance in Benin (Djegbe *et al.*, 2014) and Ghana (Mitchell *et al.*, 2012). Also, CYP6P3 has been shown to metabolize bendiocarb (Edi *et al.*, 2014) and pyriproxyfen (Yunta. C *et al.*, 2016).

Glutathion-S-transferases (GST) are one of the key classes of detoxification enzymes which are associated with insecticide resistance in mosquitoes. GSTe2, the most often studied GST in relation to insecticide resistance in mosquitoes, is associated with resistance through upregulation and through a L119F mutation which is particularly associated with DDT resistance (Riveron *et al.*, 2014), potentially contributes to the loss of efficacy of pyrethroid treated bed nets (Menze *et al.*, 2020) and is more recently associated with temephos resistance (Helvecio *et al.*, 2020). RNAi knockdown in *An. funestus* (Kouamo *et al.*, 2021) and GAL4-UAS analysis in *D. melanogaster* (Riveron et al., 2017) both demonstrate the impact of GSTe2 on pyrethroid and other classes of insecticide.

SAP2 was shown to be upregulated in full adult carcases in a laboratory colony of *An. coluzzii* from Côte d'Ivoire (Tiassalé) compared to two susceptible strains and in both RNAi knockdown and

GAL4-UAS overexpression experiments SAP2 was shown to have a role in resistance to pyrethroids (Ingham *et al.*, 2020). Additionally, analysis of the *An. gambiae* 1000 genomes project indicated a possible selective sweep in the SAP2 locus at low frequency in North West Africa (Ingham *et al.*, 2020). Unfortunately, no information is available on the impact of SAP2 overexpression on mosquito larval stages which could be important in areas attempting to implement integrated vector control programmes to combat pyrethroid resistance.

Transcriptomic analyses of field mosquitoes are essential for identifying probable candidates for insecticide resistance mechanisms. However, fold-change of gene expression can be an unreliable predictor of contribution to a phenotype such as insecticide resistance as it neglects the levels of activity and absolute expression of a protein (Evans, 2015). Also, definitively determining the contribution of individual mechanisms to resistance profiles is necessary as multiple potential mechanisms typically co-exist in field and laboratory selected mosquitoes which makes definitively identifying causative factors very difficult (Yewhalaw *et al.*, 2011). The best method currently available for validating individual insecticide resistance mechanisms is to assess each mechanism in isolation using transgenic mosquitoes (Adolfi and Lycett, 2019).

GAL4-UAS binary expression models are a useful tool for assessing the impact of upregulation of detoxification genes on resistance (Lynd and Lycett, 2012; Adolfi *et al.*, 2019). UAS transgenic lines capable of overexpressing CYP6P3, CYP6M2 (Adolfi, 2017), GSTe2 (Adolfi *et al.*, 2019) and SAP2 (Ingham *et al.*, 2020) when crossed with an appropriate GAL4 expressing line such as Ubi-A10 (Adolfi *et al.*, 2018) have been generated by the Lycett group. The effect of CYP6P3, CYP6M2 and GSTe2 overexpression on insecticide susceptibility in adults was characterised using WHO Tube assays (Adolfi *et al.*, 2019). CYP6P3 and CYP6M2 were implicated in conferring resistance to pyrethroid and carbamate insecticides and increasing susceptibility to malathion relative to susceptible control when they are overexpressed ubiquitously with Ubi-A10. Ubiquitous GSTe2 overexpression resulted in DDT and fenitrothion resistance (Adolfi *et al.*, 2019). It is not clear however how adulticide resistance relates to larval stage resistance, however, full characterisation of the impact of these genes on larval susceptibility would be incredibly time consuming using the traditional larval

assay. If the INVAPP method works well as a high-throughput larval assay for resistance detection, the time required for studies into larval resistance mechanisms may be more reasonable.

The INVAPP system has been shown to be capable of detecting fairly large differences in EC50 between strains for deltamethrin. However, it is yet to be assessed whether the system is sufficiently robust to function as a high-throughput assay to differentiate small changes in resistance for many compounds and strains in a large, complex experiment. Achieving this required the assessment of different modelling tools to analyse the data. Additionally, the system could be particularly useful if resistance in 1$^{st}$-instar larvae reflects the equivalent resistance in adult stage, as if so, this could be a very rapid tool for resistance detection in populations.

### 2.1.1 AIMS AND OBJECTIVES

- To assess the suitability of INVAPP as a high-throughput assay for identification of differential susceptibility to toxic compounds in *An. gambiae* mosquitoes known to overexpress key individual resistance markers.
- To evaluate different statistical methods for their suitability for analysis of a large and complex dataset of INVAPP results.
- To determine whether the effect of individual metabolic enzyme overexpression on larval insecticide susceptibility can be reliably predicted using the INVAPP assay.
- To assess the suitability of INVAPP as a potential proxy for the prediction of differential susceptibility in the adult stage based on the results in 1$^{st}$ instar larvae.

## 2.2 METHODS

### 2.2.1 CONTRIBUTIONS

Dr. Adriana Adolfi created the ubiquitous expression driver line (Ubi-GAL4) and UAS responder lines carrying the CYP6P3 and CYP6M2 genes. Stephanie MacIllwee and Amalia Anthousi created the UAS responder lines carrying the GSTe2 and SAP2 genes respectively. Dr. Steven Buckingham provided and assisted with the editing of some of the python code used for data extraction and analysis and gave general advice for coding in python. Professor. David Sattelle, Dr. Steven Buckingham and Dr. Freddie Partridge received and floated eggs arriving at UCL and originally developed the INVAPP system. Dr. Gareth Lycett, Amalia Anthousi and Fraser Colman assisted with mosquito maintenance and blood feeding for experiments.

### 2.2.2 *AN. GAMBIAE* REARING

*An. gambiae* were reared as described in Appendix D-xiv.

### 2.2.3 MOSQUITO STRAINS

Seven mosquito lines were used in this chapter:

A GAL4 driver/docking line - Ubi-GAL4, a homozygous *An. gambiae* transgenic driver/docking line created as described in (Adolfi *et al.*, 2018) which expresses GAL4 under the transcriptional control of a ubiquitin promotor and carries *attP* sites for ϕC31 mediated cassette exchange.

A susceptible non-transgenic laboratory strain – G3, an *An. gambiae* (M+S) wild type strain, obtained from the Malaria Research and Reference Reagent Resource Centre (MR4), which was originally isolated from the Gambia. G3 was crossed with Ubi-GAL4 for assays and served as experimental control as it expresses the same level of GAL4 as in test strains. The progeny of G3 crosses with Ubi-GAL4 are denoted ‘Ubi-GAL4/WT’.

A ‘resistant’ non-transgenic laboratory strain - Tiassalé 13 (referred to as ‘Tiassalé’ throughout) is an *An. gambiae s.s.* (M+S) wild type strain isolated from Cote d-Ivoire in 2013, which was obtained from LITE. Adults were regularly selected with 1-hour exposure to 0.05% deltamethrin. ~90% frequency of 1014F kdr allele and ~40% frequency of 280S ACE1 allele plus elevated CYP6M2 (13x), CYP6P3 (34x) and CYP6Z2/3 (5x) compared to Ngousso control was detected in adult samples in 2016 (the closest data available to the time this strain was tested).

Four UAS responder lines were used in this chapter. These lines are marked with 3xP3-driven eYFP and have *cyp6m2*, *cyp6p3, gste2* and *sap2* genes under the control of a UAS promoter. UAS-CYP6M2 and UAS-CYP6P3 are *An. gambiae* transgenic responder lines that were created from A11 as described in (Adolfi, 2017). UAS-GSTe2 and UAS-SAP2 are *An. gambiae* transgenic responder lines that were created from Ubi-GAL4 as described in (Adolfi *et al.*, 2019). To obtain larvae ubiquitously overexpressing the described genes, female UAS and male Ubi-GAL4 lines were crossed (as female Ubi-GAL4 are weakened by a fitness cost on longevity). The progeny of these crosses that overexpress genes are denoted in the format “up‘overexpressed gene’” (e.g. upGSTe2). These four GAL4-UAS transgenic strains were used as they have been well characterised in adults by the Lycett group and so permit comparison of results with previous data from the same strains.

### 2.2.4 INVERTEBRATE AUTOMATED PHENOTYPING PLATFORM (INVAPP) ASSAYS

Adult females were blood fed on day 1 using a hemotek. On day 5 afternoon, eggs laid day 4 evening / day 5 morning. When received at UCL on day 6, eggs were washed into filter paper lined, 3 litre (34 x 23 x 7 cm) trays containing 0.001% pond salt solution (~1 cm depth) and one third pellet of cat food. Trays containing larvae were incubated at 25°C and moved minimally to prevent stranding of eggs. Eggs were rinsed down the filter paper with 0.001% pond salt solution on day 7 to prevent stranding, desiccation and encourage hatching. Assays using the INVAPP system were conducted on first instar larvae on day 8 with 1440 min readings made on day 9 (Figure 2.2.1).

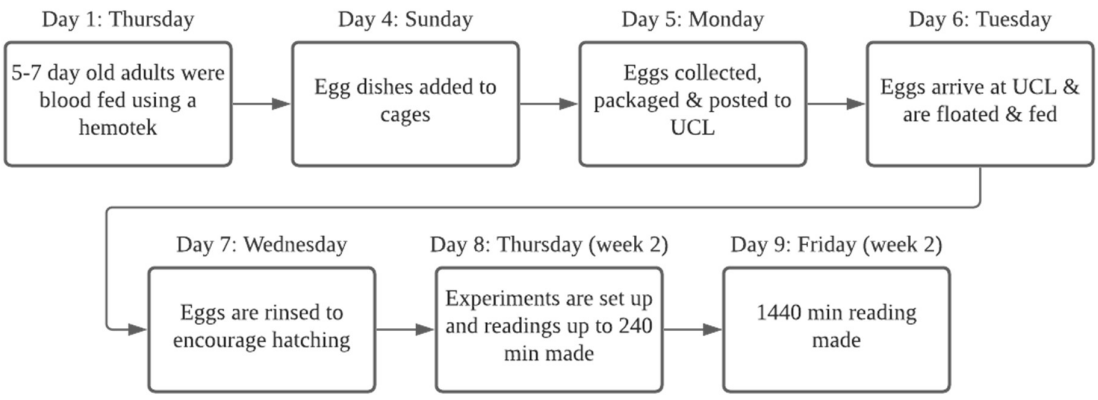


Figure 2.2.1: INVAPP Experimental Process.

Flow chart detailing the regular process followed to conduct INVAPP assays at University College London (UCL). Days of the week reflect the usual days each step was conducted on (Created using Lucidchart.com).

On day 8, using a 100 µm cell strainer 1st instar larvae were concentrated to approximately 3-10 larvae per 100 µl 0.001% pond salt solution. Immediately prior to this the remainder of the cat food pellet was removed with a 3 mL Pasteur pipette (with the end removed to widen tip). 100 µl 0.001% pond salt solution containing 3-10 first instar larvae were added to each well of a 96-well plate. A second 96 well plate was prepared with 150 µl of 0.001% pond salt solution plus insecticide solution with concentrations ranging from $1x10^{-4}$ M – $3.05x10^{-9}$ M (double the intended final concentration). The plate containing larvae was filmed prior to insecticide exposure to provide baseline readings for normalization. 100µl from each well in the plate containing the insecticides was added to the plate containing larvae resulting in final concentrations ranging from $5x10^{-5}$ – $1.525x10^{-9}$ M.

#### 2.2.4.1 INVAPP System Filming

An Andor Neo camera (resolution 2560x2160, maximum frame rate 100 frames per second) with a line-scan lens (Pentax YF3528) and LED array and acrylic diffuser illumination filmed the 96 well plate containing larvae (Figure 2.2.2), together with a 'Vectorgon' algorithm (Appendix A-i) measure

the motility of first-instar larvae. 5 or 10 stacks of 30 images, 10 ms apart were collected at approximately 5 s intervals for each time point.

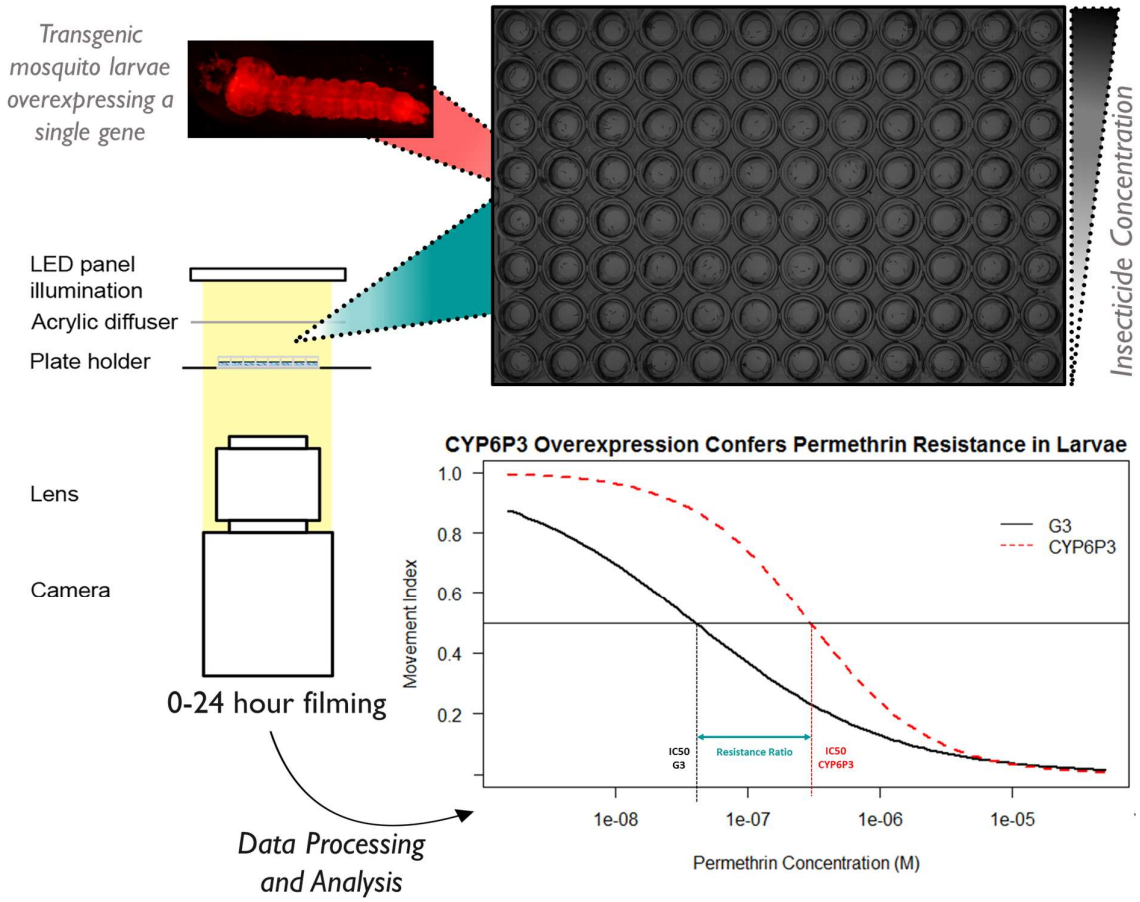


Figure 2.2.2: Schematic representation of the Invertebrate Automated Phenotyping Platform (INVAPP) workflow.

A diagram showing the key components (camera set-up, mosquito larvae in a 96-well plate, a transgenic mosquito larva and mock output data for two strains showing the normalised movement index against concentration) of the INVAPP system as used in this thesis. Diagram of camera system has been modified from (Partridge *et al.*, 2018).

#### 2.2.4.1 Calculation of Motility

Image stacks were analysed using python scripts utilising MATLAB packages (Appendix A-i). The calculation of a Movement Index (MI) was made for each well by calculation of the variance through time for each pixel and using a threshold (3 standard deviations greater than the mean variance of that

well – this threshold was determined by colleagues at UCL when developing the optimum analysis algorithm) to determine whether movement occurred in a pixel during the time frame and totalling the results for each well on a plate (Buckingham *et al.*, 2021). The mean movement index values for the 5/10 image stacks for each time point were then normalised (to control for the number of and differences in activity between larvae) by dividing by the mean MI for the 5/10 image stacks collected prior to insecticide exposure (nMI) (Appendix A-i). Following calculation of the motility in python, data were exported as a .csv file and further data analysis was conducted in R or python.

#### 2.2.4.2 Statistical Analysis

Initially a dose response 'polynomial regression with local fitting' (LOESS) curve was generated in R (v4.1.0) for each unique combination of strain, insecticide and time point using the geom_smooth() function of the package ggplott2 (v3.3.5) to visualise the data. Different data analysis algorithms were then assessed for suitability for analysis of large-scale high throughput INVAPP data for identification of resistance phenotypes. Other packages used for data manipulation and plotting in R were: cowplot (v1.1.1), dplyr (v1.0.7), extrafont (v0.17), forcats (v0.5.1), ggpubr (v0.4.0), htmltools (v0.5.2), magrittr (v2.0.1), plyr (v1.8.6), purr (v0.3.4), RColorBrewer (v1.1-2), reshape2 (v1.4.4) and tidyverse (v1.3.1). Packages used in python (v3.7.1) were: glob (v0.7), arrow (v1.1.1), pandas (v0.23.4), numpy (v1.15.4), matplotlib (v3.0.2) and scipy (v1.1.0).

##### *2.2.4.2.1 Analysis Method 1: 'estimate_EC50()' function in R*

The ec50estimator package (v0.1.0) is a new package which permits calculation of large multi-variable datasets in a single (relatively simple) line of code:

```
> ec50s <- estimate_EC50(nMI~concentration, data =data, EC_lvl = 0.5, isolate_col =
> "bioreplicate", strata_col =  c("strain","time","compound"), interval = "delta", fct = drc::LL.4())
```

The model used was a four-parameter log-logistic function (Equation 2.2.1) from the drc package (v3.0-1).

$$f(x) = c + \frac{d - c}{1 + \exp\left(b(\log(x) - \log\left(e\right))\right)}$$

Equation 2.2.1: Four-parameter log-logistic function. LL.4() - used by *estimate_EC50()* method.

b = Slope (between EC10 and EC90), c = upper limit, d = lower limit, e = EC50 – concentration at 0.5 y-value (absolute)- or midpoint – concentration at 'c / d' (relative) - (defined in function call)

Using the *estimator_EC50()* function, an 'absolute' IC50 (the concentration at which nMI = 0.5) was calculated for each replicate for each unique strain, compound and time point combination in one model. For each compound and time point combination, a t-test (*t_test()* from the rstatix package v0.7.0) specifying Ubi-GAL4/WT as the denominator/reference strain, with a Benjamini-Hochberg (BH) post hoc correction was used to assess the statistical significance of differences between Ubi-GAL4/WT and the other strains tested. Resistance ratios (RR) – the fold change in IC50 between 2 strains - were calculated by dividing the mean IC50 of the strain of interest by the equivalent mean IC50 for Ubi-GAL4/WT. RRs were calculated for each strain for each unique time and compound combination. A RR value of 1 indicates no difference; greater than 1 indicates increased tolerance; and less than 1 indicates increased susceptibility compared to the Ubi-GAL4/WT comparator strain.

#### *2.2.4.2.2 Analysis Method 2: 'curve.fit()' function in Python*

One method used previously to analyse the results of INVAPP experiments uses the *curve.fit()* function from sci.py.optimise to fit a sigmoid function (Equation 2.2.2) with the insecticide concentration and normalised movement index and calculate the pIC50 (the -log10 of the IC50) (Buckingham *et al.*, 2021). Starter values and minimum and maximum bounds were provided to the model for the pIC50 and slope parameters. These values were investigated on a smaller subset of the data testing different values until curves which reflected the raw data well were found. The 'relative' pIC50 here is calculated as the midpoint between the maximum and minimum values of nMI in the

model. A separate model was run for each compound tested. pIC50s were calculated for each replicate of each genotype and time point combination for each compound.

$$nMI = \frac{1}{1 + 10^{\frac{I-C}{H}}}$$

Equation 2.2.2: Sigmoid equation used in *curve.fit()* method for pIC50 calculation. nMI = normalised movement index, I = IC50 – concentration at 'maximum nMI / minimum nMI' (relative), C = compound concentration, H = slope.

The model output data was exported to .csv files and was further analysed in R. Statistical differences in pIC50s and then RRs were calculated as in analysis method 1 (section 2.2.4.2.1) for IC50s.

#### *2.2.4.2.3 Analysis Method 3: 'drm()' function in R*

Next, generation of models for smaller groupings of the data using the *drm()* function of the drc package was assessed as a potential alternative analysis method. For each insecticide one time point was chosen (identified as the 'best for analysis' by having a full dose response sigmoid shape curve for as many strains as possible using visual assessment of LOESS curve plots. The data was studied in depth to identify whether reducing the number of concentrations could improve the fit of the model to the raw data. The 'best' model function for the data was then found using the *mselect()* function of the drc package (to identify the most mathematically appropriate function) then, after plotting, visual assessment was used to confirm the quality of the models fit to the raw data. For all compounds the 'best' model selected was that using the three-parameter log-logistic function (Equation 2.2.3) which limits the lower limit to 0 but the upper limit can vary with strain. This model (which had strain as a grouping variable) was then compared to a simpler model (which did not have a grouping variable) using an anova to assess whether strain is a significant factor. The *compParm()* function (from drc package) was used to calculated 'relative' resistance ratios and a Z test was used to assess the significance of the ratio.

$$f(x) = \frac{d}{1 + \exp\left(b(\log(x) - \log\left(e\right))\right)}$$

Equation 2.2.3: Three-parameter log-logistic function - LL.3() - used by *drm()* method.

b = slope (between EC10 and EC90), d = upper limit, e = EC50 – concentration at midpoint – concentration at 'c / d' (relative).

### 2.2.5 WHO LARVAL ASSAY

WHO larval assays were conducted and analysed as described in (Appendix D-xix).

### 2.2.6 WHO ADULT ASSAY

WHO adult assays were conducted and analysed as described in (Appendix D-xx).

# 2.3 RESULTS

## 2.3.1 INVAPP ANALYSIS

To determine whether the INVAPP system could detect differences in IC50 between the alternative transgenic and control strains, analysis was conducted for 6 strains, testing 9 insecticides, at 16 concentrations (starting at $5x10^{-5}$ M and decreasing two-fold to $1.53x10^{-9}$ M) and readings were taken for each plate at 2, 60, 90, 120, 210, 240 and 1440 min after addition of insecticide. However, readings were not taken at 120 and 210 min for 3 compounds - fenthion, DDT and diflubenzuron - due to restricted access to the INVAPP system at that period. Various ways to analyse this large dataset were undertaken, as described below, to determine which was the most suitable.

### 2.3.1.1 Visualisation

To initially visualise the complex dataset, Figure 2.3.1 shows a LOESS function plot for each of these strains which reflects a non-parametric polynomial fit of the relationship between compound concentration and normalised movement index (nMI) separated by compound and time. From visual inspection of the LOESS curves (Figure 2.3.1) differences in response between Ubi-GAL4/WT control and at least one other strain are apparent at one or more time points for every compound tested (Table 2.3.1). The 2 min time point (Figure 2.3.1-1) shows the nMI just after the start of the experiment which fluctuates at around 1 (equal to the normalisation mobility value given from the zero-time point) for most strains and compounds, though spikes of nMI greater than 2 are seen in concentrations over ~$1x10^{-6}$ M with Tiassalé and upCYP6M2 in deltamethrin (Figure 2.3.1-E1), with upGSTe2 in temephos (Figure 2.3.1-D1); and with upCYP6M2 in malathion (Figure 2.3.1-C1). In general, after 60 min exposure or above, each strain exposed to each compound display a reduction in nMI at increasing dose and time.

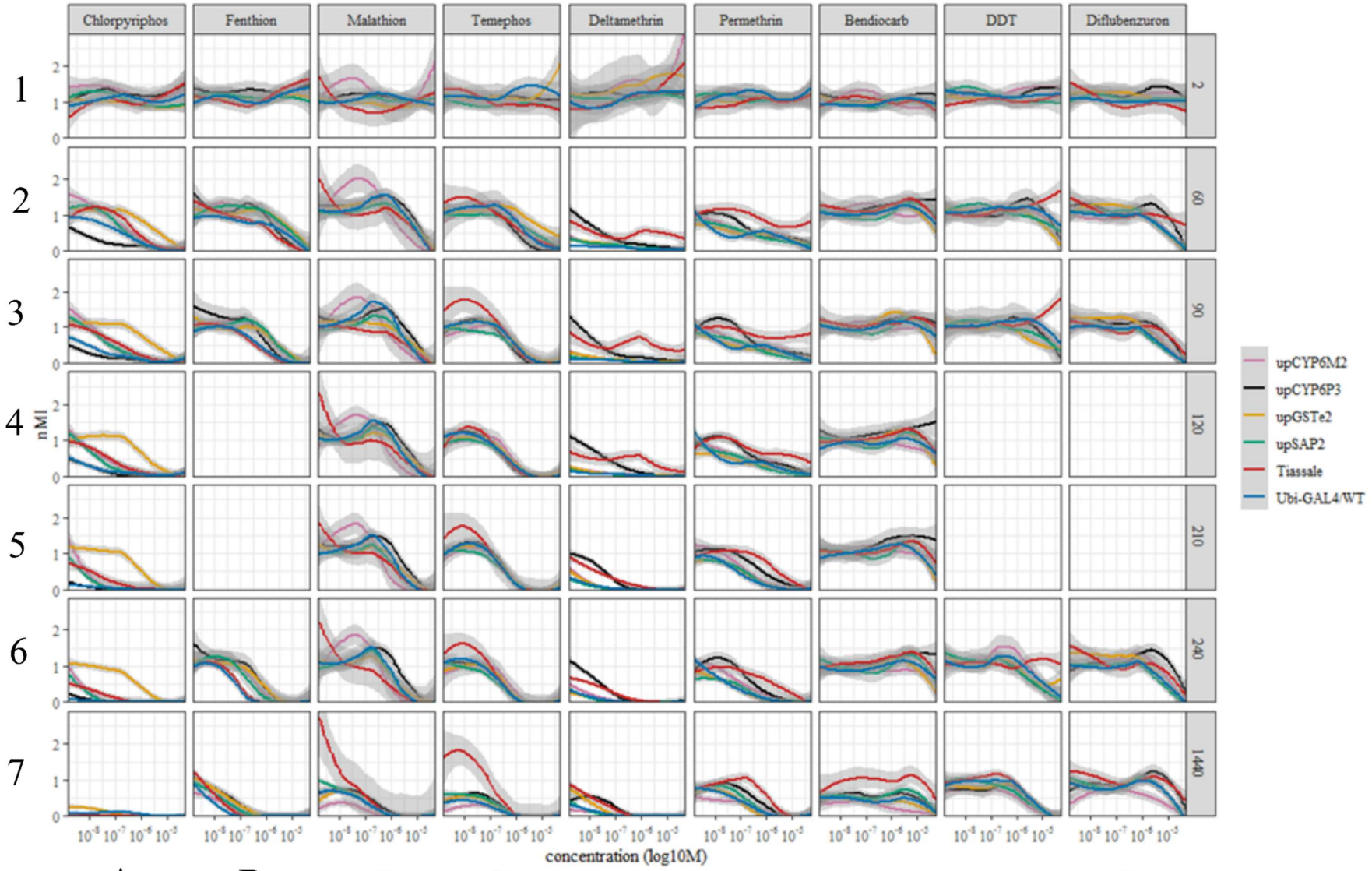
Chlorpyriphos
Fenthion
Malathion
Temephos
Deltamethrin
Permethrin
Bendiocarb
DDT
Diflubenzuron
1
2
3
4
5
6
7
2
60
90
120
210
240
1440
nMI
concentration (log10M)
A
B
C
D
E
F
G
H
I
upCYP6M2
upCYP6P3
upGSTe2
upSAP2
Tiassale
Ubi-GAL4/WT

Figure 2.3.1: INVAPP Analysis LOESS Dose Response Plots.

LOESS curves reflecting concentration against nMI for each strain, compound and time point combination divided into facet plots by compound (x) and time (y). Line colour reflects strain as defined in the legend. Plotted using the geom_smooth() function of the ggplot2 package displaying standard error as a grey shadow for each plot. Each row and column on the plot are labelled with a number (1-7) and letter (A-I) respectively to improve clarity when the figure is being discussed in the text.

The compounds which caused the least decrease in motility were bendiocarb and diflubenzuron which both only reduced nMI in the highest concentrations tested (Figure 2.3.1-G+I). With bendiocarb exposure the effects are only obvious at very high doses above $1x10^{-5}$ M and with diflubenzuron only above $1x10^{-6}$ M. The most active compounds (which reduced activity in all strains quickest at the lowest concentrations) were chlorpyriphos, deltamethrin and fenthion (Figure 2.3.1-A,B+E). At the final time point, mean nMI below 0.5 was observed in all strains following fenthion and deltamethrin exposure at all concentrations above $1x10^{-7}$ M. In chlorpyriphos at this time point all strains displayed mean nMI of below 0.5 in all concentrations.

For most strains and at most time points following exposure to malathion or temephos (and less consistently for fenthion, permethrin or DDT) there is an increase in nMI at moderate doses of these insecticides, whilst at high doses motility decreases and at low doses nMI remains ~1. In the malathion curves between the 60-240 min timepoints (Figure 2.3.1-C2-6), all of the lines show an increase in motility (above that observed in lower concentration for the same line) when exposed to concentrations between $1x10^{-7}$ M and $1x10^{-6}$ M, except for upCYP6M2 which shows similar increased motility but shifted to lower concentrations ($1x10^{-8}$ M and $1x10^{-7}$ M). This increase in activity may be due to hormesis, however attempts to model the data with the Brain-Cousens hormesis functions (*BC.4()* and *BC.5()* from the drc package) produced models that either would not converge or did not reflect the data well, tending to exaggerate the hormesis effect beyond what occurs in the data (not shown).

In the chlorpyriphos curves, the upGSTe2 strain displays differential motility of around 1 nMI at the lower range of concentrations up until 240 min (Figure 2.3.1-A6), whereas the control mosquitoes (Ubi-GAL4/WT) lost virtually all of their activity at this point. Meanwhile, the upCYP6P3 strain follows closely the responses of the control and may even show decreased activity at the 60 min time point Figure 2.3.1-A2. The other strains show intermediate responses between the upGSTe2 and control strain.

Differences between Ubi-GAL4/WT and all four transgenic crosses can be seen with 90, 240 and 1440 min fenthion exposure as motility remains around 1 in higher concentrations than Ubi-GAL4/WT (Figure 2.3.1-B3,6+7). Whereas, Tiassalé is very similar to Ubi-GAL4/WT until 1440 min when the nMI of Ubi-GAL4/WT is lower.

| | | ***TESTED STRAIN*** | | | | |
|---|---|---|---|---|---|---|
| | | **upCYP6P3** | **upCYP6M2** | **upGSTe2** | **upSAP2** | **Tiassalé** |
| ***COMPOUND*** | **Chlorpyriphos** | $\downarrow^{60}$ | $\uparrow^{60 - 240}$ | $\uparrow\uparrow\uparrow\uparrow^{60 - 240}$ | $\uparrow^{60 - 240}$ | $\uparrow^{60 - 240}$ |
| | **Fenthion** | $\uparrow\uparrow^{90, 240, 1440}$ | $\uparrow\uparrow^{90, 240, 1440}$ | $\uparrow\uparrow^{90,240, 1440}$ | $\uparrow\uparrow^{90,240, 1440}$ | $\uparrow^{1440}$ |
| | **Malathion** | $\uparrow^{210}$ | $\downarrow^{60 - 1440}$ | – | – | ? |
| | **Temephos** | – | – | – | – | ? - $\uparrow^{90- 1440}$ |
| | **Deltamethrin** | $\uparrow\uparrow\uparrow^{60 – 1440}$ | – | $\uparrow^{1440}$ | – | $\uparrow\uparrow\uparrow^{60-1440}$ |
| | **Permethrin** | $\uparrow\uparrow^{60-1440}$ | – | – | – | $\uparrow\uparrow\uparrow^{60-1440}$ |
| | **Bendiocarb** | $\uparrow\uparrow^{120-240}$ | $\downarrow^{1440}$ | – | – | $\uparrow^{1440}$ |
| | **DDT** | – | $\downarrow^{1440}$ | – | – | $\uparrow\uparrow^{60, 90, 240}$ |
| | **Diflubenzuron** | $\uparrow^{60, 90, 240, 1440}$ | $\downarrow^{1440}$ | – | – | $\uparrow^{60, 90, 1440}$ |

Table 2.3.1: Differences in susceptibility predicted visually from LOESS curves. Predictions are indicated by symbols: ↑ = increased tolerance; ↓ = decreased tolerance; – = equal susceptibility; when compared to Ubi-GAL4/WT. Increased number of arrows indicates a larger predicted difference. ? indicates that a prediction is difficult or unclear. Superscript indicates the timepoint at which the indicated difference is apparent.

The Tiassalé line showed a marked difference to the other lines following exposure to Temephos (Figure 2.3.1-D). At nearly all time points, at the lower range of concentrations up until $1x10^{-6}$ M, the Tiassalé line showed greater nMI than the control and all other lines. In addition, there appeared to be a hormesis like effect occurring at about $1x10^{-8}$ M occurring with all the lines but more pronounced in the Tiassalé. This complicates the analysis of the effect as in all except the 1440 min exposure, despite the upper asymptote being clearly higher, the slope of the curve meets the slope of the curves for the other strains. In both pyrethroid (deltamethrin and permethrin) experiments, at 60 min exposure and beyond there was increased motility in the Tiassalé and upCYP6P3 lines at some concentrations compared to the other lines. After 1440 min deltamethrin exposure upGSTe2 also displays increased motility compared to Ubi-GAL4/WT.

At 120-, 210- and 240-min bendiocarb exposures (Figure 2.3.1-G), upCYP6P3 displayed no reduction in nMI at any concentration whereas the control mosquitoes and other strains displayed some decline in the highest concentrations tested but after 1440 min exposure this difference was not evident. At 1440 the mean nMI of all strains except Tiassalé at all concentrations decreased to around 0.5. For Tiassalé the nMI remained around 1 at most concentrations. After 1440 min exposure CYP6M2 displays a slight reduction in nMI across all concentrations compared to Ubi-GAL4/WT.

Decline in nMI following DDT exposure occurred in concentrations above $1x10^{-6}$ M after 60 min exposure in all strains except Tiassalé. nMI remained around 1 for Tiassalé for all time points except 1440 min at which point the curve was very similar to that of Ubi-GAL4/WT.

After 1440 min diflubenzuron exposure a reduction in nMI at most concentrations is apparent between upCYP6M2 and Ubi-GAL4/WT. At all time points after 60 mins activity of upCYP6P3 and Tiassalé mosquitoes was higher in concentrations above $1x10^{-6}$ M than that of Ubi-GAL4/WT.

To analyse whether these observations have a statistical basis and to calculate resistance ratios for the inhibition of movement, several models were tested for reliability to describe the datasets. The first approach used the *estimate_EC50()* function in R to fit a single LL.4 model to the entire dataset. The second fitted a separate sigmoid curve model for each compound separately. The final method used an

LL.3 model for a single time point for each compound. The time point was selected based on visual inspection of the LOESS curves to identify that which had the most complete dose response curve for all of the strains. Where this was not possible the time point with a curve for Ubi-GAL4/WT - which fit the data well (preferably where this control strain had a range of nMI values at least from above 0.5 to zero) and as many other strains as possible could also be analysed - was selected.

#### 2.3.1.2 Analysis Method 1 – '*estimate_EC50()*' function in R

The *estimate_EC()* method, used to fit one model for the whole data set, successfully calculated an 'absolute' IC50 (threshold nMI = 0.5) for 679 (83.8%) of the 810 desired comparisons (unique combinations of strain, compound, timepoint and replicate). 12 (3.5%) comparisons of strain, compound and timepoint had no IC50s calculated so could not be further analysed.

Critically, as no IC50s were calculated for Ubi-GAL4/WT for 210 min exposure to chlorpyriphos and 120 min exposure to deltamethrin, comparison of IC50s and calculation of RRs was not possible for these groups. The mean IC50 predictions for 89 (26%) strain-compound-timepoint values were predicted outside the range of concentrations that were tested (i.e., were extrapolated) (Appendix A ii, Appendix A-iii), and so will not be accurate. Extrapolation of IC50s was not randomly distributed across compounds and time points, although it is not concentrated on a particular strain (all strains had between 25% and 32% of comparisons with incalculable or extrapolated IC50s). 42.6% of comparisons across all compounds for 2 min exposure were incalculable or extrapolated beyond the range of concentrations tested. The majority of deltamethrin and bendiocarb comparisons had extrapolated or incalculable IC50 values (59.5% and 61.9% respectively), whereas the same values for other compounds ranged from 14% and 27%.

Where less than 2 replicate IC50 values (either 2 or 3 replicates were performed) were calculable for a particular strain-compound-timepoint combination, statistical assessment of the difference compared to Ubi-GAL4/WT could not be done. Appendix A ii illustrates the model predictions whilst keeping the y axis limited to concentrations used in the assays. Appendix A-iii illustrates the same model predictions with no axis limits. As can be seen, very few IC50 comparisons (2 of 178 calculable

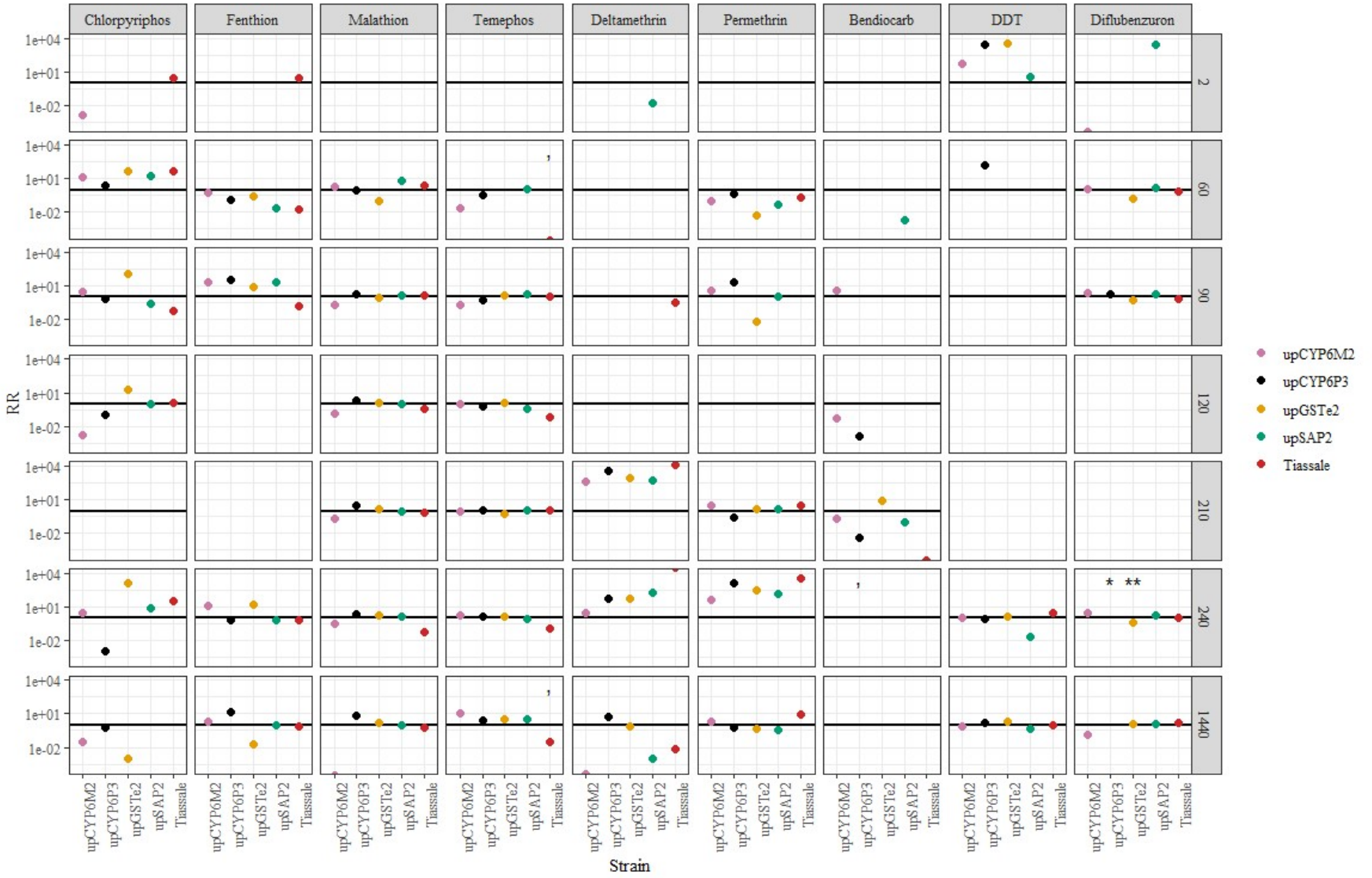
Chlorpyriphos
Fenthion
Malathion
Temephos
Deltamethrin
Permethrin
Bendiocarb
DDT
Diflubenzuron
2
60
90
120
210
240
1440
RR
1e+04
1e+01
1e-02
upCYP6M2
upCYP6P3
upGSTe2
upSAP2
Tiassale
Strain

Figure 2.3.2: RR values comparing IC50 values of Ubi-GAL4/WT with the equivalent for all other strains tested which had been calculated using the *'estimate_EC50()*'.

The y axis has been limited to view differences in values showing smaller differences. Resistance ratios calculated from meanIC50s (calculated using the *estimate _EC50()* function from the ECestimator package in R) comparing the test strains to the Ubi-GAL4/WT strain, facetted by compound (x) and exposure time (y). y axis limited at 0.001 and 10,000 to permit visualisation of values predicting small differences. Points reflect RR, p-values of <0.1 are reflected: 0.1 > , > 0.05 > * > 0.01 > ** > 0.001 > *** > 0.0001 > ****. Horizontal black line indicates RR = 1 (IC50 strain = IC50 Ubi-GAL4/WT). Where no point is visible the resistance ratio was either calculated to be outside of the range of the plot or was incalculable.

comparisons – 1.1 %) between test strains and Ubi-GAL4/WT were significantly different (Table 2.3.2). For the first of these significant comparisons, the IC50 of the test strain for 'diflubenzuron - 240 min exposure - upCYP6P3' ($t(1) = 30.7$, $p = 0.042$, IC50: Ubi-GAL4/WT $= 9.87 \times 10^{-7}$ M, upCYP6P3 $= 1.35 \times 10^{-101}$ M); was extrapolated beyond the range of tested data (Figure 2.3.2, Appendix A-iv). In the second significant comparison, neither IC50 was extrapolated 'diflubenzuron – 240 min – upGSTe2' ($t(1.91) = 24.1$, $p = 0.008$, IC50: Ubi-GAL4/WT $= 9.87 \times 10^{-7}$ M, upGSTe2 = $3.64 \times 10^{-7}$ M) (Appendix A ii).

Figure 2.3.2 illustrates the RRs calculated from the *estimate_EC50()* function with limits on the y axis (0.001 to 10,000) to permit visualisation of smaller differences. Appendix A-iv shows the same data with no axis limits so that extreme RRs can be seen. For both comparisons which have statistically significant differences have RRs less than 1 (Figure 2.3.2), 'diflubenzuron - 240 min - upCYP6P3 (RR = $1.4 \times 10^{-95}$)' and 'diflubenzuron – 240 min – upGSTe2 (RR = 0.369)', the IC50 of Ubi-GAL4/WT was not extrapolated which is important as these are the denominator of the RR comparisons. But extrapolation of the IC50 for 'diflubenzuron - upCYP6P3 – 240 min' resulted in a very small RR (mean IC50 test strain / mean IC50 Ubi-GAL4/WT) (Appendix A-iv).

| | | *TESTED STRAIN* | | | | |
|---|---|---|---|---|---|---|
| | | **upCYP6P3** | **upCYP6M2** | **upGSTe2** | **upSAP2** | **Tiassalé** |
| ***COMPOUND*** | **Chlorpyriphos** | – | – | – | – | – |
| | **Fenthion** | – | – | – | – | – |
| | **Malathion** | – | – | – | – | – |
| | **Temephos** | – | – | – | – | – |
| | **Deltamethrin** | – | – | – | – | – |
| | **Permethrin** | – | – | – | – | – |
| | **Bendiocarb** | – | – | – | – | – |
| | **DDT** | – | – | – | – | – |
| | **Diflubenzuron** | $\downarrow\downarrow\downarrow\downarrow^{240*}$ | – | $\downarrow^{240**}$ | – | – |

Table 2.3.2: Differences in susceptibility indicated by the *estimate_EC50()* analysis method.

Predictions are indicated by symbols: ↑ = statistically significant increased tolerance, ↓ = statistically significant decreased tolerance, − = equal susceptibility (no statistically significant difference) when compared to Ubi-GAL4/WT. Increased number of arrows indicates the size of resistance ratio calculated (↑/↓ <10-fold < ↑↑/↓↓ < 100-fold < ↑↑↑/↓↓↓ < 1000-fold < ↑↑↑↑/↓↓↓↓). Superscript details the time point at which significance is indicated. P-vales are represented by asterisks as follows: 0.05 > * > 0.01 > ** > 0.001 > *** > 0.0001 > ****

#### 2.3.1.3 Analysis Method 2 – '*curve.fit()*' function in python

One model which included all of the data could not be made to converge (regardless of starter values and bounds) using the sigmoid equation (Equation 2.2.2) with the *curve.fit()* function. Therefore, nine separate models were made, one for each compound tested. From these models pIC50s (-log10(IC50)) were successfully calculated for 702 (86.7%) of 810 possible comparisons (Appendix A-vi). Appendix A-vi shows the IC50 values with no axis limits and Appendix A-v shows the same data with minimum and maximum limits on the y axis to permit visualisation of the IC50s which were

predicted within the range of concentrations tested. Models could not be fitted for DDT, diflubenzuron and fenthion when the 2-, 60- and 90-min time points were included and so results are not available for these combinations from this analysis. For all other groups, a pIC50 was calculated for every strain (Appendix A-vi). pIC50 calculations were limited by bounds (max pIC50 = -10) and the *p_guess* starter function (pIC50 'guess' = -7) which were set when the model was defined. Despite this, 57 of 288 (19.8%) of mean pIC50s were extrapolated beyond the range of concentrations tested (Appendix A-v). pIC50s that were extrapolated were not evenly distributed between strains, compounds, and time points. 33% of the mean pIC50s of upSAP2 were extrapolated beyond the range of concentrations tested whereas only 8% were extrapolated for Tiassalé. All time points had under 20% of pIC50s calculated outside of the range of concentrations tested except for 2-min exposure which had 41.7% extrapolated. Bendiocarb and deltamethrin both had more pIC50 values extrapolated (47% and 38% respectively) compared to the other compounds tested (range 0% to 21%) (Appendix A-vi).

| | | ***TESTED STRAIN*** | | | | |
|---|---|---|---|---|---|---|
| | | **upCYP6P3** | **upCYP6M2** | **upGSTe2** | **upSAP2** | **Tiassalé** |
| ***COMPOUND*** | **Chlorpyriphos** | – | ↓↓↓↓$^{240**}$ | ↓↓↓↓$^{240*}$ | – | ↓↓↓↓$^{240**}$ |
| | **Fenthion** | – | – | – | – | – |
| | **Malathion** | – | – | – | – | – |
| | **Temephos** | – | – | – | – | – |
| | **Deltamethrin** | ↑↑$^{210*}$ & ↓↓↓↓$^{90*}$ | ↓↓↓↓$^{90*}$ | – | – | – |
| | **Permethrin** | ↑$^{240*}$ | – | – | ↓↓$^{2**}$ | ↑↑$^{210*}$ & ↑↑$^{240**}$ |
| | **Bendiocarb** | – | – | – | – | – |
| | **DDT** | ↑↑↑↑$^{240*}$ | – | – | ↑↑↑↑$^{240*}$ | – |
| | **Diflubenzuron** | ↓↓↓↓$^{240**}$ | – | – | – | – |

Table 2.3.3: Differences in susceptibility indicated by the *curve.fit()* analysis method.

Predictions are indicated by symbols: ↑ = statistically significant increased tolerance, ↓ = statistically significant decreased tolerance, − = equal susceptibility (no statistically significant difference) when compared to Ubi-GAL4/WT. Increased number of arrows indicates the size of resistance ratio calculated (↑/↓ <10-fold < ↑↑/↓↓ < 100-fold < ↑↑↑/↓↓↓ < 1000-fold < ↑↑↑↑/↓↓↓↓). Superscript details the time point at which significance is indicated. P-vales are represented by asterisks as follows: 0.05 > * > 0.01 > ** > 0.001 > *** > 0.0001 > ****.

| Insecticide | Exposure time (min) | Strain | IC50 | df | t | p-value | RR |
|---|---|---|---|---|---|---|---|
| DDT | 240 min | upCYP6P3 | $4.96x10^{-6}$ M | 1.68 | -30.48 | 0.015 | $3.5x10^{4}$ |
| DDT | 240 min | upSAP2 | $4.69x10^{-6}$ M | 1 | -35.8 | 0.0425 | $3.3x10^{4}$ |
| permethrin | 240 min | Tiassalé | $1.46x10^{-6}$ M | 3.94 | -10.04 | 0.003 | 36.7 |
| permethrin | 240 min | upCYP6P3 | $2.85x10^{-7}$ M | 3.17 | -6.49 | 0.015 | 7.14 |
| permethrin | 210 min | Tiassalé | $2.4x10^{-6}$ M | 3.92 | -5.35 | 0.03 | 30.3 |
| deltamethrin | 210 min | upCYP6P3 | $3.25x10^{-8}$ M | 1.95 | -19.15 | 0.015 | 49.88 |
| | | | | | | | |
| chlorpyriphos | 240 min | upCYP6M2 | $3.4x10^{-9}$ M | 3.1 | 9.74 | 0.005 | $5.1x10^{-9}$ |
| chlorpyriphos | 240 min | upGSTe2 | $8.23x10^{-7}$ M | 2.2 | 7.38 | 0.023 | $1.2x10^{-6}$ |
| chlorpyriphos | 240 min | Tiassalé | $5.79x10^{-9}$ M | 3.95 | 8.32 | 0.005 | $8.65x10^{-9}$ |
| deltamethrin | 90 min | upCYP6M2 | $2.02x10^{-10}$ M | 1 | 83.43 | 0.04 | $2.02x10^{-10}$ |
| deltamethrin | 90 min | upCYP6P3 | $3.46x10^{-8}$ M | 1 | 35.45 | 0.045 | $3.46x10^{-8}$ |
| permethrin | 2 min | upSAP2 | $1.2x10^{-10}$ M | 2.01 | 27.51 | 0.005 | 0.0819 |
| diflubenzuron | 240 min | upCYP6P3 | $1.4x10^{-9}$ M | 1.7 | 69.1 | 0.003 | $2.2x10^{-4}$ |

Table 2.3.4: Summary of significant results from *'curve.fit()'* analysis detailing IC50, resistance ratio (RR) and statistical values.

Summary of the comparisons from the '*curve.fit()*' analysis for which the IC50 parameter was found to be significantly different from that of Ubi-GAL4. Statistical values included are the results of a t-test with Benjamini-Hochberg (BH) post hoc correction comparing the IC50 parameters.

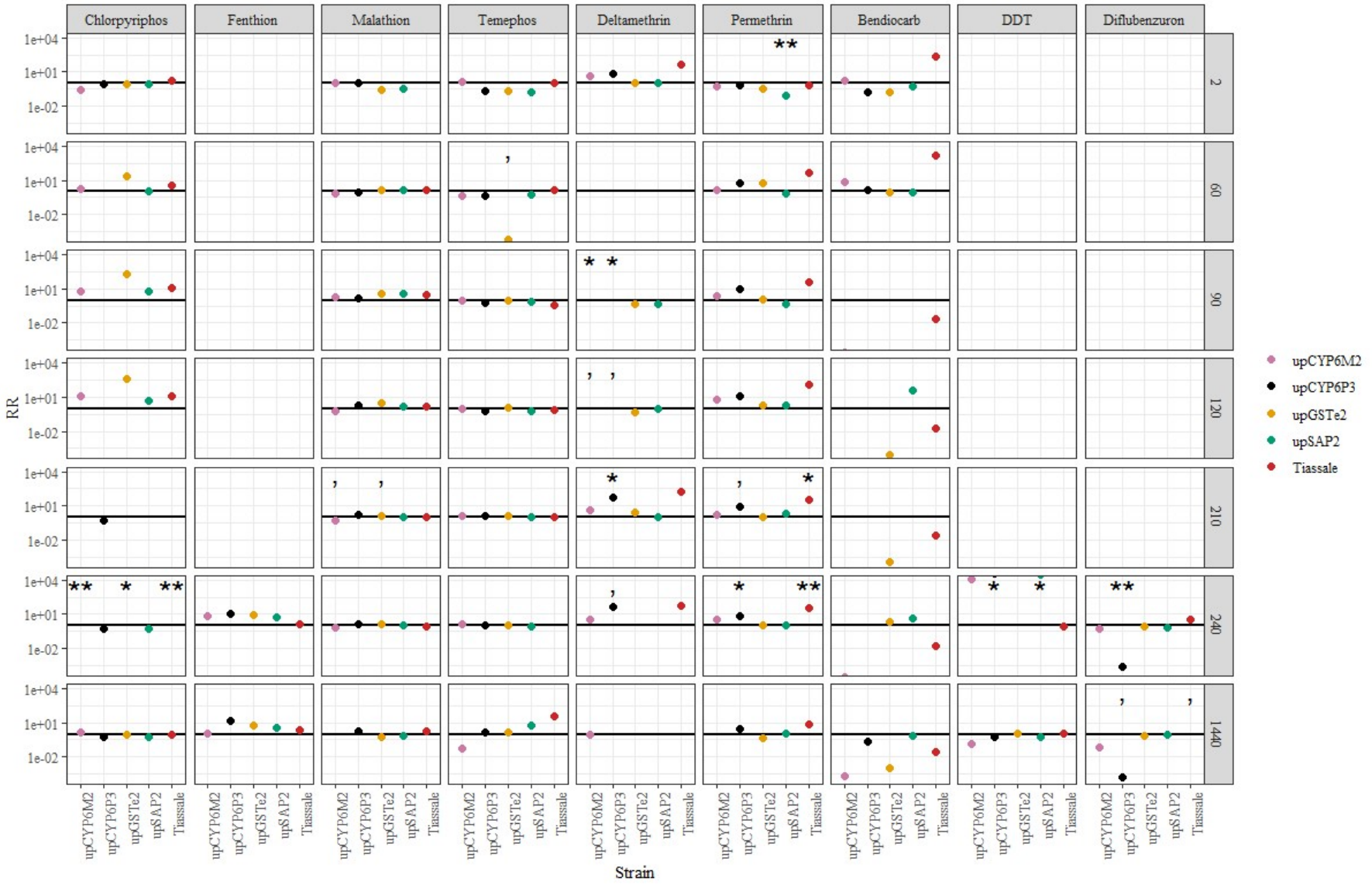
Chlorpyriphos
Fenthion
Malathion
Temephos
Deltamethrin
Permethrin
Bendiocarb
DDT
Diflubenzuron
2
60
90
120
210
240
1440
RR
1e+04
1e+01
1e-02
upCYP6M2
upCYP6P3
upGSTe2
upSAP2
Tiassale
Strain

Figure 2.3.3: RR values comparing IC50 values of Ubi-GAL4/WT with the equivalent for all other strains tested which had been calculated using the *'curve.fit()*'.

Resistance ratios calculated from meanIC50s (calculated using the curve.fit() function from the scip.py package in python) comparing the test strains to the Ubi-GAL4/WT strain, facetted by compound (x) and exposure time (y). y axis limited at 0.001 and 10,000 to permit visualisation of values predicting small differences. Points reflect RR, p-values of <0.1 are reflected: 0.1 > , > 0.05 > * > 0.01 > ** > 0.001 > *** > 0.0001 > ****. Horizontal black line indicates RR = 1 (IC50 strain = IC50 Ubi-GAL4/WT).

pIC50 comparisons and RR calculations of test strains with Ubi-GAL4/WT were possible for all 240 comparisons (missing are those which could not be modelled) (Appendix A-vii, Figure 2.3.3 and Table 2.3.3). 13 comparisons were found to be statistically significant.

6 comparisons of the IC50 parameter with Ubi-GAL4/WT were significant with RRs greater than 1 thus predicting an increase in resistance and significantly increased susceptibility was predicted for 7 comparisons with RRs less than 1 (Table 2.3.4). Appendix A-vii shows the calculated RR values with no axis limits to show all of the data. Figure 2.3.3 shows the same data with y axis limits of 0.001 to 10,000 to permit visualisation of smaller RRs. Table 2.3.3 highlights the size and direction of the differences which are significant.

#### 2.3.1.4 Analysis method 3: 'drm()' function in R

Next, it was investigated whether analysing the data with one model for each compound at a given time point would be a better approach. With this function it was not possible to fit a model which includes all of the data. Therefore, for each compound, a single time point, for which a dose response curve for most strains could be made, which also reflected the raw data best (determined by visual assessment of LOESS curves (Figure 2.3.1) and comparison of raw data to the *drm()* model plots) was selected for this analysis. Note that the time point selected for, and concentration range included in this analysis varied depending on insecticide.

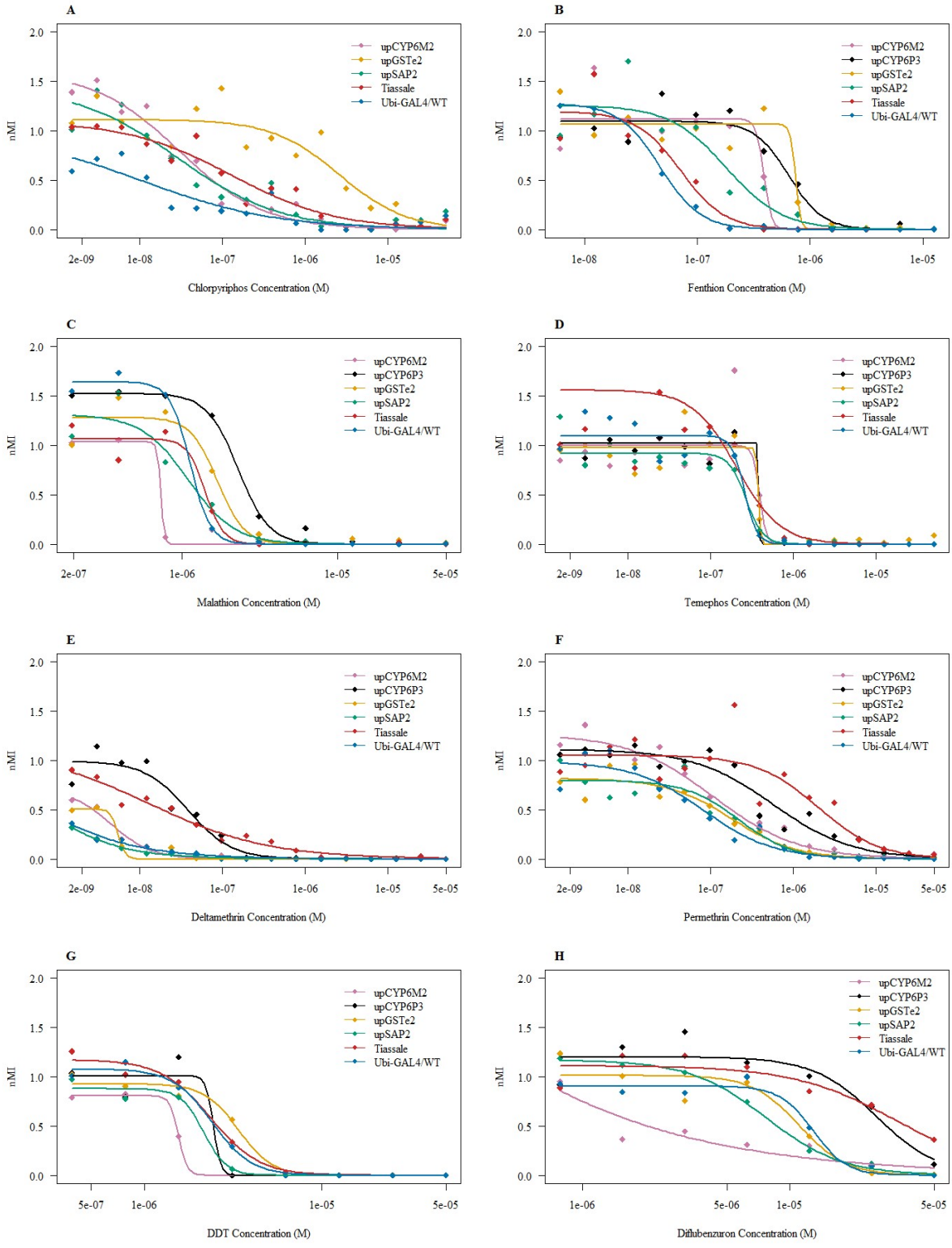


Figure 2.3.4: Dose response plots generated by the *drm()* function LL.3 model for single time points for 8 compounds.

Individual plots for different compounds (time point and concentration range modelled is noted after compound): chlorpyriphos – 90 min, $1.525x10^{-9}$ – $5x10^{-5}$ M (A), fenthion – 240 min, $6.1x10^{-9}$ – $2x10^{-5}$ M (B), malathion - 210 min, $1.95x10^{-7}$ – $5x10^{-5}$ M (C), temephos – 240 min, $1.525x10^{-9}$ – $5x10^{-5}$ M (D), deltamethrin – 210 min, $1.53x10^{-9}$ – $5x10^{-5}$ M (E), permethrin – 210 min, $1.53x10^{-9}$ – $5x10^{-5}$ M (F), DDT – 1440 min, $3.905x10^{-7}$ – $5x10^{-5}$ M (G) and diflubenzuron – 1440 min, $7.81x10^{-7}$ – $5x10^{-5}$ M (H). Points represent mean nMI at each tested concentration. Separate lines and points for each strain tested.

| Insecticide | Concentrations | Exposure time | df | F | p-value |
|---|---|---|---|---|---|
| Chlorpyriphos | $1.525x10^{-9}$ – $5x10^{-5}$ M | 90 min | 12 | 17.99 | < 0.001 |
| Fenthion | $6.1x10^{-9}$ – $2x10^{-5}$ M | 240 min | 15 | 7.38 | < 0.0001 |
| Malathion | $1.95x10^{-7}$ – $5x10^{-5}$ M | 210 min | 15 | 7.46 | < 0.0001 |
| Temephos | $1.525x10^{-9}$ – $5x10^{-5}$ M | 240 min | 15 | 2.36 | 0.0027 |
| Deltamethrin | $1.525x10^{-9}$ – $5x10^{-5}$ M | 210 min | 15 | 38.3 | < 0.001 |
| Permethrin | $1.525x10^{-9}$ – $5x10^{-5}$ M | 210 min | 16 | 9.16 | < 0.0001 |
| DDT | 3.905x10-7 – 5x10-5 M | 1440 min | 15 | 3.98 | < 0.0001 |
| Diflubenzuron | 7.81x10-7 – 5x10-5 M | 1440 min | 15 | 5.32 | < 0.0001 |

Table 2.3.5: ANOVA results from drc package analysis comparing the model including strain as a grouping factor with a model without strain as a grouping factor which was otherwise identical detailing the concentrations and exposure time data included in the LL.3 model.

The 3-parameter log-logistic function (Equation 2.2.3) was identified as the best model for 8 of 9 compounds. No *drm()* model containing Ubi-GAL4/WT could be found (no model function or subset of data could be identified which permitted successful model convergence but the *drm()* function) for bendiocarb at any time point. Also, no model could be found at any time point for upCYP6P3 for chlorpyriphos. Therefore, comparisons for bendiocarb and for upCYP6P3-chlorpyriphos are absent from this analysis. The *drm()* function calculates a p-value to reflect the confidence in the parameters (including IC50) in the model and uses the associated errors when calculating p-values for RRs.

Figure 2.3.4 presents the dose response curves predicted by the model and Figure 2.3.5 presents the RRs for each strain compared to Ubi-GAL4/WT.

| | | ***TESTED STRAIN*** | | | | |
|---|---|---|---|---|---|---|
| | | **upCYP6P3** | **upCYP6M2** | **upGSTe2** | **upSAP2** | **Tiassalé** |
| ***COMPOUND*** | **Chlorpyriphos** | / | – | – | – | – |
| | **Fenthion** | ↑↑$^{240**}$ | ↑$^{240***}$ | ↑↑$^{240**}$ | ↑$^{240*}$ | – |
| | **Malathion** | ↑$^{210**}$ | ↓$^{210*}$ | – | – | – |
| | **Temephos** | – | – | – | – | – |
| | **Deltamethrin** | – | – | – | – | – |
| | **Permethrin** | – | – | – | – | ↑↑$^{210*}$ |
| | **Bendiocarb** | / | / | / | / | / |
| | **DDT** | – | ↓$^{1440***}$ | – | – | – |
| | **Diflubenzuron** | – | ↓↓$^{1440****}$ | – | – | – |

Table 2.3.6: Summary of the differences in susceptibility indicated by the *drm()* analysis method.

Predictions are indicated by symbols: ↑ = statistically significant increased tolerance, ↓ = statistically significant decreased tolerance, − = equal susceptibility (no statistically significant difference) when compared to Ubi-GAL4/WT. Increased number of arrows indicates the size of resistance ratio calculated (↑/↓ <10-fold < ↑↑/↓↓ < 100-fold < ↑↑↑/↓↓↓ < 1000-fold < ↑↑↑↑/↓↓↓↓). Superscript details the time point at which significance is indicated. P-vales are represented by asterisks as follows: 0.05 > * > 0.01 > ** > 0.001 > *** > 0.0001 > ****. '/' indicates that the comparison could not be assessed.

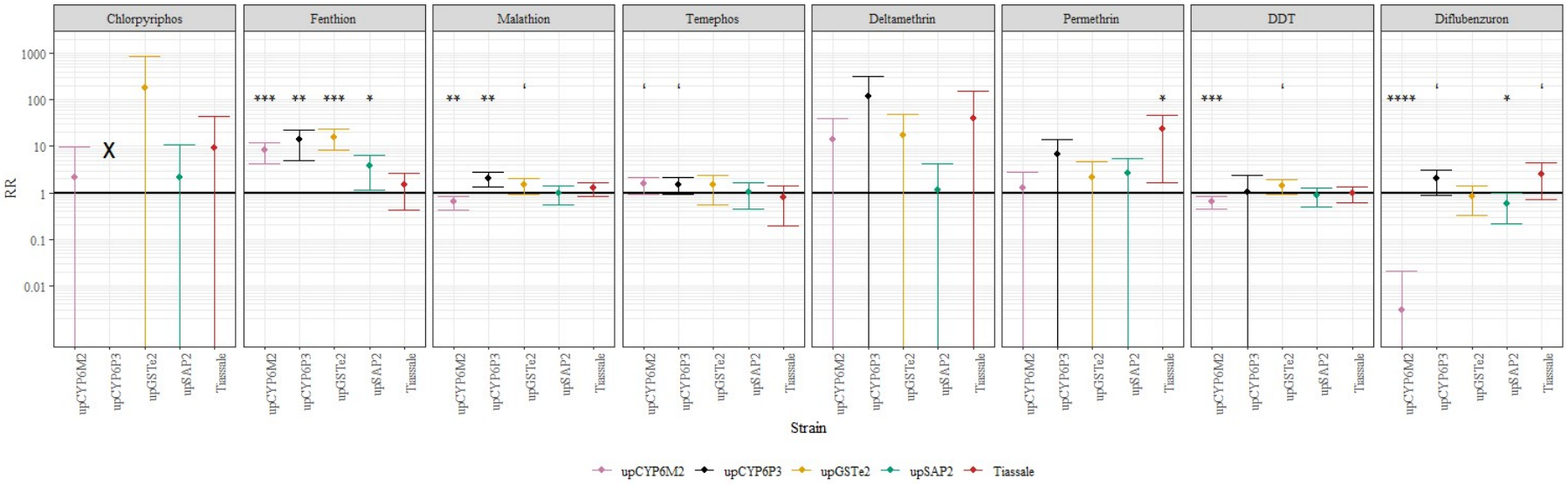


Figure 2.3.5: Plot presenting the RRs (compared to Ubi-GAL4/WT) calculated by the *drm()* function LL.3 model and indicating those comparisons which are statistically significant.

Grouped by compound (time point and concentration range modelled is noted after compound): 'chlorpyriphos – 90 min, $1.525x10^{-9}$ – $5x10^{-5}$ M'; 'fenthion – 240 min, $6.1x10^{-9}$ – $2x10^{-5}$ M'; 'malathion - 210 min, $1.95x10^{-7}$ – $5x10^{-5}$ M'; 'temephos – 240 min, $1.525x10^{-9}$ – $5x10^{-5}$ M'; 'deltamethrin – 210 min, $1.53x10^{-9}$ – $5x10^{-5}$ M'; 'permethrin – 210 min, $1.53x10^{-9}$ – $5x10^{-5}$ M'; 'DDT – 1440 min, $1x10^{-7}$ – $5x10^{-5}$ M' and 'diflubenzuron – 1440 min, $5x10^{-7}$ – $5x10^{-5}$ M'. Points represent RR (mean IC50 test strain / mean IC50 Ubi-GAL4/WT). Black X indicates a strain where a model could not be fitted. Error bars represent 95% confidence intervals (CI). Where lower 95% CI was calculated to be negative (which is illogical) the error bar reaches the x axis. p-values of <0.1 are reflected: 0.1 > , > 0.05 > * > 0.01 > ** > 0.001 > *** > 0.0001 > ****.

In every compound for which a successful model was identified the ANOVA p-value was found to be less than 0.05 indicating a significant impact of strain on the model fit (specifically the slope and IC50 parameters in the LL.3 model used here) (Table 2.3.5). Despite this only in 5 of 8 models was a significant difference in IC50 identified for one or more strain when compared to Ubi-GAL4/WT (Figure 2.3.5, Table 2.3.6). For chlorpyriphos, no significant difference ($p>0.59$ for all strains) was observed for any strain when compared to Ubi-GAL4/WT despite large resistance ratios for some strains (upGSTe2 = 182.3) as the IC50 parameter prediction confidence for Ubi-GAL4/WT was poor ($IC50=1.44x10^{-8}$ M, $p=0.588$) which will impact the confidence in all comparisons. Similarly, deltamethrin susceptibility did not significantly differ in any line when IC50s were compared to Ubi-GAL4/WT ($IC50=3.22x10^{-10}$ M, $p=0.239$). This is again likely due to the fact that the IC50 parameter for Ubi-GAL4/WT was not predicted with confidence. On the other hand, although no significant differences in the IC50 parameter were found compared to Ubi-GAL4/WT ($IC50=2.55x10^{-7}$ M, $p=3.2x10^{-7}$) following 240 min temephos exposure this is not unexpected as the resistance ratios calculated are not large.

Some strains displayed increase resistance to the compounds tested. A significant reduction in fenthion susceptibility compared to Ubi-GAL4/WT ($IC50=4.66x10^{-8}$ M, $p=3.28x10^{-5}$) was observed for upSAP2 (RR=3.86, p=0.0386), upGSTe2 (RR=15.87, p=0.000143), upCYP6M2 (RR=8.32, p=0.000348) and upCYP6P3 (RR=13.84, p=0.0045). A reduction in malathion susceptibility compared to Ubi-GAL4/WT ($IC50=1.12x10^{-6}$ M, $p=9.3x10^{-13}$) was observed for upCYP6P3 (RR =2.04, p=0.0051). A 1.55-fold increase in susceptibility compared to Ubi-GAL4/WT was observed for upCYP6M2 (RR = 0.65, p=0.001).

Conversely, other strains displayed increased susceptibility following exposure to certain compounds. The only significant difference in the IC50 parameter which was observed in permethrin susceptibility compared to Ubi-GAL4/WT ($IC50=8.25x10^{-8}$ M. p=0.0119) was for Tiassalé (RR = 24.16, p = 0.0437). A 1.54-fold increase in DDT susceptibility compared to Ubi-GAL4/WT ($IC50=2.4x10^{-6}$ M, $p=4.42x10^{-11}$) was observed for upCYP6M2 (RR=0.648, p=0.00078). Increased susceptibility,

compared to Ubi-GAL4/WT, was also observed for upCYP6M2 (RR=0.00296, $p<2.2x10^{-16}$) and upSAP2 (RR=0.593, p=0.0364) following diflubenzuron exposure.

### 2.3.2 WHO LARVAL ASSAYS

To follow up on some of the predicted resistance phenotypes detected in the *drm()* function models from the INVAPP analysis, a limited range of manual assays were performed to determine whether similar resistance could be detected in standard WHO assays. The results for each insecticide were modelled by *drm()* using a 2-parameter log-logistic function (Equation 6.4.1) and are plotted in Figure 2.3.6.

In the analysis of the data collected using INVAPP using the *drc* package, upCYP6P3 did not display significant increase in resistance despite strong implications in adult resistance. It is possible that insecticide resistance phenotypes vary between adult and larval stages, so this was investigated further. upGSTe2 was included as permethrin resistance is not associated with GSTe2 upregulation. Approximate F-test ANOVA comparison of LL.2 models with and without grouping data by strain suggests a significant impact of strain on slope and IC50 parameters ($F(4)=42.711$, $P<0.001$). A 7.05-fold increase in RR, compared to Ubi-GAL4/WT ($IC50 = 2.99x10^{-8}$ M), was observed for upCYP6P3 ($p = 0.00046$) but no significant difference was observed for upGSTe2 (RR=1.24, p=0.3557) (Figure 2.3.6A).

To assess whether the INVAPP system is incapable of detecting small differences, a WHO assay using temephos was conducted for comparison. An approximate F-test ANOVA comparison of LL.2 models with and without grouping by strain indicates no significant effect of strain on slope and IC50 parameters ($F(4) = 0.828$, $P = 0.511$). No significant difference was indicated when comparing specific strains: upCYP6P3 (RR = 1.34, p = 0.187) and upGSTe2 (RR = 1.08, p = 0.71) (Figure 2.3.6B).

A

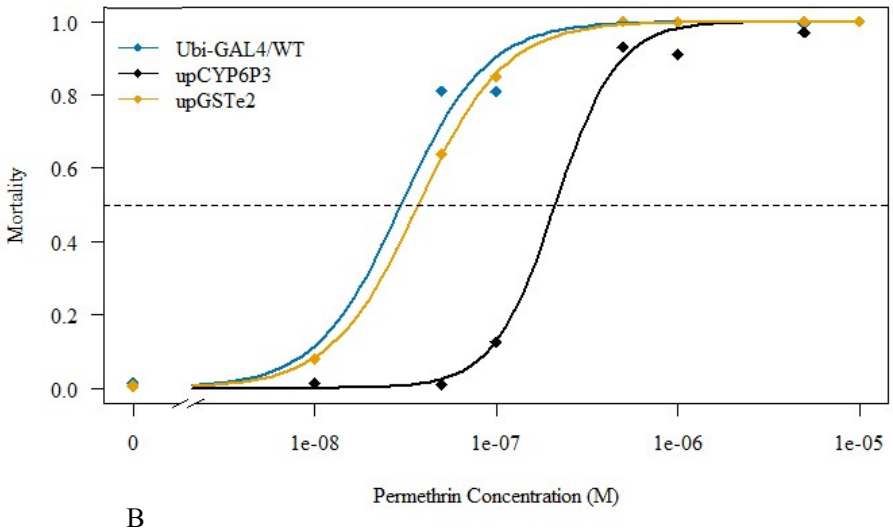
Ubi-GAL4/WT
upCYP6P3
upGSTe2
Mortality
1.0
0.8
0.6
0.4
0.2
0.0
0
1e-08
1e-07
1e-06
1e-05
Permethrin Concentration (M)

B

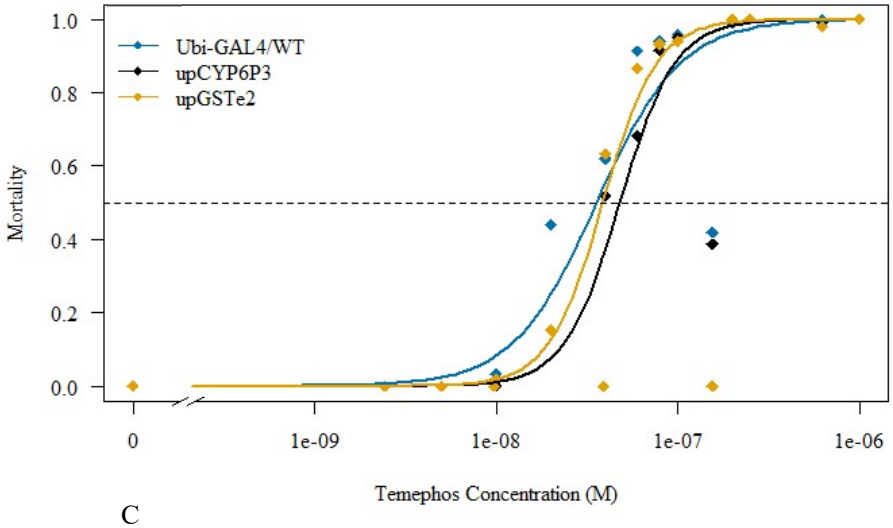
Ubi-GAL4/WT
upCYP6P3
upGSTe2
Mortality
1.0
0.8
0.6
0.4
0.2
0.0
0
1e-09
1e-08
1e-07
1e-06
Temephos Concentration (M)

C

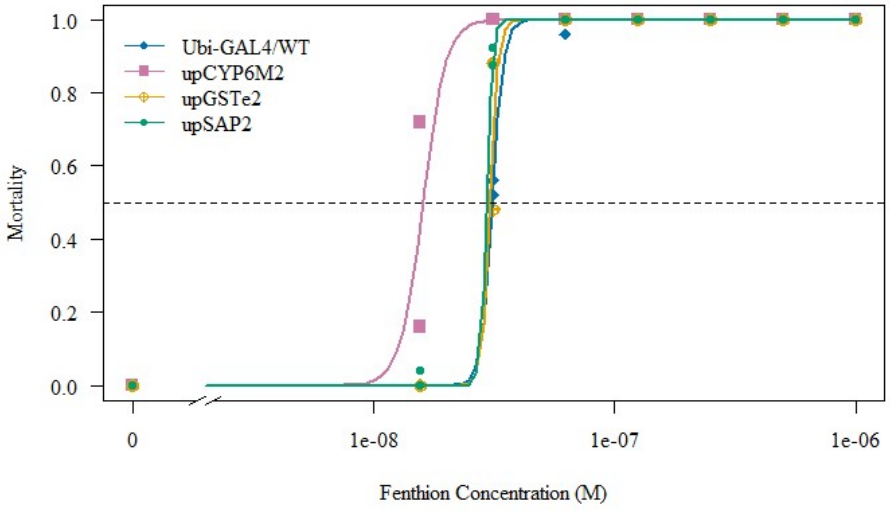
Ubi-GAL4/WT
upCYP6M2
upGSTe2
upSAP2
Mortality
1.0
0.8
0.6
0.4
0.2
0.0
0
1e-08
1e-07
1e-06
Fenthion Concentration (M)

Figure 2.3.6: WHO Assay larval resistance characterization.

Permethrin (A), temephos (B), fenthion (C). All strains were modelled using the LL.2 function in the drc package in R and the fitted curve plotted with mean points for each measured concentration, n=3 (left). Horizontal dashed line indicates y value (0.5) used for calculation of LC50s.

In the INVAPP assay several strains displayed resistance which was not expected for an OP insecticide. For the WHO assay an approximate F-test ANOVA comparison of LL.2 models with and without grouping by strain indicates a significant effect of strain on slope and IC50 parameters ($F(6) = 20.9$, $P<0.001$). Significant increase in susceptibility was detected compared to Ubi-GAL4/WT (IC50 = $3.1x10^{-8}$ M, $p < 2.2x10^{-16}$) for upCYP6M2 (RR = 0.516, $p < 2.2x10^{-16}$) and upSAP2 (RR = 0.947. $p = 0.036$). No significant difference was detected for upGSTe2 (RR = 0.979, $p = 0.247$) (Figure 2.3.6C).

### 2.3.3 WHO ADULT TUBE ASSAY

As part of initial characterisation of the upGSTe2 transgenic line (Adolfi et al 2019), a series of WHO bioassays were performed to follow resistance phenotypes in adults. The data as presented in (Adolfi *et al.*, 2019) is included in Appendix A-viii. Adulticide assays for upCYP6P3, upCYP6M2 and upSAP2 were conducted prior to the start of this project by other lab members. In the context of this project, determining whether the potential resistance observed in INVAPP larval assays to fenthion was shown against a similar adult targeted organophosphate, fenitrothion, was of particular interest.

In the adult assay, the upGSTe2 line displayed less than 90% mean mortality and thus resistance for two compounds (Figure 2.3.7): DDT (mean percentage mortality = 7.37 %, $t(13.8) = 32.56$, $p = 1.93x10^{-14}$) and fenitrothion (mean percentage mortality = 7.72 %, $t(3) = 48.43$, $p = 1.94x10^{-5}$). Reduced sensitivity was also shown against malathion (mean percentage mortality = 89.3 %, $t(5) = 2.04$, $p = 0.097$) but was not significant. No significant difference was detected for bendiocarb (mean percentage mortality = 97.9 %, $t(1) = 1$, $p = 0.5$) and permethrin (mean percentage mortality = 95.7 %,

t(1) = -1, p = 0.5). Statistical analysis could not be conducted for deltamethrin as all values were identical (100% mortality), but it is clear that no difference has been detected here.

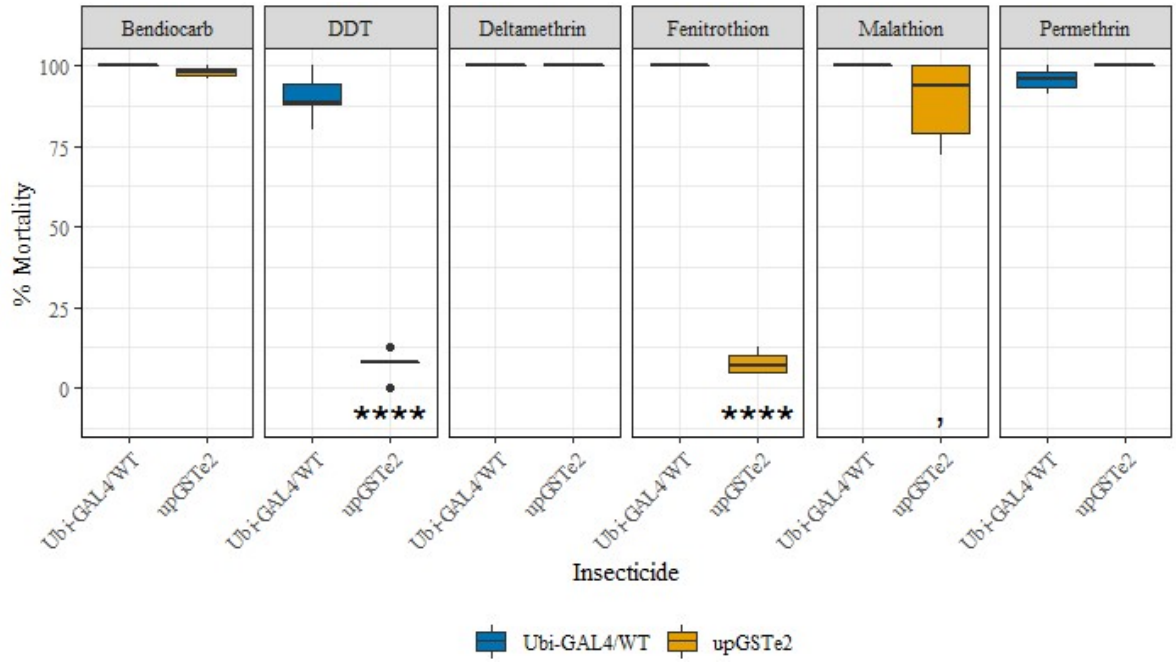


Figure 2.3.7: WHO adult tube assay results (modified from (Adolfi et al., 2019)). Box plots indicate: largest value (plotted as a point if this is greater than 1.5 times the interquartile range from the upper hinge), third quantile, median, first quantile and smallest value (plotted as a point if this is greater than 1.5 times the interquartile range from the lower hinge). p-values of <0.1 are reflected: 0.1 > , > 0.05 > * > 0.01 > ** > 0.001 > *** > 0.0001 > **** > 0.00001.

## 2.4 DISCUSSION

At the beginning of this project, the primary aim of the work was to assess the capabilities of INVAPP to detect subtle differences in resistance between multiple strains of mosquitoes in a high-throughput assay. However, due to a halt in access to the screening platform due to the COVID pandemic, only a limited number of replicate experiments could be performed. As such, much of the work undertaken was to assess different models available to analyse the large dataset produced from even this limited experimentation. Further replication of the experiments described here would have provided a better dataset for a full assessment of the capabilities of the INVAPP system as a high-throughput assay for insecticide resistance detection. However, with the data available, attempts were made to find the 'best' approach for statistical analysis which represents the data most accurately, for as many unique combinations of factors as possible. The results of the most appropriate approaches used are presented in this thesis, and below is a discussion on the experiment analysis and potential changes to the design which may improve the data quality.

### 2.4.1 ASSESSMENT OF ALTERNATIVE DATA ANALYSIS METHODS

Many approaches and variations on the analysis were initially attempted on subsets of the dataset including use of raw MI values (the approach used in (Partridge *et al.*, 2021)), general linear models and generalised linear mixed models (using binomial, Poisson and negative binomial distributions). These approaches proved unsuccessful and so are not presented in detail in the Results but collection and inclusion of data from more experimental replicates (and several other alterations which are discussed later) may well impact considerably on the quality of outputs and predictions of all the models tested. The dose response models which are presented here showed more promise, not only in that the output better reflected the data, but also in the time required to run the analysis. The time required is important when analysing data sets of this size otherwise the high-throughput nature of the method is lost. It is generally best to fit all the data for an experiment in one model as using individual

models can generate inaccurate standard errors for model parameters (Keshtkar, Kudsk and Mesgaran, 2021), but this often is not possible with datasets of this size.

Three different analysis methods are presented here to analyse the large INVAPP data set. Each approach uses a different function in R or python to fit models of common dose-response mathematical equations to the data: 1. '*estimate_EC50()*' four-parameter log-logistic (Equation 2.2.1) in R; 2. '*curve.fit()*' – sigmoid (Equation 2.2.2) in python; 3. '*drm()*' - three-parameter log-logistic (Equation 2.2.3) in R.

First the data was visualised by plotting LOESS curves to give a general representation of the shape of the data for each unique combination of strain, compound and exposure time. From visual inspection of the LOESS curves, predictions were made as to which of the comparisons of the test strains with Ubi-GAL4/WT control may indicate differences in insecticide tolerance. Several possible differences were noted from the LOESS curves (Table 2.3.1 and Figure 2.3.1) and although these predictions do not have a firm statistical basis they have value in identifying where the most likely differences are prior to comparing the output of the statistical models. It was expected that some of these predictions were not found to be significant by the three analysis methods given the variation in the data. However, some of the significant differences that were identified by the *estimateEC50()* and *curve.fit()* functions were unexpected or the opposite of what was predicted from visual inspection of the LOESS curves, and from what would be expected from the known resistance of adults from these strains to some of the tested compounds. Potentially indicating that the models are not suitable.

The only common significant comparison between the LOESS, *drm()* and *curve.fit()* analyses was decreased susceptibility of Tiassalé following 210 min permethrin exposure. For this comparison the RR was similar for *drm()* and *curve.fit()* methods having been calculated as 24.2- and 30.3-fold respectively as was the IC50 at $1.99 \times 10^{-6}$ M and $2.4 \times 10^{-6}$ M respectively. No comparison was significant in both *estimate_EC50()* and *drm()* analyses. We have previously shown the Tiassalé larvae to be resistant to deltamethrin (RR = 10) using an INVAPP assay with 60 min exposure (Buckingham *et al.*, 2021).

#### 2.4.1.1 Analysis method 1 – '*estimate_EC50()*' function in R

Analysis method 1, using the *estimate_EC50()* function, is the fastest of the three methods to complete but provides the least control of model design. IC50s for the entire data set were calculated in one four-parameter log-logistic (Equation 2.2.1) model separated by each unique: replicate, strain, compound and timepoint. When using the *estimate_EC50()* function there is no option to set bounds (limits of the maximum and minimum parameter values) or values for the starter function (estimates of values to guide the model and help it to fit). This does remove some potential investigator bias in determining the limits of the model and potentially influencing the output, which is desirable. However, the inability to plot the dose response curves generated by the model which made comparison of the *estimate_EC50()* model fit with the raw data difficult. Comparing the calculated IC50s with the equivalent LOESS curves allowed crude assessment of whether they were close to the concentration which would be predicted visually. Despite the insensitivity of this approach many very large and obvious errors were identified. Very few results (1.1%) were found to be statistically significant and since a threshold of $p < 0.05$ was used it is possible that this number of significant results would occur through random chance.

The *estimate_EC50()* and *curve.fit()* models both found a significant, very large increase in diflubenzuron susceptibility for upCYP6P3 compared to Ubi-GAL4/WT after 240 min exposure for which visual inspection of the LOESS curves indicates a clear decrease in susceptibility. The IC50 concentrations predicted by both models was much lower than expected suggesting that they have made poor predictions. The LOESS curve for upCYP6P3 only just crosses 0.5 nMI which could contribute to poor model fitting, but it is unclear why the IC50 has been predicted to be so low in both cases. It is possible that the slight hormesis effect has affected the model fit but unfortunately, as the model fits cannot be plotted on top of the raw data it is difficult to ascertain why this is the case. The *drm()* analysis of diflubenzuron was conducted on the data for 1440 min exposure and so the comparisons discussed here were not analysed using the method. The *estimate_EC50()* model also indicated a significant though more modest (0.369-fold) increase in susceptibility of upGSTe2 after 240 min exposure to diflubenzuron which was not predicted from the raw data as the curves of

upGSTe2 and Ubi-GAL4/WT appear to overlap. But the IC50 for both Ubi-GAL4/WT and upGSTe2 were predicted to be ~10-100-fold lower than would be visually estimated from the LOESS curves which suggests some error in the analysis.

Ultimately, no conclusions could be drawn from the *estimate_EC50()* function regarding insecticide resistance as there is little confidence in the accuracy of the very few significant results generated. In its current form despite being the quickest and simplest to conduct, the prevalence of incalculable and extrapolated IC50 values combined with the inability to plot the dose response outcome of the model, make the *estimate_EC50()* function unsuitable for this analysis. The EC50estimator package is relatively new (v0.1.0, released 07.09.2020) so it is possible that updates may improve its functionality but in its current form, despite the speed at which analysis can be conducted, this method would not be recommended for use with INVAPP data sets of this size and complexity.

#### 2.4.1.2 Analysis method 2 – '*curve.fit()*' function in Python

The second programme tested, the *curve.fit()* function, aims to fit a model with a sigmoid equation (Equation 2.2.2), and was the method used in the first publication of the INVAPP analysis method in mosquitoes for calculation of pIC50 ($-\log_{10}$IC50) (Buckingham *et al.*, 2021). The *curve.fit()* function predicted a relative pIC50 for every desired value where a model could converge (86.7%). The plots for this method could not be made with the raw data plotted alongside when time was included in the model. The *curve.fit()* method requires input, by the investigator, of a value estimation plus minimum and maximum limits for pIC50 and slope parameters of the model for the optimizer start function. This is unlike the other methods described here which use self-starter functions which are optimised to the equation used to generate the model. When used here, providing these starting values forced the model to make fewer pIC50 predictions which were extrapolated outside of the range of concentrations. When comparing these pIC50 values with the LOESS plots these predictions are clearly incorrect for 2 min and it is likely that it has made erroneous predictions for many other pIC50 values.

From the *curve.fit()* analysis, 13 comparisons with Ubi-GAL4/WT were statistically significant. However, only four significant comparisons (permethrin-210 min-Tiassalé; permethrin-240 min-upCYP6P3; permethrin-240 min-Tiassalé and deltamethrin – 210 min – upCYP6P3) from this model agree with the predicted differences when looking at the LOESS plots. The significant results of 7 comparisons: 'chlorpyriphos – 240 min – all strains'; 'deltamethrin – 90 min – upCYP6P3'; plus 'diflubenzuron – 240 min – CYP6P3' (which was discussed above) are clearly incorrect as increased susceptibility is predicted while reduced susceptibility is indicated from visual inspection of LOESS plots.

The remaining comparisons indicated significant differences where no difference is indicated on the LOESS curves. As LOESS curves are not a statistical method of analysis and so significant differences of small magnitude which are predicted through modelling could reasonably be correct, even if they are not obvious from LOESS curves. However, where the *curve.fit()* analysis disagrees with the LOESS curve examination, the magnitude of the RRs predicted are generally different by several orders of magnitude or more and so were clearly erroneous. These errors and the inability to fully assess the reasons for them, highlight the importance of comparing the model fit to plotted raw data. In a data set of this size, it is highly likely that poorly fitted plots for a few comparisons (even if the model fits most of the data well) will result in significant results which are wrong.

Unlike the *estimate_EC50()* method, the *curve.fit()* method was able to make some predictions of significant differences which are in line with the predictions from the equivalent LOESS curves, so are thought to accurately reflect differences present in the data. The *curve.fit()* method could potentially be used for analysis of this type of data set but more detailed determination of appropriate starter values and bounds would likely be required for each model generated rather than the same values for each model as was used here. However, this would introduce a further source of investigator bias into the analysis method and increase the time required for data analysis which is undesirable for high-throughput analysis. Without further development the *curve.fit()* method is likely not suitable for analysis of high-throughput INVAPP dose response data, unless perhaps, the data provided was improved considerably by replication.

#### 2.4.1.3 Analysis method 3 – '*drm()*' function in R

The third approach using the *'drm()'* function was unable to fit all data in one model or all of the timepoints in separate models for each compound. Given these limitations, this method was used to plot one timepoint for each compound. Many strain-compound-timepoint combinations could not be modelled (an error was produced by R indicating that the model "could not converge") using this method. Unfortunately, this includes Ubi-GAL4/WT exposed to bendiocarb for all timepoints so this compound could not be assessed using this method. Additionally, for several compounds, to fit models even for the time point with complete curves, the range of concentrations modelled had to be reduced to acquire a model that represented the data well. Despite this, the method has several features which are beneficial for this analysis. The choice of whether to use the self-starter function or to input starter values is good. Where possible the use of a self-starter is preferable, particularly when the analysis may be conducted by inexperienced statisticians, but input of starter values can improve the model fit. Lack of investigator bias is one of the benefits of the INVAPP system over the WHO larval assay and so introducing this bias into the data analysis is undesirable. The drc package also has a very useful plot function with settings for plotting the output of each strain individually or together and alongside the data (with options for all points, average points, error bars etc.) which allows visualisation of how well the model fits for each strain.

The RR for all 9 significant comparisons predicted by the *drm()* function were in the same direction (increased or decreased susceptibility) and with roughly similar magnitudes to what was expected from the LOESS curves. Several of the differences which were predicted from the LOESS plots were insignificant in the *drm()* analysis (most notably for chlorpyriphos) but the model plots are a good representation of the raw data in most cases and so it is expected that this insignificance is due to the insufficiency in replication of the data rather than a failure of the model.

Conducting the *drm()* function analysis, was far more time consuming than the other two methods, only a subset of the data was analysed, and the range of concentrations modelled was reduced for some compounds. This was because in many cases the *drm()* function produced an error (unable to

converge) when the requested model was unable to fit the data (e.g. if the range of nMI values in the data is insufficient or too variable to calculate an IC50). This was common when the curve of the plot was too linear, either when larvae were moving in all concentrations (particularly the 2 min exposure time for all compounds), if all the larvae had stopped moving (died) in most/all concentrations or if the variability at the upper asymptote was too high (often when a hormesis like effect was seen in the LOESS plots). Variability at the upper asymptote was often counteracted by removing some of the lower concentrations from the model which improved the model fit in some cases. The *estimate_EC50()* and *curve.fit()* methods do not produce an error in these situations and instead either make predictions which are often incorrect or do not return a value which carries a higher risk of false significant predictions.

The approach used to calculate the IC50, absolute or relative, also impacts the likelihood of the value being calculated through extrapolation. Particularly, high levels of extrapolation occurred in the *estimate_EC50()* model as only an absolute IC50 (when IC50 is calculated from a defined value of nMI, in this model nMI = 0.5) can be calculated using the *estimate_EC50()* function. The other strategies presented (*curve.fit()* and *drm()*) calculate IC50s relative to the upper and lower asymptotes of each model. This distinction is very important to the resulting IC50. Unlike the WHO larval assay data (which has asymptotes limited between 0 and 100% by experimental plausibility – more than 100% of the mosquitoes cannot die), nMI can plausibly be (and often is) greater than 1. This is because motility (unlike mortality) is not a binary outcome and so it is biologically possible for the larvae in a well to move more after exposure to a compound than before the compound was added. Both approaches are imperfect for this situation however the results indicate that relative IC50s are more appropriate, assuming that the experiment is well designed (the upper and lower asymptotes for all strains reflect complete survival and mortality respectively).

### 2.4.2 COMPARISON OF THE INVAPP RESULTS WITH RESISTANCE DATA FROM WHO LARVAL ASSAYS

Although, using the *drm()* method reduced the number of comparisons in the data which could be analysed and increased the time required for analysis, the results appear to be far more reliable (at least in terms of reflecting the raw data) so it appears this approach should be taken forward for the analysis of further replicates of the experiments. However, this does not mean that the INVAPP data necessarily reflects the resistance status that would be determined by standard WHO larval assays. For example, some of the results which were seemingly accurately predicted by the *drm()* method, did not agree with the WHO assays of 3rd instar larvae. The results for temephos were promising as no resistance was detected in any of the INVAPP analysis or in a WHO larval assay with upCYP6P3 and upGSTe2 when compared to Ubi-GAL4/WT. Similarly, upCYP6P3 displayed permethrin resistance of 7.05- and 7.14-fold in the WHO larval assay and in the *curve.fit()* analysis respectively. A RR of 6.86 was calculated for this comparison using the *drm()* method but the difference was not found to be statistically significant. upGSTe2 permethrin susceptibility was also assessed using a WHO larval assay but no significant difference was found. This is consistent with the results of the INVAPP assay. However, when upGSTe2 and upSAP2 were compared to Ubi-GAL4/WT using the WHO larval assay for susceptibility against fenthion, no significant difference was detected. This is concerning as a significant increase was found for both strains using the *drm()* method to analyse the results of the INVAPP assay. Furthermore, upCYP6M2 was tested in both assays and displayed increased susceptibility in the WHO assay but increased resistance in the INVAPP assay when analysed with the *drm()* method. As the increased resistance in all three strains was clearly visible at several time points in the LOESS curves it is unlikely that this is a poor prediction by the analysis.

Diflubenzuron is one of a limited number of larvicides on the market and so resistance would be of serious concern to those in countries utilizing its mosquitocidal properties for vector control. A resistant CHS allele has been identified in *C. pipiens* (Fotakis et al., 2020) however upregulation of detoxification enzymes has yet to be investigated. Both upCYP6M2 displayed increased susceptibility

to diflubenzuron, which has not been previously documented but could potentially be utilized to combat resistance in areas with CYP6M2 overexpression. Diflubenzuron resistance has only recently been reported for the first time in mosquitoes in *C. pipiens* larvae collected in Italy, where resistance ratio (LC50) increased from 32-fold in 2015 to 128-fold in 2016 (exceeding recommended potable water concentrations) and was attributed to a point mutation in the *Cp*CHS gene (Grigoraki *et al.*, 2017b).

There are several possible reasons that the INVAPP and WHO assays would produce different results for the same strain. First, it is possible that confounding factors have influenced the results of one or both assays. These could include the use of differences in container size, outcome measurement, larval density, exposure time or transport of eggs to a different environment between the two assay platforms. The most likely factors to have influenced the results are the use of different larval stages, measuring different outcomes (i.e., death versus motility - which means that although the INVAPP data may be accurate it may not be measuring 'resistance' as defined by WHO) or the exposure time (e.g., earlier time points in the INVAPP assay could be indicating tolerance which does not ultimately influence 24 hr survival).

This could be studied further by carrying out WHO assays using 1$^{st}$ instar larvae in comparison. Also, the INVAPP assay should be repeated ensuring that the concentrations tested produce 'full' sigmoid curves for all strains at 1440 min as the differences appear to have lessened at this time point on the LOESS curves. Although after this length of exposure the curve for most strains has all nMI values below one which makes assessment of differences more difficult. Another way to investigate the impact of mosquito stage on insecticide resistance is to compare the results here to the results for the same strain exposed to the same or similar compounds as adults.

### 2.4.3 COMPARISON OF INVAPP RESULTS WITH RESISTANCE DATA FROM ADULTS

One of the benefits of using GAL4-UAS lines for this experiment is that they have been very well characterised as adults and require no selection to maintain their resistance profiles, so resistance phenotypes are expected to be consistent across generations. Although the insecticide resistance conferred by expression of the same genes in adults and larvae does not have to be conserved, there are several surprising results in the analysis conducted here. Only the significant results from the INVAPP assay which appear to reflect the raw data are discussed here.

The result indicating that CYP6M2 increases susceptibility, as was observed in adults of the same strain (Adolfi *et al.*, 2019), supports the theory that CYP6M2 could be contributing to the oxidative sulphuration required for malathion activation (Voice *et al.*, 2012). This could be investigated further using metabolomic analyses to quantify the ratio of malaoxon to malathion in mosquitoes upregulating CYP6M2. Tiassalé was found to be significantly resistant to permethrin which was also demonstrated using the INVAPP system previously (Buckingham *et al.*, 2021). Tiassalé is documented to overexpress CYP6P3 and CYP6M2 and carries G119S ACE1 and 1014F *kdr* mutations resistance to pyrethroids, organophosphates and DDT were expected (Williams *et al.*, 2019). However, of the significant results indicated by the drc method these were the only results which supported previous evidence, though it should be noted that for some results there was very little or no prior understanding of the expected phenotype.

Worryingly, several other results conflict with the other evidence available which brings the methods accuracy and specificity into question. upCYP6P3 displayed reduced susceptibility to malathion, suggesting that CYP6P3 overexpression causes increased tolerance to malathion contradicting previous work with this strain which indicates slightly increased susceptibility testing the same strains in the adult stage using WHO Tube assays (Adolfi *et al.*, 2019). CYP6P3 is predicted to metabolize and confer resistance to deltamethrin (Adolfi *et al.*, 2019; Yunta *et al.*, 2019) and permethrin (Djouaka *et al.*, 2008; Muller *et al.*, 2008) and although resistance was indicated in the first two

analysis methods these results were unreliable and the drc method did not indicate significant differences. Meanwhile, upCYP6M2 demonstrated an increase in susceptibility to DDT in the INVAPP assay but CYP6M2 has not been shown to deplete DDT effectively *in vitro* (Adolfi *et al.*, 2019; Yunta *et al.*, 2019).

Ultimately these results bring into question the accuracy and sensitivity of the INVAPP method for detecting resistance phenotypes which are thought to be present. This could indicate an issue with the models used for the INVAPP system or a lack of repetition, but it is also possible that 1st instar larval susceptibility is a poor proxy for adult tolerance to some of the compounds.

### 2.4.4 USE OF INVAPP FOR MOSQUITO LARVAE INSECTICIDE SUSCEPTIBILITY ASSESSMENT

The success of the INVAPP system with parasitic nematodes highlights its potential for compound screening in other motile organisms such as mosquito larvae. The same platform (Figure 2.2.2) with another algorithm (Vectorgon) was highly effective at measuring the motility of both *Ae. aegypti* and *An. gambiae* mosquito larvae for screening toxic compounds (Buckingham *et al.*, 2021). INVAPP has also been used in a high throughput screen of the MMV Pandemic response box against *Ae. aegypti*, identifying camptothecin and its derivatives, topotecan and rubitecan, as having larvicidal properties. Although not included in this thesis, I showed that camptothecin was toxic to adult mosquitoes when included in a blood meal (Partridge *et al.*, 2021). Camptothecin also has known activity against some pest species and has been shown to block Zika virus replication in human cells (Song *et al.*, 2021). Further chemical analysis and modification could potentially develop a related compound which is more suitable for mosquito control in the future. This highlights INVAPPs potential for the identification of compounds from classes previously not used as insecticides for further development. INVAPP is sufficiently high-throughput to screen a 'Pathogen Box library' of ~500 compounds and sufficiently sensitive to distinguish between deltamethrin sensitive and resistant strains in both species (*An. gambiae* – G3 and Tiassalé, *Ae. aegypti* – New Orleans and Cayman, respectively) (Buckingham

*et al.*, 2021). However, assessment of insecticide resistance was only conducted for one compound and two mosquito strains at a time.

The experimental set-up of the INVAPP assay proved to be easily adaptable to screening of many strains and compounds over a wide range of concentrations. Relative to the other methods available for assessment of insecticide resistance in mosquitoes (particularly the WHO larval assay (WHO, 2005)) the INVAPP assay is more efficient in terms of the quantity of data that can be collected in a single day. In one day (10 h) it is feasible to manually collect the results for up to twelve 96-well plates with time points up to 240 min (a 24 h timepoint can be collected the following day). The entire process (including taking the 0 and 2 min timepoint readings and adding the compound) requires ~30 min set up time per plate (by experienced personnel). The use of 96-well plates in the assay permits the use of pipetting systems (e.g., pipetting robots, multi-well and multi-dispensing pipettes) for experimental set up to further increase efficiency. As 96-well plates are smaller than 200 mL pots (each of which is somewhat comparable to one well) and are stackable, the INVAPP assay requires far less physical space than the WHO larval assay. This is important as lack of sufficient bench space can be a limiting factor to the size of WHO larval assay conducted. With robotics, the throughput would increase again.

Another element of the INVAPP assay design which reduces the time required and permits automation is the use of 1$^{st}$-instar larvae in the tests. This reduces the rearing time required by ~4 days (for the strains tested here, exact reduction may vary depending on the strains tested) and they are sufficiently small to be used with standard pipettes for rapid dispensing. The use of 1$^{st}$-instar larvae should reduce the confounding impact of rearing conditions compared to 3$^{rd}$-instar larvae (which are used in the WHO larval assay) as nutrition and density are known to impact insecticide susceptibility in later larvae (Owusu, Chitnis and Müller, 2017). Additionally, as the INVAPP assay includes collection of data prior to compound addition for normalisation, the number of larvae in each well does not need to be accurately measured. The assay performs well when the number of larvae is between 3 and 10 per well (personal communication, data not shown). However, the use of the earlier life stage will likely reduce the lethal concentration, as younger mosquitoes have been shown to be

more susceptible (Ong and Jaal, 2018). Comparisons with the WHO larval assay will also be confounded by the variation in exposure time and the different outcome measurements.

Unlike the WHO larval assay which measures mortality, as INVAPP measures motility it is a real time behavioural assay which uses larval motility as a proxy for mortality. It is important to be aware that some insecticides act through paralysis, and this should be considered when evaluating the results. The normalised movement index (nMI) calculated from an INVAPP experiment is a non-binary measurement of a behavioural characteristic. This facilitates the collection of information about the activity response of larvae to compounds. For example, when exposed to malathion and temephos (and less consistently for fenthion, permethrin and DDT) strains exhibited greater nMIs in the higher concentrations immediately before the descending slope of the dose response curve than in the lower concentrations of the same plot (Figure 2.3.1). This biphasic dose response is suggestive of a hormesis effect caused by these compounds. Hormesis is an adaptive response of biological organisms to a moderate stress which is strongly linked with (though not exclusively to) exposure to toxic compounds (Mattson, 2008). This effect is unlikely to be detected in a binary outcome assay such as the WHO larval assay as typically results are only recorded at a single time point (usually 24 h). In the data collected using the INVAPP system, the hormesis like effect was not reflected well using typical hormesis functions (*BC.4()* or *BC.5()* – Brian-Cousens models) as they either were unable to converge or substantially over predicted the size of the hormesis effect far beyond the data provided to the model. The *mselect()* function in the drc package was used to confirm that the log-logistic models were more appropriate for use with these data despite not reflecting the hormesis effect well. This effect was not investigated further here, but additional replication of the assays would allow more accurate assessment of hormesis, as well as insecticide resistance with this technology.

#### 2.4.4.1 Improvements to experimental design for INVAPP assays

Ultimately, despite the ease of experimental set-up, very little can be concluded from the results of these assays in terms of the impact of the upregulation of the genes tested on insecticide resistance. The *drm()* method (and *curve.fit()* method for some comparisons) may be the best model to use, however the variability observed must be improved to make full use of this high-throughput method for dose response analysis. There are several alterations which could be made to the experimental design and early analysis which may improve the quality of the data and reduce the time required for analysis. Several of these suggestions require further experimentation to test the benefit, but unfortunately it was not possible to do this during this project.

For some compounds, the data may have been improved if the range of concentrations tested was more appropriate for the exposure times. The range of concentrations tested is very important to the calculation of either a relative or absolute IC50 and the likelihood of extrapolated calculations. For example, part of the difficulty in analysing the data for chlorpyriphos (and potentially why some apparent large differences were not significant) was that the only strain with a full sigmoid dose response curve after 60 minutes was upGSTe2. If a range of concentrations were tested in which the strains all survive at the lowest few concentrations at endpoint, the results are likely to be less variable.

There are several possible approaches to addressing the time component of the analysis. One is to focus on a single time point as is used in the WHO assay, which would remove some of the complexity from the analysis. This would be acceptable but would not be utilising the potential of the INVAPP system. A second approach is to collect data for multiple time points but ensure that the time points are evenly spaced, so that the parameter can be treated as a true numerical and not categorical variable. This could help with the analysis and improve the models used but would mean unfortunate working hours in this manual assay. Finally, given more time to study these models it may be prudent to remove the 2 min time point from the analysis, as it clearly does not have a dose response curve, and this may be impacting the fitting of curves at other time points.

Another possibility for improving the quality of the data which does not require further experimentation but could not be conducted here due to patent restrictions, would be to alter the MI extraction algorithm parameters. There are a few options on how this could be altered that may improve the reliability of the output data. For example, the number of images considered could be increased which would smooth the variation in the output. In these experiments, 30 images were taken per image stack, however only 3 images (the first, 15$^{th}$ and last) are used in the extraction analysis. Increasing the number of frames used, however would cause an exponential increase in computing power needed which would be expensive. An alteration to the algorithm which could be assessed without additional computing power would be to change the number of standard deviations (std) from the mean required to meet the threshold for a 'motile pixel'. The number required could be either increased or decreased. For INVAPP analysis of *Caenorhabditis elegans* a reduced threshold of 1 std from the mean is used (Partridge *et al.*, 2018; Faravelli *et al.*, 2019). Reducing the std threshold would most likely result in more 'motile pixels' potentially increasing the sensitivity but also increasing the potential for 'false positives' when a dead larva in a well shifts slightly because of a moving larva in a well. Conversely, increasing the std threshold could result in not detecting slow moving, filter feeding or spasming larvae, thus decreasing the sensitivity of the assay.

A convenient way in which to modify the collection of the data is to increase the time between images of the image stack. In the existing method 30 images are taken at 10 ms intervals. If the time between images was increased to, for example, 50 ms (or potentially longer) the larvae that are moving in the well may have moved further. This would result in a higher MI for larvae that would have been detected moving with 10 ms intervals but may also detect very slow-moving larvae more definitively or larvae which happened not to move in the shorter time frame.

Another change to data collection could be to further increase the number of image stacks (technical replicates) taken at each timepoint. During preliminary optimisation of the INVAPP system for mosquito larvae, the number of image stacks collected was increased from 3 to 10 stacks per plate per timepoint. This number could be increased further to gather a more accurate measure of well motility without substantially increasing the time required to conduct the experiment as image stacks can be

collected around 5 s apart. This could be beneficial particularly for the 0 min time point as variability is higher when the larvae are alive, and this time point is used to normalise all the data derived from that well. It is possible that taking more readings would permit systematic removal of values either with predefined cut offs (e.g., values which are a certain number of standard deviations from the mean) or a system where a set number of the highest and lowest values are removed (e.g., if 20 values are taken the highest and lowest 5 values could be removed). This approach would depend on the MI values for each well and timepoint having a normal distribution to ensure that the data is not being artificially skewed.

Increasing the number of larvae tested could improve the reliability of the data. One solution from an experimental design perspective would be to increase the number of technical replicates conducted for each well in the experiment. Here the experiment was conducted in triplicate but given the variability detected in some cases it may be necessary to increase the number of technical replicates conducted. An alternative would be to increase the number of different larval batches which are tested for each strain.

A large change to the experimental design which could provide a range of different experimental options would be to use large wells (e.g., 6-, 12- or 24-well plates) for the experiment. 6-well plates have been used previously with the INVAPP system for *C. elegans* analysis and permitted analysis of more larvae in one experiment (Faravelli *et al.*, 2019). Increasing the well size could increase the number of larvae tested per well or permit testing of 3$^{rd}$ instar larvae. The high-throughput nature of the assay would be reduced but it may be suitable for routine assays.

### 2.4.5 CONCLUSION

In conclusion, the INVAPP assay is relatively simple to conduct however the analysis of such a large data set was complicated as high levels of variance proved an issue in most instances. This variance caused poor model fitting and insignificant calculation of IC50 concentrations. In the *drm()* method, this prevented model convergence or caused prediction of IC50s with high p-values and in *estimate_EC50()* and *curve.fit()* methods, it resulted in high levels of extrapolated predictions of

IC50/pIC50. The *estimate_EC50()* method is promising in the time in which analysis can be conducted but produced the most unreliable results, so in its current form is an inappropriate method for analysing high-throughput INVAPP data. The *curve.fit()* method appeared to make accurate predictions for a few comparisons that were verified by WHO assays, but is unlikely to be reliable for high-throughput INVAPP analysis, as the starter values and bounds would need to be modified for each model which would introduce a substantial investigator bias. The *drm()* method was identified as likely to be the most reliable method, despite the time required and the inability to analyse much of the dataset. Even so, the results for fenthion disagree with the data from WHO assay and although this may be due to differences in assay design such as larval stage, this should be investigated further before firm conclusions can be drawn about the suitability of the *drm()* method. There is insufficient data available to accurately assess whether larval resistance is a good proxy for adult resistance (or $1^{st}$ for $3^{rd}$ instar larval resistance), so further comparative data is required. Finally, the modifications suggested to improve the experimental design may improve the sensitivity of the INVAPP assay to detect small differences in resistance between mosquito strains.

# *In vivo* phenotypic characterisation of CCEae3A upregulation on insecticide susceptibility using transgenic GAL4-UAS *Anopheles gambiae*

## 3.1 INTRODUCTION

The role of carboxylesterases in conferring OP resistance, as such compounds have become one of the mainstays of chemical larval source management, was investigated. Increasing insecticide resistance is reducing the effectiveness of larviciding programmes and improving our understanding of the mechanisms behind resistance is important for effective insecticide resistance management and developing new control methods (Dusfour *et al.*, 2019). For OP and carbamate insecticides (including temephos) the target is acetylcholinesterase (*ace1*), however, the ACE1 insensitive mutation (G280S), which is widespread in *Anopheles* mosquitoes is uncommon in *Ae. aegypti* and *Ae. albopictus* as the SNP required involves codon usage which is unlikely to occur (Weill *et al.*, 2004). Despite this, resistance to temephos has still been widely detected in *Aedes* mosquitoes and this has been attributed primarily to metabolic resistance. This mechanism is not driving OP larvicide resistance in *Aedes* mosquitoes and so the cause is likely to involve detoxification enzymes.

After reviewing the literature, CCEae3A was identified as the gene with the strongest evidence supporting a role in larvicide resistance, particularly in relation to temephos resistance in both *Ae. aegypti* and *Ae. albopictus* (Poupardin *et al.*, 2014; Grigoraki *et al.*, 2015; Grigoraki *et al.*, 2016; Goindin *et al.*, 2017; Grigoraki *et al.*, 2017a; Seixas *et al.*, 2017; Marcombe *et al.*, 2019).

Overexpression of carboxylesterase enzymes, CCEae3A (AAEL023844) and CCEae6a (AAEL015264), 60- and 29-fold respectively, was first identified in temephos resistant (9.85-fold) *Ae. aegypti* from the Nakhon Sawan (NS) region of Thailand following a control programme using temephos (Poupardin *et al.*, 2014). Several amino-acid polymorphisms were identified in CCEae3A from NS mosquitoes which could play a role in increasing resistance to temephos and other organophosphates (Poupardin *et al.*, 2014).

*Ae. albopictus* orthologues, CCEae3A (AALF007796) and CCEae6a, have also been implicated in temephos resistance as *Ae. albopictus* larvae selected in the laboratory with temephos, displayed upregulation of CCEae3A and CCEae6A (27- and 12- fold respectively using RT-qPCR) which was thought to contribute to a 6.4-fold increase in LC50 (Grigoraki *et al.*, 2015).

CCEae3A was also identified as being overexpressed (2.1-3.4-fold) in *Ae. aegypti* which had not been exposed to temephos on Madeira Island (Portugal) (Seixas *et al.*, 2017) and *Ae. aegypti* from the French West Indies displayed temephos and malathion resistance in which CCEae3A (but not CCEae6A) was overexpressed (19.2 - 60.4-fold) in addition to GSTe2 and several cytochrome genes, (Goindin *et al.*, 2017).

CCEae3A-CCEae6a co-amplification was identified in both *Ae. aegypti* and *Ae. albopictus* (Poupardin *et al.*, 2014; Grigoraki *et al.*, 2015) and amplification of CCEae3A alone was only identified in *Ae. albopictus* (Grigoraki *et al.*, 2017a). CCEae3A copy number has also been correlated with adult malathion resistance in *Ae. aegypti* from Laos (Marcombe *et al.*, 2019).

CCEae3A from both species is expected to sequester and has been confirmed to metabolize temephos from its oxon to its less toxic monoester. An immunolocalization experiment indicated that CCEae3A localises primarily in the nerve cord and malpighian tubules when overexpressed (Grigoraki *et al.*, 2016).

Thus far, all research implicating CCEae3A in resistance to organophosphate insecticides has studied wild-type mosquitoes where CCEae3A was found to be overexpressed following selection with temephos or other insecticides. In all cases other genes were identified as upregulated in addition to CCEae3A and the presence of point mutations were not investigated. It is difficult therefore, to elucidate the precise role that CCEae3A alone has on resistance to temephos and other organophosphates from the available data. The GAL4-UAS system is a well-established tool for assessing the impact of detoxification genes on insecticide resistance in mosquitoes but has been used predominantly for the study of insecticide resistance genes in adults (Lynd and Lycett, 2011; Lynd and Lycett, 2012; Adolfi, 2017; Adolfi *et al.*, 2018; Adolfi *et al.*, 2019; Grigoraki *et al.*, 2020). As in

the Ubi-GAL4 system (Adolfi *et al.*, 2018) in which a polyubiquitin promoter drives GAL4 expression, GAL4 is also highly expressed in larval tissues, it was reasonable to assume its use could be adapted to examine resistance mechanisms in mosquito larvae.

### 3.1.1 AIMS AND OBJECTIVES

The first aim was to functionally characterise the impact of CCEae3A overexpression in an insecticide susceptible background on resistance using the GAL4-UAS binary expression system. A second aim was to characterise the role of CCEae3A overexpression in the susceptibility of adults to insecticides. Finally, the effect of CCEae3A expression on fecundity and longevity were assessed to examine potential fitness costs resulting from overexpression.

# *3.2* METHODS

General methods for plasmid cloning (including details of buffers used), embryo injection, mosquito rearing, insecticide resistance assays and fitness cost assessment are detailed in Appendix D- General Methods.

## 3.2.1 CONTRIBUTIONS

Amalia Anthousi, Fraser Coleman and Dr. Gareth Lycett assisted with mosquito maintenance. Professor Hilary Ranson provided DH10β cells glycerol stock containing a plasmid carrying CCEae3A cDNA for cloning.

## 3.2.2 PLASMID CONSTRUCTION

The insertion plasmid was designed as described in (Poulton *et al.*, 2021). The 1669-bp CCEae3A (AAEL023844-RA) cDNA sequence was amplified from DH10β cells glycerol stock - containing a plasmid carrying cDNA from CCEae3A amplified from the temephos resistant Nakhon Sawan 2 strain (Poupardin *et al.*, 2014; Grigoraki *et al.*, 2016) - using primers CCEfor and CCErev (Appendix B-ix) which carry a 5' extension of 5 random bases plus an EcoRI and XhoI restriction site respectively. The amplified fragment and responder plasmid pSL**attB*:YFP:Gyp:UAS14i:Gyp:*attB* (Lynd *et al.*, 2019) were digested using EcoRI and XhoI (NEB) following manufacturers protocol. The digested responder plasmid was dephosphorylated using rSAP as per manufacturers recommendations following digestion. Both fragments (CCEae3A=1675bp, backbone=7467bp) were isolated by gel electrophoresis and purified as described in Appendix D-xxv and Appendix D-xxvi. The digested plasmid backbone and CCEae3A insert were incubated with T4 ligase (NEB) then transformed into MegaX DH10B™ T1R Electrocomp™ *E. coli* cells (Invitrogen) and selected using 100 μg/mL ampicillin as described in Appendix D-xxix. Positive clones were identified by colony PCR (Appendix D-xxiv) using CCEseqfor and CCErev primers (Appendix B-ix). Correct insertion of

the selected clone of *pSL-attB-YFP-Gyp-UAS-3A-Gyp-attB* was confirmed by sequencing (Appendix D-xxxii) using the following primers: UASp, CCErev, CCEseqfor and CCEseqrev (Appendix B-ix).

### 3.2.3 CREATION OF LINES BY ΦC31-MEDIATED CASSETTE EXCHANGE

150 ng/µL ϕC31 integrase encoding integrase helper plasmid (pKC40) (Ringrose, 2009; Pondeville *et al.*, 2014) and 350 ng/µL responder plasmid were injected into embryos (

Appendix D-xvii) of the docking line Ubi-GAL4 (expressing GAL4 controlled by a ubiquitin promoter, marked with CFP driven by 3xP3 and carrying 2 inverted *attP* sites) (Adolfi *et al.*, 2018). Emerging $F_0$ were screened to select those expressing transient eYFP fluorescence (a variable level of fluorescence at the posterior of larvae that is believed to reflect the amount of plasmid, which was injected into embryos, thus the likelihood of success). These $F_0$ individuals were outcrossed to wild-type G3 in sex-specific founder cages. $F_1$ larvae identified as eYFP (cassette exchange) and eYFP + eCFP (cassette integration) in nerve cord and eye were individually crossed with Ubi-GAL4 or G3 (WT) respectively in excess. PCR was used to confirm cassette orientation was performed after LIVAK DNA extraction (Livak, 1984) of exoskeletons left behind when adults emerge. Orientation confirmation was conducted as in (Adolfi *et al.*, 2019) using ITRL1R, Redseq_4R and piggybacR_R2 (Appendix B-ix).

#### 3.2.3.1 Homozygous cassette 'exchange' line establishment: UAS-3A.hom

UAS-3A (eYFP+) were crossed with Ubi-GAL4 (CFP+) mosquitoes and the F2 progeny screened to isolate individuals with eYFP+/eCFP+ fluorescence (UAS-3A-3xP3-eYFP on one allele, Ubi-GAL4-3xP3-eCFP on the other), which were then intercrossed. The F3 progeny of this cross (which due to mendelian inheritance consists of: 25% eYFP+/eYFP+ with both alleles, 'UAS-3A-3xP3-eYFP'; 50% eYFP+/eCFP+ carrying one of each cassette, 'UAS-3A-3xP3-eYFP_ Ubi-GAL4-3xP3-eCFP'; and 25% eCFP+/eCFP+ with both alleles, 'Ubi-GAL4-3xP3-eCFP') were screened for eYFP+ only fluorescence as these individuals are homozygous for the cassette allowing establishment of a homozygous UAS-3A line (UAS-3A.hom). Homozygosity of this line was monitored through regular

screening for eYFP presence and absence of eCFP. To establish ubiquitous expression of CCEae3A, UAS-3A.hom females were crossed with Ubi-GAL4.hom males. The progeny of these crosses (UAS-3A_Ubi-GAL4) were used for resistance testing and expression analysis.

#### 3.2.3.2 Cassette 'integration' line establishment: Ubi-GAL4:UAS-3A (3A+)

'eYFP+ eCFP+' fluorescent pupae were selected when screening F2 progeny from 'eYFP+ eCFP+ × G3' cross and a stock created. The population was initially maintained as a mixed positives stock (3A+.mix) for several generations (through removal of non-fluorescent individuals at pupal stage) and later a homozygous population established by separating homozygous (3A+/3A+) individuals by intensity of fluorescence (Figure 3.3.3). Homozygosity was successfully confirmed by crossing ~100 3A+/3A+ females with male G3 and ~100 random males with female G3 then screening the progeny for non-fluorescent offspring which would indicate presence of heterozygotes (3A+/WT) in the parental population. When 3A+/WT were required for experimentation 3A+/3A+ males were crossed with G3 females.

### 3.2.4 CCEAE3A TRANSCRIPT EXPRESSION ANALYSIS

#### 3.2.4.1 Sample collection and extraction

For transcriptional and bioassay analysis, UAS-3A.hom were crossed with homozygous Ubi-GAL4 to acquire transheterozygous Ubi-GAL4/UAS-3A progeny which express CCEae3A from single alleles of the driver and responder. When required for experiments homozygous 3A+ (3A+/3A+) were taken from pure stocks, and heterozygous 3A+/WT and WT (WT/WT) were collected when required following YFP based screening (Figure 3.3.3) of an unpurified mix of genotypes that were kept as a backup colony.

Three biological replicates of 3$^{rd}$ instar larvae and adults were collected in pools of 10 and 5 respectively in 1000µL TRIzol Reagent (Invitrogen) then RNA extracted following manufacturers instructions. Turbo DNA-Free kit (Ambion) and oligo(dT) SuperScript III First-Strand Synthesis

System (Life Technologies) protocols were followed for ~5 µg RNA to remove genomic DNA and reverse transcribe ~500 ng RNA respectively.

#### 3.2.4.2 RT-qPCR

1×Brilliant III Ultra-Fast SYBR Green qPCR Master Mix (Agilent Technologies 600882) was used with 3AqPCRfor and 3AqPCRrev (Appendix B-ix) for assessment of CCEae3A transcript quantity. Potential primers were designed using Benchling on either side of intron1-2 (13.8 kb) to permit detection of undesired amplification of genomic DNA. A standard curve was generated using 6 concentrations of cDNA (0.33 ng/µL, 0.11 ng/µL, 0.037 ng/µL, 0.0123 ng/µL, 0.0041 ng/µL and 0.00137 ng/µL) from 3A+/3A+ and WT/WT larvae using MXPro analysis software and a primer pairing which demonstrated amplification of a single product (single peak on dissociation curve), efficiency of 90 – 110 % and R squared > 0.99 in 3A+/3A+ and no amplification in WT/WT samples was selected. Primers qS7fw, qS7rv, qEFfw and qEFrv (Appendix B-ix) were used to quantify the housekeeping genes – ribosomal protein S7 (S7) (AGAP010592) and elongation factor (EF) (AGAP005128). 0.1 ng cDNA was included for each reaction. 3 biological and 4 technical replicates were conducted for each sample and primer pairing.

#### 3.2.4.3 Analysis

Ct values were calculated for all samples at a threshold of dR = 6311 up to a maximum of 35 cycles. The mean Ct (dR) was calculated for technical replicates for all samples and primer sets. Then, the mean Ct (dR) of the house keeping genes (S7 and EF) was calculated for each biological replicate. The ΔCt method was used to adjust CCEae3A mean Ct values with the calculated mean CT in housekeeping genes for each replicate that produced a Ct for all 3 genes. The 2^-ΔΔCt method was then used to compare the expression levels between strains (calculating the fold change expression of the GOI relative to that of a second strain using normalised Ct values which had been adjusted using two housekeeping genes) and a two-tailed t-Test used to assess the significance of the difference. In control samples: Ubi-GAL4/Ubi-GAL4, Ubi-GAL4 /WT and WT/WT, both reference genes

amplified at levels similar to other samples but did not amplify beyond the threshold dR for CCEae3A and so a ΔCt could not be calculated. This is expected as CCEae3A is not expressed in *An. gambiae* and none of these lines carry the transgene for expression. Therefore, mean Ct values (with standard deviation) are reported and two tailed t-tests were used to compare homozygous and heterozygous transgenic samples $2^{-\Delta\Delta Ct}$ values.

## 3.2.5 INSECTICIDE RESISTANCE CHARACTERIZATION

### 3.2.5.1 Larval Susceptibility Assessment

The appropriate volume of temephos, chlorpyriphos or fenthion $1\times10^{-4}$ M stock (dissolved in acetone) to achieve the desired concentrations ($2.14\times10^{-9}$ – $2.14\times10^{-6}$ M, $2.44\text{x}10^{-10}$ – $1\text{x}10^{-6}$ M, $1.37\text{x}10^{-9}$ – $2\text{x}10^{-6}$ M respectively) was added to 200 ml of $dH_2O$ with 25 third-instar larvae. Counting and analysis is described in Appendix D-xix.

### 3.2.5.2 Adult Susceptibility Assessment

#### *3.2.5.2.1 WHO Adult Tube Assay*

WHO tube assays were used initially to test adult susceptibility following Appendix D-xx. Adults were exposed for 60 min to standard diagnostic doses of the following insecticides – malathion, bendiocarb, alphacypermethrin, permethrin, deltamethrin, DDT (4 h exposure as lower exposure times did not kill most of the control adults), fenitrothion (2 h exposure as recommended), pirimiphos methyl, propoxur and dieldrin.

#### *3.2.5.2.2 Adult Tarsal Assay*

Malathion, bendiocarb and alpha-cypermethrin were investigated further using tarsal assays (Appendix xxi). The compounds were dissolved in acetone and tested at concentrations from $3.9\text{x}10^{-4}$ – 0.3 %, $2.56\text{x}10^{-6}$ – 1 % and $2.56\text{x}10^{-7}$ – 0.1 % respectively.

### 3.2.6 FITNESS COST ASSESSMENT

#### 3.2.6.1 Fecundity

This experiment was repeated 3 times with different batches of mosquitoes. For each batch 3 cups of 5 females per strain were tested. Adult female mosquitoes were selected randomly from a cage of approximately 250 adults (5-7 days post emergence) and transferred to 8 oz paper cups. Each batch was armfed, ensuring all individuals had visibly engorged. 3 days later individuals were separated into 50 mL paper cups (covered with net secured with an elastic band), containing 5ml distilled water (+0.1% PondSalt) and lined with Whatman filter paper. The females were allowed to lay eggs overnight. The number of eggs laid was counted the next day and the number of larvae to hatch counted for 48 hours. If no eggs were laid overnight this was noted and those individuals were left to lay for a further night and the same process followed with a day delay.

#### 3.2.6.2 Longevity

This experiment was conducted 3 times, monitoring 5 cups of 10 adults for each sex as is described in Appendix D-xviii.

# 3.3 RESULTS

## 3.3.1 PLASMID CONSTRUCTION

CCEae3A cDNA (1675bp) extracted from adults from the Nakhon Sawan 2 collections in Poupardin *et al.*, 2014 (Poupardin *et al.*, 2014)was cloned into pSL**attB*:YFP:Gyp:UAS14i:Gyp:*attB* (Lynd et al., 2019) to create pSL**attB*:YFP:Gyp:UAS-3A:Gyp:*attB* (

Figure 3.3.2). The selected clone was sequenced, and 7 amino acid changes were identified (Figure 3.3.1) compared to the available vectorbase sequence (AAEL023844). 6 of these substitutions were also identified in sequencing by (Poupardin *et al.*, 2014) for the same strain but the leucine to phenylalanine substitution at codon 4 was not.

```
                          1                                                                                                   100
CCEae3a vectorbase tr... MSTLERVITQLSAGKVQGCKSALPNGNSYCFYRGIPYAKPPVGELRFRPPVALERFEEEVLDCSYERSSCYAYMHFPPTVAVSEDCLYANVYTPIDPTEI
CCEae3a + P135 Sequen... MSTFERVITQLSAGKVQGCKSALPNGNSYCLYRGIPYAKPPVGELRFRPPVALERFEEEVLDCSYERSSCYAYMHFPPTVAVSEDCLYANVYTPIDPTEI
 ....................................................................................................................................

                          101                                                                                                 200
CCEae3a vectorbase tr... ERTIPLPVMVWIHGGGFIAGSGDAAIYGPRYIVQEGVIVVTFNYRLGPLGFLYFPEKGIYGNMGLKDQRFLLKWVQENISKFGGDPDNVTIFGESAGGAS
CCEae3a + P135 Sequen... ERTLPLPVMVWIHGGGFIAGSGDAAIYGPRYIVQEGVIVVTFNYRLGPLGFLYFPEKGIYGNMGLKDQRFLLKWVQENISKFGGDPDNVTIFGESAGGAS
 ....................................................................................................................................

                          201                                                                                                 300
CCEae3a vectorbase tr... CHLQYLCESSRKYFHKAICQSGVAFTVWTEQMDAVSKTRNLAKFVGCVAESDDEIYETLMSAPADDLIAGSEQCVSDLDRSIYRIFAFSPVVEPKESEDP
CCEae3a + P135 Sequen... CHLQYLCESSRKYFHKAICQSGVAVTVWTEQMDAVSKTRNLAKFVGCVAESDDEIYETLMSAPADDLIAGSEQCVSDLDRSIYRIFAFSPVVEPKESEDP
 ....................................................................................................................................

                          301                                                                                                 400
CCEae3a vectorbase tr... FITENYVDILRNPNMTNIPLILGLTSNEAICFIQNLSVELYANDAKLFVPPQLAVPEDRLLQVGEEVKRFYFENRTVSSENLQFLLDFVSDCMFVIPVCV
CCEae3a + P135 Sequen... FITENYVDILRNPNMTNIPLILGLTSNEAICFIQNLSVELYANDAKLFVPPQLAVPEDRLLQVGEEVKRFYFDDRTVSSENLQFLLDFVSDCMFVIPVCV
 ....................................................................................................................................

                          401                                                                                                 500
CCEae3a vectorbase tr... ASELHSRYQHSAPQYFYCFSFEGKSNHIKAMFQNDYQLEGAAHADELTYMFEASFFTTEEMDTDSQEYKIRKAMCRMWTNFAKCGNPTPDEDQLDILWQP
CCEae3a + P135 Sequen... ASELHSRYQHSAPQYFYCFSFEGKSNHIKAMFQNDYQLEGAAHADELTYMFEASFFTTEEMDTDSQEYKIRKAMCRMWTNFAKCGNPTPDEDQLDILWQP
 ....................................................................................................................................

                          501                                                 554
CCEae3a vectorbase tr... VEKIDPDQEKYNIRALDLNEPSKMVDHPFEKRVNFWKRLFEKYGGNYLLHRALQ
CCEae3a + P135 Sequen... VEKIDPDQEKYNIRALDLNEPSKMVDHPFEKRVNFWKQLFEKYGGNYLLHRALQ
 ....................................................................................................................................
```

Figure 3.3.1: *pSL-attB-YFP-Gyp-UAS-3A-Gyp-attB* and vectorbase (AAEL023844) Amino Acid Alignment Sequencing.

Amino Acid translation of CCEae3A in pSL-attB-YFP-Gyp-UAS-3A-Gyp-attB (bottom) aligned to CCEae3A vectorbase sequence (AAEL023844)(top). Mismatched amino acids highlighted in red.

### 3.3.2 CREATION OF LINES BY ΦC31-MEDIATED CASSETTE EXCHANGE

UAS-3A and 3A+ lines were generated in docking line Ubi-GAL4 (eCFP:*attP*) (Adolfi *et al.*, 2018) using site-directed ϕC31 integration by injecting *pSL-attB-eYFP-Gyp-UAS-3A-Gyp-attB* (

Figure 3.3.2), and integrase helper plasmid (pKC40) (Ringrose, 2009). The Ubi-GAL4 line carries 2 inverse attP sequences flanking the GAL4 /CFP cassette. If recombination-mediated cassette exchange (RMCE) occurs at this locus, transgene exchange occurs which results in the UAS-3A-3xP3-eYFP cassette replacing the Ubi-GAL4-3xP3-eCFP cassette (

Figure 3.3.2). This exchange can occur in two potential orientations of the cassette. Alternatively, if only a single *attP* site is involved in recombination with a single *attB* on the donor plasmid, then all of the donor plasmid will integrate next to the Ubi-GAL4-3xP3-eCFP cassette at this locus. Since the locus and donor plasmid carry 2 *att* sites each, this could potentially occur in 4 potential integration orientations (

Figure 3.3.2). If RCME occurs, distinction between exchange or integration can be made in $F_1$ larvae as mosquitoes in which an exchange occured only bear eYFP fluorescence, whereas integration leads to progeny carrying both eCFP and eYFP fluorescence.

Table 3.3.1 summarizes the injection experiments that resulted in successful RMCE events as identified in $F_1$ by eYFP+ (Figure 3.3.3A) and integration events as identified by eYFP+/eCFP+ (Figure 3.3.3B) from progeny of $F_0$ pooled individuals with eYFP+ partial fluorescence.

One eYFP+ (Figure 3.3.3A) $F_1$ female confirmed by PCR to have a successful exchange event in the A orientation from 3A-4 was crossed with Ubi-GAL4, and their progeny interbred (as described in methods) to obtain a homozygous UAS-3A line (

Figure 3.3.2A, Table 3.3.1). One eYFP+/eCFP+ (Figure 3.3.3B) $F_1$ female confirmed by PCR to have a successful integration event from 3A-2 was maintained for analysis (

Figure 3.3.2C, Table 3.3.1). The distribution of eYFP fluorescence displayed by 3A+ pupae was more widespread than normally seen in transgenics produced with the 3xP3 promoter as the ubiquitously

expressed GAL4 transcription factor acts weakly on the 3xP3 promoter driving eYFP expression beyond the normal range of the 3xP3 promoter. Additionally, there is an obvious difference in the intensity of eYFP fluorescence between heterozygous and homozygous

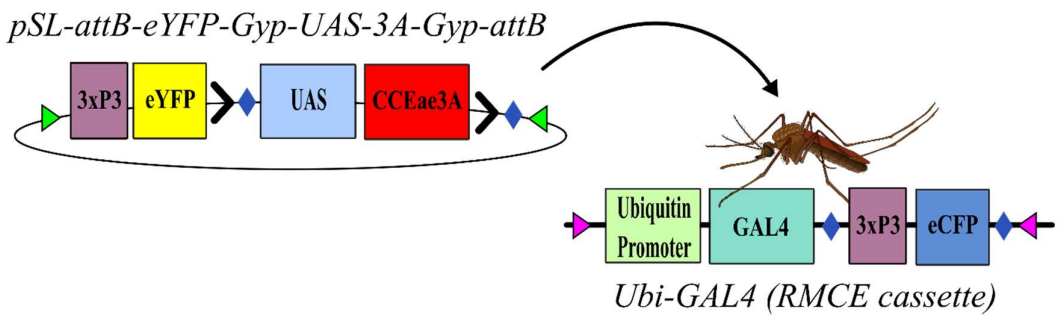


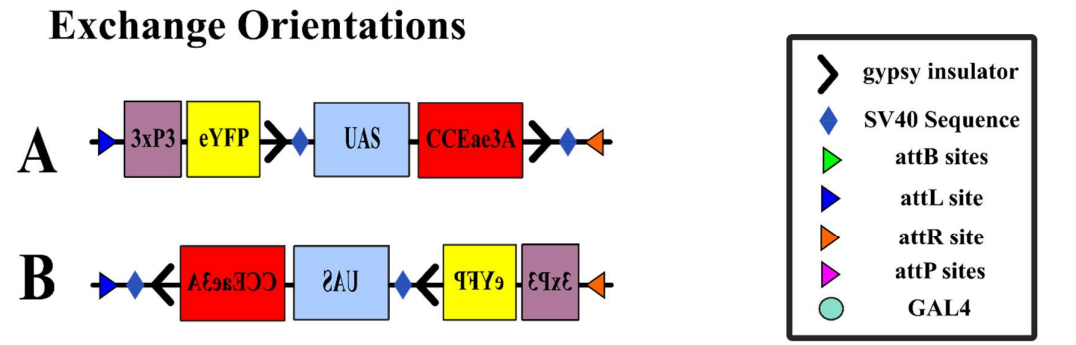


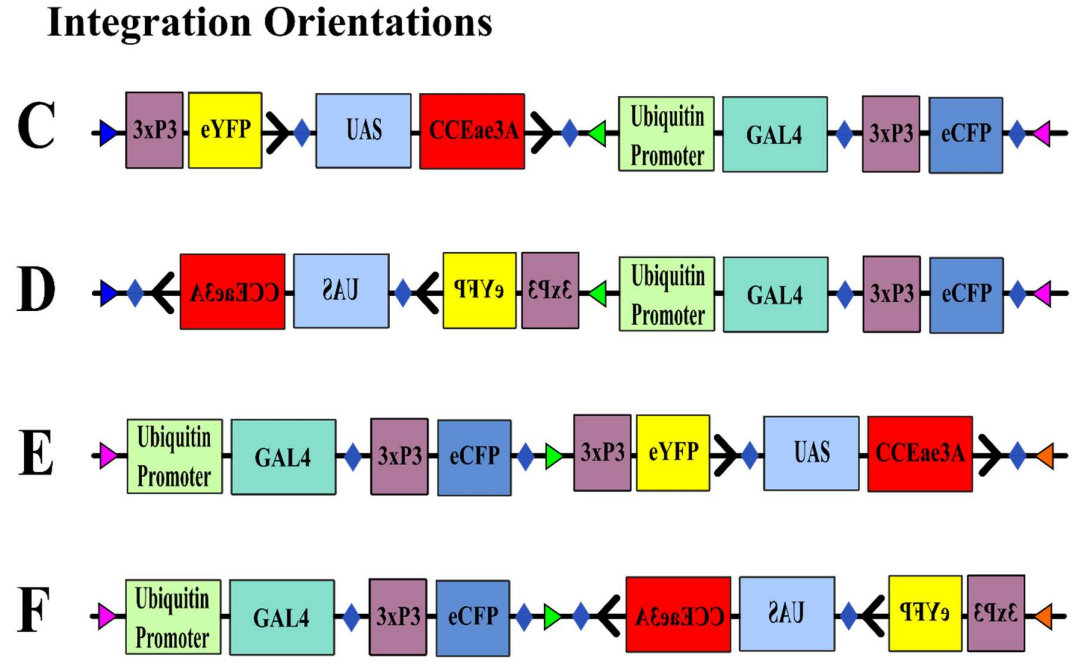


Figure 3.3.2: RMCE cassette structure and orientation possibilities following exchange or integration.

Key details of the *pSL-attB-eYFP-Gyp-UAS-3A-Gyp-attB* plasmid and Ubi-GAL4 RMCE cassettes (Top). Cassettes can insert in six orientations designated: A – forward UAS-3A

(exchange), B – reverse UAS-3A (exchange), C – forward-UAS-3A_Ubi-GAL4 (integration), D – reverse-UAS-3A_Ubi-GAL4 (integration), E – Ubi-GAL4_forward-UAS-3A (integration), F – Ubi-GAL4_reverse-UAS-3A (integration).

states. The fluorescence in homozygote 3A+/3A+ pupae is also more widespread throughout the pupa than in heterozygotes. Wild type pupae display no eYFP fluorescence. This enabled the ready selection of 3A+ homozygotes following inbreeding (Figure 3.3.3B).

Establishment of homogeneous UAS-3A.hom and 3A+/3A+ lines was confirmed when outcrossing to G3 (wild type) failed to produce any eYFP+ offspring (results not shown).

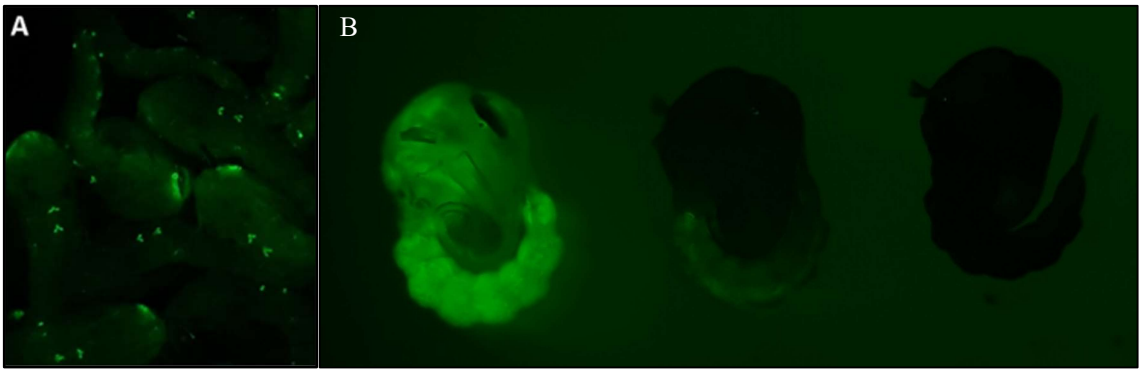


Figure 3.3.3: Images of eYFP fluorescence of CCEae3A GAL4-UAS pupae.
(A) 3xP3-YFP+ Fluorescent UAS-3A.hom pupae and (B) Left = 3A+/3A+, middle = 3A+/WT, right = WT/WT pupae.

| F0 pools (number and sex of positive hatchlings) | F1 Transgenics: Number Identified and sex | | Orientation of Cassette Exchange |
|---|---|---|---|
| | YFP+ (Exchange) | YFP+/CFP+ (Integration) | |
| **Set A: Ubi-GAL4 (154 injected)** | | | |
| 3A-1 (10♂) | 1♂† | 0 | n/a |
| 3A-2 (12♀) | 0 | 1♀ | 1 F1 ♀-C* |
| **Set B: Ubi-GAL4 (175 injected)** | | | |
| 3A-3 (27♂) | 2♀ | 0 | 2 F1 - ♀-A x2 |
| 3A-4 (39♀) | 4♀**, 1♂ | 2♀, 1♂ | 6 F1 - ♀-A x3**, B x1, Dx2 |

Table 3.3.1: Establishment of UAS-3A and 3A+ lines by RMCE strategy for crossing, screening and orientation confirmation.

Each pool refers to a cross of single sex $F_0$ individuals identified with eYFP+ partial fluorescence as larvae crossed with excess G3 of the opposite sex. Highlighted bars indicate the docking line injected, and number of eggs injected (in brackets) for each set of injections that produced successful $F_1$ offspring. Cassettes can insert in six orientations designated: A – forward UAS-3A (exchange), B – reverse UAS-3A (exchange), C – forward-UAS-3A_Ubi-GAL4 (integration), D – reverse-UAS-3A_Ubi-GAL4 (integration), E – Ubi-GAL4_forward-UAS-3A (integration), F – Ubi-GAL4_reverse-UAS-3A (integration) (

Figure 3.3.2). Orientation was determined from $F_1$ individuals. n/a = not applicable. † Did not survive to adulthood. *Indicates the $F_1$ individual used to establish iso-female 3A+ line. **Indicates the $F_1$ individual used to establish iso-female UAS-3A responder line. ♀ = female, ♂ = male.

### 3.3.3 CCEAE3A EXPRESSION ANALYSIS

To confirm and semi-quantify transcription of CCEae3A in the lines, qPCR was conducted on adult and 3rd instar larvae cDNA. Primer pair 3AqPCRfor and 3AqPCRrev were found to amplify a single product and demonstrated efficiency values (107.6%) and R squared (0.994) suitable for expression

analysis with 3A+/3A+ adult samples and no amplification in WT/WT samples at a fluorescence threshold of 6311 dR.

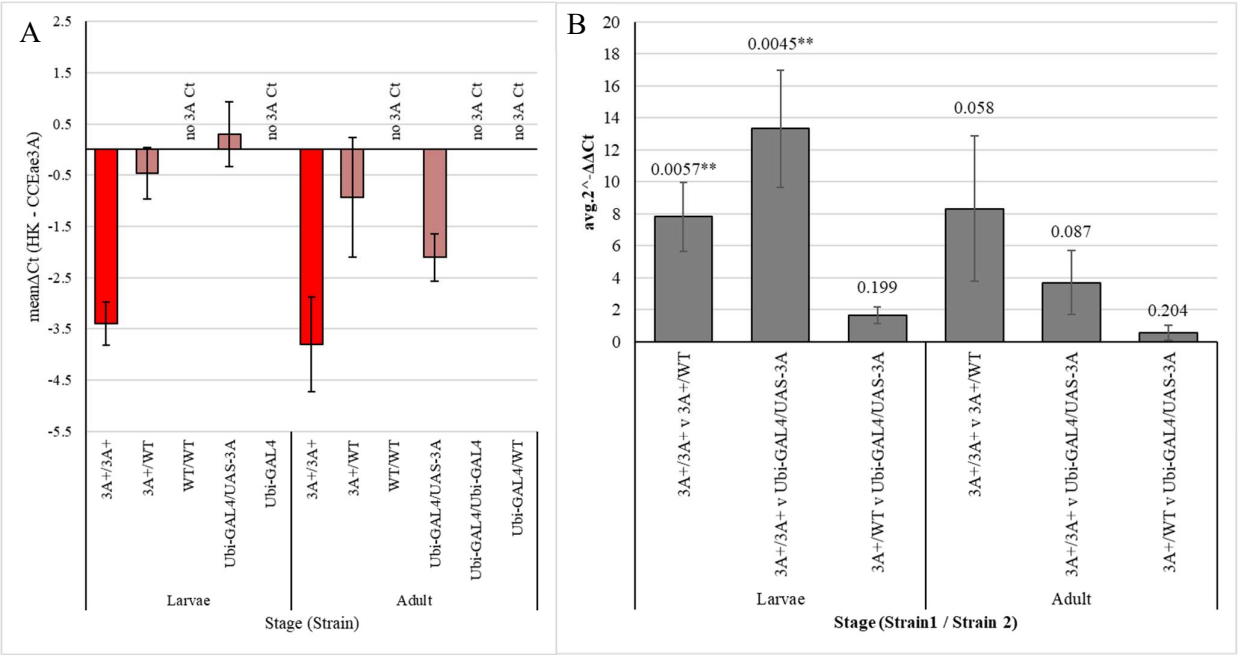


Figure 3.3.4: qPCR results for the CCEae3A GAL4-UAS strains confirming expression of CCEae3A in the genetically modified strains.

mean ΔCt values (mean Ct Housekeeping genes - Ct CCEae3A) of replicates for each stage and strain pairing (A); mean 2^-(ΔΔCt) – comparing the CCEae3A expression between different strains. Values above bars indicate the p-value from a two-tailed t-test (p-value: 0.001 < ** < 0.01 < * < 0.05) (B). Error bars on all plots = ± standard deviation of the mean.

In adult and larvae control samples: Ubi-GAL4/Ubi-GAL4, Ubi-GAL4/WT and WT/WT, both reference genes amplified at levels similar to other samples but did not amplify beyond the threshold dR for CCEae3A and so a ΔCt could not be calculated. Therefore, mean Ct values (with standard deviation) are plotted to demonstrate similar Cts in housekeeping genes (Figure 3.3.4A) and meanΔCt values in Figure 3.3.4B. Whereas CCEae3A was detected in abundance in all genetically modified strains. The Ct values for these strains were analysed using the 2^-(ΔΔCt) method.

To examine if there were significant differences in CCEae3A expression between the genetically modified strains, pairwise comparison of strains for both larvae and adults was performed, and the difference was evaluated using a two-tailed t-test (Figure 3.3.4C). In larval samples, significant increases between 3A+/3A+ and 3A+/WT (7.81-fold, $t(2) = -6.1$, $p = 0.026$) and Ubi-GAL4/UAS-3A (13.31-fold, $t(2) = -5.4$, $p = 0.033$) were detected but the difference between 3A+/WT and Ubi-GAL4/UAS-3A (1.65-fold, $t(2) = -2.2$, $p = 0.16$) was not significant. In adult samples, there was no significant difference between 3A+/3A+ and 3A+/WT (8.31-fold, $t(2) = -2.8$, $p = 0.11$), 3A+/3A+ and Ubi-GAL4/UAS-3A (3.68-fold, $t(2) = -2.2$, $p = 0.16$) or between Ubi-GAL4/UAS-3A and 3A+/WT (2.33-fold, $t(2) = -1.1$, $p = 0.39$).

## 3.3.4 INSECTICIDE RESISTANCE CHARACTERISATION

### 3.3.4.1 Larval Susceptibility Assessment

In order to confirm the expectation that CCEae3A confers resistance to temephos in larval stages the genetically modified strains were tested using a WHO larval assay. From the temephos dose response analysis (*EDcomp*(), drc package, R (Ritz *et al.*, 2015)), LC50s of $1.98 \times 10^{-7}$ M, $4.47 \times 10^{-8}$ M and $3.31 \times 10^{-8}$ M were calculated for 3A+/3A+, 3A+/WT and WT/WT respectively with a 2-parameter log-logistic model (LL.2 - Equation 6.4.1) including strain as a grouping parameter (Figure 3.3.5A).

An ANOVA with approximate F-test comparing this model with a model identical other than removal of strain as a grouping factor was significant ($F(118,114) = 24.8$, $p < 0.001$), indicating that the dose-response curves for the different strains are not identical. 3A+/3A+ overexpression resulted in a statistically significant 5.98-fold increase in LC50 compared to WT/WT ($p = 2.71 \times 10^{-6}$) and 4.42-fold increase compared to 3A+/WT overexpression ($p = 7.53 \times 10^{-6}$) (Figure 3.3.5A). Whereas 3A+/WT overexpression increases LC50 1.35-fold compared to wild type ($p=0.048$) (Figure 3.3.5A, Table 3.3.2).

WHO larval assays to assess temephos resistance were also conducted on the Ubi-GAL4/UAS-3A crosses. LC50 values of $5.01 \times 10^{-8}$ M and $3.57 \times 10^{-8}$ M were calculated for Ubi-GAL4/UAS-3A and

Ubi-GAL4/WT crosses respectively (Figure 3.3.5B). An ANOVA with approximate F-test comparing the LL.2 analysis model with strain as a grouping factor to an identical model without strain as a grouping factor was not significant ($F(142,140) = 2.3$, $p = 0.099$).

As only 3A+/3A+ displayed significant resistance to temephos (Figure 3.3.5, Table 3.3.2) which is similar to ratios in previous studies, this line was used in all further analysis compared to Ubi-GAL4/Ubi-GAL4 control.

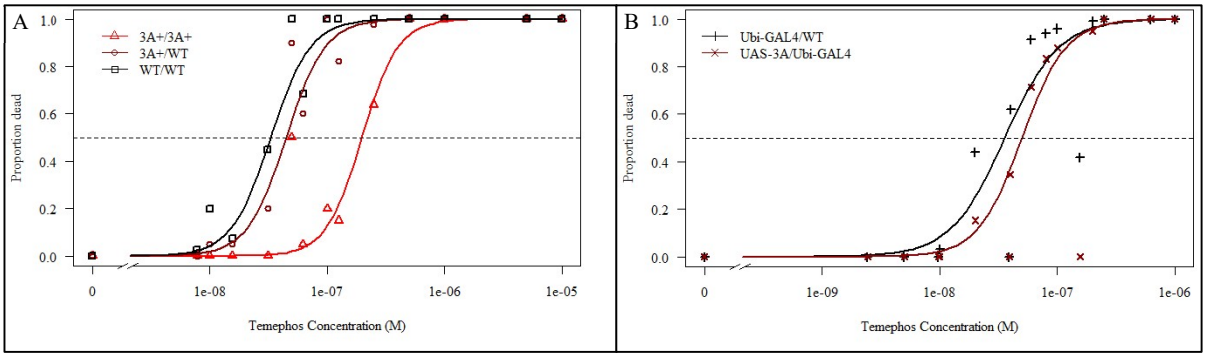


Figure 3.3.5: Temephos WHO larval assay results testing 3rd instar larval susceptibility for strains expressing different levels of CCEae3A.

3A+/3A+ - 'red' (n=2), 3A+/WT – 'dark red' (n=3) and WT/WT – 'black' (n=3) (A). Ubi-GAL4/UAS-3A bipartite system – 'dark red' and Ubi-GAL4/WT – 'black' (n = 5) (B). Horizontal dashed line indicates y value (0.5) used for calculation of LC50s. Points are mean values for tested concentrations.

| Strain 1 | Strain 2 | RR | Std. Error | t-value | p-value | |
|---|---|---|---|---|---|---|
| 3A+/3A+ | 3A+/WT | 4.42 | 0.72915 | 4.6937 | $7.53 \times 10^{-6}$ | *** |
| 3A+/3A+ | WT/WT | 5.98 | 1.00861 | 4.9391 | $2.71 \times 10^{-6}$ | *** |
| 3A+/WT | WT/WT | 1.35 | 0.17612 | 2.002 | 0.04766 | * |
| Ubi-GAL4/UAS-3A | Ubi-GAL4/WT | 1.4 | 0.21974 | 1.8364 | 0.06842 | · |

Table 3.3.2: WHO temephos larval assay resistance ratios (RR) for LC50 and Z-test results.

p value - *** < 0.001 ** < 0.01 * < 0.05 · < 0.1, ns > 0.1

A WHO larval assay was also conducted to assess the effect of CCEae3A expression on chlorpyriphos susceptibility. An LL.2 model including strain as a grouping factor (Figure 3.3.6A) compared to a

model identical without inclusion of strain as a factor using an ANOVA with approximate F-test indicated a significant impact of strain on model fit ($F(92,90) = 244$, $p < 0.01$). LC50s of $1.38x10^{-7}$ M and $2.07x10^{-8}$ M were calculated for 3A+/3A+ and Ubi-GAL4/Ubi-GAL4 respectively. The difference between these LC50s (RR = 6.6) was significant using Z-test ($t = 4.2$, $p = 5.64x10^{-5}$).

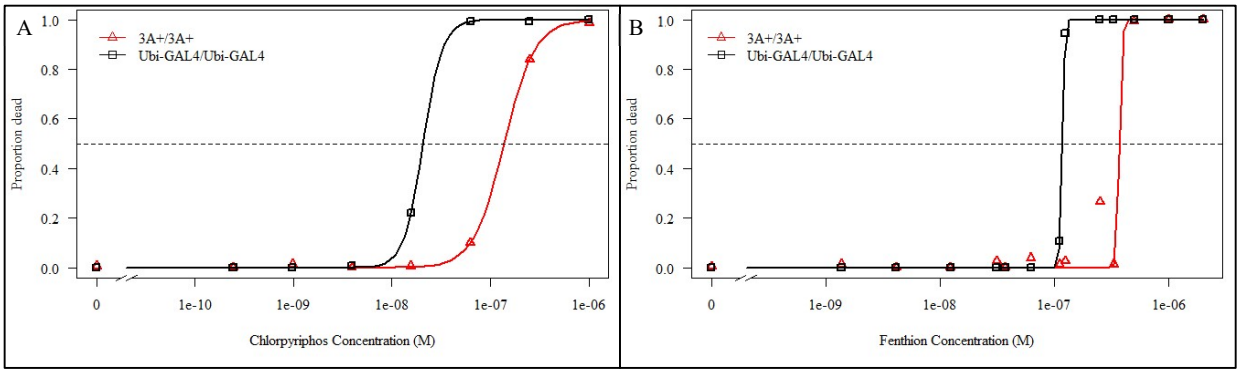


Figure 3.3.6: Chlorpyriphos (A) and fenthion (B) WHO larval assay results. Comparing 3A+/3A+ – 'red', with Ubi-GAL4/Ubi-GAL4 – 'black'. Horizontal dashed line indicates y value (0.5) used for calculation of LC50s. Points are mean values for tested concentrations for chlorpyriphos (n = 6) and fenthion (n=9).

In similar fenthion assays, strain and thus CCEae3A expression was also found to have a significant effect on model fit when a LL.2 model (Figure 3.3.6B) including strain as a grouping factor was compared to an identical model without including strain as a factor using an ANOVA with approximate F-test ($F(142,140) = 650$, $p < 0.01$). The difference between 3A+/3A+ and Ubi-GAL4/Ubi-GAL4 LC50s ($3.7x10^{-7}$ M and $1.2x10^{-7}$ M respectively) was 3.2-fold and was found to be significant using a Z-test ($t = 7.5$, $p = 6.1x10^{-12}$).

#### 3.3.4.2 Adult Susceptibility Assessment

##### *3.3.4.2.1 WHO Tube Assay*

According to WHO guidelines mortality of less than 90% is indicative of resistance which is then confirmed using a Welch's T-test. Full susceptibility in 3A+/3A+ was indicated for pyrethroids –

deltamethrin (98% mortality) and permethrin (99% mortality) – and the organochlorine dieldrin (100% mortality) (Figure 3.3.7). Following exposure to DDT, 3A+/3A+ did display mortality below 90% however this was also observed in Ubi-GAL4/Ubi-GAL4 control samples (Figure 3.3.7). As standard papers were unable to achieve 100% mortality in controls (even following 4 h exposure) the results for DDT remain inconclusive (Ubi-GAL4/Ubi-GAL4 = 94% mortality, 3A+/3A+ = 86% mortality).

Resistance was indicated in 3A+/3A+ to organophosphates: fenitrothion (2% mortality), pirimiphos methyl (4% mortality), malathion (4% mortality) and carbamates: propoxur (6% mortality) and bendiocarb (4% mortality) (Figure 3.3.7). One pyrethroid: alphacypermethrin (90.7% mortality) is defined as inconclusive according to WHO definitions and requires further testing (Figure 3.3.7). Alpha-cypermethrin was thus selected for dose response analysis by variable dose tarsal assays, as despite displaying only marginal resistance by mortality, noticeable increase in the time taken for death during the experiment was observed in 3A+/3A+ individuals compared to Ubi-GAL4/Ubi-GAL4 controls.

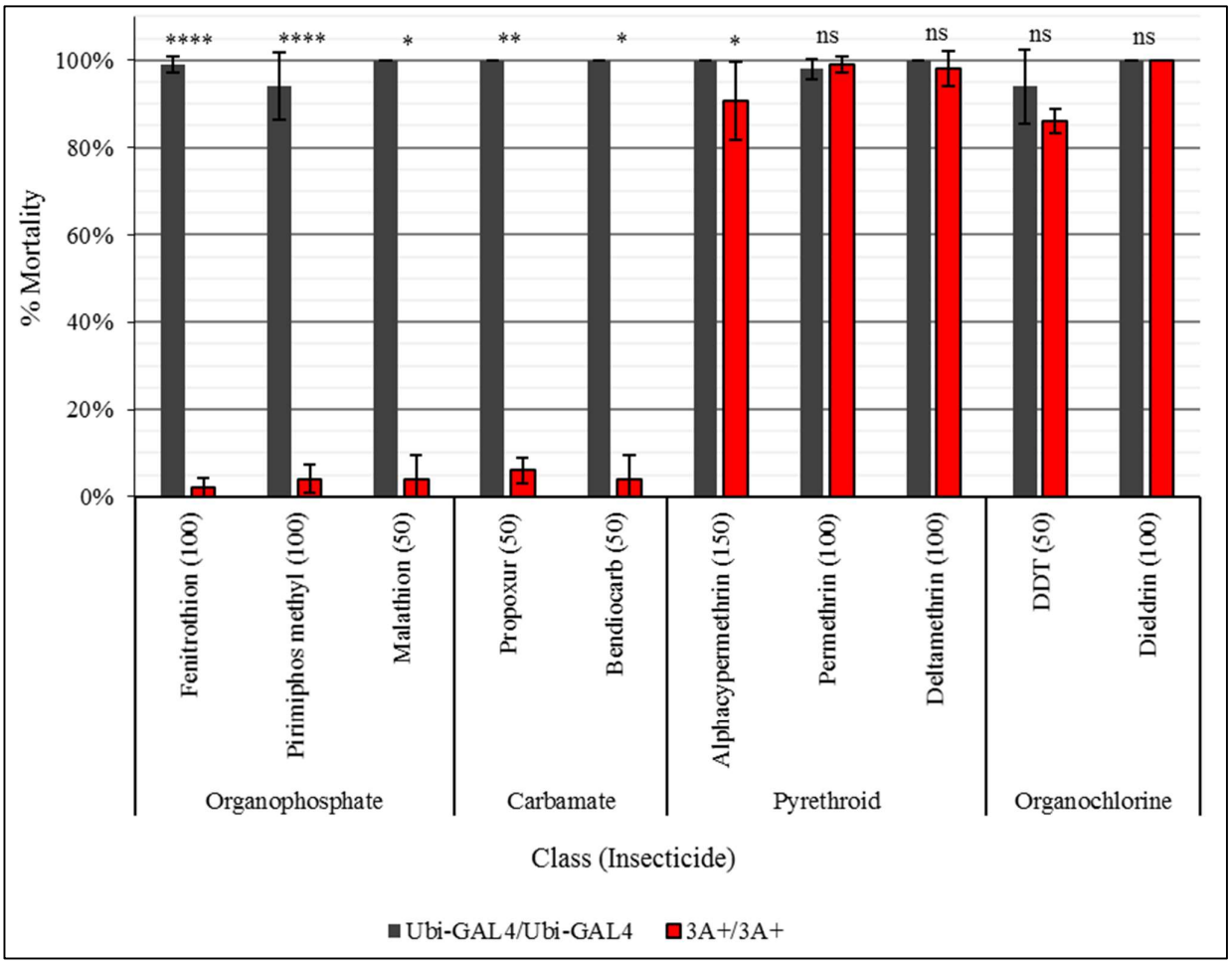


Figure 3.3.7: CCEae3A overexpression leads to resistance against OP and carbamates but not pyrethroids or OCs.

3A+/3A+ = 'red', Ubi-GAL4/Ubi-GAL4 = 'black'. Adults were exposed to all compounds for 1 h except fenitrothion for which the standard exposure time is 2 h and DDT for which a 4 h exposure for which this length of exposure was required to kill most control mosquitoes. Error bars = standard deviation. Star: Welch's T-test (p value - **** < 0.0001, *** < 0.001, ** < 0.01, * < 0.05, · < 0.1, ns > 0.1). Numbers in brackets after compound name indicates the number of mosquitoes tested for each strain (tested in tubes of ~25 females).

*3.3.4.2.2 Dose Response Tarsal Assays*

To quantify the level of resistance conveyed by CCEae3A to adults more accurately, dose response assays were performed for the pyrethroid, alpha-cypermethrin. In addition, malathion and bendiocarb, as representatives of other classes for which resistance was also detected were also assayed. Strain (and thus CCEae3A expression) was implicated as a significant factor in influencing model fit using an ANOVA with approximate F-test for malathion ($F(70,68) = 448.1$, $p < 0.01$), bendiocarb ($F(118,116) = 80.0$, $p < 0.001$) and alphacypermethrin ($F(118,116) = 60.4$, $p < 0.001$) (Figure 3.3.8A-C). For the controls, LC50s of 0.0012 %, $3.79 \times 10^{-5}$ % and $4.58 \times 10^{-5}$ % were calculated for malathion, bendiocarb and alphacypermethrin respectively. Whereas LC50s of 0.0419 %, $7.02 \times 10^{-4}$ % and $4.45 \times 10^{-4}$ % were calculated for 3A+/3A+ for malathion, bendiocarb and alphacypermethrin respectively. Z-test analysis (Figure 3.3.8D) confirmed that the difference between the LC50 of the two strains for each compound was significant. RRs for malathion, bendiocarb and alphacypermethrin were calculated as 35.5, 18.5 and 9.7 respectively (Figure 3.3.8D).

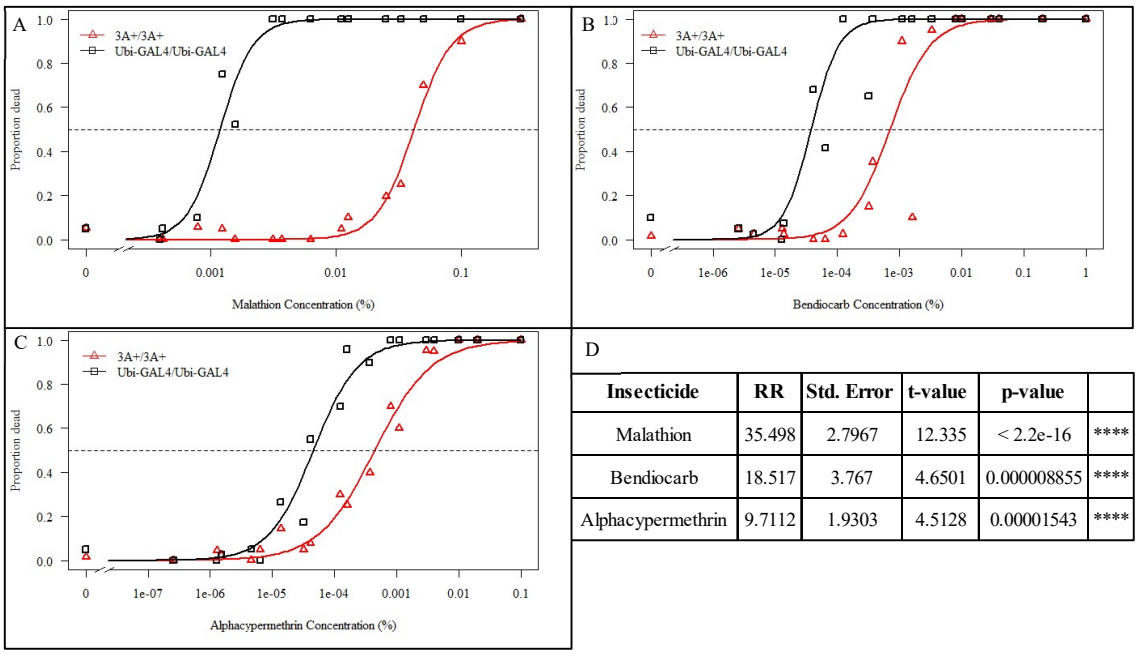


D

| Insecticide | RR | Std. Error | t-value | p-value | |
|---|---|---|---|---|---|
| Malathion | 35.498 | 2.7967 | 12.335 | < 2.2e-16 | **** |
| Bendiocarb | 18.517 | 3.767 | 4.6501 | 0.000008855 | **** |
| Alphacypermethrin | 9.7112 | 1.9303 | 4.5128 | 0.00001543 | **** |

Figure 3.3.8: CCEae3A overexpression tarsal assay results.

Malathion (n=4) (A) and bendiocarb (n =6) (B) and alphacypermethrin (n=6) (C) adult tarsal assay LL.2 model fit plots comparing 3A+/3A+ – 'red', with Ubi-GAL4/Ubi-GAL4 –

'black'. Horizontal dashed line indicates y value (0.5) used for calculation of LC50s. Points are mean values for tested concentrations. (n = 6). Table detailing statistical outcomes of Z-test analysis comparing the LC50 values of 3A+/3A+ and Ubi-GAL4/Ubi-GAL4 (p value - **** < 0.0001, *** < 0.001, ** < 0.01, * < 0.05, · < 0.1, ns > 0.1) (D)

## 3.3.5 FITNESS COST ASSESSMENT

### 3.3.5.1 Fecundity

Several mechanisms of insecticide resistance have been predicted to impact other life history trait of mosquitoes including fecundity and longevity. Figure 3.3.9 displays a summary of the fecundity data for the 3A+/3A+ strain in comparison to the control (Ubi-GAL4/Ubi-GAL4). An independent two-tailed t-test found significant reductions in the mean number of eggs laid (Figure 3.3.9A), number of larvae hatched (Figure 3.3.9B) and the hatch rate (Figure 3.3.9C) in 3A+/3A+ (98.1 eggs, 58.1 larvae, and 48 % hatch rate) when compared to Ubi-GAL4/Ubi-GAL4 (123.6 eggs, 93.7 larvae and 64 % hatch rate). Significance values for the t-tests are indicated in Figure 3.3.9D.

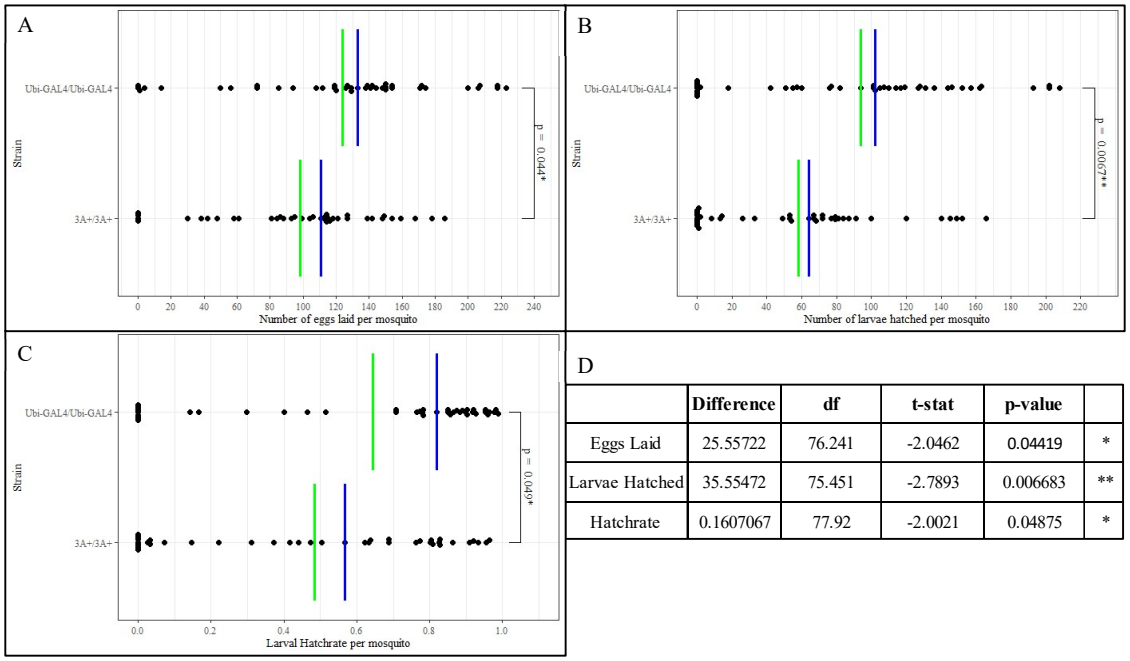


D

| | Difference | df | t-stat | p-value | |
|---|---|---|---|---|---|
| Eggs Laid | 25.55722 | 76.241 | -2.0462 | 0.04419 | * |
| Larvae Hatched | 35.55472 | 75.451 | -2.7893 | 0.006683 | ** |
| Hatchrate | 0.1607067 | 77.92 | -2.0021 | 0.04875 | * |

Figure 3.3.9: Effect of CCEae3A expression on fecundity and fertility

The number of eggs laid (A), number of larvae hatched (B) and proportion of larvae hatched (hatch rate – number of larvae / number of eggs for each female) (C) per mosquito with vertical lines indicating mean (green) and median (blue) and a table reporting the results of an independent two-tailed T-test (D). P-values of this test are also highlighted in individual plots beside brackets (p value - **** < 0.0001, *** < 0.001, ** < 0.01, * < 0.05, · < 0.1, ns > 0.1). Each point = results from an individual female. df = degrees of freedom.

#### 3.3.5.2 Longevity

In longevity assays, significant impacts of both strain (Figure 3.3.10A, p = 0.00018) and sex (Figure 3.3.10B, p = 0.00025) were determined with a log rank test, although only 1 day difference in the median survival time when comparing strain (3A+/3A+ 17 days, Ubi-GAL4/ Ubi-GAL4 18 days) or sex (females 17 days, males 18 days) was found. Log rank tests then confirmed significant differences between 3A+/3A+ and Ubi-GAL4/ Ubi-GAL4 survival curves for both females (Figure 3.3.10C, p = 0.00021) and males (Figure 3.3.10D, p = 0.035). However, no difference in the median survival time was observed for females (17 days) and only one day difference for males (3A+/3A+ 17 days, Ubi-GAL4/Ubi-GAL4 18 days). Although, there are visible differences between the female strain curves, this does not occur at the median (0.5 relative survival probability). Female 3A+/3A+ have almost identical survival until ~ day 17 at which point the rate of death increases above that of Ubi-GAL4/ Ubi-GAL4 leading to 100% death at 26 days, as compared to 30 days for control (Figure 3.3.10C). Whereas male 3A+/3A+ display increased death until ~ 17 days compared to controls. after which point around the same proportion survive until day 29 when only a small proportion (5%) of controls survive (up until 36 days) (Figure 3.3.10D).

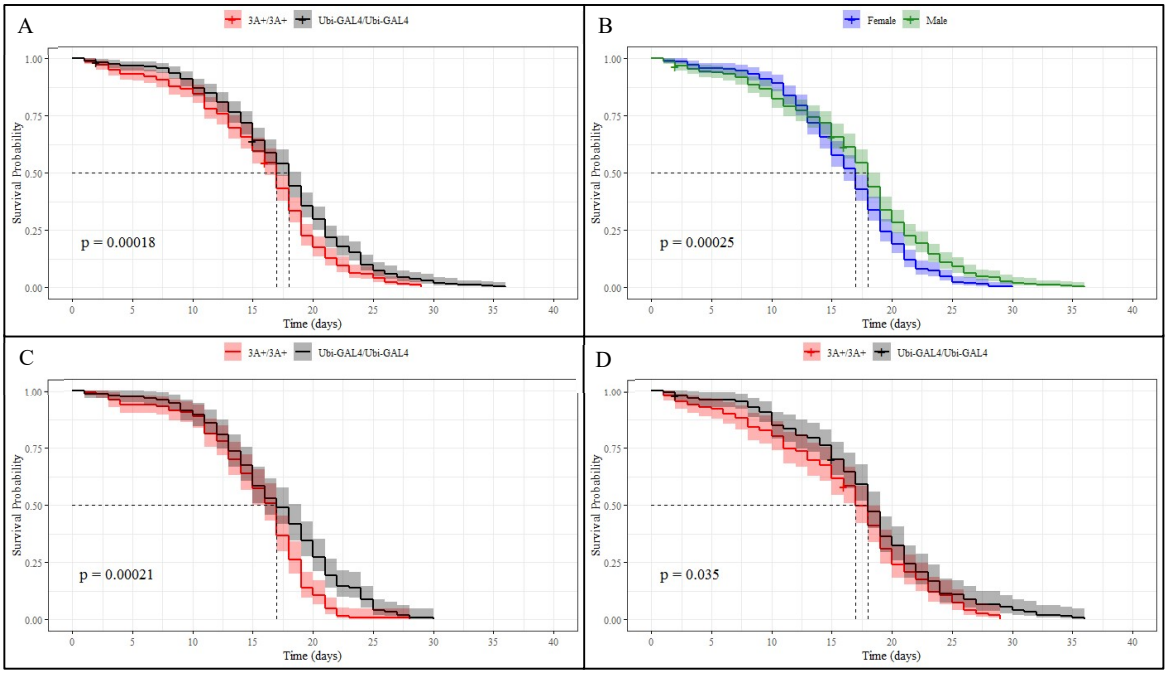


Figure 3.3.10: Longevity Assay Survival Curves.

Kaplan-Meier plots of all data separated by strain (A) all data separated by sex (B) female data separate by strain (C) and male data separated by strain (D). P-values reported are the result of a log rank test comparing the curves in the same panel. Shadows represent the 95% confidence intervals for each day. Dotted line highlights the median survival probability for each plot.

## 3.4 DISCUSSION

### 3.4.1 LINE CREATION AND CCEAE3A EXPRESSION ANALYSIS

Functional characterisation of key resistance mechanisms *in vivo* is crucial to demonstrate causal effects of individual genes on resistance phenotypes. *pSL-attB-YFP-Gyp-UAS-3A-Gyp-attB* plasmid was successfully produced using cDNA from Nakhon Sawan C2 (Poupardin *et al.*, 2014; Grigoraki *et al.*, 2016) for cloning here. This cDNA clone was selected as the Nakhon Sawan C2 strain it was extracted from, demonstrated the strongest temephos resistance phenotype (9.85-fold) of those tested in (Poupardin *et al.*, 2014). When sequenced here, 7 amino acid changes compared to the vectorbase sequence were identified after sub-cloning of *pSL-attB-YFP-Gyp-UAS-3A-Gyp-attB*. One mutation (L4F) which was not present when the gene was sequenced in 2014 (Poupardin *et al.*, 2014) may have been introduced during cloning despite the use of polymerase enzymes with proof reading capabilities. The quality of the sequencing data was good and the peak for the SNP causing the amino acid change is clear so the mutation is not thought to be a sequencing error. However, the new mutation is found in the signal peptide and so would not be expected to alter enzyme activity.

*In silico* structure prediction by (Poupardin *et al.*, 2014) identified that the other 6 SNPs in Nakhon Sawan C2 may result in the folded protein lacking a hairpin loop between Y283 and G293 which may impact OP stabilization in the active site. However, later evidence indicated no difference in kinetic constants for the temephos oxon when recombinant activity derived from the susceptible and Nakhon Sawan C2 clones were later compared. So the mutations are not thought to impact resistance despite the potential structural change (Grigoraki *et al.*, 2016). High-performance liquid chromatography/mass spectrometry analysis of this CCEae3A clone suggested that CCEae3A may preferentially metabolise the less toxic mono-oxygenated form of the temephos oxon but the results were not entirely conclusive (Grigoraki *et al.*, 2016). The Nakhon Sawan C2 clone was selected for the current project as producing the strongest phenotype in the transgenic lines was desirable,

however it could be interesting in the future to conduct similar experiments with CCEae3A derived from a susceptible strain to define the impact of the mutations *in vivo*.

Following RMCE and line establishment, the expression of CCEae3A in all the expected transgenic *An. gambiae* lines was confirmed. *An. gambiae* does not express a known orthologue of CCEae3A and so it is difficult to estimate what level of upregulation there is compared to the *Ae. aegypti* or *Ae. albopictus* counterpart genes. Expression in qPCR experiments is typically analysed using the 2^-ΔΔCt method which first adjusts for the Ct values detected for housekeeping genes (to account for variation in the amount of cDNA added to the reaction) then compares the expression of the gene of interest to comparator (usually control) samples. As it is not possible to divide 'no Ct', this traditional approach was not possible here. The expression level of CCEae3A achieved is at least that of the highly expressed housekeeping genes. As control mosquitoes (Ubi-GAL4/Ubi-GAL4 and Ubi-GAL4/WT) do not express CCEae3A and thus produced no Ct this method was inappropriate.

Instead, the mean Ct values for all strains and genes are presented in Figure 3.3.4A confirming the expression of housekeeping genes. 2^-ΔΔCt results are reported for all comparisons (for the same life cycle stage) of genetically modified lines for adults and larvae. Expression of CCEae3A was detected in all three lines tested (3A+/3A+, 3A+/WT and Ubi-GAL4/UAS-3A) in both adult and 3$^{rd}$ instar larval samples. There was no significant difference in expression between the integration line (3A+/WT) heterozygotes compared with the Ubi-GAL4/UAS-3A transheterozygotes in both adults and larvae. This indicates that there is no effect of having the responder and driver on the same allele. However, significantly increased expression of CCEae3A was detected in 3A+/3A+ homozygous individuals carrying two copies of both driver and responder (range = 3.68 – 13.31 across 4 comparisons with single copy strains). This was surprising as a doubling of expression was expected, though this has not been quantified previously. One possible explanation is that 3A+/3A+ individuals produce twice the number of GAL4 molecules but that this is above a threshold for its breakdown at the same rate of production and as a result GAL4 accumulates over time increasing the production of CCEae3A mRNA. This could be examined by analysis of GAL4 transcript expression and protein presence. Additionally, it would be interesting to generate mosquitoes carrying two copies of GAL4

and one copy of UAS-3A and vice versa through the appropriate crosses to determine which has the most impact on mRNA production.

The possibility of determining the absolute expression of CCEae3A in the transgenic samples was considered but as reports of upregulation in previous publications have only reported differential expression compared to a susceptible strain (Strode *et al.*, 2012; Poupardin *et al.*, 2014; Grigoraki *et al.*, 2017a; Seixas *et al.*, 2017; Marcombe *et al.*, 2019) this was unlikely to provide more clarity on the level of expression here compared to that observed in field resistant strains. Finally, it is important to consider that the differential expression ratio may not directly correlate with equivalent ratios of increasing resistance, if a threshold of expression is required before resistance is conferred.

It should be highlighted that *An. gambiae* was used as a model to express the *Ae. aegypti* CCEae3A gene, since the lab had developed the necessary genetic tools, e.g., GAL4 drivers and RCME lines, in this mosquito species for functional genetic analysis. This does introduce caveats on the generalisation from our model system to *Aedes* mosquitoes. As mentioned, one key difference with relevance to this study is that *An. gambiae* does not express an orthologue to CCEae3A. This means that the transgene transcription level was difficult to meaningfully compare to the 60-fold upregulation reported in Nakhon Sawan 2 *Ae. aegypti* that showed 5.9 – 9.85-fold RR to temephos. In the same strain there was also RR of 29.1-fold reported to permethrin, and many other genes including CCEae6A and several P450s were also found to be upregulated which may also metabolise these insecticides (Poupardin *et al.*, 2014).

In addition, in the transgenic lines, CCEae3A expression is controlled by a polyubiquitin promoter which results in widespread expression throughout the whole body, although not equally in all tissues (Adolfi *et al.*, 2019). In *Ae. aegypti* (Grigoraki *et al.*, 2016) demonstrated through immunohistochemistry that CCEae3A expression is localized to the malpighian tubules and nervous system. The transgenic lines have high expression in the nervous tissue, but is undetectable in the malphigian tubules (Adolfi *et al.*, 2019). These differences in localisation complicate the interpretation of phenotypic impacts but may suggest that malphigian tubule expression of CCEae3A is not critical for resistance to the insecticides tested.

The best approach available at the beginning of this project was employed here but other methodologies which have since been published in *Ae. aegypti* or are used in other insects like *D. melanogaster* could be used to permit CCEae3A expression in the correct tissues in the future. As CRISPR-Cas9 technology has developed rapidly and homology directed repair can now be used in *Ae. aegypti* mosquitoes (Li *et al.*, 2017) it could be possible to over-express CCEae3A in the natural spatiotemporal location through insertion of a construct such as this – 'GAL4-3xP3-RFP-UAS' – directly before the start codon of CCEae3A (so that GAL4 is expressed by the endogenous promoter) or using CRISPRa technology which uses a catalytically dead Cas9 with a transcriptional effector which increases gene expression (Dominguez, Lim and Qi, 2016; Ewen-Campen *et al.*, 2017; Waters *et al.*, 2018) (though this has not yet been published in mosquitoes). The use of model organisms has been crucial to the progress made in the field particularly using transgenics and I believe that this is an appropriate use of a model organism which is very closely related to the organism of interest.

## 3.4.2 LARVAL INSECTICIDE SUSCEPTIBILITY

### 3.4.2.1 Temephos

Temephos is a commonly used chemical larvicide to target *Aedes* mosquitoes in the larval stage (George *et al.*, 2015) and is the main insecticide studied so far as exposure has been demonstrated to select for CCEae3A upregulation. CCEae3A upregulation has been associated with temephos resistance (Strode *et al.*, 2012; Poupardin *et al.*, 2014; Grigoraki *et al.*, 2015; Grigoraki *et al.*, 2017a; Seixas *et al.*, 2017; Marcombe *et al.*, 2019). Only 3A+/3A+ CCEae3A expressing larvae displayed substantial resistance to temephos (5.98-fold change in LC50 compared to controls). Single copy CCEae3A expression by 3A+/WT and Ubi-GAL4/UAS-3A displayed RRs of 1.35 and 1.4 (Table 3.3.2). This indicates that a threshold of CCEae3A expression may be required to confer meaningful resistance to temephos. The temephos resistance observed in the transgenic lines provides further evidence to the predictions made from *in vitro* studies which had shown that CCEae3A is capable of sequestering and metabolising the temephos-oxon (Grigoraki *et al.*, 2016) and upregulation of

CCEae3A correlates with temephos resistance in the NK2 strain (Poupardin *et al.*, 2014). Simulated field assays, using concentrations of temephos which are normally used for insecticide control, have shown that *Ae. aegypti* larvae of similar RR to those generated here will significantly impact the duration of temephos efficacy and the number of mosquitoes caught in the field (Montella *et al.*, 2007).

The LC50 of the NK2 strain (Poupardin *et al.*, 2014) was 50.59 nM (converted from 0.0236 ppm) and the LC50 of the transgenic 3A+/3A+ strain was 198 nM. The 4-fold difference in the LC50 of 3A+/3A+ compared to NK2 could be explained in many ways. There are several differences between the two test species involved which would affect general fitness and thus resistance. These include comparing long-term laboratory reared mosquitoes to recent field acquired strain, the *An. gambiae* background susceptibility compared to that of *Ae. aegypti* and that the NK2 strain is carrying other resistance mechanisms which may increase the susceptibility. Despite this, and the resistance ratio of 5.98-fold in 3A+/3A+ is of a similar magnitude to the resistance ratio found for NK2 (5.90 and 9.85 compared to Phatthalung (wild-type) and New Orleans (laboratory) strains respectively). The magnitude of LC50 calculated for 3A+/3A+ is also similar to that in several other studies where CCEae3A specifically was upregulated in *Ae. aegypti*:

RR = 13 – 36 (LC50s not reported) (Marcombe *et al.*, 2012);

LC50 = 264 – 500 nM, RR = 15.3 – 29.1 (Goindin *et al.*, 2017)

LC50 = 200 nM, RR = 2.31 (Marcombe *et al.*, 2019);

and in *Ae. albopictus*:

LC50 = 103 - 274 nM, RR = 16 – 42.6 (Grigoraki *et al.*, 2015);

Although the RRs are often ~ 3-10 times greater in these latter studies, perhaps indicating other mechanisms are also involved in resistance.

As the most resistant strain generated and easiest to assay (since it didn't involve crosses to generate), the 3A+/3A+ strain was assayed against other further compounds. Use of only this line restricted the

analysis to only one level of overexpression, however due to restrictions on time and space for rearing and experimentation this was the best approach. It could be interesting in the future to study the effect of different levels of CCEae3A overexpression on the insecticide resistance and fitness cost phenotypes which have been identified here, using 3A+/WT or new genetically modified mosquito strains. This is the first instance of this type of GAL4-UAS integration line being used for functional characterisation in mosquitoes (though the strategy was proposed in (Adolfi *et al.*, 2019) and a similar line overexpressing GSTe2 was used for examination of the synergistic relationship between *kdr* L1014F and GSTe2 (Grigoraki *et al.*, 2021).

#### 3.4.2.2 Chlorpyriphos and Fenthion

Larvae of the 3A+/3A+ strain also displayed resistance to both chlorpyriphos (6.64-fold) and fenthion (3.18-fold) OPs. In the published reports on CCEae3A characterisation these insecticides were not assayed, but from the current data it would appear that CCEae3A is active against a range of OPs. Esterase involvement in chlorpyriphos resistance has been implicated by synergist studies on a known resistant line with S,S,S, tributyl phosphorotrithioate (DEF), though the specific genes involved were not identified (Rodríguez *et al.*, 2001). Fenthion also has not been directly linked to CCEae3A upregulation, but again the esterase family have been linked to fenthion resistance in C*ulex* mosquitoes through increased production in resistant strains (Stone and Brown, 1969). The cross resistance to different larvicides caused by CCEae3A is concerning as it indicates quite broad-spectrum activity against insecticidal esters.

### 3.4.3 ADULT INSECTICIDE SUSCEPTIBILITY

#### 3.4.3.1 Organophosphates

In total resistance to six different organophosphate insecticides was shown when CCEae3A is expressed and as such conclude that in areas with CCEae3A overexpression, organophosphate insecticides are highly likely to be less effective as a control tool.

#### *3.4.3.1.1 Malathion*

Consistent with previous reports where CCEae3A upregulation has been correlated with resistance, ubiquitous expression of CCEae3A was sufficient to confer resistance to malathion (Goindin *et al.*, 2017; Marcombe *et al.*, 2019; Balaska *et al.*, 2020; Sene *et al.*, 2021). In tarsal assays 3A+/3A+ displayed 35.5-fold increase in LC50. In further support of this finding in the absence of malathion and temephos resistance, CCEae3A was not found to be overexpressed (Rahman *et al.*, 2021). The combination of malathion and temephos resistance conferred by CCEae3A is concerning as although many countries are adopting rotational or mosaic combinations of different insecticides for insecticide resistance management (Dusfour *et al.*, 2019), these insecticides are often still crucial components due to the lack of alternative effective and approved compounds.

#### *3.4.3.1.2 Fenitrothion*

High levels of fenitrothion resistance (<5% mortality) were observed in WHO assays in the 3A+/3A+ line. In wild caught populations upregulation of CCEae3A by between 1.8 and 11.1-fold have been correlated with fenitrothion resistance (70-90% mortality) in Senegal (Sene *et al.*, 2021). However, a separate study in which fenitrothion resistance was not detected in *Ae. aegypti* from Maderia island which upregulated CCEae3A at 2.1 - 3.4-fold compared to controls (Seixas *et al.*, 2017). In both cases the increase in expression is relatively low. It is possible that a high threshold of CCEae3A expression is required for an individual to survive exposure to fenitrothion, which may be analysed by assaying the heterozygous transgenic lines which have lower levels of CCEae3A expression. In doing so, it must be borne in mind that the ubiquitous expression pattern in the line tested here may not be representative of the field mosquitoes.

#### *3.4.3.1.3 Pirimiphos methyl*

WHO diagnostic resistance (<5% mortality) to the phosphorothioate, pirimiphos methyl, in 3A+/3A+ was also shown. Our study demonstrates though that high levels of CCEae3A expression can lead to

strong pirimiphos methyl resistance. However, a strong link between CCEae3A upregulation and pirimiphos methyl resistance has not previously been demonstrated. While pirimiphos methyl resistance was found in all populations tested in the Senegal study quoted above (Sene *et al.*, 2021), there was not a direct correlation to CCEae3A upregulation as not all the populations had upregulated CCEae3A. Nevertheless, in the Senegal mosquitoes, CCEae3A may have been contributing to resistance, in conjunction with the other mechanisms present (Sene *et al.*, 2021). Since pirimiphos methyl is one of very few newly registered compounds for public health use in IRS, as well as being one of only very few insecticides which is used for both larval and adult (contact and smoke spray) control (WHO, 2016), the emergence of resistance through esterase overexpression may have serious consequences for control.

#### 3.4.3.2 Carbamates

3A+/3A+ mosquitoes also displayed extremely high WHO diagnostic resistance (<7% mortality) to both carbamates, propoxur and bendiocarb, and recorded an 18.5-fold RR for bendiocarb in a dose response tarsal assay. Previous WHO diagnostic resistance to bendiocarb (below 63% mortality) and propoxur (below 78% mortality) has been associated (though not exclusively, as several other mechanisms were also present) with CCEae3A upregulation in the Senegal study (Sene *et al.*, 2021). Bendiocarb resistance (60-75% mortality) has also been observed in the Maderia Island *Ae. aegypti* mosquitoes with slightly upregulated CCEae3A (Seixas *et al.*, 2017), but as nearly 100% mortality was observed when co-exposed with PBO, it was concluded that the resistance was largely the result of P450 metabolism. As with fenitrothion it is possible that the low level of CCEae3A upregulation was not sufficient to confer resistance in the Madeira population. Although we have shown here that high levels of CCEae3A alone can confer strong resistance to bendiocarb. This is the second class of insecticides to which CCEae3A appears to confer resistance to the key members that are used for vector control, reducing the pool of alternative compounds further.

#### 3.4.3.3 Pyrethroids

##### *3.4.3.3.1 Permethrin and Deltamethrin*

In WHO assays 3A+/3A+ displayed full susceptibility to permethrin and deltamethrin despite both compounds containing ester groups. There has been no evidence in previous studies with CCEae3A upregulation that directly contradicts these results (Marcombe *et al.*, 2012; Goindin *et al.*, 2017; Seixas *et al.*, 2017; Marcombe *et al.*, 2019; Sene *et al.*, 2021). In previous studies, pyrethroid resistance in mosquitoes overexpressing CCEae3A was more strongly associated with other classes of known pyrethroid metabolising enzymes which were also overexpressed. These enzymes, particularly P450s are thus more likely to be responsible for reductions in mortality observed previously.

##### *3.4.3.3.2 Alphacypermethrin*

Potential resistance to alphacypermethrin (90.7% mortality) was detected in diagnostic WHO assays, during which it was observed that 3A+/3A+ resisted knockdown for greater time than controls. This phenotype has not been associated with CCEae3A previously. A RR of 9.71 was then confirmed though dose response assays. Alphacypermethrin, which is primarily composed of the most active cis isomers of cypermethrin, contains an ester group which has been shown to be cleaved during toxicity studies in mammals, presumably by carboxylesterases (Pronk *et al.*, accessed: 2021). Alpha-esterases have been implicated in pyrethroid resistance previously in *Ae. aegypti* (Rodríguez, Bisset and Fernández, 2007; Lee *et al.*, 2014) though even in these cases the role of alpha-esterases has been questioned. In previous mosquito studies, when CCEae3A upregulation and alphacypermethrin resistance have been co-detected (Sene *et al.*, 2021) other mechanisms of resistance have also been present and the alphacypermethrin resistance has been attributed entirely to resistance mechanisms such as *kdr* and cytochrome P450 upregulation (Smith, Kasai and Scott, 2016). This raises cause for concern as the focus of research to recover pyrethroid effectiveness is on approaches which circumvent P450 upregulation such as piperonyl butoxide (PBO) (Gleave *et al.*, 2021) or chlorfenapyr (Kouassi *et al.*, 2020) inclusion on bed nets which may not have the desired effect on carboxylesterase

driven resistance. Although most research into combatting pyrethroid resistance has been conducted on *Anopheles* mosquitoes, PBO resistance has been reported previously in *Ae. aegypti* in Florida Keys (Scott *et al.*, 2020). Although, resistance was not detected to permethrin and deltamethrin the alphacypermethrin resistance detected here is concerning, particularly for areas employing mosaic or rotational insecticide use, as this further reduces the number of available alternative insecticides to replace malathion for outdoor spraying measures.

#### 3.4.3.4 Organochlorines

No resistance was detected to dieldrin (and none is expected to DDT though the results were inconclusive) and this is expected as organochlorines do not possess the carboxylester group which is required for hydrolysis metabolism or sequestration. This at least means there is a compound class which does not appear to be impacted by CCEae3A.

CCEae3A has been shown here to confer resistance to all the members tested of two insecticide classes (organophosphates and carbamates) plus alphacypermethrin (a type II pyrethroid) which includes some of the most used compounds for *Aedes* control. Resistance was not detected against permethrin, deltamethrin and dieldrin which is positive, however, *Aedes* control is typically achieved through larval control and pyrethroids and organochlorines are not approved as larvicides as they cannot be used in potable water and are environmentally toxic. Also, control programmes are now encouraged to involve rotation of different insecticide classes to reduce the spread of resistance (Dusfour *et al.*, 2019). This is far less likely to be successful if the pool of insecticides without existing resistance is limited to two compound classes (one of which is reduced by at least one compound in alphacypermethrin) which share a target site. This kind of suboptimal intervention could create a strong selection pressure on the *vgsc* target site resulting in resistance to both classes and compounding control efforts further still.

### 3.4.4 FITNESS COSTS

Although insecticide resistance mechanisms are often selected for due to strong insecticide selection pressure, the upregulation of some enzymes can result in fitness costs that reduce the likelihood of the mechanism reaching fixation or being selected for when insecticides are not present. Reductions in the number of progeny produced which are associated with insecticide resistance can reduce population size and impact the rate at which and potential for a mechanism to become prevalent in a field population. Reduced longevity is particularly important when it is reduced below the minimum incubation time for pathogen spread thus reducing the proportion of the population which survive long enough to transmit pathogens.

#### 3.4.4.1 Fecundity and Fertility

Significant though fairly moderate reductions in egg laying, larval hatching and hatch rate were observed in 3A+/3A+ compared to Ubi-GAL4/Ubi-GAL4 mosquitoes (Figure 3.3.9). These fitness parameters have not been quantified in the GAL4-UAS mosquitoes previously generated in the lab. The moderate nature of the reduction did not impact our ability to maintain a stable laboratory colony, although, it is clear that the very high levels of CCEae3A expressed in these mosquitoes impacts fitness in comparison to those mosquitoes only expressing GAL4. It is difficult to assess how relevant this is to natural populations that are likely to produce much less CCEae3A.

Previous work had noticed a negative association between fecundity and temephos resistance of ~50% (Diniz *et al.*, 2015) in mosquitoes displaying upregulated alpha esterases (Diniz *et al.*, 2015). It should be noted, however, that CCEae3A was not tested for individually and that both the difference in fecundity and longevity are far greater in that study than is observed here and it is therefore most likely that other mechanisms were contributing to the fitness costs.

#### 3.4.4.2 Longevity

Significant reductions in adult longevity were observed for 3A+/3A+ compared to Ubi-GAL4/Ubi-GAL4 with sexes combined and for males and females analysed separately but these differences were small with either 1 day or no change in the median adult life span despite obvious differences on Kaplin-Mayer curves (Figure 3.3.10).

Female 3A+/3A+ adults began to die at a faster rate from around day 17 resulting in far fewer individuals living beyond 22 days than for Ubi-GAL4/Ubi-GAL4. If the longevity difference was physiologically relevant for CCEae3A overexpressing mosquitoes, it could be crucial as the proportion of CCEae3A overexpressing females who live long enough to take multiple blood feeds, incubate and transmit arboviruses is reduced. The extrinsic incubation time of arboviruses increases as temperature decreases and so in low temperatures, particularly for viruses with longer incubation periods such as West Nile virus, the likelihood of an individual overexpressing CCEae3A transmitting an arbovirus could be reduced compared to those which do not (Winokur *et al.*, 2020). This is quite speculative though since the level of CCEae3A expressed in the transgenic mosquitoes is likely to be much higher than that observed in the field as in 3A+/3A+ CCEae3A is expressed ubiquitously whereas in the field expression is restricted to specific tissues (malpighian tubules and nerve cord).

In males the pattern was slightly more complicated as there was an increase in the rate of death in the first week of life after which the rate slowed before accelerating around day 25 which resulted in far fewer mosquitoes surviving beyond that time than in Ubi-GAL4/Ubi-GAL4. Again, if this was a physiologically relevant amount of CCEae3A causing this mortality, the increase in early death observed could have an impact on mating in the field. A decrease in mating was not observed in our laboratory cages, however this would not necessarily be reflective of mating in a field setting as the number of factors which influence mating success is far reduced in laboratory colonies.

### 3.4.5 CONCLUSIONS

Three genetically modified lines which express CCEae3A were generated using RMCE and a GAL4-UAS system and expression was confirmed using qPCR. Single copy levels of expression were not sufficient to confer significant resistance to temephos but temephos resistance was observed under dual copy expression (3A+/3A+). This line was used for subsequent experiments as it produced the strongest phenotype for temephos resistance. CCEae3A expression was found to confer resistance to all organophosphate and carbamate insecticides tested. Surprisingly, alphacypermethrin resistance was also associated with this enzyme for the first time. This is very concerning as cross resistance to members of three classes of insecticide were found for this one enzyme.

The role of CCEae3A overexpression in resistance to several of the compounds tested was unclear prior to this study as insecticide selection results in multiple molecular changes which can be difficult to unravel. Here we demonstrate the importance of investigating and characterising suspected resistance mechanisms in isolation to accurately characterise the potential effect. This will become increasingly important as around the world countries adopt resistance management practices such as insecticide rotation and molecular screening of resistant populations for 'known' resistance markers. Poor understanding of cross resistance and of the role of individual molecular mechanisms could result in failures to curb resistance spread and reduced efficacy of mosquito control programmes.

# Acetyl Choline Esterase (ACE1) localisation and characterisation of resistance and fitness cost phenotypes of the G280S mutant.

## 4.1 INTRODUCTION

Acetyl cholinesterase 1 (ACE1), AGAP001356, the molecular target of organophosphate (OP) and carbamate insecticides (Weill *et al.*, 2002), is a serine hydrolase enzyme with an asymmetric dimeric structure (Cheung *et al.*, 2018; Han *et al.*, 2018). ACE1 functions in cholinergic synapses to terminate synaptic transmission through rapid hydrolysis of the neurotransmitter acetylcholine (ACh) to choline and acetate (Downes and Granato, 2004). The primary role of ACh is to activate acetylcholine receptors in the synapses of the central nervous system (CNS) mediating neurotransmission (Fukuto, 1990; Thany and Tricoire-Leignel, 2011) by driving channel opening which permits cation penetration through the synaptic membrane (Hirata, 2016). When ACE1 is inhibited, ACh accumulates in the synaptic cleft resulting in continuous hypercholinergic activity causing convulsions and death (O'Brien, 1967; Chambers, Meek and Chambers, 2010a). OP insecticides inhibit ACE1 function through phosphorylation of the enzyme's serine hydroxyl moiety in the active site (Cheung *et al.*, 2018). Carbamate insecticides cause the same effect, however the inhibition of each ACE1 is temporary as carbamylated ACE1 can reactivate but the inhibition is sufficient to cause mortality (Fukuto, 1990).

OP and carbamate insecticides (particularly malathion, bendiocarb and pirimiphos methyl) are important tools for the control of *An. gambiae* particularly as alternatives to or in combination with pyrethroid insecticides, since pyrethroid resistance is widespread (Asidi *et al.*, 2005; N'Guessan *et al.*, 2010; Akogbeto *et al.*, 2011; Agossa *et al.*, 2014; Tchicaya *et al.*, 2014). However, OP and carbamate resistance has also been detected across sub-Saharan Africa often associated with duplication of large gene clusters that include the *ace1* gene (Djogbénou *et al.*, 2008; Djogbénou *et al.*, 2009; Essandoh, Yawson and Weetman, 2013; Edi *et al.*, 2014; Assogba *et al.*, 2015; Djogbénou *et al.*, 2015; Weetman *et al.*, 2015; Assogba *et al.*, 2016; Ibrahim *et al.*, 2016; Assogba *et al.*, 2018; Elanga-Ndille *et al.*,

2019; Grau-Bové *et al.*, 2021), and a single nucleotide polymorphism resulting in substitution of a glycine with a serine in the *ace1* target site. The single codon change GGC to AGC, which causes the glycine to serine substitution, was first linked to carbosulfan and propoxur resistance in an *An. gambiae* strain from the Yaokoffikro suburb of Bouaké in Ivory coast and was named, G119S based on the *Torpedo californica* (electric ray) partial crystal structure (N'Guessan *et al.*, 2003; Weill *et al.*, 2003; Weill *et al.*, 2004). In the complete annotation of the *An. gambiae ace1* gene the mutation occurs in codon 280 (Anopheles gambiae 1000 Genomes Consortium, 2017). In this chapter it will be referred to as G280S.

The G280S substitution is positioned in the active-site gorge of ACE1, which is reduced in size by a larger side chain (-H to -$CH_2OH$), causing steric crowding which inhibits access of both natural substrate (ACh) and inhibitors (OP and carbamate insecticides). *An. gambiae* ACE1-280S activity on ACh was shown to be substantially reduced, compared to G280 and G280S enzymes *in vitro* (Cheung *et al.*, 2018; Han *et al.*, 2018). The level of enzyme activity reduction predicted suggests that other co-evolved mechanisms are likely present to compensate, which would include *ace1* CNV (Wong *et al.*, 2012; Engdahl *et al.*, 2015). As the potency of inhibitor binding is also reduced for the 280S enzyme (Alout *et al.*, 2008; Ahoua Alou *et al.*, 2010; Engdahl *et al.*, 2015; Cheung *et al.*, 2018), this likely imparts resistance to OP and carbamate resistance.

The G280S mutation in *An. gambiae* has been associated with OP and carbamate resistance in many countries in Africa including more than once in Benin, Cameroon, Côte d'Ivoire and Guinea (Djogbénou *et al.*, 2007; Djogbenou *et al.*, 2008; Ahoua Alou *et al.*, 2010; Padonou *et al.*, 2012; Essandoh, Yawson and Weetman, 2013; Weetman *et al.*, 2015; Camara *et al.*, 2018; Zoh *et al.*, 2018; Bamou *et al.*, 2019; Collins *et al.*, 2019; Elanga-Ndille *et al.*, 2019; Stica *et al.*, 2019; Ahadji-Dabla *et al.*, 2020; Diouf *et al.*, 2020; Fagbohun *et al.*, 2020; Gueye *et al.*, 2020; Keïta *et al.*, 2020; Nkemngo *et al.*, 2020; Oumbouke *et al.*, 2020). Understanding the role of *ace1* in resistance and its fitness effects are crucial for resistance management strategies that rely upon accurate prediction of the impact of potential resistance mechanisms. Further to this, improving our understanding of the normal

function of important target site proteins may well contribute to the development of novel compounds or new approaches for vector control.

To date, in all the studies of *ace1* described above, the studies have been conducted using field or laboratory selected mosquitoes, and so there were likely to be many co-evolved resistance and fitness compensatory mechanisms (e.g., *kdr* mutations, metabolic gene upregulation) which complicate interpretation of the phenotypic effects of *ace1* mutation. Even in phenotypic studies of selective breeding to place a*ce1* mutations into a susceptible genetic background (Djogbénou *et al.*, 2007; Luc, Valérie and Philip, 2010; Alout *et al.*, 2014), one cannot rule out the very probable co-selection of compensatory mechanisms.

With the advent of genome editing technology, these obstacles can be overcome to a large extent by introduction of the 280S mutation to the genome of an otherwise susceptible *An. gambiae* strain. In this chapter the use of CRISPR-Cas9 to introduce the 280S *ace1* mutation into the well characterised Ngousso lab strain, and the subsequent characterisation of the insecticide resistance and fitness phenotypes that result from this single base pair change is described. Other 'susceptible' strains were available (e.g. G3, Kisumu), however, they were either less well characterised, were a mixture of *An. gambiae* and *An. coluzzii* or carried fitness costs which were worse than that of Ngousso that would increase the difficulty of line maintenance.

In addition, further characterisation of the *ace1* gene was performed by using genetic modification to localise its spatial and temporal transcription profiles. Transcript profiling was achieved by using 2A protospacer sequence technology for the first time in mosquitoes to tag an endogenous gene.

2A protospacers are ~19-22 amino acid oligopeptides which permit translation of multiple separate proteins from a single mRNA strand (Wang *et al.*, 2015). 2As contain a cleavage site which is recognised by host cell ribosomes which cleave the growing peptide by "ribosomal skipping", "stop-go" or "stop-carry" depending on the origin of the 2A sequence. This system allows co-expression of genes in the natural expression pattern of the first target gene without requiring an understanding of transcriptional control and without fusion to the protein of interest. In one approach for transcript

profiling, the 2A sequence is inserted in frame (usually using a CRISPR-Cas9 homology directed repair (HDR) design) immediately before the stop codon of the target gene and carries the second gene in frame immediately downstream of the 2A sequence. The ensuing large mRNA is translated until the 2A sequences are reached and translation of the first protein is terminated. Thereafter the second protein is translated. In the end, both proteins in theory should be produced in stoichiometric amounts in the same tissues where the target protein is synthesised. By including a fluorescent protein as the second gene, the expressing tissues can be identified microscopically, depending on the level of expression.

2A peptides were first used for functional genetic analysis to study T-cell receptor:CD3 complexes in mice (Szymczak *et al.*, 2004). The F2A peptide, from the foot and mouth disease virus, has been used previously in *An. gambiae* (Galizi *et al.*, 2014), but in this case was not used to tag an endogenous gene. After starting this project, the T2A sequence, from the *Thosea asigna* virus, was successfully used to tag neuronal genes in *Ae. aegypti* with calcium marker genes and QF transactivators (Shankar *et al.*, 2020; Zhao, Tian and McBride, 2021). In this thesis, I attempted to use the F2A peptide combined with an eYFP marker to localise *ace1* transcription in *An. gambiae*.

### 4.1.1 AIMS AND OBJECTIVES

- To determine the spatio-temporal localisation of ace*1* transcription.
- To use CRISPR-Cas9 to introduce the ACE1-G280S SNP into a strain with an insecticide sensitive genetic background.
- To determine the resistance profile and identify fitness costs associated with possession of both homozygous 280S and heterozygous G280S *ace1* alleles.

## 4.2 MATERIALS AND METHODS

General methods for plasmid cloning, embryo injection, mosquito rearing, insecticide resistance assays and fitness cost assessment are detailed in Appendix D – General Methods.

### 4.2.1 CONTRIBUTIONS

Dr Tony Nolan provided the pBac[AttB-3xP3-RFP-zpg-hCas9-U6-BsaI-AttB] plasmid for cloning. Fraser Colman and Dr. Gareth Lycett assisted with mosquito rearing and assay preparations. Dr. Aitor Casas-Sanchez provided training and advice for confocal microscopy. Dr. Amy Lynd provided advice for designing LNA SNP detection assays.

### 4.2.2 PLASMID CONSTRUCTION

Four plasmids were generated for CRISPR-Cas9 HDR genome editing to create two new transgenic lines: ACE1-F2A-eYFP (for localisation of *ace1* transcription) and ACE1-G280S (to study the G280S mutation in isolation). The genome sequence of ~ 1 kb both up and down stream of both planned insertion sites was sequenced from genomic DNA which had been extracted from pools of 5 adult Ngousso (Appendix D-xxii) prior to design of gRNAs and primers for plasmid construction. For each line a gRNA-Cas9 plasmid and a template plasmid were designed and constructed for embryonic injection (

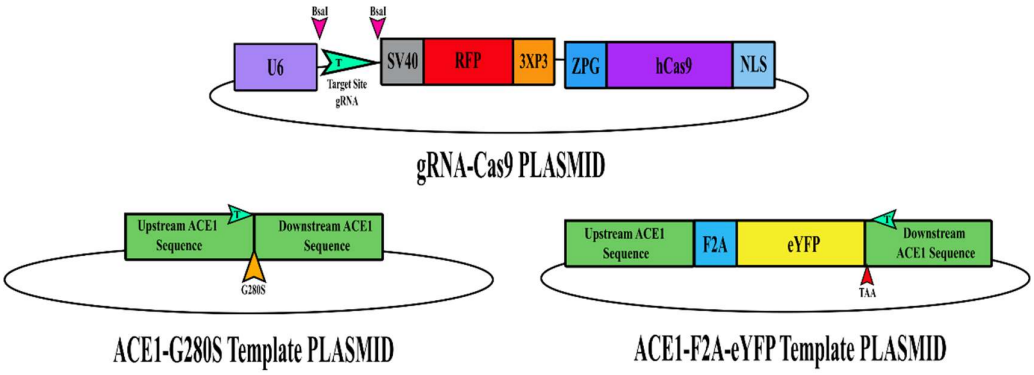

Figure 4.2.1). Guide RNAs (gRNA) were designed using *chopchop.com* (Labun *et al.*, 2019) for each line. The gRNA for ACE1-F2A-eYFP was targeted as close to the *ace1* stop codon as possible, in the UTR, and 2 bases were altered to remove the PAM site in the template plasmid. The PAM site of the gRNA used for ACE1-G280S included the G280S SNP and so the desired SNP changed the PAM site, meaning that no further alteration was required to prevent re-cutting. All plasmids were sequenced (Appendix D-xxxii) prior to embryonic injection (

Appendix D-xvii).

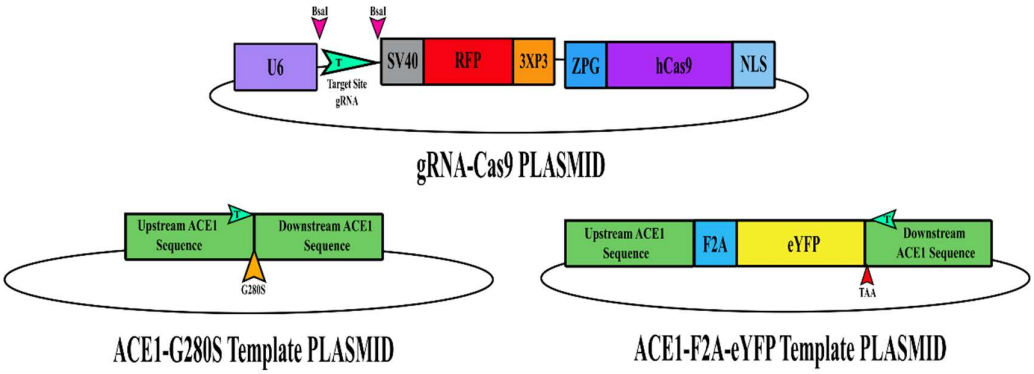


Figure 4.2.1: Plasmids for CRISPR-Cas9 homology-directed repair of *ace1*. Diagrammatic representation of the basic organisation of the key components of gRNA-Cas9 plasmid used for both ACE1-F2A-eYFP and ACE1-G280S lines (top), the ACE1-G280S template plasmid (left) and the ACE1-F2A-eYFP template plasmid (right). The blue arrow (G) indicates the binding location and direction for the gRNA used to direct cutting of the genome for each line (note: the template plasmids are not cut as the PAM sequence was altered to prevent recutting after successful modification, arrows indicate the equivalent location on the genome at which they bind).

#### 4.2.2.1 Guide RNA – Cas9 plasmids

Standard complementary oligos were ordered (one forward and one reverse for each gRNA) which carry the overhang required for ligation into the BsaI digested backbone (forward = TGCT, reverse = AAAC). These oligos (Appendix C-x) were annealed by adding 1 µL of each primer (100 µM) and

2.5 µL NaCl (1 M) to a 50 µL total reaction and incubating at 95˚C for 5 min then 2 min long incubations at 85˚C, 75˚C, 65˚C, 55˚C, 45˚C, 35˚C, 25˚C and 20˚C, then held at 4˚C. The NEB® Golden Gate Assembly Kit (BsaI-HF®v2) (#E1601) was used to insert the annealed gRNAs into *pBac[AttB-3xP3-RFP-zpg-hCas9-U6-BsaI-AttB]* (Kyrou *et al.*, 2018) using a standard reaction set up (100 µM plasmid backbone and 20 µM annealed oligos) and the following thermocycler settings: [37˚C - 3 min, 16˚C – 4 min] x 25 cycles, 50˚C – 5 min, 80˚C – 5 min, 4˚C – infinite hold. 2 µL of the golden gate reaction was added to the transformation which was conducted as described in Appendix D-xxix. All oligo sequences are provided in Appendix C-x.

#### 4.2.2.2 CRISPR-Cas9 Template Plasmids

Template plasmids (the template for HDR) were produced using Gibson assembly (

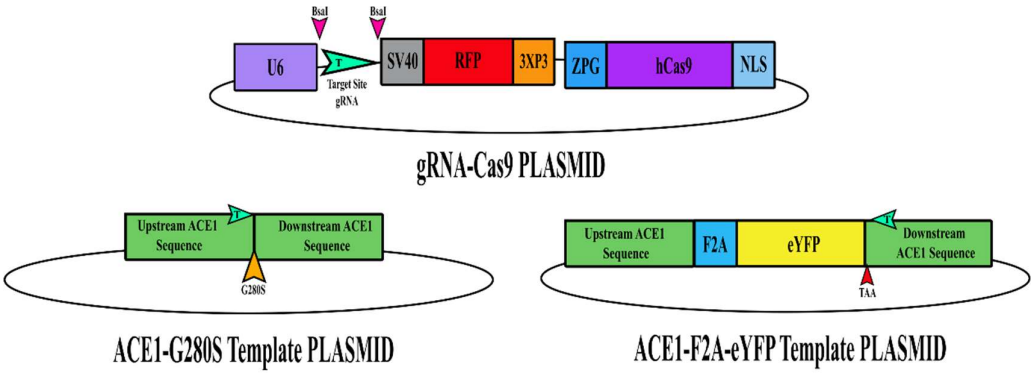


Figure 4.2.1). The backbone plasmid, Puc19, was digested using EcoRI and BamHI and the desired fragment extracted from an agarose gel (Appendix D-xxv and Appendix D-xxvi). Each insertion fragment was generated by PCR – except for the F2A fragment for which complementary primers (F2Afor3 and F2Arev3) were ordered then annealed (100 pM of each primer in a Phusion PCR reaction with no template) prior to amplification (1:10000 annealing mix added to a Phusion PCR reaction with Gibson assembly primers including overlapping sequences). The eYFP fragment was amplified from the *pSL[attB-YFP-Gyp-UAS-14i-Gyp-attB]* plasmid. Up- and down-stream complementary sequences (~1 kb up or down stream of the gRNA binding site) for both lines were amplified by PCR from Ngousso genomic DNA (extracted using the LIVAK procedure (Appendix D-

xxii) from 5 adult females). Each fragment was run on an agarose gel and extracted as described in Appendix D-xxv and Appendix D-xxvi.

The 280S SNP was introduced on the overlapping and binding sequences of the PCR primers and presence confirmed in plasmid clones following transformation and miniprep using AluI digestion (not shown). Primer sequences and uses are detailed in Appendix C-x. The Gibson assembly reaction for ACE1-F2A-eYFP was incubated for 60 min and for ACE1-G280S was incubated for 15 min at 50˚C. Both plasmids were used to transform *E. coli* (Appendix D-xxix), then underwent miniprep (Appendix D-xxx), sequence verification (Appendix D-xxxii), followed by midi-preparation (Appendix D-xxxi) and finally ethanol precipitation (Appendix D-xxviii).

#### 4.2.2.3 Injections

100 ng/µL gRNA-Cas9 and 300 ng/µL template plasmids were combined to make the injection mix and embryonic injections performed as described in

Appendix D-xvii.

### 4.2.3 IMAGING ACE1-F2A-EYFP

Embryos were collected, bleached and fixed as in (Poulton *et al.*, 2021). ACE1-F2A-eYFP larval samples of different stages were starved overnight, anesthetised (5% tricane and 0.5% tetramizole) then set in 1% low melting point agarose (Sigma-Aldrich CH-123-10G) on a slide and secured with a coverslip. Larvae were imaged within 1 h following knock out with anaesthetic. Adult samples were knocked down on ice for 10 mins then dissected in 1X PBS and set in low melting point agarose on a slide and coverslip. Adult dissections consisted of removal of the head (which was then cut in 2 along the ventral-dorsal and apical-posterior axes), legs, and wings; dissection of midgut, ovaries and malpighian tubules, using the standard method of pulling from the terminal abdominal segment, and then separation of thorax and abdomen. The thorax was then cut laterally, opened up and positioned so that the internal structure faced the coverslip. The abdomen was cut from anterior to posterior on

the lateral side (to avoid the nerve cord) opened out and the internal side laid against the coverslip. Each dissected component was set in 1% low melting point agarose (Sigma-Aldrich CH-123-10G) on a coverslip and slide for imaging.

Standard imaging was conducted using a Samsung Galaxy S9 using 'pro' mode (SM-G960F) which permits control of ISO, aperture and shutter speed, through the eyepiece of a fluorescent microscope (Leica MZFLIII with a Leica mercury lamp attached). Images were taken aiming to replicate what can be seen by eye. Confocal imaging was conducted on a Zeiss LSM 880 AxioObserver using a 10X objective (excitation wavelength = 514 nm, emission wavelength = 547 nm, detection wavelength = 527-568) and analysed using Zen 3.4 (blue edition).

### 4.2.4 ACE1-G280S LINE ESTABLISHMENT (CROSSING STRATEGY)

Screening of $F_0$ larvae was carried out by assessment of transient RFP fluorescence, encoded on the Cas9/gRNA plasmid, in the posterior tissues. Larvae displaying mosaic transient fluorescence were reared to adulthood (as they were far more likely to produce positive $F_1$ transgenics than those not displaying transient fluorescence) and females added to a cross with Ngousso males of the same age, as indicated in the results. This cross was fed and resultant progeny reared to pupal stage. Pupae were collected individually to eclose, and then pupae casings collected in 45 µl $dH_2O$ + 5 µL proteinase K. These were shaken with a ball bearing for 2 min at 20 $s^{-1}$ then incubated at 95˚C for 30 min to extract DNA.

As with ACE-F2A-eYFP, the plasmids used for injections of ACE1-G280S carry a 3xP3-RFP construct which is expressed in a mosaic pattern in those injected larvae which have taken up the plasmid well, so it was possible to narrow the pool of $F_o$s to those most likely to produce positive progeny. However, in contrast to all other transgenic mosquitoes used in this thesis, the ACE1-G280S line is not designed to insert an endogenous fluorescent marker to aid identification of positive transgenics. It would have been tricky to insert a marker at the same time as the SNP without disrupting the *ace1* gene as the G280S SNP is in the middle of the gene. It was therefore necessary to screen each generation using molecular PCR-based methods to identify individuals carrying the SNP.

Molecular screening was also required to genotype the individuals included in subsequent phenotypic characterisation *post hoc*.

A restriction fragment length polymorphism (RFLP) assay (Weill *et al.*, 2004) was used to detect the ACE1 G280S genotype of each sample in the $F_1$ generation. 5 µL of extracted DNA was then included in a 10µL DreamTaq PCR reaction with 0.3125 nM dNTPs, 0.5 µM of each primer (Appendix C-x) 1X DreamTaq buffer green and 0.1 µL DreamTaq. Thermocycler settings used were: 95˚C – 3 min, [95˚C – 30 s, 63.8˚C – 30 s, 72˚C – 30 s] X30, 72˚C – 10 min, 12˚C – infinite hold. On completion of the PCR, 0.1 U AluI restriction enzyme was added to each reaction and reactions were incubated for 15 minutes at 37˚C. All samples were run on a 2% agarose gel and the results assessed as 280S homozygote (presence of bands at 203 and 72 bp), G280S heterozygote (presence of bands at 275, 203 and 72 bp), G280 homozygote (presence of one band at 275 bp) or failed reaction (no bands present) (

Figure 4.3.3).

This same RFLP approach was attempted with the $F_2$ generation but provided very poor results. The TaqMan assay, described in (Bass *et al.*, 2010), was used to genotype the $F_2$ samples. This assay permitted identification of sufficient samples to cross together to produce an enriched $F_3$ generation but distinction between G280 and G280S samples in the results was unreliable. Therefore, a modified TaqMan style assay using probes containing locked nucleic acids (LNAs) (Johnson, Haupt and Griffiths, 2004) was designed and tested. This assay was optimised using the $F_3$ generation and was used for all genotyping from the $F_4$ generation onwards as it gave more robust distinction between homozygous G280 and G280S heterozygotes.

Due to the difficulties faced in establishing a homozygous 280S line in the first few generations all experiments were conducted on adults or larvae from of unknown genotype heterozygous G280S parents which were subsequently genotyped using the LNA assay protocols described in section

4.3.2.2 (Appendix C-xii and Appendix C-xiii). A homozygous line was established in the $F_8$ generation, but this was after the experiments in this thesis were conducted.

When describing the mosquitoes in this section the following naming convention was followed: 'G280' refers to individual which were found to only possess the susceptible GGC allele in molecular screening; 'G280S' refers to individuals which were found to possess both the susceptible GGC allele and the resistant AGC allele in molecular screening and '280S' refers to individuals which were found to posses only the resistant AGC allele in molecular screening.

### 4.2.5 ACE1-G280S INSECTICIDE RESISTANCE TESTING

WHO adult tube (malathion, propoxur and fenitrothion), tarsal (malathion) and larval (temephos) assays were conducted as described in Appendix D-xx using mixed populations of ACE1-G280S expected to include all three possible genotypes. Due to the difficulties faced in establishing a pure breeding homozygous 280S line in the first few generations, all the resistance testing was conducted blind on adults or larvae generated from heterozygous G280S parents. Once a robust LNA assay, described in section 4.3.2.2 (Appendix C-xii and Appendix C-xiii), was developed that distinguished all three genotypes, all the test mosquitoes (i.e. dead and alive) were subsequently genotyped.

WHO adult tube assays were modified slightly from the description in Appendix D-xx as a range of exposure times were tested for each insecticide to assess the resistance present more precisely. Also, for tarsal and WHO assays, immediate knockdown was not recorded for individuals as it was not possible to link this information to an individual's genotype post-hoc.

In each assay, individuals dead at 24 hours were collected (adults using tweezers, larvae using a glass Pastuer pipette and removing the water) in 96-well plates, recording the well used, alongside the other relevant experimental details (including mortality status at 24 hours) for the individual. Alive individuals were then collected (adults were held at -20°C for at least 10 minutes) in the same manner. DNA was extracted and LNA reactions were conducted as described in section 4.3.2.2, Appendix C-xii and Appendix C-xiii to establish the genotype of each individual.

Analysis was conducted using log-logistic models (using the drc package in R) to calculate LC50 (larval and tarsal assays) or LT50 (WHO adults tube assays) using one model for each different insecticide and experiment with genotype included as a factor. One WHO assay, fenitrothion, was analysed with a linear regression as this was the suitable model for the data collected.

## 4.2.6 ACE1-G280S FITNESS COST EVALUATION

### 4.2.6.1 Longevity

Longevity was assessed following the method described in Appendix D-xviii. As a mixed population was used, dead individuals were collected in 96-well plates, recording the day of death and well number with the other relevant experimental details. Individuals were then genotyped post hoc using the LNA method described in section 4.3.2.2.

### 4.2.6.2 Fecundity

Following genotyping of ACE1-G280S mixed progeny pupae casings using the LNA assay described in section 4.3.2.2 separate crosses of G280, G280S and 280S males and females were set-up.

#### *4.2.6.2.1 Egg Laying*

Each cross was blood fed, then 3 days later females were aspirated into individual egg laying tubes (Figure 4.2.2). On day 5 the number of eggs laid were counted and rinsed into a 250 mL plastic pot lined with filter paper and filled approximately half full of water. If an individual had not laid any eggs on day 5, they were not removed from the tube until day 9. If eggs were laid in this time they were counted and prepared for hatching as before. All individuals were kept alive for dissection if required later.


Figure 4.2.2: Individual egg laying tube.

Tube containing ~ 1 mL pond salt water, a circle of filter paper and a female mosquito who should lay eggs onto the damp filter paper.

#### *4.2.6.2.2 Larval hatching*

On days 6 and 7 eggs were washed down and ground fish food added to each pot. On day 8 the number of larvae hatched in each pot was counted.

#### *4.2.6.2.3 Insemination and Unlaid Egg Development*

Females which did not lay any eggs or that laid eggs which did not hatch were dissected to establish whether they had mated and whether or not any egg development had occurred. Individuals were knocked down on ice for 10 minutes then moved onto a slide with a drop of 1X PBS using tweezers.

Using dissecting pins, the thorax was detached from the abdomen. As most individuals dissected were gravid it was not possible to remove the ovaries and midgut in the normal way. Therefore, the final segment was detached, spermatheca separated, crushed and then the presence or absence of sperm determined under 400X magnification.

The remainder of the abdomen was cut along the dorsal side from anterior to posterior with dissecting scissors. The structure of the ovaries and developing eggs were noted.

# 4.3 RESULTS

## 4.3.1 ACE1-F2A-EYFP

### 4.3.1.1 Establishment

Following injections, F0 progeny were screened as larvae to identify transient RFP fluorescence (which indicates that the larvae have been injected successfully with plasmid). Only those larvae with transient RFP fluorescence were kept and reared to adulthood, then separated by sex and crossed with WT Ngousso adults of the opposite sex as indicated in Table 4.3.1. The progeny of this cross ($F_1$) were screened for eYFP fluorescence and positive individuals (57) crossed together (Table 4.3.1). 4 larvae died before adulthood. From the progeny of this $F_2$ cross, homozygote individuals were putatively identified by fluorescence intensity and crossed again in order to establish a homozygous colony. The distinction between homozygote and heterozygote individuals was not completely robust, and so a few generations of screening and removing heterozygote and wild type individuals was required before a fully homozygote line was established. Homozygosity was confirmed by setting up reciprocal crosses of 50 ACE1-F2A-eYFP individuals with 50 Ngousso individuals and screening the progeny for individuals lacking fluorescence which would identify heterozygosity in the parents.

| **Number of eggs injected (Number hatched)** | **$F_0$ pools - number and sex of positive hatchlings (number and sex of Ngousso included in cross)** | **$F_1$ positive transgenics – Number positive larvae (*number and sex of positive $F_1$ adults crossed together*) / Total** |
|---|---|---|
| 300 (62) | 3 ♀ (*18*♂) | 61 (*30* ♀ + *27*♂) / 100 |
| | 2 ♂ (*19*♀) | 0 |

Table 4.3.1: Details of the establishment of the $F_1$ generation of ACE1-F2A-eYFP line following CRISPR-Cas9 genome editing.

NB: despite identification of 3 positive $F_0$ females all progeny recorded were laid by a single female. 1 founder from 5 transient positive $F_0$ (20%) with a positivity rate in $F_1$ generation of 61%.

#### 4.3.1.2 Imaging

In ACE1-F2A-eYFP, the eYFP expression is weak in heterozygotes, but of sufficient intensity to identify through screening. However, to characterise the expression profile and attempt to image individuals, even homozygotes, it was necessary to starve larvae overnight (due to the high autofluorescence of larval food) and to dissect adults to reveal the inner tissues.

In embryos, no signal was observed at any of the time points (1, 12, 24 and 36 h) examined after laying following fixation and clearing of the exochorion by bleaching (Poulton *et al.*, 2021). Observation by low magnification stereo fluorescence microscopy comparing ACE1-F2A-eYFP and Ngousso (wild type) larvae indicated eYFP expression in the abdominal and thoracic nerve cord and ganglia, Figure 4.3.1A,B. Depending on the opacity of the head capsule between individuals, expression could also be detected in the brain Figure 4.3.18B.

Because of time constraints, only preliminary confocal imaging could be performed to examine expression in more detail. From these images it is difficult to discern low level expression from autofluorescence (which both appear as various shades of purple/fuschia). However, the ventral nerve cord shows clear and robust expression (Figure 4.3.1C,D) and expression is again detected in the brain Figure 4.3.1D. There is potentially expression in the neurons that lead away from the ganglia and the connected neuromuscular junctions Figure 4.3.1C,D,E). There may also be eYFP signal detected in the larval antenna, (Figure 4.3.1C,E), although it is more difficult to distinguish. The absence of eYFP expression in the eyes and the presence of eYFP expression in the brain permits distinction of the line described here from other lines which express eYFP driven by the 3xP3 promoter.

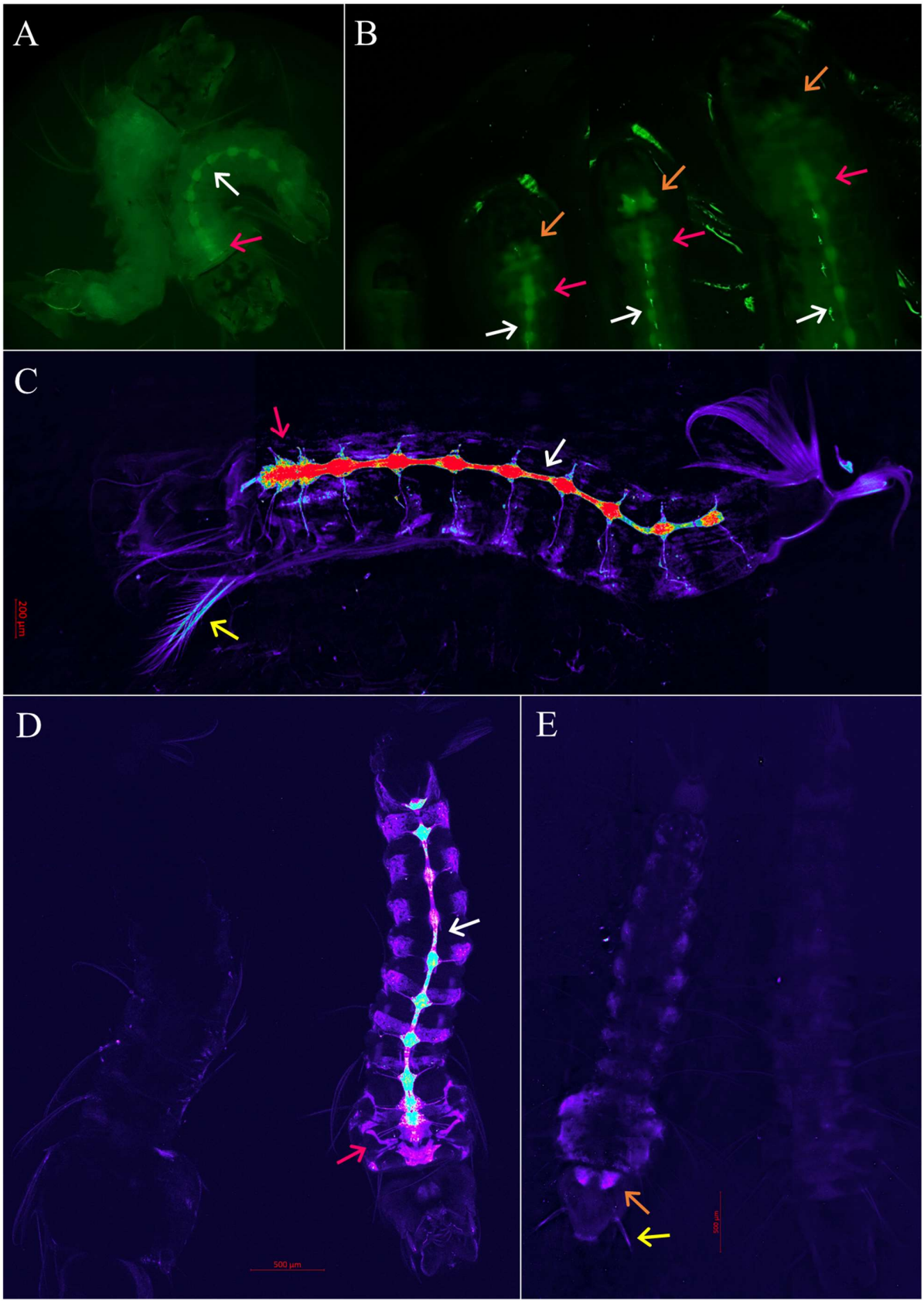
A
B
C
200 µm
D
500 µm
E
500 µm

Figure 4.3.1: Localisation of ACE1 transcription in larval stages.

An image at ~20X magnification on a fluorescent microscope with eYFP filter taken with mobile phone camera - Comparison of 4$^{th}$ instar larvae (ventral) wildtype Ngousso (left) and ACE1-F2A-eYFP (right) (A). An image at ~20X magnification of ACE1-F2A-eYFP larvae – left to right = 1$^{st}$, 2$^{nd}$, 3$^{rd}$ and 4$^{th}$ – (ventral side) expressing eYFP – note image was taken as a single image but has been cropped to reduce blank space (B). A weighted average orthogonal projection combined image of a z-stack confocal microscopy image of a (ventral) 2$^{nd}$ instar ACE1-F2A-eYFP larvae (rainbow 2 LUT – strongest signal = red, weakest signal = purple) (C). Comparison of wildtype Ngousso (left) and ACE1-F2A-eYFP (right) 4$^{th}$ instar larvae (ventral) using standard deviation orthogonal projection combined images of a confocal microscopy z-stack (rainbow 2 LUT – strongest signal = red, weakest signal = purple) with low weight T-PMT (white, visible light representation) to provide frame of reference for the eYFP signal (D). Comparison of (dorsal) wildtype Ngousso (right) and ACE1-F2A-eYFP (left) 4$^{th}$ instar larvae using weighted average orthogonal projection combined images of a confocal microscopy z-stack (rainbow 2 LUT – strongest signal = red, weakest signal = purple) with low weight T-PMT (white, visible light representation) to provide frame of reference for the eYFP signal (E). All larvae were starved overnight prior to imaging to permit visualisation of eYFP fluorescence without the substantial background signal from food. Arrows indicate signal in nerve cord (white), brain (orange), thoracic ganglia (pink), antenna/hairs/bristles (yellow).

In adults, eYFP expression appeared lower than in larvae and was limited to nervous tissues. The strongest expression was detected in abdominal nerve cord (Figure 4.3.2A,B) and thoracic sub-oesophageal ganglion (Figure 4.3.2E). Expression was also observed in the antenna (Figure 4.3.2 D). In pupae, eYFP expression was seen in the nerve cord and in the head (Figure 4.3.2F) but at much lower levels than in larvae. Dissection of the pupae head was attempted but did not help discern the exact tissues of expression.

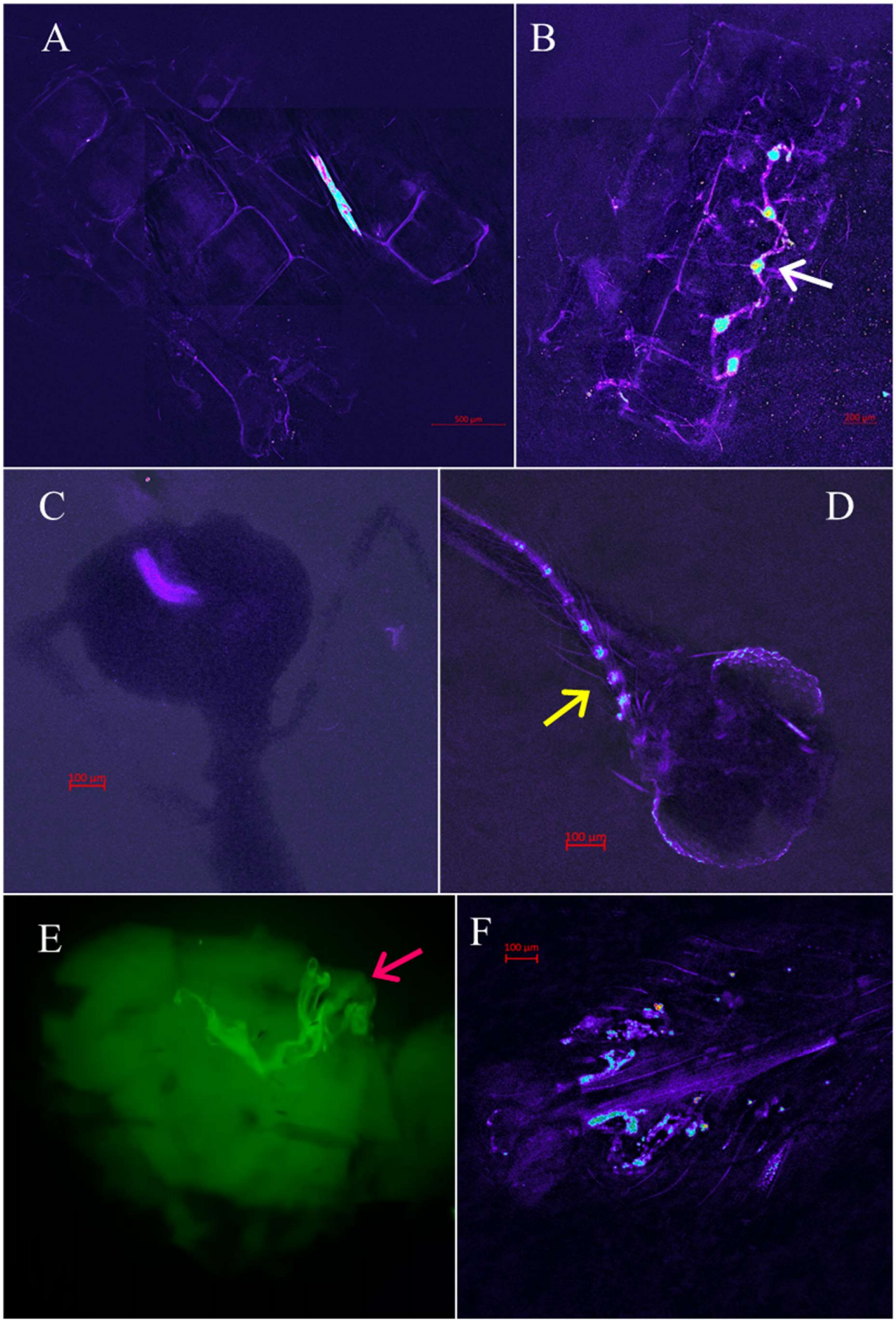


Figure 4.3.2: Localisation of ACE1 transcription in adults and pupae.

Weighted average orthogonal projection combined images of z-stack confocal microscopy images of wildtype Ngousso (A) and ACE1-F2A-eYFP (B) adult dissected abdomen highlighting eYFP expression (rainbow 2 LUT – strongest signal = red, weakest signal = purple). Weighted average orthogonal projection combined images of z-stack confocal microscopy images of wildtype Ngousso (C) and ACE1-F2A-eYFP (D) adult dissected head, displaying T-PMT (white, visible light representation) to provide frame of reference for eYFP expression (rainbow 2 LUT – strongest signal = red, weakest signal = purple). Image of dissected thorax of ACE1-F2A-eYFP from a fluorescent microscope (~30X magnification) with YFP filter. White arrow indicates what is believed to be the sub-oesophageal ganglion expressing eYFP thus indicating ace1 expression (E). Weighted average orthogonal projection combined image of z-stack confocal microscopy images of ACE1-F2A-eYFP pupae highlighting eYFP expression (rainbow 2 LUT – strongest signal = red, weakest signal = purple) (F). Arrows indicate signal in the abdominal nerve cord (white), antenna (yellow) and thoracic ganglia (pink).

## 4.3.2 ACE1-G280S

### 4.3.2.1 Establishment

Next a HDR CRISPR-Cas9 method was used to introduce the *ace1*-G280S SNP into an insecticide susceptible strain (Ngousso) to permit phenotypic characterisation of the SNP isolated from other mechanisms of resistance. As in the case of the F2A lines, $F_0$ progeny from 280S construct injected embryos were screened as larvae to identify transient RFP fluorescence and these were crossed with wild type Ngousso adults of the opposite sex, as indicated in Table 8.2. The $F_1$ generation of 29 individuals was genotyped using the RFLP-method (

Figure 4.3.3) and from this six G280S individuals were identified and intercrossed with WT Ngousso. However, this genotyping method had a very high failure rate when scaled up for use in the $F_2$ generation on larger numbers of samples. The $F_2$ generation was thus screened using an existing

TaqMan probe-based assay (Bass *et al.*, 2010). However, the results from this assay (particularly when using pupae casings as a source of DNA) were again not good enough to reliably separate G280 homozygote and G280S heterozygote samples. Therefore, the $F_2$ generation was kept as a mixed population which was expected to contain some G280 homozygotes, in addition to the desired G280S heterozygotes and 280S homozygotes.

| **Number of eggs injected (Number hatched)** | **$F_0$ pools - number and sex of positive hatchlings (number and sex of Ngousso included in cross)** | **$F_1$ positive transgenics – Number positive larvae (*number and sex of positive $F_1$ adults crossed together*) / Total** |
|---|---|---|
| 417 (82) | 3 ♀ ( *15*♂ ) | 6 ( *4*♀ + *2*♂ ) / 29 |
| | 1 ♂ ( 8♀ ) | 0 |

Table 4.3.2: Details of the establishment of the $F_1$ generation of ACE1-G280 line following CRISPR-Cas9 genome editing.

NB: despite identification of 3 positive $F_0$ females all progeny recorded were laid by a single female. 1 founder from 4 transient positive $F_0$ (25%) with a positivity rate in $F_1$ generation of 20.7%.

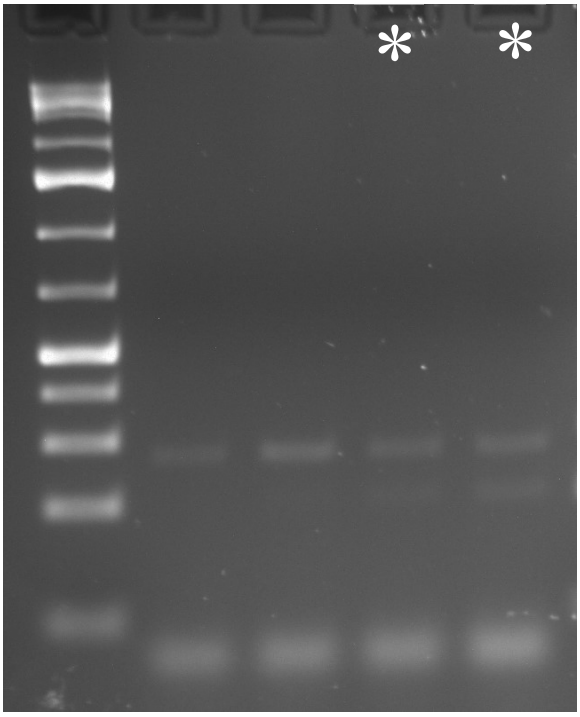

Figure 4.3.3: ACE1-G280S RFLP Example Results

Subset of the results from $F_1$ generation of ACE1-G280S with * indicating positive (G280S) heterozygotes which were identified, Ladder is a GeneRuler 1 kb plus – band sizes are the same as the equivalent band on the ladder in panel A (Thermo Scientific).

Between the $F_2$ and $F_3$ generation, I designed probes which contained locked nucleic acids (LNA) and optimized an assay which had a greater distinction between these pupal casing samples that considerably improved the robustness of genotyping. The LNA assay was used for all subsequent genotyping (including all experiments described here). However, the $F_3$ generation was established with only G280S heterozygotes, as an attempt to breed from only 280S homozygous individuals didn't succeed. This was likely due to small numbers used and the associated fitness costs of the 280S allele as described below. An iso-female homozygous line was established after multiple attempts in generation 8 which is now somewhat stable (however this was after the assays in this thesis were conducted).

#### 4.3.2.2 Locked Nucleic Acids Assay Optimisation

Optimisation of the ACE1-G280S LNA assay found that the primers used in the TaqMan assay (Appendix C-x) provided effective amplification and did not interfere with probe binding (a newly designed set blocked HEX probe binding). Probe sequences detailed in Appendix C-x produced sufficient amplification (Figure 4.3.4A,B) and were able to distinguish between the three desired genotypes (Figure 4.3.4C). The G280-HEX probe produces almost no detectable background signal but does not allow clear distinction of homozygote G280 and heterozygote amplicons based on the HEX signal alone (Figure 4.3.4A). Conversely, homozygote 280S and heterozygotes produce FAM signals at distinct levels which could permit determination of 280S samples from other genotypes using this probe alone. However, the 280S-FAM probe consistently produces a low-level background signal (typically up to ~1000 dR) which, if sufficient DNA is not included in the reaction at the beginning, can make determination of samples as either G280 or G280S difficult (Figure 4.3.4B).

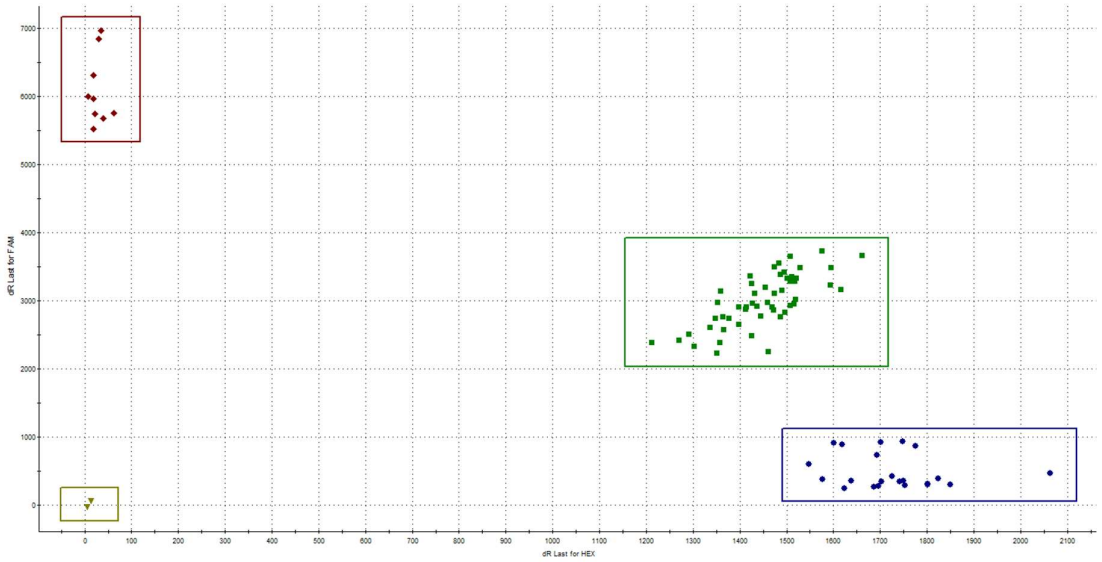


Figure 4.3.4: Example output from LNA Assay.

Example LNA results using the optimal thermocycler settings (95˚C – 3 min, [95˚C – 5 s, 63˚C – 30 s] x40). Note the annealing temperature of 63˚C is different from the standard temperature (60˚C). Example dR Last fluorescence value dual scatterplot for HEX (x-axis) and FAM (y-axis) (C). Data shown are from the LNA genotyping of WHO malathion 15-min exposure rep 1 following optimal settings for adult samples detailed in Appendix C-xii and Appendix C-xiii. The typical clusters of the three possible genotypes (G280 - only HEX detected (blue); G280S – both HEX and FAM detected (green); and 280S – only FAM detected (red)) and 'failed' reactions (neither probe detected (yellow)) are indicated.

Although the optimisation experiments are not detailed here, the final extraction volumes, LNA reaction and template volumes detailed in Appendix C-xii and Appendix C-xiii, and the thermocycler settings (95˚C – 3 min, [95˚C – 5 s, 63˚C – 30 s] x40), were found to provide the best distinction between genotype clusters. Note that the annealing temperature is higher than that typically used in LNA or TaqMan assays as this provided more reliable results. It was also found that detection of both probes improved when extractions were conducted in a standard PCR machine as opposed to a hybridiser or water bath. When extractions were conducted in a PCR machine, 1 h at 95˚C was sufficient for robust results in the LNA assay. When this was not possible and a water bath or incubator had to be used, the temperature had to be set as high as possible (99˚C) and the incubation

time increased to ~4 hours in order to achieve sufficient extraction to reliably distinguish between genotypes using the LNA assay. Typical results of a successful genotyping assay (WHO assay malathion, 15 min exposure) are shown in Figure 4.3.4.

#### 4.3.2.3 Insecticide Resistance Testing

##### *4.3.2.3.1 WHO Adult Tube Assay*

WHO Tube assays were conducted for three insecticides at four different exposure times. The WHO resistance definition was not met for any genotype following malathion exposure as the mortality from 60 min exposure was 100% for all genotypes (Figure 4.3.5A). However, a significant reduction in mean mortality following 15 min malathion exposure was found using a two-tailed t-test between G280 (77.2%) and 280S (24.5%) genotypes ($t(21) = 3.727$, $p=0.00125$), but not between G280 and G280S (81.9%) genotypes ($t(16) = -0.46$, $p=0.653$).

For propoxur, both G280S and 280S genotypes meet the WHO definition of resistance at the standard exposure time (60 min) as survival was greater than 10% (Figure 4.3.5B). A two-tailed t-test confirmed that the difference in mortality between G280 (100%) and G280S (62.5%) genotypes ($t(3) = 12.18$, $p=0.0012$) but not between G280 and 280S (15%) genotypes ($t(1) = 5.67$, $p=0.111$).

Following fenitrothion exposure, WHO defined resistance was detected for the 280S genotype as mean mortality was 66.9% and the difference in mortality compared to G280 (100%) was confirmed by two-tailed t-test ($t(6) = 2.54$, $p=0.044$). 100% mortality was found for the G280S genotype, so resistance is not suggested (Figure 4.3.5C).

To examine the results of the time course experiments in more detail, the data was modelled using either a three-parameter log-logistic (malathion and propoxur) using the *drm()* function or a linear regression (fenitrothion) model using the *lm()* function. When a model which includes genotype as a grouping factor was compared using an ANOVA to a simpler model with no grouping factor significant differences were found for both malathion ($F(54,179) = 3.608$, $p<0.0001$) and propoxur

(F(36,179) = 5.572, p<0.0001). However, no significant differences were found in the LT50 for any comparison of genotypes for either insecticide using a Z-test. The LT50s of G280 and G280S for malathion and 280S for propoxur were not significantly calculated (p > 0.3) in the models. This is most likely as the data is higher (malathion) or lower (propoxur) than 50% for all time points so the model must extrapolate beyond this to calculate the LT50.

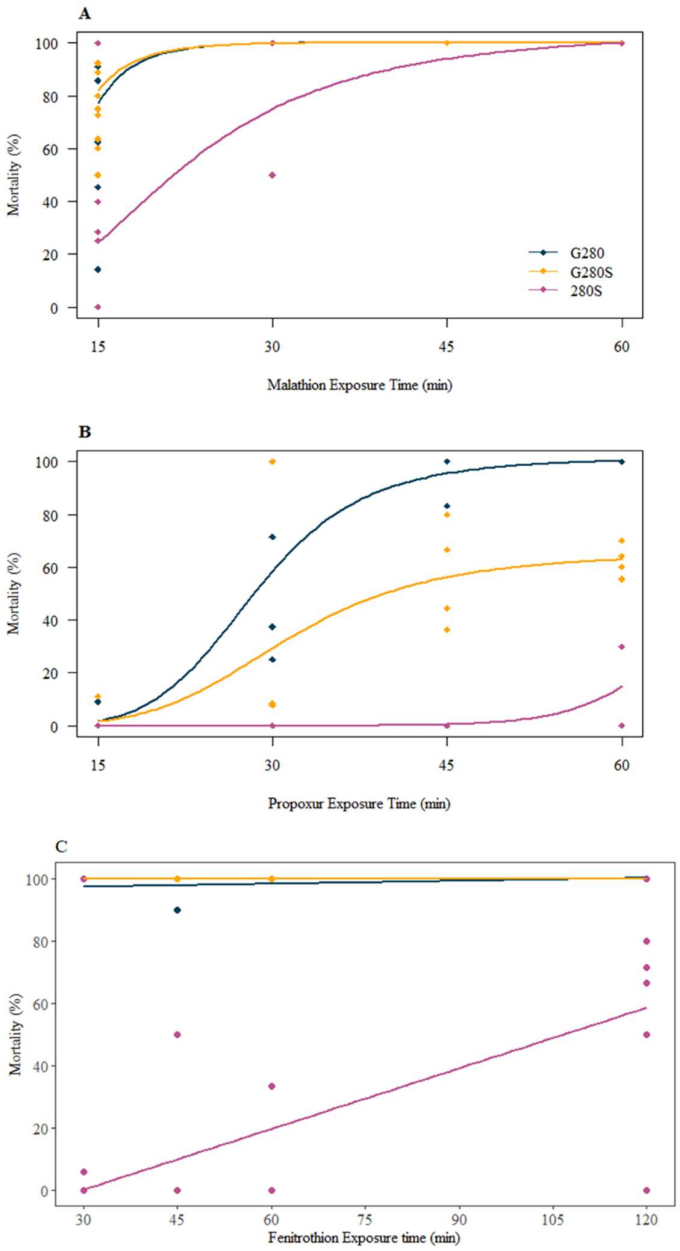

Figure 4.3.5: WHO adult tube assay results showing the impact of the ACE1-G280S mutation on insecticide susceptibility.

Plots reflecting three-parameter log-logistic models for malathion (A) and propoxur (B) and a linear regression model for fenitrothion (C). Points reflect mortality in each tube tested.

An ANOVA of the linear regression model for fenitrothion identified genotype as a significant factor in the model ($F(2) = 96.051$, $p < 2x10^{-16}$). 280S was identified as a significant coefficient in the model ($t = -11.810$, $p < 2x10^{-16}$), whereas G280S which displayed 100% mortality at all exposure times was not ($t = 12.055$, $p = 0.8399$).

#### *4.3.2.3.2 Tarsal Assay – Malathion*

Since the WHO results for malathion indicated a level of resistance, but not at the diagnostic dose (Figure 4.3.5A), a more detailed comparison was performed using tarsal assay exposures to different doses of insecticide. An ANOVA, comparing a three-parameter log-logistic model for the malathion tarsal assay data with genotype as a grouping factor with a simpler model which does not, indicated a significant effect of genotype on model output ($F(182,188) = 24.04$, $p<0.001$).

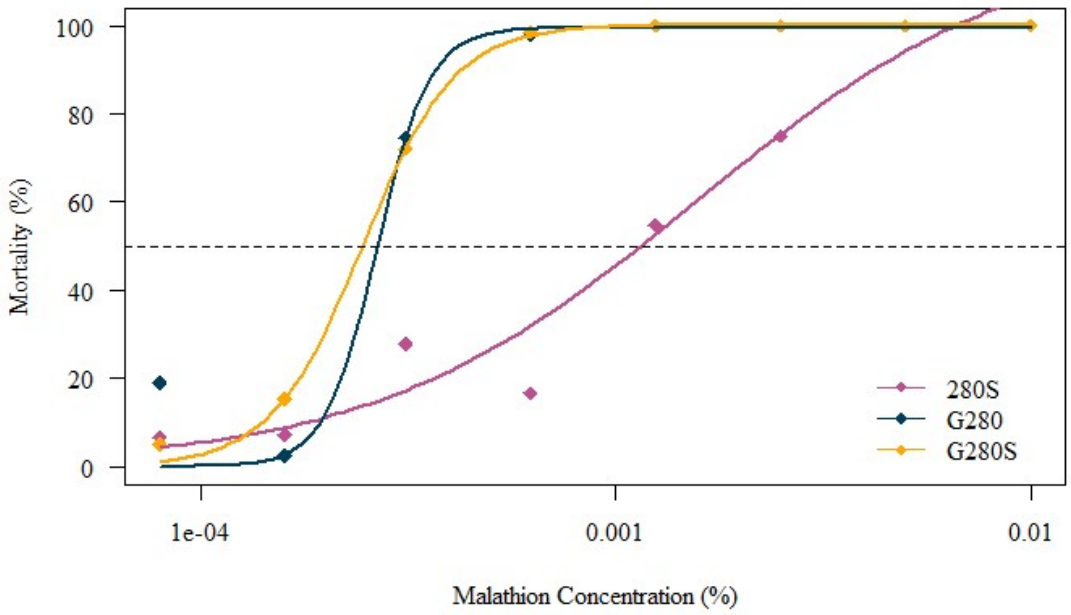

Figure 4.3.6: Tarsal assay assessment of the impact of the ACE1-G280S mutation on malathion susceptibility.

Plotted result of a three-parameter log-logistic model. Points represent the mean mortality for each genotype at each concentration.

Significant LC50 resistance ratios (RR) were identified by z-test for comparisons of 280S (0.0016 %) with both G280 (RR = 5.87, t = 2.16, p = 0.032) and G280S (RR = 6.36, t = 2.22, p = 0.028) but not for the comparison of G280 (0.00027 %) and G280S (RR = 1.08, t = 0.127, p = 0.506)

#### *4.3.2.3.3 WHO Larval Assay*

A WHO larval assay was used to assess whether the genotypes displayed resistance to the commonly used OP, temephos (

Figure 4.3.7). The results were analysed as a two-parameter log-logistic model using an ANOVA and genotype was found to have a significant effect (F(174,180) = 3.06, p = 0.0071). Comparison of RRs indicated a small but significant 1.62-fold reduction in susceptibility for G280S ($5.61x10^{-8}$ M) compared to the G280 ($3.44x10^{-8}$ M) genotype (RR = 1.62, t = 2.53, p = 0.0124). No significant difference was detected for 280S ($3.88x10^{-8}$ M) in comparison to either G280 (RR = 1.12, t = 0.897, p = 0.37) or G280S (RR = 1.44, t = 1.74, p = 0.083) genotypes.

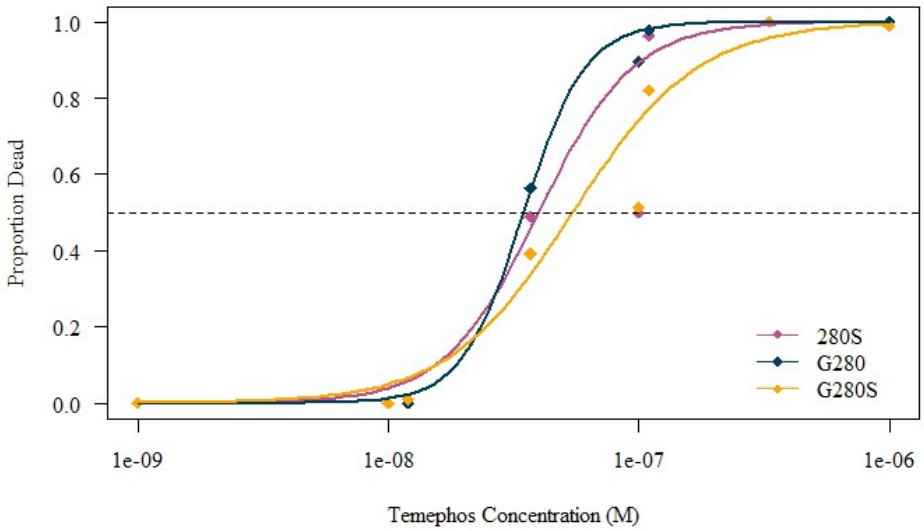

Figure 4.3.7: Effect of ACE1-G280S mutation on temephos susceptibility in a WHO larval assay.

Points represent the mean proportion dead for each concentration tested for each genotype.

#### 4.3.2.4 Fitness Cost Evaluation

##### *4.3.2.4.1 Longevity*

Log rank tests were used to assess the significant differences in the median survival time for various comparisons of adult G280, G280S and 280S genotypes and sex. A significant impact of genotype on longevity was found (Figure 4.3.8A, $p = 5.12x10^{-8}$). Median survival was 20 days for both G280 and G280S and 18 days for 280S. There was no significant difference between G280 and G280S genotypes (Figure 4.3.8B, p=0.71), whereas a significant difference was found between G280 and 280S genotypes (Figure 4.3.8C, $p=9.02x10^{-7}$).

No difference in median survival time was found between males and females (19 and 20 days respectively) when all genotypes were analysed together (Figure 4.3.8D, p=0.1355). There was also no difference between males and females for G280 – both 20 days - (Figure 4.3.8E, p=0.6904), or for G280S – both 20 days – (Figure 4.3.8F, p=0.317). However, a significant difference between male and female median survival, 17 and 18 days respectively, was found for the 280S genotype (Figure 4.3.8G, p=0.045).

Median survival time differed significantly by genotype for both female (Figure 4.3.8H, p=0.00289) and male (Figure 4.3.8I, $p=1.02x10^{-6}$) adults when analysed separately. The median survival time was 20 days for G280 and G280S for both sexes and was 18 days for female 280S and 17 days for male 280S.

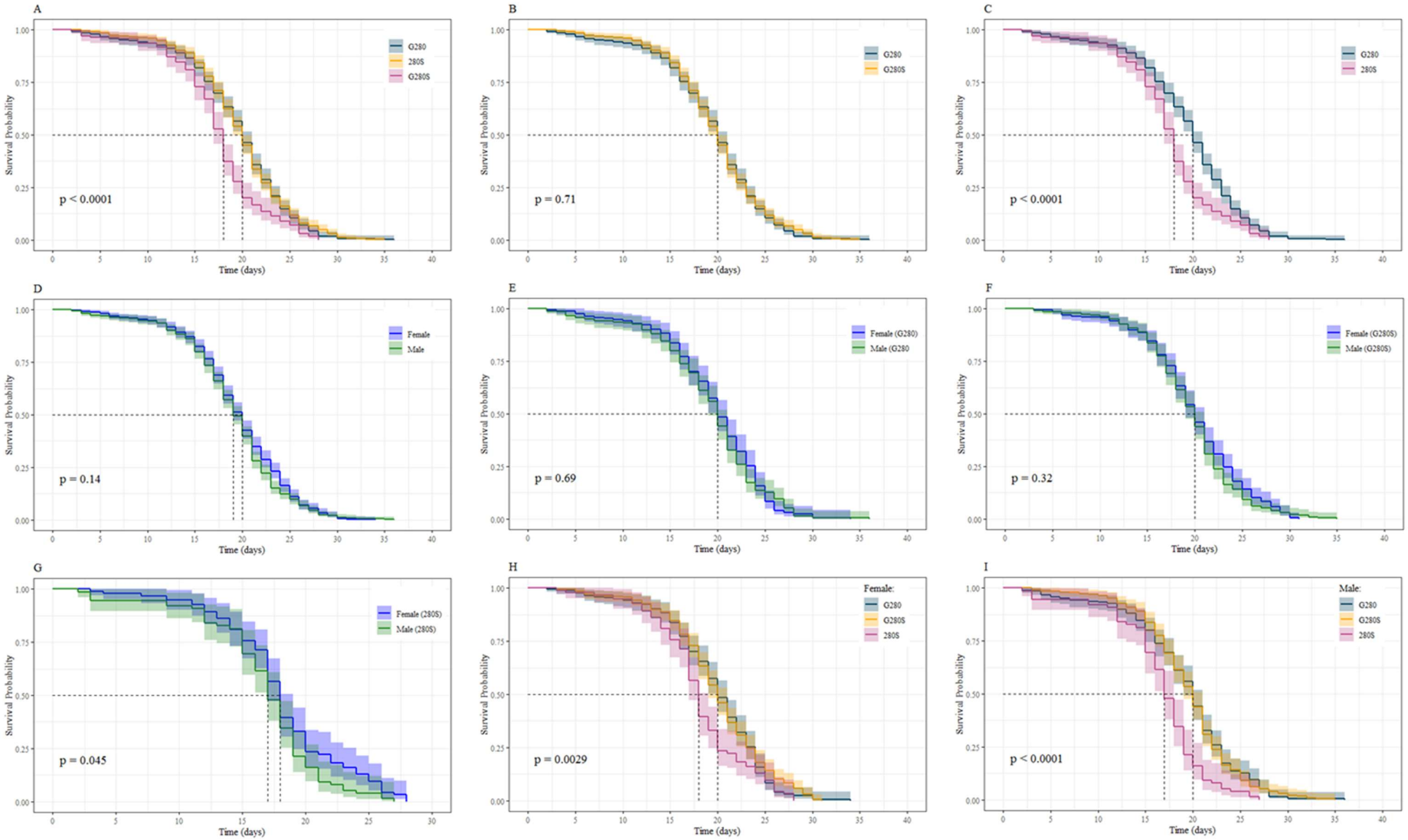
A
Survival Probability
Time (days)
G280
280S
G280S
p < 0.0001
B
G280
G280S
p = 0.71
C
G280
280S
p < 0.0001
D
Female
Male
p = 0.14
E
Female (G280)
Male (G280)
p = 0.69
F
Female (G280S)
Male (G280S)
p = 0.32
G
Female (280S)
Male (280S)
p = 0.045
H
Female:
G280
G280S
280S
p = 0.0029
I
Male:
G280
G280S
280S
p < 0.0001

Figure 4.3.8: Impact of the ACE1-G280S mutation on adult longevity.
Kaplan-Meier graphs with separate curves depicting the probability of death happening each day for: all genotypes – G280, G280S, 280S (A), only G280 and G280S genotypes (B), only G280 and 280S genotypes (C), each sex including data for all genotypes (D), each sex for G280 (E), each sex for G280S (F), each sex for 280S (G), each genotype for females (H), and each genotype for males (I). Black dotted lines highlight the median time to death. Confidence shadows indicate the 95% confidence interval for each step in the curve. P value is the result of a log.rank test.

#### *4.3.2.4.2 Fecundity and fertility*

Fecundity was assessed in three (G280 males x G280 females; G280S males x G280S females; and 280S males x 280S females) of the nine possible genotype crosses. This was due to limitations in time and the number of mosquitoes available. In the following figures and text, the genotype refers to that of both parents.

The number of eggs laid by individual females was identified as significantly affected by genotype ($\chi^2(2) = 12.25$, $p=0.00219$) by asymptotic K-sample Brown-Mood median test. A significant reduction in median number of eggs laid in 280S (mean = 37.5, median = 0) was found compared to G280 (mean = 67.5, median = 68) ($Z = -2.4019$, $p=0.01631$) and G280S (mean = 85.9, median = 75.5) ($Z = -4.05$, $p=5.13\times10^{-5}$) using a Brown-Mood median test. No significant difference was found for G280S compared to G280 ($Z = -0.813$, $p=0.416$).

An asymptotic K-sample Brown-Mood median test indicated that the number of larvae hatched per female was significantly affected by genotype ($\chi^2(2) = 33.978$, $p=4.186\times10^{-8}$). A significant reduction in the number of larvae hatched was found for 280S (mean = 8.58, median = 0) when compared to G280 (mean = 48.0, median = 15) ($Z = -3.5$, $p=0.000465$) and G280S (mean = 15.5, median = 68) ($Z = -5.5773$, $p=2.44\times10^{-8}$) using a Brown-Mood median test. No significant difference was found for G280S compared to G280 ($Z = -1.47$, $p=0.295$).

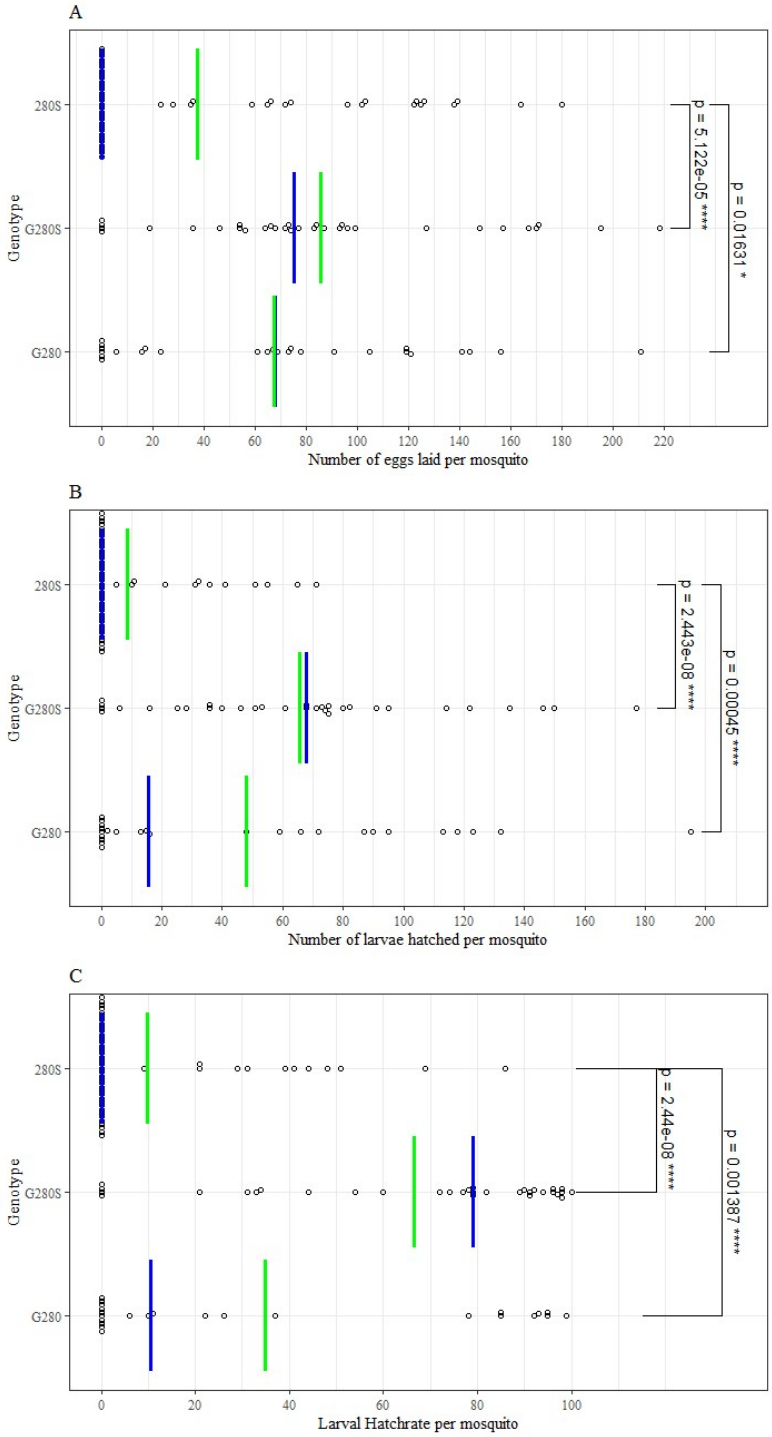


Figure 4.3.9: Impact of ACE1-G280S genotype on fecundity and fertility.

Blue line indicates the median, green the mean. Each point represents the results for a single female for: number of eggs laid (A), number of larvae hatched (B) and the individual

larval hatch rate (C). p-values were calculated using an asymptotic two-sample Brown-Mood median test.

The hatch rate (number eggs laid / number larvae hatched) was calculated for each female. Significant impact of genotype on hatch rate ($\chi^2(2) = 33.978$, $p=4.186x10^{-8}$) was found by an asymptotic K-sample Brown-Mood median test. An asymptotic two-sample Brown-Mood median test found a significant reduction in the median hatch rate of 280S (mean = 9.92 %, median = 0 %) compared to G280 (mean = 72.9 %, median = 17.2 %) ($Z = -3.197$, $p=0.0014$) and G280S (mean 66.9 %, median = 79.5 %) ($Z = -5.577$, $p=2.44x10^{-8}$). No impact was detected when G280 and G280S were compared ($Z = -1.571$, $p=0.116$).

Due to the large percentage of 280S homozygotes which laid no eggs and the low hatch rate of the eggs that were laid, spermatheca dissections were carried out on females which did not produce any larvae, to establish whether this is due to lack of mating. Three G280 homozygote (of 4 dissections conducted) individuals were removed from all analysis due to lack of sperm detected in dissections or absence of signs of blood feeding. 100% of G280S (n=2) and 280S (n=46) homozygotes were found to carry sperm. While conducting dissections to confirm insemination it was noted that most of the female 280S homozygotes (n=46, 87%) being studied were gravid and carrying eggs which appeared to have developed normally. No structural abnormalities were visually identified in the dissected ovaries (when dissections could be completed without damaging both ovaries).

## 4.4 DISCUSSION

In this chapter two transgenic lines were successfully established following genomic modification via CRISPR-Cas9 HDR: ACE1-F2A-eYFP and ACE1-G280S. For both lines homozygous colonies were established, though for ACE1-G280S this was after the phenotypic characterisation presented here was conducted. The ACE1-F2A-eYFP line permitted localisation of the primary tissues of *ace1* transcription and phenotypic characterisation of ACE1-G280S has highlighted insecticide resistance and fitness cost phenotypes which add to our understanding of the observed evolution of this mutation in field populations.

### 4.4.1 CRISPR MUTAGENESIS

The efficiency of any mosquito genome modification technique is greatly influenced by the quality of embryo injections. However, the CRISPR-Cas9 HDR system used here was capable of inserting a 795 bp sequence in the tagging experiment, at high efficiencies even with low $F_0$ embryo survival. Greater than 50% of the progeny from the pooled $F_0$ females produced fluorescently tagged *ace1* progeny. These were the progeny of a single female however, in which case 1 in 5 $F_0$ females (that transiently expressed the dsRed marker) gave rise to CRISPR modified progeny.

This successful F2A transgenic was achieved following many alterations to the design of the experiment including; changing the promoter controlling Cas9 expression from *vasa* (Papathanos *et al.*, 2009) to *zpg* (Kyrou *et al.*, 2018; Hammond *et al.*, 2021); design and cloning of two different gRNAs; changing the injection pressure settings; and altering the ratio and concentration of plasmids injected. Only the successful approach is presented here, and it is difficult to separate which of these changes were most relevant to the success, due to confounding factors such as the quality of injections and the number and quality of embryos injected. The *zpg* promoter was selected as it has better restriction of expression to the germline when compared to the *vasa* promoter (Kyrou *et al.*, 2018).

Following success in acquiring positive $F_1$ transgenics for ACE1-F2A-eYFP, the same methodology was employed for creation of ACE1-G280S, and ACE1-G280S transgenics were acquired from the

first round of injections. There are several possible contributory factors as to why this line was established with less difficulty including that; the method was optimised; I was more experienced at performing embryo injections at the time of injecting; the gRNA used may have been more efficient; and only a single nucleotide polymorphism was introduced compared to a 795 bp fragment. Although only two CRISPR lines have been produced here, it is interesting to note that they were both derived from isofemale $F_0$s, and 1 in 3 females produced mutated progeny.

When (Grigoraki *et al.*, 2021) introduced the L1014F SNP into Kisumu *An. gambiae*, a single $F_0$ female from 24, which transiently expressed the dsRed marker, gave rise to genetically modified offspring (in comparison 4 out of 22, 18%, of $F_1$ offspring were GM). From this limited set of data a range of 1 in 3 to 1 in 24 $F_0$ adults producing modified progeny confirms that CRISPR Cas9 methodology is highly efficient in *An. gambiae*. (Hoermann *et al.*, 2021) show wide variation in success between the three lines generated using Cas9 (expressed using a vasa promoter), where they modified the regulatory sequences of 3 midgut specific loci. They do not separate the number of $F_0$ transient positives by sex or by the number of females which produced positive $F_1$s. The number of $F_1$s from the number of transient positive $F_0$s was 6 from 9, 117 from 10 and 1 from 18 (Hoermann *et al.*, 2021). The equivalent results here of 61 $F_1$s from 5 $F_0$s for ACE1-F2A-eYFP and 6 $F_1$s from 4 $F_0$s for ACE1-G280S are similar and also variable. (Hammond *et al.*, 2016) created 2 lines disrupting genes known to impact female sterility using *vasa* controlled Cas9. They do not report the number of individuals which produced positive $F_1$ progeny but do separate the results by sex. 263 positive $F_1$s from 8 female $F_0$s and 13 $F_1$s from 2 female $F_0$s were identified for the two lines generated. Some other published work in *An. gambiae* uses the vasa promoter to express Cas9 successfully for HDR but did not publish efficiency data for the line (Galizi *et al.*, 2016; Kyrou *et al.*, 2018). This efficiency of CRISPR-Cas9 modification compares very favourably to that produced by the many RMCE experiments performed in the same laboratory over the past 6 years in which, on average, 1 in 20 $F_0$ adults produced GM progeny (Adolfi *et al.*, 2021).

### 4.4.2 ACE1 TRANSCRIPTIONAL LOCALISATION

The uses of 2A protospacers are particularly versatile as they permit expression of transgenes in the spatio-temporal localisation of existing genes with only knowledge of their coding sequence, often requiring no understanding of the regulatory sequences and mechanisms involved. The F2A protospacer was selected for use to identify the spatio-temporal location of transcription of *ace1* using the transgenic line ACE1-F2A-eYFP, as it had previously been shown to function in *An. gambiae* mosquitoes (Galizi *et al.*, 2014), but in that case had been used with a highly active testes specific promoter and the construct had been inserted through PiggyBac mutagenesis, rather than site specific genome insertion to tag expression of an endogenous gene. Whether the expression of the *ace1* gene would be sufficient to produce detectable fluorescence through the F2A co-expression was unknown.

As it transpired, eYFP expression, although faint in 1$^{st}$ instar larvae, was sufficient to allow screening for successful genome modification. No expression was detected in embryos following fixing and bleaching. Although these treatments may reduce fluorescence, it would suggest that *ace1* levels in embryonic stages are low. However, this is inconsistent with mRNA expression analysis using qPCR which found high expression in early embryos, which then reduced expression until the adult stage when expression levels increased (Zhao, Wang and Jiang, 2013). It must be remembered though that the eYFP protein is quite stable (Okita, Sato and Schroeder, 2004) and thus the signal observed will likely accumulate with time, and so fluorescence intensity may not be an accurate measure of temporal transcription rates. This could be overcome potentially if eYFP was substituted for a rapidly degrading fluorophore such as destabilized eGFP (Li *et al.*, 1998), however the overall signal produced would be obviously reduced.

From the imaging conducted thus far, eYFP fluorescence and thus *ace1* transcription appears to be localised primarily to nervous tissues and is observed most in the large larval nerve cord ganglia. In larvae, *ace1* also appears to be transcribed in the larval brain, and potentially in the antenna and sensory neurons leading off the ganglia. This transcription located in the nerve cord and brain is typical of the expression seen from the synthetic neuronal 3xP3 promoter which is often used to mark

mosquito transgenics (Volohonsky *et al.*, 2015). A clear distinction from the 3xP3 expression profile is that ACE1-F2A-eYFP expression was not detected in the developing eye or the anal papillae.

ACE1 expression in these *An. gambiae* neuronal tissues was clearly expected for a protein that functions in neurotransmission, and the distribution is similar to that reported in *D. melanogaster* using *in situ* hybridisation to localise transcription. However, in *D. melanogaster*, expression is seen throughout the developing embryo, which supports the idea of insufficient accumulation of eYFP for detection in these early stages (Fisher *et al.*, 2012). To improve localisation or to study genes which have even lower expression, one possibility would be to use a brighter fluorescent protein than eYFP (e.g. mGreenLantern (Campbell. BC *et al.*, 2020)) which would produce a stronger signal per molecule produced. Another approach could be to replace the fluorescent protein with GAL4 in the design used here (adding a 3xP3_fluorescent protein after GAL4 to permit fluorescent screening of transgenics) and generate a second transgenic line with a fluorescent protein controlled by a UAS promoter (e.g. UAS-mCD8:mCherry (Adolfi *et al.*, 2018)). The GAL4 transactivator acts to amplify the signal produced, since each molecule of GAL4 synthesised will produce multiple mRNAs of the GOI.

Other approaches may also improve the isolation of fluorescently tagged 2A transgenics. In the $F_1$ ACE1-F2A-eYFP generation, eYFP intensity was only just discernible and great care was needed to identify those individuals which were carrying the transgene. In hindsight, the design may have been improved through inclusion of a second different fluorescent protein (e.g. RFP) (controlled by a non-neuronal promoter (e.g., Actin5C (Pinkerton *et al.*, 2000)) between the stop codon of eYFP and the downstream UTR of *ace1*. Although further moving the relative position of the UTR may influence the expression of *ace1* itself, addition of this transgenic marker would make identification in the $F_1$ generation and subsequent screening and line maintenance easier. Such methods would also be required for genes that have expected expression profiles late in development or in tissues hidden by cuticle, where the logistics of screening becomes a severe drawback.

Further analysis of the ACE1-F2A-eYFP line is required. Only preliminary confocal studies were performed, and greater time is needed for detailed analysis and potentially optimisation of fixation

conditions to obtain clearer images with appropriate control comparison. More detailed assessment of the expression between different larval instars, different times of day and at different times between larval moults is required to fully understand the spatio-temporal expression patterns of *ace1* in larval stages. In adults, the impact of malaria or lymphatic filariasis parasite infection, blood feeding and egg laying on *ace1* expression would be interesting to investigate. It is possible that increased expression of *ace1* could influence mosquito parasite and viral refractoriness, alter blood feeding behaviour, blood meal digestion and/or reproduction, all of which have the potential to increase or decrease mosquito numbers and mosquito fitness and thus pathogen transmission. Additionally, the impact of insecticide exposure, both lethal and sublethal, on expression would be important to study in both adult and larval stages. Accumulation due to the stability of eYFP however may make accurate assessment of expression changes in response to stimuli difficult to detect.

As the genome of *An. gambiae* has been fully sequenced, the design of new transgenic lines using 2A protospacers is relatively simple and there are a wide range of approaches (in combination with other transgenic methods such as GAL4-UAS) which could prove useful for the manipulation and study of genes of interest (GOI). A bipartite GOI-T2A-GAL4 with UAS-eYFP system is quite versatile and could be utilised to localise many genes. A single design which is suitable for all levels of GOI expression is unlikely however, as the possible modifications described to increase the fluorescent protein signal could cause too much signal to permit accurate localisation of for highly expressed genes unless their expression is restricted to a very small number of tissues. In such a case GAL4 would not be required and a standard fluorescent protein (e.g., eYFP) may be sufficient.

A major advantage of the bipartite system would be that the 'GOI-F2A-GAL4' line described above could also be crossed with a 'UAS-GOI' line to achieve gene overexpression in the same spatio-temporal location as the GOI. This could be achieved through addition of the UAS sequence immediately upstream of the GOI start codon using CRISPR-Cas9 (if a lethal phenotype is not caused) or introduction of a UAS-GOI coding sequence elsewhere in the genome (which could be achieved using RCME). Using this approach may produce tissue specific upregulation which is more representative of those observed in field resistant mosquitoes than the approaches taken until now (for

example in this thesis) using the polyubiquitin promoter (Adolfi *et al.*, 2018). Approaches similar to this have been used in many organisms including *D. melanogaster* (Diao and White, 2012; Lee *et al.*, 2018; Harnish *et al.*, 2019; Kanca *et al.*, 2019; Kondo *et al.*, 2020). It is a particularly useful approach when using newer CRISPR-Cas9 based systems such as CRISPaint which do not require new donor plasmids to be made for each GOI (Bosch *et al.*, 2020). *Ae. aegypti* transgenic lines combining the GAL4-UAS system and T2A were attempted recently for pan neuronal expression however the attempt was unsuccessful and an alternative Q system was used instead (Zhao, Tian and McBride, 2021). The Q system is a binary expression system (similar to but independent of the GAL4-UAS system) which uses a transcription factor – QF, QF2 or $QF2^{W}$ – that activates a QUAS promoter. The GAL4-UAS system is not as well established in *Ae. aegypti* (Matthews, Younger and Vosshall, 2019) as it is in *An. gambiae* so it is likely that GAL4 based T2A systems could be optimised more quickly in *An. gambiae*. Alternatively, the Q system may also prove useful in *An. gambiae* in combination with GAL4-UAS to upregulate multiple genes in different spatio-temporal patterns as the systems function independently of each other (Riabinina *et al.*, 2015).

### 4.4.3 ACE1-G280S PHENOTYPIC CHARACTERISATION

The SNP in the *ace1* gene which results in a glycine to serine substitution at position 280 (denoted G280S) has been strongly linked with reductions in susceptibility to OP and carbamate insecticides. However, our knowledge thus far comes from studies in which the mosquitoes were selected with insecticides either in the field or intensively in the laboratory which means that the phenotype of G280S has been difficult to definitively define separated from the phenotypes due to other concurrent changes. Here we addressed this issue using CRISPR-Cas9 genomic modification to introduce the SNP (GGC to AGC) into the susceptible *An. gambiae* Ngousso strain. This new line was successfully established though there were some initial difficulties to produce a homozygous 280S colony. The phenotypic experiments described here were thus conducted on a mixed population of G280, G280S and 280S individuals which were genotyped post hoc. This means that the experiments were conducted blind and that individuals from each genotype were raised, exposed or held together in the

same pot, cup, tube or plate for the duration of the experiment, thus controlling for the impact of replicate (e.g., WHO insecticide paper variation) and investigator bias. However, this approach was more expensive and time consuming to conduct - due to the sample collection and genotyping required, and the number of individuals of each genotype was not known at the start of the experiment, so large numbers were tested to ensure that the experiments were not underpowered, further increasing the time required.

The GGC to AGC base change results in the generation of an AluI restriction site which has been used in the past in an RFLP assay for ACE1-G280S genotyping (Weill *et al.*, 2004). New primers were designed specifically for Ngousso and the assay was trialled for genotyping pupae casings prior to creation of the transgenic ACE1-G280S line. However, when this method was used on higher numbers of mosquitoes in the $F_2$ generation (~300 individuals) it was not producing sufficient successful reactions. In future, when optimising an assay like this, it should be tested on larger numbers of samples during optimisation to reduce the risk of these issues when scale up is attempted.

As a result, the $F_3$ generation was genotyped using a TaqMan assay (Bass *et al.*, 2010) which is more expensive but was expected to provide better results than the RFLP assay. The TaqMan assay did perform better as there were far fewer failed reactions however the distinction between G280 and G280S genotypes was poor – particularly for DNA extracted from pupae casings. Therefore, a novel LNA probe assay was designed and optimised which provided better differentiation between G280 and G280S samples and very few failed reactions. This LNA assay was used from the $F_4$ generation onwards for genotyping of progeny for colony maintenance and for all assays presented here. The LNA assay was designed using the same primers as in the TaqMan assay (which has been used for genotyping a variety of strains) so it is expected that it will be as successful for genotyping strains other than Ngousso, however this has yet to be tested.

Using the WHO diagnostic standard, 280S mosquitoes were classified as resistant to fenitrothion and propoxur, but were susceptible to malathion, and G280S were resistant to only to propoxur. Differences in malathion susceptibility were detected in 280S homozygotes under reduced exposure

times and when dose response tarsal assays were performed. However, no difference in malathion susceptibility between G280S and G280 were detected under any of the assays performed.

These data provide new insight into the level of resistance conferred by *ace1* mutation, particularly for malathion (5.87-fold increase in LC50 in 280S compared to G280) and would suggest for most insecticides tested the WHO assay would fail to detect the emergence of single copy heterozygotes for the G280S mutation unless other resistance mechanisms were also present. In future, tarsal assays should be conducted for propoxur and fenitrothion to provide similar data. Additionally, testing of bendiocarb and pirimiphos methyl should be prioritized given their extensive use for IRS.

It was particularly surprising that no significant resistance was conferred to temephos by either 280S or G280S genotypes, in fact a slight (though significant) increase in susceptibility was found for G280S. It would be interesting to repeat the temephos assays to confirm this fitness effect on the G280S mosquitoes, and whether small differences in 280S resistance could be detected on further replication with more concentrations tested.

It was interesting to compare these results to the laboratory strain, AcerKis, which is an *An. gambiae* strain which is homozygous for the 280S mutation and was obtained by introgression and selection with propoxur (Djogbénou *et al.*, 2007). It was later shown that this line also carries a duplication of the 280S gene, and so expression of *ace1* would be expected to have increased in comparison (Assogba *et al.*, 2016). It may also have carried over confounding metabolic resistance mechanisms too. Compared to the lack of resistance to temphos shown by the pure ACE1-280S larvae, AcerKis displayed a RR of 30.6-fold. In WHO assays in adults, diagnostic resistance was indicated to propoxur and fenitrothion for AcerKis, as was shown in ACE1-280S but AcerKis also displayed resistance to malathion at diagnostic dose (Assogba *et al.*, 2014). AcerKis was not found to be resistant to pirimiphos methyl (Medjigbodo *et al.*, 2021) but ACE1-G280S has been strongly linked with pirimiphos methyl resistance from bioinformatics based analyses of the 1000 genomes project data (Grau-Bové *et al.*, 2021), and so it would be interesting to discover whether ACE1-280S display such resistance.

Overall, then, AcerKis show similar resistance profiles to ACE1-280S but with higher magnitudes of difference to a susceptible strain. The main exception is the resistance to temephos in larvae which is observed in the AcerKis line but has not been observed in ACE1-280S. As mentioned, the increased resistance is likely to be produced by the combined upregulation of *ace1* expression due to gene duplication and the 280S mutation which would point to a synergistic or additive effect of expression and the mutation. It would be informative to generate transgenic strains which overexpress the wild type and 280S forms to examine this.

Gene duplication of 280S is observed widely in the field and has been associated with improving fitness costs caused by the mutation (Assogba *et al.*, 2015). The generation of ACE1-280S here allowed the direct analysis of fitness resulting from the G280S mutation. The results showed that longevity of 280S adults was significantly reduced, although only by 3 days compared to both G280 and G280S genotypes with no effect observed for G280S heterozygotes compared to G280 homozygotes. The reduction was slightly (but significantly) greater in male 280S compared to female 280S, while no impact of sex on longevity of G280 and G280S was observed.

In contrast to the longevity studies, large and significant reductions in egg laying, larval hatching and hatch rate were observed for 280S compared to both G280 and G280S genotypes. Again, no difference was observed for G280S heterozygote individuals compared to G280 homozygotes. Interestingly, those 280S females that did not produce larvae had mated and blood feeding and egg development looked normal. This suggests that the ACE1-280S mutation is inhibiting oviposition. The exact mechanism of this would be difficult to decipher. Reduction in acetylcholine esterase activity in *C. elegans* has been shown previously to reduce egg laying (Bany, Dong and Koelle, 2003). Meanwhile, in *D. melanogaster* it has been determined that silencing cholinergic neurons (which are dependent on ACE1 to function correctly) results in the number of eggs laid being reduced massively and egg jamming of the oviduct (Oliveira-Ferreira, Gaspar and Vasconcelos, 2021). It is possible that disruption of nervous signalling due to the inefficient ACE1 enzyme relating to egg expulsion, means that oviposition is not triggered. Alternatively, ACE1 could have a secondary function which has not yet been described which impacts oviposition signalling likely in one or more

of the other neuron types implicated in different aspects of oviposition signalling (Oliveira-Ferreira, Gaspar and Vasconcelos, 2021).

These findings improve our understanding of why 280S homozygotes are not observed in the field. 280S despite having moderate impacts on insecticide susceptibility, also causes a slight reduction in longevity and large reduction in fecundity. When combined with the predicted massive reduction in the turnover rate of the ACh natural product described previously (Wong *et al.*, 2012; Engdahl *et al.*, 2015) it is unsurprising that single copy 280S homozygotes are not observed widely in the field. However, no significant effect on fecundity or fecundity rate was found for AcerKis which is homozygous for 280S (Alout *et al.*, 2016). As has been proposed previously, it is likely that compensatory mechanisms such as duplication or co-evolved mutations counteract the fitness cost associated with 280S in AcerKis (Assogba *et al.*, 2015). In the field most individuals with duplication of *ace1* carry a mixture of G280 alleles and 280S alleles, but rarely are homozygous for either allele, yet mosquitoes without duplication tend to possess only the G280 allele (Grau-Bové *et al.*, 2021). It should be noted that establishment of the homozygous ACE1-280S strain took several attempts because of infertility and may have involved selection for a line that has such compensatory mechanisms, which could be explored further. This line was not used in the analysis presented here however.

Noticeably higher than normal mortality was not observed during larval development, so this was not prioritised for experimentation though there has been evidence of increased mortality in larval and pupal stages in the AcerKis strain (Luc, Valérie and Philip, 2010; Assogba *et al.*, 2015) so could be investigated further in the ACE1-280S homozygous line which is now available. A developmental cost of 280S was noted though from the genotyping of adults derived from heterozygous crosses during the bioassays and longevity assays. A substantial reduction in the proportion of expected 280S homozygotes was observed from G280S parents.

Table 4.4.1 shows the proportion of each genotype in each of the bioassay experiments conducted in this chapter. Assuming mendelian inheritance the genotypes of G280, G280S and 280S are expected to make up 25 %, 50 % and 25 % of the population respectively. However, 280S consistently makes

up less than 20% (mean = 17.9 %) and G280 makes up more than 30% (mean = 32.6 %) of the mosquitoes included in each experiment. G280S made up around half (mean = 49.5%) of the mosquitoes in each experiment. A Chi squared goodness of fit test confirmed that the observed frequencies differ significantly from that which is expected with mendelian inheritance ($\chi^2 = 206.6$, $p = 1.39 \times 10^{-45}$). This is likely the result of a reduction in larval hatching and/or other fitness costs resulting in a reduction in 280S homozygotes from heterozygote parents.

| | **Number of each genotype identified in each assay** | | |
|---|---|---|---|
| | **G280** | **G280S** | **280S** |
| **WHO Assays (1433)** | 452 | 704 | 277 |
| **Tarsal Assay (833)** | 256 | 452 | 125 |
| **Larval Assay (1476)** | 474 | 728 | 274 |
| **Longevity Assay (986)** | 361 | 456 | 169 |
| **Total (4728)** | **32.6 %** | **49.5 %** | **17.9 %** |

Table 4.4.1: Number of ACE1-G280S genotypes identified through *post hoc* genotyping for each experiment and cumulative frequency for each genotype. Number of each genotype in each assay. Number in brackets reflects the raw number of mosquitoes in each group. The mosquitoes for each assay were the progeny of G280S parents so the expected frequency is 25%, 50% and 25% for G280, G280S and 280S respectively. The total number of mosquitoes in each experiment is noted in brackets below the experiment name.

Copy number variations (CNV) including *ace1* has been reported several times in *An. gambiae* and are predicted to increase insecticide resistance by compensating for the fitness costs of the 280S genotype (Djogbénou *et al.*, 2008; Djogbénou *et al.*, 2009; Luc, Valérie and Philip, 2010; Edi *et al.*, 2014; Assogba *et al.*, 2015; Djogbénou *et al.*, 2015; Weetman *et al.*, 2015; Assogba *et al.*, 2016;

Assogba *et al.*, 2018; Grau-Bové *et al.*, 2021). From analysis of the 1000 genome project data *(Anopheles gambiae* 1000 Genomes Consortium, 2017) it was found that presence of 280S homozygotes in the field was very rare and only occurred when the individual had greater than seven copies of ACE1. Wild type G280 homozygotes were the most common genotype in the data and in only one case was there any duplication, all other duplication included at least one *ace1* copy with the 280S mutation (Grau-Bové *et al.*, 2021). In this work I have shown that stable homozygous lines can be generated in the lab, but it would appear for resistance to be selected in the field, copies of the wild type *ace1* allele are needed to compensate for the fitness costs associated with the mutation. Because the ACE1 protein is a dimer, the presence of wild type peptides in the dimer may provide a balance of neuronal activity and insecticide resistance that gives the selective advantage in the presence of insecticide pressure.

Transgenic methods could be used to analyse the impact of *ace1* duplication/upregulation in several ways. Modification of ACE1-G280S with a GAL4-UAS system could be used to upregulate *ace1* or CRISPR-Cas9 could be used to introduce defined duplications to the line. The latter would provide more control of different combinations of G280S genotype between copies. Introducing the whole duplication seen in the field may be preferable, as it would result in the most realistic mutants, however typically very large clusters of genes are duplicated often spanning a region of 200 kb (Grau-Bové *et al.*, 2021). Inserting a fragment of this size is not feasible currently so a smaller insert focusing on *ace1* may be necessary.

In summary, homozygous ACE1-280S has been shown here to reduce susceptibility to malathion, fenitrothion and propoxur in adults and heterozygous G280S to reduce propoxur susceptibility in adults and temephos susceptibility in larvae. However, 280S was also shown to slightly reduce longevity and substantially reduce fecundity and fertility. The combination of moderate insecticide resistance and severe fitness costs likely explains why 280S homozygotes are not found in the field without many copies, which is thought to compensate for the fitness cost of the mutation.

# General Discussion

## 5.1 DETECTION OF CROSS RESISTANCE BETWEEN LARVAL AND ADULT STAGES

The primary focus of this thesis has been to characterise potential mechanisms of insecticide resistance in mosquito larvae and investigate their effect on insecticide susceptibility in adult stages and on adult fitness through genetic approaches. Previous work in the laboratory had created a series of *An. gambiae* GAL4-UAS transgenic lines to overexpress selected P450 and GST genes in a ubiquitous pattern throughout the development of the insect. These lines had been characterised in relation to insecticide resistance in adult stages and taken together these genes conferred cross resistance to pyrethroids, a carbamate, an organochloride and an OP (Adolfi *et al.*, 2019; Ingham *et al.*, 2020). To explore this further, Chapter 3 describes the production and testing of transgenic lines expressing a carboxylesterase, which completes a set of lines that cover members of the three main detoxifying gene families. The CCEae3A lines conferred resistance to an expanded set of insecticide classes, including all OPs and carbamates tested, as well as a member of the pyrethroid class. This latter finding is novel and emphasises the point that cross resistance through metabolic activity can be widespread. As well as validating a role for CCEae3A in resistance, the CCEae3A lines can be used alongside the other metabolic gene expressing lines to screen new compounds for liability to resistance from existing enzyme activity prior to expensive field trials (Lees *et al.*, 2020).

Since this panel of transgenic lines express the metabolic resistance genes in the larval stage, they were utilised in chapter 2 to explore the use of the INVAPP system to rapidly screen for relative resistance in larvae. This system has clearly shown promise as a high-throughput screen of chemical libraries, where acute toxicity of hundreds (and potentially thousands) of compounds can be rapidly assessed. In this project the interest was whether the system could detect (small) differences in resistance between mosquito strains expressing different individual metabolic genes. In hindsight, initial optimisation of the INVAPP system could have been conducted on a smaller subset of strains

and compounds (albeit at a wider range of concentrations), gradually adding complexity as opposed to starting with such a large experiment. Also, for this subset, complete paired data of compounds and strains using the INVAPP and WHO larval assays for comparison could have been collected.

Issues with access to the INVAPP system due to the COVID pandemic affected the optimisation of data collection, and focused attention on the analysis of the INVAPP assay data that was obtained early in the project. Despite the problems described in Chapter 2, some evaluation of the results was possible. None of the detoxification enzymes (CYP6P3, CYP6M2, GSTe2 and SAP2) tested using the INVAPP assay conferred temephos resistance, which was supported through WHO assays. Similarly, the data was largely supportive of CYP6P3 and Tiassale permethrin resistance as has been shown previously in adults. However, the results from INVAPP suggested a reduction in susceptibility in all 4 genetically modified strains tested when exposed to fenthion. This result was brought into question when compared to results from WHO assay of the same compound and strains where no change in resistance was found with GSTe2 and SAP2 lines and the opposite effect in CYP6M2 lines was observed. Conclusions became even more difficult as GSTe2 was shown to confer resistance to the similar compound fenitrothion in adults, highlighting how the phenotype may vary between not only adult and larval stage, but potentially between different larval stages. Meanwhile, results from the WHO assays support the assertion that CYP6M2 metabolises malathion to a more toxic form resulting in increased susceptibility when it is overexpressed in both larvae and adults.

Temephos, a key OP larvicide, was tested in all three chapters but only CCEae3A expression was found to confer strong resistance. CCEae3A upregulation was strongly linked to temephos resistance (Grigoraki *et al.*, 2015; Grigoraki *et al.*, 2016; Grigoraki *et al.*, 2017a; Seixas *et al.*, 2017; Marcombe *et al.*, 2019; Balaska *et al.*, 2020) prior to this study and this activity has been demonstrated *in vivo* for the first time. CCEae3A has been primarily reported as upregulated following selection by temephos but here it was found the CCEae3A also confers resistance to all OP and carbamate insecticides tested using WHO larval and tube assays and to alphacypermethrin as adults.

Meanwhile, ACE1 is generally considered as the target for the OP temephos and in spite of this, no resistance was detected in strains carrying the homozygous 280S amino acid substitution and

heterozygote G280S displayed only 1.6 fold resistance, despite being strongly linked with OP and carbamate resistance (Ahoua Alou *et al.*, 2010; Essandoh, Yawson and Weetman, 2013; Elanga-Ndille *et al.*, 2019; Keïta *et al.*, 2020). Despite very strong correlation with resistance to other OP insecticides there is a distinct lack of evidence suggesting ACE1-G280S confers resistance to temephos despite being the target site for OPs. It is unknown why this is the case, but it may provide some further insight into the apparent absence of the G280S substitution in *Aedes* mosquitoes. Only one report of ACE1-G280S has been reported in *Aedes* (Muthusamy and Shivakumar, 2015). The near absence of ACE1-G280S in *Aedes* mosquitoes has previously been attributed to gene constraints. But low magnitudes of resistance to malathion, fenitrothion and propoxur combined with longevity and fecundity fitness costs associated with ACE1-G280S may further explain why ACE1-G280S is very rarely found in *Aedes* mosquitoes.

Going forward, the 3A+/3A+ could be evaluated using INVAPP with temephos, chlorpyriphos and fenthion to optimise and compare with existing 3$^{rd}$ instar larval data and adult data. It would also be useful when the system is fully optimised to use INVAPP for rapid analysis of the ACE1-280S, ACE1-G280S and ACE1-280S lines now that a stable homozygous line has been established.

Taken together the data provides important information on the molecular mechanisms which are driving insecticide resistance in larval stage and has confirmed the capability of the GAL4-UAS system to be used for studying insecticide resistance in larvae which is novel. Though ultimately, there is not sufficiently clear data to fully understand the relationship between adult and larvae (or even 1$^{st}$ to 3$^{rd}$ instar larval) insecticide resistance but there are suggestions that it is not necessarily the same for different compounds, even from the same class.

## 5.2 COMBINING TRANSGENIC METHODS FOR *IN VIVO* FUNCTIONAL ANALYSIS

Several different transgenic methods have been employed for this project including two methods of genome modification (ϕC31 RMCE and CRISPR Cas9 HDR) and three different types of alterations

(GAL4-UAS, SNP and F2A-eYFP). There are several modifications which could improve and build upon the approaches used here in future work on these and other genes related to insecticide resistance.

Firstly, although this project has focused on studying resistance mechanisms in isolation for functional characterisation, it is also important to acknowledge that mechanisms rarely occur alone in the field. It is possible to study the impact of combining resistance mechanisms in a controlled environment using transgenic mosquitoes such as 3A+/3A+ crossed with UAS-responder lines for other genes of interest or modified lines with SNPs. This approach was taken by (Grigoraki *et al.*, 2021) to investigate the combined effect of GSTe2 upregulation and the L1014F *kdr* mutation on resistance to DDT and pyrethroid insecticides. In this thesis, it was shown that GSTe2 upregulation alone does not reduce susceptibility to permethrin, but when combined with the 1014F *kdr* mutation, provided a synergistic interaction that increased resistance seen from the mutation alone. This is critical evidence that the transgenic approach can be used to study synergism between different resistance mechanisms.

A similar experiment crossing the ACE1-G280S line created in Chapter 4 with the GSTe2 line used by (Grigoraki *et al.*, 2021) could be easily conducted. This would be particularly interesting as both mechanisms appear to cause resistance to fenitrothion, though only for ACE1-280S homozygotes not heterozygotes. In chapter 2, upGSTe2 did not display a significant reduction in malathion sensitivity in a WHO tube assay, but the results do warrant further investigation as mean mortality was just below 89.3% thus meeting the WHO definition for resistance. ACE1-G280S (homozygote 280S or heterozygote G280S) did not meet the WHO definition of resistance with a 1 h exposure but homozygote 280S did show reduced susceptibility with a 15-minute exposure in a WHO tube assay and displayed a 5.87-fold increase in LC50 in a malathion tarsal assay. No difference in malathion susceptibility was demonstrated for heterozygote ACE1-G280S but it would be interesting to investigate whether there is synergism with GSTe2 overexpression. GSTe2 upregulation has been found in the same mosquito populations as ACE1-G280S before in field mosquitoes (Hamid-Adiamoh *et al.*, 2020; Meiwald *et al.*, 2020; Piameu *et al.*, 2021) though mostly at modest levels of

upregulation and low proportions of G280S in the population. This may suggest the resistance given by the molecular changes are currently balanced by the demonstrated fitness cost/s of G280S and potentially co-GSTe2 overexpression.

Similar experiments could be conducted using the 3A+/3A+ strain created in Chapter 3 crossed with the ACE1-G280S strain created in Chapter 4. This was not possible during this project as the ACE1-280S homozygous line was not established in the time available. Although, CCEae3A is not an *An. gambiae* gene and there is not an ortholog in *An. gambiae*, it would still be interesting to study the impact of its upregulation combined with ACE1-280S, as a representative of the carboxylesterase group of detoxification enzymes.

Examination of co-upregulation of detoxification enzymes would also be interesting. Ubi-GAL4 integration lines are already available for CCEae3A and GSTe2 which could be crossed to the available UAS-responder lines (Poulton *et al.*, 2021). However, combinations of detoxification genes, that are only available as UAS-lines, such as CYP6P3, CYP6M2, or SAP2 would require the creation of new lines. These could be created in the same manner using ϕC31 RMCE in Ubi-GAL4 and selecting larvae with integration events. However, the 'design' opportunities of other gene editing approaches may be superior. The ultimate goal would be to increase expression of a GOI in the endogenous spatio-temporal pattern, rather than relying on a crude ubiquitous expression pattern or 'selected' tissue specific promoters.

A new approach combining CRISPR-Cas9 and GAL4-UAS could permit not only upregulation, but also control of the spatio-temporal manner of expression beyond what is currently possible with the GAL4 lines that are available. The GAL4 system has so far relied on discovery of promoters that we think the resistance genes are driven by. Lack of knowledge of this information and the trial and error in promoter discovery have limited this experimentation. However, as was shown in Chapter 4 through the first time use of F2A to define the expression pattern of GOI in *An. gambiae*, the CRISPR-Cas9 approach is highly efficient at harnessing endogenous gene regulation in this mosquito species. This HDR methodology could be adapted through insertion of a cassette immediately before the start codon of the gene of interest (GOI) which for instance contains 'GAL4-3xP3-eYFP-UAS'

which would result in transcription of GAL4 in the endogenous spatio-temporal pattern of the GOI and amplify its expression through the GAL4 transcription factor. Such methodology could also be extended by simultaneously creating base pair changes in the GOI to simultaneous study the overexpression of mutant alleles in the 'correct' endogenous tissues.

Another use of these lines could be for co-localisation of gene expression. A 'GAL4-3xP3-eYFP-UAS-GOI' line could also be crossed with UAS-mCD8:mCherry to drive mCherry expression in the same pattern as the GOI (Adolfi *et al.*, 2018). Alternatively, if 'F2A-GAL4-3xP3-eYFP' was introduced immediately before the stop codon of a gene, GAL4 expression would still occur in the same spatio-temporal pattern and could be crossed to a line carrying an exogenous copy of the gene controlled by a UAS promoter elsewhere in the genome. This methodology would be particularly useful if upregulation of the gene was lethal or carried a severe fitness cost. Another option with this type of bipartite system is to introduce RNAi 'hairpin' sequences as described in (Poulton *et al.*, 2021) for controlled knockdown of the GOI when crossed with one of the driver lines described above.

An entirely different approach to achieve tissue specific upregulation, that is yet to be published in mosquitoes, but has been developed in *D. melanogaster,* uses a modified Cas9 for gene upregulation or activation CRISPRa (Ewen-Campen *et al.*, 2017; Waters *et al.*, 2018). In this case, the Cas9 utilized has been modified to remove its DNA cleavage activity but retains its ability to be guided to specific DNA targets through guide RNAs. The modified Cas9 (dCas9) is fused to a transcription activator, and so when combined with a guide RNA that targets the promoter region of the GOI, directs expression of that gene. It would need to be assessed to what extent 'true' endogenous transcription patterns were conserved in the mosquito, but the CRISPRa is versatile. The extent of transcriptional activation could be modified by using different strength transcriptional activation domains (Lynd et al, 2012). A further advantage of the system is that multiple genes could be regulated simultaneously by using a number of different guide RNAs.

Currently in mosquitoes such modifications would have to be created using a HDR mechanism, which although efficient in *An. gambiae,* as demonstrated in Chapter 4, can be time consuming and

expensive to generate the necessary reagents. In human cells and *D. melanogaster,* a CRISPaint knock-in system has been developed in which CRISPR-Cas9 is used to cut the genome, then non-homologous end joining relied upon to insert a linear dsDNA fragment. The CRISPaint system does not require the use of homology arms as the location of insertion is driven solely by a gRNA and the recombinational activity of exogenous linear DNA. Thus, the system is less expensive and labour intensive for plasmid cloning and has been developed for the creation of knockout lines, as well as GAL4 lines like those described above (Schmid-Burgk *et al.*, 2016; Bosch *et al.*, 2020). The efficiency of correct insertion may be lower than HDR however, as this method appears to be favour deletions rather than precise insertion repair (Bosch *et al.*, 2020). I started to work on developing this system in *An. gambiae,* however had not succeeded prior to the end of the project, though little optimisation had been attempted. Successful development of this technique could increase the rate at which transgenic mosquitoes could be generated by substantially reducing the cloning and gene synthesis requirements. Libraries of transgenic *D. melanogaster* were possible using this technique (Bosch *et al.*, 2020), however the physical space and time required for maintenance would likely prevent the generation and screening of libraries in mosquitoes.

## 5.3 FINAL CONCLUSIONS

Overall, the work conducted in this thesis has improved the understanding of insecticide resistance mechanisms in mosquito larvae and shown that there is substantial cross resistance with adult resistance. It was also demonstrated that the GAL4-UAS system can be used for functional characterisation of individual genes on mosquito larvae. Attempts were made to develop and optimise the INVAPP assay for high throughput analysis resulting in identification of several alterations for improving the output data variability. A binary GAL4-UAS expression system upregulating CCEae3A was used to highlight unknown relationships between CCEae3A upregulation and insecticide resistance ultimately concluding that increased expression of this gene alone is capable of increasing resistance to members of 3 different insecticide classes. The use of F2A-eYFP fusion to tag the *ace1* gene was shown to be highly efficient in *An. gambiae* for the first time and paves the way for

further utilisation of this technology in mosquitoes. Finally, the production and characterisation of ACE1-G280S improved our understanding of evolutionary forces of insecticide resistance and fitness costs of mutation in a key insecticide target site.

# Appendices

## 6.1 APPENDIX A – CHAPTER 2 APPENDICES

```
#importing the libraries required for this analysis


import glob
import arrow
import pandas as pd
```

```
#This chunk makes the function which calculates and extracts the movement index for
each well from stacks of images of 96-well plates and pairs the data for each well
with the experimental data (exposure time, insecticide etc.) recorded in the condit
ions file.


def guess_genotype(name):
    '''
    Guess the genotype from the file name
    '''
    import re


    s = re.compile('([A-Z]*)_')
    if s.search(name):
        return s.search(name).groups()[0]


def guess_replicate(name):
    '''
    Guess the replicate value based on the file name
    '''
    import re
    s = re.compile('min (\d)')
    if s.search(name):
        return s.search(name).groups()[0]


def guess_exposure(name):
    '''
    Guess the replicate value based on the file name
    '''
```

```
    import re
    s = re.compile('([0-9]*)min ')
    if s.search(name):
        return s.search(name).groups()[0]

def guess_plateno(name):
    fname = name.split('/')[-1]
    return fname[:12]

def doVar(directory):
    import numpy as np
    import glob
    from skimage.io import imread
    images = glob.glob(directory+'/*tif')
    images = np.array([imread(images[0]), imread(images[15]), imread(images[-1])])
    varimg = np.var(images, axis=0)
    varimg = varimg > varimg.mean()+3*varimg.std()
    return varimg

def getSum(rowColList):
    '''
    Take a list (A) of lists (B) where each element of A is a row
    and each element of B is a well, then sum the number of positive
    (movement-detected) pixels in each well, returning as an array
    '''
    import numpy as np
    nrows = len(rowColList)
    ncols = len(rowColList[0])
    out = np.ones((nrows,ncols))*np.nan
    for row in range(out.shape[0]):
        for col in range(out.shape[1]):
            out[row,col] = rowColList[row][col].sum()
    return out

def getRowsCols(df, nrows=8, ncols=12):
    '''
    Split an image into 12 columns and 8 rows.
    Returns a list of lists that can be passed to getSum().
```

```
    '''
    import numpy  as np
    f = np.array_split(df, nrows,0)
    f = [np.array_split(x,ncols,1) for x in f]
    return f

def loadConditions(conditions):
    '''
    Read in the conditions file.  Must be either excel or csv.
    Must be in this format (order of columns not important):
    row    col    cmpd    concentration
    0        0        DMSO    1e-7
    etc
    '''
    import pandas as pd
    ftype = conditions.split('.')[-1]
    if ftype=='xlsx':
        fn = pd.read_excel
    if ftype == 'csv':
        fn = pd.read_csv
    conditions = fn(conditions)
    return conditions

def doAll(directory, conditionsFile):
    '''
    do the var analysis and merge with conditions
    '''
    import pandas as pd
    # get in the conditions
    conds = loadConditions(conditionsFile)

    # do variance
    mvts = doVar(directory)
    mvts = getRowsCols(mvts)
    mvts = getSum(mvts)

    # get the expt params
    exposure = guess_exposure(directory)
```

```
    plateNo = guess_plateno(directory)
    replicate = guess_replicate(directory)
    genotype = guess_genotype(directory)

    # turn into a dataframe
    out = []
    for row in range(8):
        for col in range(12):
            out.append([row, col, exposure, plateNo, replicate, genotype, mvts[row,
col]])
    out = pd.DataFrame(out)
    out.columns = ['row','col', 'exposure', 'plateNo', 'replicate', 'genotype', 'mv
tIndex']

    # merge with conditions
    out = out.merge(conds)

    return out

    # merge with the conditions
```

```
#Directing the program to the folder containing the image stacks

directory1 = '/media/bethpoulton/Seagate Backup Plus Drive/PhD/UCL INVAPP/GM Testin
g/GM 2 Testing/20180927 GM 2.1 Testing/20180927 Plate 1/'
```

```
#Importing the conditions file containing the experimental data which matches the i
mage stacks being analysed

conditions1 = '/media/bethpoulton/Seagate Backup Plus Drive/PhD/UCL INVAPP/GM Testi
ng/GM 2 Testing/20180927 GM 2.1 Testing/20180927 Plate 1/20180927conditions1.xlsx'
```

```
#Running the function generated above on the data just imported

imdirs = glob.glob(directory1+'/*')
thelot1 = []
for d in imdirs:
    thelot1.append(doAll(d, conditions1))
    print(d)
```

```
#Completes formation of the dataframe.

thelot1 = pd.concat(thelot1)
```

```
print(thelot1)
```

```
thelot1.head()
```

```
thelot1.tail()
```

```
directory2 = '/media/bethpoulton/Seagate Backup Plus Drive/PhD/UCL INVAPP/GM Testin
g/GM 2 Testing/20180927 GM 2.1 Testing/20180927 Plate 2/'
```

```
conditions2 = '/media/bethpoulton/Seagate Backup Plus Drive/PhD/UCL INVAPP/GM Testi
ng/GM 2 Testing/20180927 GM 2.1 Testing/20180927 Plate 2/20180927conditions2.xlsx'
```

```
imdirs = glob.glob(directory2+'/*')

thelot2 = []

for d in imdirs:

    thelot2.append(doAll(d, conditions2))

    print(d)
```

```
thelot2 = pd.concat(thelot2)
```

```
print(thelot2)
```

```
thelot2.head()
```

```
thelot2.tail()
```

```
#merging thelot1 and thelot2 so all of the data is in one data frame.


exptData = thelot1.append(thelot2, ignore_index = True)

print(exptData)
```

```
#saving the raw data before calculation of the nMI

exptData.to_csv('/media/bethpoulton/Seagate Backup Plus Drive/PhD/UCL INVAPP/GM Tes
ting/GM 2 Testing/20180927 GM 2.1 Testing/20180927 GM 2.1 Testing Raw Data.csv')
```

```
#Subsetting exptData.alldata - extracting only 0min exposure

# grouping this subset by plate number, row, col, genotype, compound, concentration
, bioreplicate, technical replicate, and exposure
```

```
#printing the mean of mvtIndex for each group (well on the plate)


ZeroExp = exptData.loc[exptData['exposure']=='0']

gZero = ZeroExp.groupby(['row', 'col', 'genotype', 'cmpd', 'concentration', 'plateN
o', 'bioreplicate', 'tecreplicate'])

print(gZero.mean())
```

```
#Subsetting exptData.alldata - extracting only 2 min exposure

# grouping this subset by plate number, row, col, genotype, compound, concentration
, bioreplicate, technical replicate, and exposure

#printing mean


TwoExp = exptData.loc[exptData['exposure']=='2']

gTwo = TwoExp.groupby(['row', 'col', 'genotype', 'cmpd', 'concentration', 'exposure
', 'plateNo', 'bioreplicate', 'tecreplicate'])

print(gTwo.mean())
```

```
#Subsetting exptData.alldata - extracting only 60 min exposure

# grouping this subset by plate number, row, col, genotype, compound, concentration
, bioreplicate, technical replicate, and exposure

#printing mean


SixtyExp = exptData.loc[exptData['exposure']=='60']

gSixty = SixtyExp.groupby(['row', 'col', 'genotype', 'cmpd', 'concentration', 'expo
sure', 'plateNo', 'bioreplicate', 'tecreplicate'])

print(gSixty.mean())
```

```
#Subsetting exptData.alldata - extracting only 90 min exposure

# grouping this subset by plate number, row, col, genotype, compound, concentration
, bioreplicate, technical replicate, and exposure

#printing mean


NintyExp = exptData.loc[exptData['exposure']=='90']

gNinty = NintyExp.groupby(['row', 'col', 'genotype', 'cmpd', 'concentration', 'expo
sure', 'plateNo', 'bioreplicate', 'tecreplicate'])

print(gNinty.mean())
```

```
#Subsetting exptData.alldata - extracting only 120 min exposure

# grouping this subset by plate number, row, col, genotype, compound, concentration
, bioreplicate, technical replicate, and exposure

#printing mean
```

```
OneTwentyExp = exptData.loc[exptData['exposure']=='120']

gOneTwenty = OneTwentyExp.groupby(['row', 'col', 'genotype', 'cmpd', 'concentration
', 'exposure', 'plateNo', 'bioreplicate', 'tecreplicate'])

print(gOneTwenty.mean())
```

```
#Subsetting exptData.alldata - extracting only 210 min exposure

# grouping this subset by plate number, row, col, genotype, compound, concentration
, bioreplicate, technical replicate, and exposure

#printing mean


TwoTenExp = exptData.loc[exptData['exposure']=='210']

gTwoTen = TwoTenExp.groupby(['row', 'col', 'genotype', 'cmpd', 'concentration', 'ex
posure', 'plateNo', 'bioreplicate', 'tecreplicate'])

print(gTwoTen.mean())
```

```
#Subsetting exptData.alldata - extracting only 240 min exposure

# grouping this subset by plate number, row, col, genotype, compound, concentration
, bioreplicate, technical replicate, and exposure

#printing mean


TwoFortyExp = exptData.loc[exptData['exposure']=='240']

gTwoForty = TwoFortyExp.groupby(['row', 'col', 'genotype', 'cmpd', 'concentration',
'exposure', 'plateNo', 'bioreplicate', 'tecreplicate'])

print(gTwoForty.mean())
```

```
#Subsetting exptData.alldata - extracting only 1440 min exposure

#grouping this subset by plate number, row, col, genotype, compound, concentration,
bioreplicate, technical replicate, and exposure

#printing mean


TwentyFourHourExp = exptData.loc[exptData['exposure']=='1440']

gTwentyFourHour = TwentyFourHourExp.groupby(['row', 'col', 'genotype', 'cmpd', 'con
centration', 'exposure', 'plateNo', 'bioreplicate', 'tecreplicate'])

print(gTwentyFourHour.mean())
```

```
#Assigning the mean value datasets names so that the function doesn’t have to be in
the code later.


g_0 = gZero.mean()

g_2 = gTwo.mean()
```

```
g_60 = gSixty.mean()
g_90 = gNinty.mean()
g_120 = gOneTwenty.mean()
g_210 = gTwoTen.mean()
g_240 = gTwoForty.mean()
g_1440 = gTwentyFourHour.mean()
```

```
#Adding the averaged mvtIndex for each exposure in place of the mvtIndex column


g_0.rename(columns={'mvtIndex': 'mi0'}, inplace=True)
g_2.rename(columns={'mvtIndex': 'mi2'}, inplace=True)
g_60.rename(columns={'mvtIndex': 'mi60'}, inplace=True)
g_90.rename(columns={'mvtIndex': 'mi90'}, inplace=True)
g_120.rename(columns={'mvtIndex': 'mi120'}, inplace=True)
g_210.rename(columns={'mvtIndex': 'mi210'}, inplace=True)
g_240.rename(columns={'mvtIndex': 'mi240'}, inplace=True)
g_1440.rename(columns={'mvtIndex': 'mi1440'}, inplace=True)
```

```
#merging the dataframes containing the average values of MI into one table in ten s
teps, one for each
#exposure time - ending in Average data which contains a separate column with MI pe
r row for each timepoint


mer1 = g_0.merge(g_2, how='left', on=['row', 'col', 'genotype', 'cmpd', 'concentrat
ion', 'plateNo', 'bioreplicate', 'tecreplicate'])
mer2 = mer1.merge(g_60, how='left', on=['row', 'col', 'genotype', 'cmpd', 'concentr
ation', 'plateNo', 'bioreplicate', 'tecreplicate'])
mer3 = mer2.merge(g_90, how='left', on=['row', 'col', 'genotype', 'cmpd', 'concentr
ation', 'plateNo', 'bioreplicate', 'tecreplicate'])
mer4 = mer3.merge(g_120, how='left', on=['row', 'col', 'genotype', 'cmpd', 'concent
ration', 'plateNo', 'bioreplicate', 'tecreplicate'])
mer5 = mer4.merge(g_210, how='left', on=['row', 'col', 'genotype', 'cmpd', 'concent
ration', 'plateNo', 'bioreplicate', 'tecreplicate'])
mer6 = mer5.merge(g_240, how='left', on=['row', 'col', 'genotype', 'cmpd', 'concent
ration', 'plateNo', 'bioreplicate', 'tecreplicate'])
AverageData = mer6.merge(g_1440, how='left', on=['row', 'col', 'genotype', 'cmpd',
'concentration', 'plateNo', 'bioreplicate', 'tecreplicate'])
```

```
print(AverageData)
```

```
#Normalising the data for each exposure time by dividing the columns in the merged
table.
```

```
#This creates a list of results (indexed by the python indexing) ...


t2t0 = list(AverageData['mi2'] / AverageData['mi0'])
t60t0 = list(AverageData['mi60'] / AverageData['mi0'])
t90t0 = list(AverageData['mi90'] / AverageData['mi0'])
t120t0 = list(AverageData['mi120'] / AverageData['mi0'])
t210t0 = list(AverageData['mi210'] / AverageData['mi0'])
t240t0 = list(AverageData['mi240'] / AverageData['mi0'])
t1440t0 = list(AverageData['mi1440'] / AverageData['mi0'])
```

```
#... which are now added to the merged dataframe.


AverageData['t2t0'] = t2t0
AverageData['t60t0'] = t60t0
AverageData['t90t0'] = t90t0
AverageData['t120t0'] = t120t0
AverageData['t210t0'] = t210t0
AverageData['t240t0'] = t240t0
AverageData['t1440t0'] = t1440t0
```

```
#Because of the group by functions python makes the first 5 columns indexes which c
an make them hard to work with.
#So this reindexes the dataframe and ensures that the data is indexed based solely
on pythons'hidden-but will be shown now' system.
#printing the final data set containing the normalised values for each well and eac
h exposure time.


AverageData = AverageData.reset_index()
print(AverageData)
```

```
#Exporting the final data.frame to a .csv file


AverageData.to_csv('/media/bethpoulton/Seagate Backup Plus Drive/PhD/UCL INVAPP/GM
Testing/GM 2 Testing/20180927 GM 2.1 Testing//20180927 GM 2.1 Testing Analysis.csv'
)
```

Appendix A-i: Python code for extraction of MI from INVAPP image stacks (Vectorgon) and calculation of the nMI.

An example of the code used for analysing the image stacks collected during an INVAPP experiment. First the relevant package libraries are imported. Second the function for

calculation of the movement index (MI or mvtIndex) for each well on each plate and attribution of this value to the correct experimental details (insecticide, strain, concentration etc.) is made. An object directing the programme to a folder containing the data to be analysed is created. A conditions file containing the experimental details for each well is imported. The function is then run, outputting a data.frame and the raw data saved as a .csv file. The normalised movement index is then calculated. A separate data.frame for each time point is created. For each data.frame the mean MI is calculated for each individual well (ensuring that a separate value is calculated for each unique combination of plate number (the unique value assigned to each plate at the start of the experiment), row, column, genotype, insecticide, concentration and exposure time). Then for each timepoint, the mean MI was divided by the mean MI at the 0 min time point (prior to addition of the insecticide) matching the data using the same parameters as when calculating the mean to ensure that the correct values are used. Finally, these data are combined into a single data frame containing a column with the nMI (meanMI-at-Tmin / meanMI-at-0min) for each time point (T) which is then exported as a .csv file. Text preceded with the # symbol is not runnable code and is used as comment to describe what the code in that chunk does. Code chunks 1-17 are the Vectorgon which was originally written by Dr. Steve Buckingham and with his assistance was edited for this analysis using image stacks as opposed to movie files.

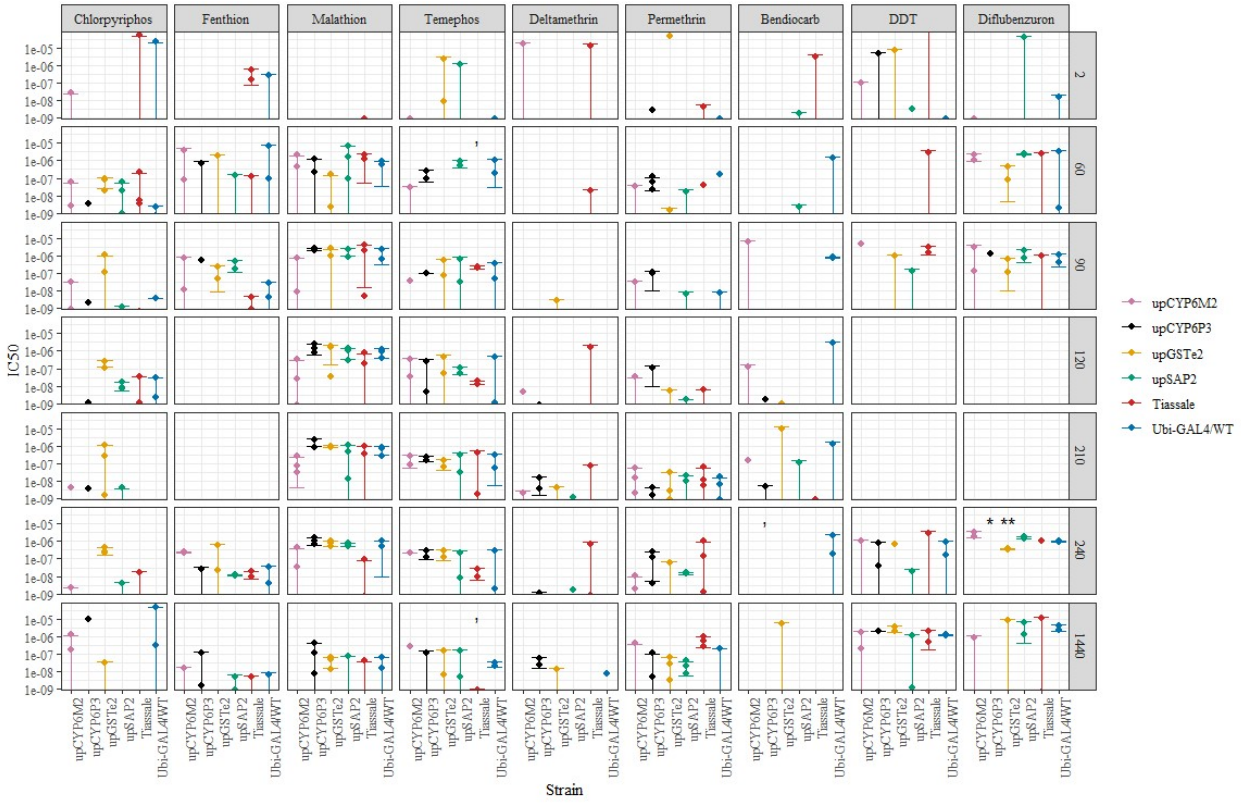


Appendix A ii: IC50 values calculated using the *'estimate_EC50()'* analysis method.

Absolute IC50s calculated using the *estimate _EC50()* function from the EC50estimator package in R facetted by compound (x) and exposure time (y). The y axis has been limited at $5x10^{-5}$ and $1.53\ x10^{-9}$ M to permit visualisation of values predicted within the range of concentrations tested. Error bars reflect the standard deviation of the mean IC50, points reflect the individual IC50s calculated for each replicate, p-values of <0.1 are reflected: 0.1 > , > 0.05 > * > 0.01 > ** > 0.001 > *** > 0.0001 > ****.

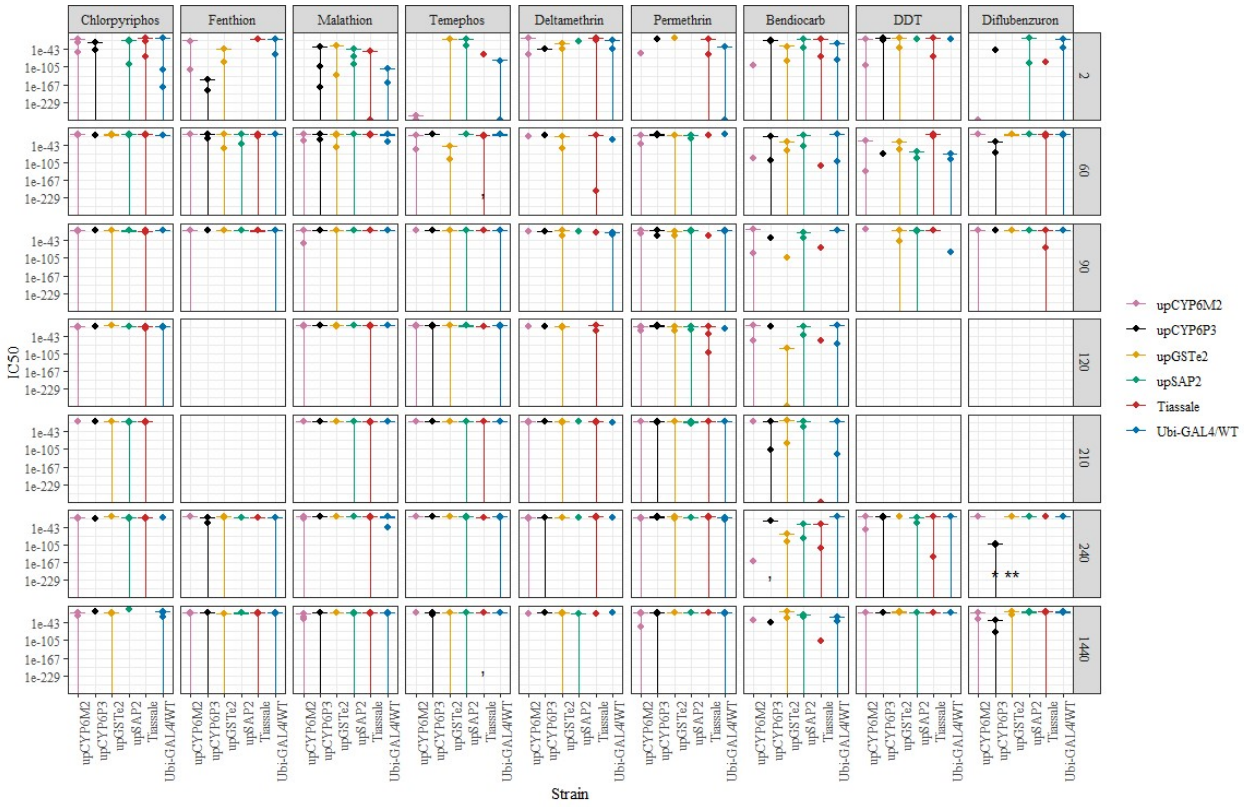


Appendix A-iii: 'estimate_EC50()' IC50s no axis limits.

Absolute IC50s calculated using the estimate _EC50() function from the ECestimator package in R facetted by compound (x) and exposure time (y). Error bars reflect the standard deviation of the mean IC50, points reflect the individual IC50s calculated for each replicate, p-values of <0.1 are reflected: 0.1 > , > 0.05 > * > 0.01 > ** > 0.001 > *** > 0.0001 > ****. Where lower confidence limit was calculated to be negative which is illogical it has been formatted to reach the bottom of the plot area.

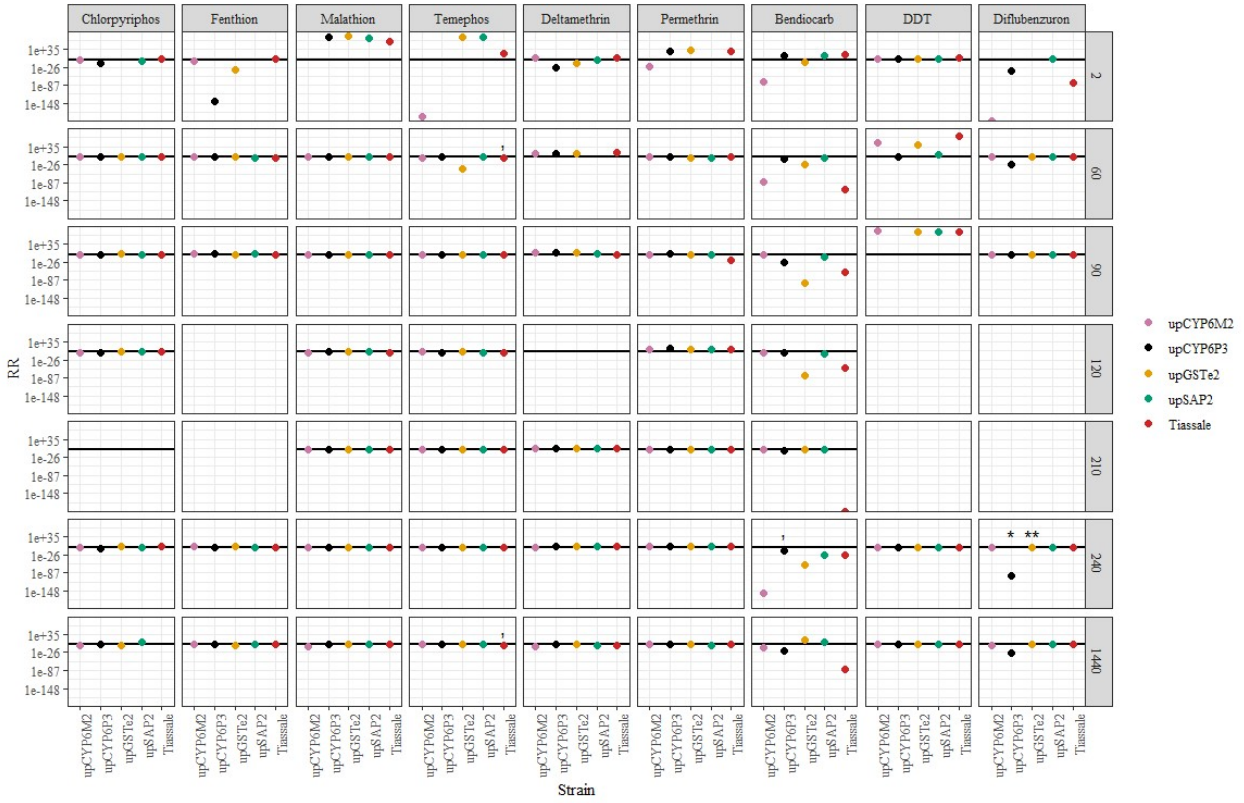


Appendix A-iv: 'estimate_EC50()' resistant ratios (RR) - no axis limits.

Resistance ratios calculated from meanIC50s (calculated using the estimate _EC50() function from the ECestimator package in R) comparing the test strains to the Ubi-GAL4/WT strain, facetted by compound (x) and exposure time (y). Points reflect RR, p-values of <0.1 are reflected: 0.1 > , > 0.05 > * > 0.01 > ** > 0.001 > *** > 0.0001 > ****. Horizonal black line indicates RR = 1 (IC50 strain = IC50 Ubi-GAL4/WT).

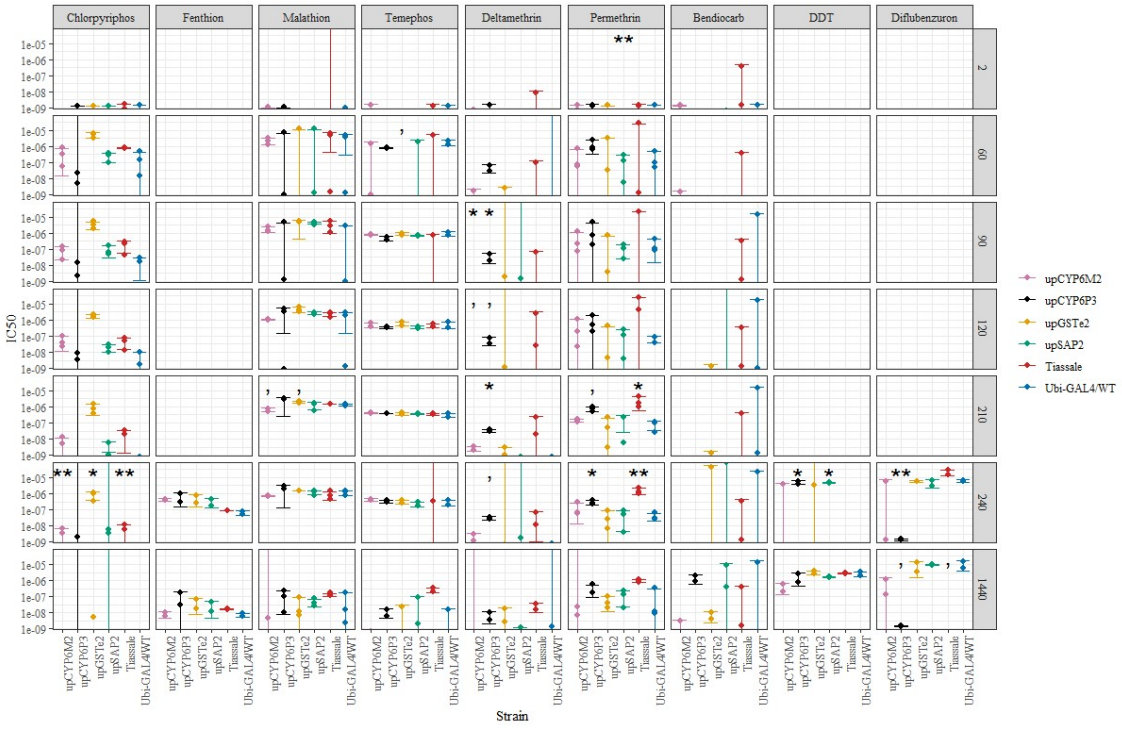


Appendix A-v: IC50 values calculated using the *'curve.fit()'* method.

Relative IC50s (calculated using the *curve.fit()* function from the scip.py package in python) facetted by compound (x) and exposure time (y). The y axis has been limited at $5x10^{-5}$ and $1.53\ x10^{-9}$ M to permit visualisation of values predicted within the range of concentrations tested. Error bars reflect the standard deviation of the mean IC50, points reflect the individual IC50s calculated for each replicate, p-values of <0.1 are reflected: 0.1 > , > 0.05 > * > 0.01 > ** > 0.001 > *** > 0.0001 > ****.

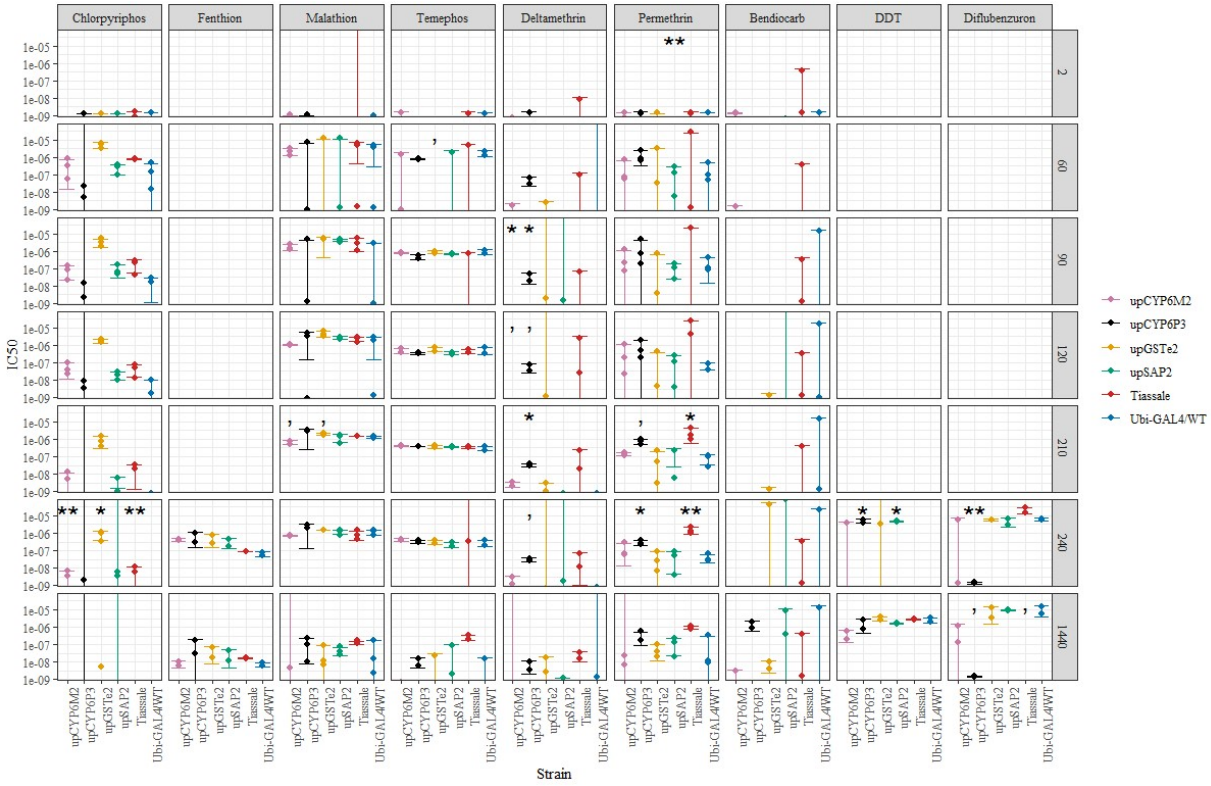


Appendix A-vi: 'curve.fit()' IC50s no axis limits.

Relative IC50s (calculated using the curve.fit() function from the scip.py package in python) facetted by compound (x) and exposure time (y). Error bars reflect the standard deviation of the mean IC50, points reflect the individual IC50s calculated for each replicate, p-values of <0.1 are reflected: 0.1 > , > 0.05 > * > 0.01 > ** > 0.001 > *** > 0.0001 > ****. Where lower confidence limit was calculated to be negative which is illogical it has been formatted to reach the bottom of the plot area.


Appendix A-vii: 'curve.fit' resistant ratios (RR) - no axis limits.

Resistance ratios calculated from meanIC50s (calculated using the curve.fit() function from the scip.py package in python) comparing the test strains to the Ubi-GAL4/WT strain, facetted by compound (x) and exposure time (y). Points reflect RR, p-values of <0.1 are reflected: 0.1 > , > 0.05 > * > 0.01 > ** > 0.001 > *** > 0.0001 > ****. Horizonal black line indicates RR = 1 (IC50 strain = IC50 Ubi-GAL4/WT).

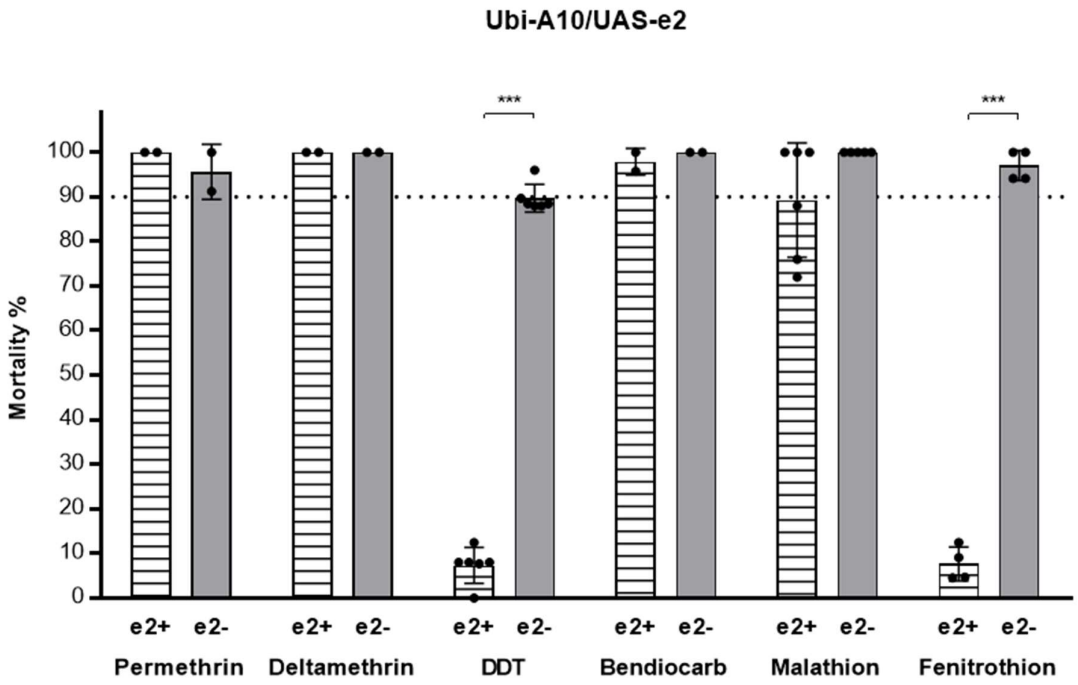


Appendix A-viii: Effect of ubiquitous GSTe2 Overexpression on insecticide susceptibility in WHO Tube assays.

Effect of ubiquitous GSTe2 overexpression under control of the Ubi-A10 (e2+) compared to Ubi-A10 controls (e2-) on adult female mosquito survival in WHO Tube assays. Data from Figure 2.3.7 as is presented in (Adolfi et al., 2019).

# 6.2 APPENDIX B – CHAPTER 3 APPENDICES

| Primer Name | Primer Sequence | Used For |
|---|---|---|
| CCEfor2 | GACTGGAATTCCATTATGTCCACTTTGGA | cDNA amplification |
| CCErev2 | GTATTCTCGAGTCATTGCAATGCTCGATG | cDNA amplification |
| CCEseqfor | ATTGTGGTGACGTTCAACTATCG | Sequencing cDNA + plasmid, Colony PCR |
| CCEseqrev | CTCGAGTCATTGCAATGCTCGATG | Sequencing cDNA + plasmid, Colony PCR |
| CCErev | CTCGAGTCATTGCAATGCTCGATG | Sequencing plasmid |
| UASp | GCAAGGGTCGAGTCGAGCGGAGACTCTAGC | Sequencing plasmid |
| ITRL1R | TGACGAGCTTGTTGGTGAGGATTCT | Orientation confirmation |
| Redseq_4R | CGAGGGTTCGAAATCGATAA | Orientation confirmation |
| piggybacR_R2 | TTTGCCTTTCGCCTTATTTTAGA | Orientation confirmation |
| qS7fw | AGAACCAGCAGACCACCATC | qPCR of Ribosomal Protein S7 |
| qS7rv | GCTGCAAACTTCGGCTATTC | qPCR of Ribosomal Protein S7 |
| qEFfw | GGCAAGAGGCATAACGATCAATGCG | qPCR of Elongation Factor |
| qEFrv | GTCCATCTGCGACGCTCCGG | qPCR of Elongation Factor |
| 3A qPCR for | TAGCTGTCACTGTGTGGACC | qPCR for CCEae3a |
| 3A qPCR rev | ACATTGTTCACTGCCAGCTA | qPCR for CCEae3a |

Appendix B-ix: Sequences of primers used in Chapter 3 and their uses.

## 6.3 APPENDIX C – CHAPTER 4 APPENDICES

| Primer Name | Purpose | Sequence |
|---|---|---|
| ACE1-G280S_LNA_F1 | Forward primer used in ACE1-G280S LNA and TaqMan Assays (Bass *et al.*, 2010) | GGCCGTCATGCTGTGGAT |
| ACE1_G280S_LNA_R1 | Reverse primer used in ACE1-G280S LNA and TaqMan Assays (Bass *et al.*, 2010) | GCGGTGCCGGAGTAGA |
| ACE1_3'utr_gRNA_a_F | Forward primer sequence for ACE1-F2A-eYFP gRNA | tgctgAGCTTAAACGAACTAGGCCA |
| ACE1_3'utr_gRNA_a_R | Reverse primer sequence for ACE1-F2A-eYFP gRNA | aaacTGGCCTAGTTCGTTTAAGCTc |
| ACE1e5G119SgRNAno1F | Forward primer sequence for ACE1-G280S gRNA | tgctgATGCTGTGGATCTTCGGCGG |
| ACE1e5G119SgRNAno1R | Reverse primer sequence for ACE1-G280S gRNA | aaacCCGCCGAAGATCCACAGCATc |
| F2Afor3 | Forward primer for annealing step of creation and preparation of F2A sequence for inclusion in template plasmid. | GGAAGCGGAGTGAAACAGACTTTGAATTTTGACCTTCTCAAGTTGGCGGGAGACG |
| F2Arev3 | Reverse primer for annealing step of creation and preparation of F2A sequence for inclusion in template plasmid. | AGGTCCAGGGTTGGACTCCACGTCTCCCGCCAACTTGAGAAGGTCAAAATTCAAA |
| F2Afor4 | Forward primer for the amplification step for F2A (binds half on ACE1-upstream sequence and half on F2A) | CGACCGTCAGATTCATACAAGGAAGCGGAGTGAAACAGAC |
| F2Arev4 | Reverse primer for the amplification step for F2A (binds half on eYFP sequence and half on F2A) | TCCTCGCCCTTGCTCACCATAGGTCCAGGGTTGGACTCCA |
| Upfor | Forward primer for amplification of ACE1 upstream sequence for ACE1-F2A-eYFP Gibson assembly (binds half on Puc19 plasmid and half on the upstream sequence). | CAGGTCGACTCTAGAGGATCTCCCGTTCGTGCCGGTGGTC |
| Uprev2 | Reverse primer for amplification of ACE1 upstream sequence for ACE1-F2A-eYFP Gibson assembly (binds half on F2A and half on the upstream complementary sequence). | GTCTGTTTCACTCCGCTTCCTTGTATGAATCTGACGGTCGCCG |
| eYFPfor2 | Forward primer for amplification of eYFP for ACE1-F2A-eYFP Gibson assembly (binds half on F2A and half on eYFP) | GTCTGTTTCACTCCGCTTCCTTGTATGAATCTGACGGTCGCCG |
| eYFPrev | Reverse primer for amplification of eYFP for ACE1-F2A-eYFP Gibson assembly (binds half on the ACE1 downstream | CATCAATGGGGTAGTAATTATTACTTGTACAGCTCGTCCATGC |

| Primer Name | Purpose | Sequence |
|---|---|---|
| | complementary sequence and half on eYFP) | |
| Downfor | Forward primer for amplification of the ACE1 downstream complementary sequence for ACE1-F2A-eYFP Gibson assembly (binds half on the ACE1 downstream complementary sequence and half on eYFP) | TGGACGAGCTGTACAA GTAATAATTACTACCC CATTGATGGCCT |
| Downrev | Reverse primer for amplification of the ACE1 downstream complementary sequence for ACE1-F2A-eYFP Gibson assembly (binds half on the ACE1 downstream complementary sequence and half on Puc19 plasmid) | AAAACGACGGCCAGTG AATTACGGGTTCGCGA CAATCCAA |
| MutUpfor | Forward primer for amplification of the ACE1 complementary sequence for ACE1-G280S Gibson assembly (binds half to Puc19 plasmid and half on ACE1- upstream complementary sequence | CAGGTCGACTCTAGAG GATCTTCCAACAGCCT CATTCACTCAT |
| MutUprev | Reverse primer for amplification of the ACE1 upstream complementary sequence for ACE1-G280S Gibson assembly (binds half to ACE1 downstream and half on ACE1- upstream complementary sequences). Has G280S SNP included in primer | GTACACGTCCAGGGTG GCGGTGCCGGAGTAGA AGCTGCCG |
| MutDownfor | Forward primer for amplification of the ACE1 downstream complementary sequence for ACE1-G280S Gibson assembly (binds half to ACE1 downstream and half on ACE1- upstream complementary sequences). Has G280S SNP included in primer | CGGCAGCTTCTACTCCg gCACCGCCACCCTGGA CGTGTAC |
| MutDownrev | Reverse primer for amplification of the ACE1 downstream complementary sequence for ACE1-G280S Gibson assembly (binds half to ACE1 downstream complementary sequence and half on Puc19 Plasmid). | AAAACGACGGCCAGTG AATTCTTTGCTGCGGT GCGTGTAC |
| 2ASeqFor1 | Forward primer for ACE1 sequencing | AAGCTGAGCGATGCGG TCGAG |
| 2ASeqFor2 | Forward primer for ACE1 sequencing | CGCAGCAAAGGCAACC CGTGG |
| 2ASeqFor3 | Forward primer for ACE1 sequencing | TCTGATCGTGCTGCTG GTGTC |

| Primer Name | Purpose | Sequence |
|---|---|---|
| 2ASeqFor4 | Forward primer for ACE1 sequencing | TACGCATGAACTACTACTTCCCTC |
| 2ASeqRev1 | Reverse primer for ACE1 sequencing | GGTGTAGCCGAGGGTGGGGTT |
| 2ASeqRev2 | Reverse primer for ACE1 sequencing | CTCCCTCGGTTCTGCTCTAAAGG |
| 2ASeqRev3 | Reverse primer for ACE1 sequencing | CTCCTGGTAACGAGTTACGAAGC |
| 2ASeqRev4 | Reverse primer for ACE1 sequencing | AGGTGTATTTGTGTAGTTTGTGTG |
| MutSeqFor1 | Forward primer for ACE1 sequencing | ATTCCCCTTTCACAGACAATTG |
| MutSeqFor2 | Forward primer for ACE1 sequencing | ATTTCAGACGCATTTTTTACACC |
| MutSeqFor3 | Forward primer for ACE1 sequencing | GAGGACTGTCTGTACATTAACGTG |
| MutSeqFor4 | Forward primer for ACE1 sequencing | ACGAACCGAGCAAGCTGAGCG |
| MutSeqRev1 | Reverse primer for ACE1 sequencing | TGCCCAACTCGGCATCTATAATT |
| MutSeqRev2 | Reverse primer for ACE1 sequencing | TGGTCGTACACGTCCAGGGTG |
| MutSeqRev3 | Reverse primer for ACE1 sequencing | CTCGTCCAGGAACGCACCGTC |
| MutSeqRev4 | Reverse primer for ACE1 sequencing | CAGTATCGCATGATCTTCCGGC |
| M13Rev | Reverse primer for sequencing inserts into the Puc19 plasmid | CAGGAAACAGCTATGACCATG |
| M13For | Forward primer for sequencing inserts into the Puc19 plasmid | GTTTTCCCAGTCACGAC |
| U6Prom | Forward primer for sequencing gRNAs in gRNA-Cas9 plasmids | TGCGCTTGAAGGGTTGATCG |
| For ACE1 G280S diagnostic | Forward primer for ACE1-G280S RFLP genotyping assay | GTACATTAACGTGGTGGCAC |
| Rev ACE1 G280S diagnostic | Reverse primer for ACE1-G280S RFLP genotyping assay | GTACATTAACGTGGTGGCAC |

Appendix C-x: Table detailing primer sequences

| Probe Name | 5’ Modification | Sequence | 3’ Modification |
|---|---|---|---|
| LNA_ACE1_G280_Probe | HEX | AAG+C+C+GCC+GC | IABkFQ |
| LNA_ACE1_280S_Probe | 6-FAM | AG+C+T+GCC+GC+C | IABkFQ |

Appendix C-xi: Table detailing probe sequences and modifications

+ symbol after base in sequence column indicates that it is a locked nucleic acid.

| Sample Type | Volume of 1X STE used for extraction | LNA Reaction Volume | Volume of Template included in LNA assay |
|---|---|---|---|
| 1st-2nd Instar Larvae | 10 µL | 10 µL | 2 µL |
| 3rd-4th Instar Larvae | 20 µL | 10 µL | 2 µL |
| Pupae Casings | 10 µL | 20 µL | 4 µL |
| Adults | 50 µL | 10 µL | 2 µL |

Appendix C-xii: Details of G280S-LNA reaction set-up for different sample types

| **10 µL Reaction** | **Stock Concentration** | **Final Concentration** | **N=1** | **N=100** |
|---|---|---|---|---|
| $dH_20$ | | | 1.6 µL | 160 µL |
| Primetime IDT master mix | *2X* | 1X | 5 µL | 500 µL |
| Primer: *ACE1_G280S_LNA_F1* | *10 µM* | 0.5 µM | 0.5 µL | 50 µL |
| Primer: *ACE1_G280S_LNA_R1* | *10 µM* | 0.5 µM | 0.5 µL | 50 µL |
| Probe: *LNA_ACE1_G280_probe* | *10 µM* | 0.2 µM | 0.2 µL | 20 µL |
| Probe: *LNA_ACE1_280S_probe* | *10 µM* | 0.2 µM | 0.2 µL | 20 µL |
| DNA Template | | | 2 µL | - |
| **Total** | | | 10 µL | **8 µL** per reaction |

| **20 µL Reaction** | **Stock Concentration** | **Final Concentration** | **N=1 (µL)** | **N=100 (µL)** |
|---|---|---|---|---|
| dH20 | | | 3.6 µL | 360 µL |
| Primetime IDT master mix | *2X* | 1X | 10 µL | 1000 µL |
| Primer: *ACE1_G280S_LNA_F1* | *10 µM* | 0.5 µM | 1 µL | 100 µL |
| Primer: *ACE1_G280S_LNA_R1* | *10 µM* | 0.5 µM | 1 µL | 100 µL |
| Probe: *LNA_ACE1_G280_probe* | *10 µM* | 0.1 µM | 0.2 µL | 20 µL |
| Probe: *LNA_ACE1_280S_probe* | *10 µM* | 0.1 µM | 0.2 µL | 20 µL |
| DNA Template | | | 4 µL | - |
| **Total** | | | 20 µL | **16 µL** per reaction |

Appendix C-xiii: ACE1-G280S LNA Master mix optimized set up.

# 6.4 APPENDIX D - GENERAL METHODS

### Appendix D-xiv: *An. gambiae* Rearing

Adult *An. gambiae* mosquitoes at least 5 days old were blood fed using human red blood cells plus plasma (NHS Blood Donation Service) in a Hemotek membrane feeding system. Three days later soaked Whatman paper was added to the cage for egg laying, which were washed into distilled water with 0.1% PondSalt (Pond guardian tonic salt - Blagdon) the following day. Larvae were fed ground Tetramin™ fish food daily and their water was replaced daily before feeding. Pupae were collected and placed in a stock cage when not required for experiments. All adult mosquitoes were fed *ad libitum* with cotton wool soaked in distilled water with 0.1% PondSalt and white sugar cube wet daily with 0.1% PondSalt.

### Appendix D-xv: Screening of fluorescent mosquitoes

Mosquitoes carrying red, yellow or cyan fluorescent (RFP, eYFP or eCFP respectively) protein controlled by the 3xP3 promoter were screened as described in (Poulton *et al.*, 2021) using a Leica MZ FLIII fluorescence stereo microscope fitted with DsRed, YFP and CFP filters (Leica Microsystems).

### Appendix D-xvi: Sexing of mosquito pupae

Mosquitoes were sexed either as pupae as described in (Poulton *et al.*, 2021) or using standard adult morphological characteristics by separating pupae to emerge individually in 25 mL tubes.

### Appendix D-xvii: Microinjections

Fire polished quartz micropipettes (OD 1.0 mm; ID 0.7 mm) (World Precision Instruments Inc.) were pulled using a Sutter P-2000 needle puller using the following settings: HEAT = 650; FIL = 4, VEL = 25, DEL = 145, PUL = 200.

Needles were back-filled with 1-2 µL of the desired plasmid mix with Microloader pipette tips (Eppendorf).

Female adult mosquitoes were forced to lay eggs as described in (Poulton *et al.*, 2021) and aligned as in (Lobo *et al.*, 2006) and injected as described in (Lombardo *et al.*, 2009).

### Appendix D-xviii: Longevity

For each technical replicate for each sex, within 24 hours of emergence, 9-11 adults were aspirated into a 200 ml paper cup covered with netting secured with rubber bands. Adults were maintained with 10% sucrose ad libitum supplied on cotton wool daily (covered to prevent evaporation), mortality counted and dead individuals removed every 24 hours until all individuals had died. Mortality was defined as an inability to stand or fly. Differences in longevity were assessed using Kaplan-Meier Curves and Fisher exact test.

### Appendix D-xix: WHO Larval Assay

Larval susceptibility was assessed using WHO standard larval assays (WHO, 2005). The appropriate volume of insecticide concentrated stock (dissolved in acetone) to achieve the desired concentrations was added to 200 ml of 0.01% pondsalt water with 25 third-instar larvae in a 250 mL clear deli pot (Cater for You Ltd. SP8OZ). Mortality was assessed visually after 24 hours continuous exposure. Moribund larvae were recorded as dead. 2-parameter log-logistic models (Equation 6.4.1) were generated using the 'drc package' (Ritz *et al.*, 2015) in R (version 4.1.0) and the comparm() function used to calculate and assess the significance of the differences in LC50.

$$f(x) = \frac{1}{1 + \exp\left(b(\log(x) - e)\right)}$$

Equation 6.4.1: Two-parameter log-logistic model

lower limit = 0, upper limit = 1, slope = b, ED50 = e

### Appendix D-xx: WHO Adult Tube Assay

Adult insecticide susceptibility was assessed using WHO Tube bioassays (WHO, 2018b). 20-25 female 2-5 days post emergence adults were exposed for a pre-determined time to standard diagnostic doses of insecticide on filter paper and mortality assessed at 24 h. Statistical differences in mortality were assessed using a two-tailed t-test assuming unequal variances in R or excel.

### Appendix xxi: Adult Tarsal Assay

Tarsal (leg parts) exposure of adults was achieved through coating of glass plates with 500 µL insecticide in solvent (typically acetone or ethanol) across a range of concentrations and allowing the solvent to evaporate for at least 1 h on an orbital shaker. A plastic 25 mL deli pot with a small hole (used to aspirate mosquitoes in and out) fits tightly into the plate creating a chamber. For each plate, 7-15 (ideally 10) 2-5 day old female adults were aspirated into a 200 mL paper cup covered with netting (secured with elastic bands) and held in the testing room for at least 1 h before being transferred to the chamber and the small hole covered with a square of parafilm. Exposure time was recorded (typically 30 min). The small size of the chamber forces contact with the insecticide. At the end of the exposure time, adults are aspirated from the chamber back into their cup, provided with sugar *ad libatum* on cotton wool and mortality is record 24 hours post exposure. The 'drc' package (Ritz *et al.*, 2015) in R (version 4.1.0) was used to generate 2-parameter log-logistic models (Equation 6.4.1) for estimation of and assessment of significance of differences in LC50.

### Appendix D-xxii: LIVAK DNA Extraction – modified from (Livak, 1984)

LIVAK Buffer (1.6 mL 5 M NaCl, 5.48 g sucrose, 1.57 g Tris, 10.16 mL 0.5 M EDTA, 2.5 mL 20% SDS and $dH_2O$ to a final volume of 100 mL – filter sterilised and stored in 1 mL aliquots) was prewarmed (65˚C – 15 min) and mixed. 100 µL LIVAK buffer was added for each adult mosquito and ground using an electric mortar and plastic pestle. Incubated immediately at $65^{O}C$ for 30 min. Condensation was collected by brief centrifugation 14 µL 8 M potassium acetate was added and mixed by gentle pipetting before incubating on ice for 30 min. DNA was separated from the mosquito

tissues by centrifuging at 13000 RPM at 4˚C for 20 min and transferring the supernatant to a clean tube. A second spin was carried out if required to remove all debris. 200 µL 100 % ethanol was added, the tube was flicked to mix and centrifuged at 13000 RPM for 15 min at 4˚C. The supernatant is removed taking care not to disturb the white smear/pellet (DNA). 100 µL 70% ice cold ethanol is used to wash the pellet then centrifuged at 13000 RPM for 10 min at 4˚C. The supernatant was removed ensuring that the smear/pellet was not disturbed, and the tube left on the bench for 5 – 10 min to allow the pellet to dry before resuspending the pellet in 100 µL $dH_2O$ (prewarmed to 60˚C).

### Appendix D-xxiii: PCR for Cloning

PCR reactions for cloning were conducted using Phusion High-Fidelity DNA Polymerase (Thermo Scientific) and working solutions of 2.5 mM dNTPs mix (Sigma) and 10 µM primers (IDT) in a T100 thermal cycler (BioRad).

### Appendix D-xxiv: Colony PCR

Colony PCR was conducted using DreamTaq polymerase (Thermo Scientific EP0702). Primers were selected that bridge the insertion and the backbone of the plasmid so that a failed insertion provides a negative result. Products were usually between 200 and 500 bp. 10 µL PCR reactions with 0.25 µM dNTPs, 0.5 µM of each primer, 0.1 µL DreamTaq and $nfH_2O$ to a total volume of 10 µL. DNA template was added by picking a colony from an agar plate using a pipette tip, dipping the colony in the PCR reaction (taking care not to remove reaction volume in the pipette tip) and storing the tip in a 1.5. mL Eppendorf. Colony PCRs were run according to the best annealing temperatures for the primer pairs used with a basic thermocycler setting of: 95˚C – 5 min, [95˚C – 10 s, annealing temperature – 10 s, 72˚C – 20 s], 72˚C – 5 min, 4˚C – hold.

### Appendix D-xxv: Agarose gel electrophoresis

For DNA visualisation, samples were loaded and run on a 0.8-2% agarose gel prepared with TAE buffer (ThermoFisher) which contained MidoriGreen (GeneFlow) for staining. Orange loading dye was added to each sample (if a buffer containing a dye, e.g., DreamTaq Green Buffer, was not used)

to a final concentration of 1X. Samples were loaded alongside a 1 kb plus ladder and images were acquired using a G-box transilluminator and Gene snap image acquisition software (SynGene).

### Appendix D-xxvi: DNA extraction and purification from agarose gel

DNA extraction was always conducted on DNA bands cut from an agarose gel following gel electrophoresis. Gel bands were incubated at 50˚C until the gel liquified. 1 mL buffer QG (Sigma) with 1.5 mg/mL diatomaceous earth (Sigma) added, was added and mixed then the mixture was passed through a Promega miniprep column twice and washed twice with 1 mL merlin P5 (NaCl (200 mM), Tris (20 mM), EDTA (5 mM) and 1 volume ethanol) buffer before eluting in prewarmed 20-50 µL nf$H_2O$.

### Appendix D-xxvii: Sticky ends ligation

For 'sticky ends' ligation, digested inserts were combined with digested vector (50-100 ng) in a molar ratio of 3:1 in a final volume of 10 µL with T4 DNA ligase and incubated at 16˚C overnight.

### Appendix D-xxviii: DNA ethanol precipitation

1/10$^{th}$ volume of 3 M sodium acetate then 2.5 volumes of 100% ice-cold ethanol were added to the DNA to be precipitated and mixed by gentle pipetting. DNA was pelleted by centrifuging at 13000 RPM at 4˚C for 20 min. A second spin was carried out if required to remove all supernatant without disturbing the smear/pellet. 1000 µL 70% ice cold ethanol is used to wash the pellet then centrifuged at 13000 RPM for 10 min at 4˚C. The supernatant was removed ensuring that the smear/pellet was not disturbed, and the tube left on the bench for 5 – 10 min to allow the pellet to dry before resuspending the pellet.

*When storing plasmids at 1000 ng/*µL: d$H_2O$ (prewarmed to 60˚C) calculated by – (starting plasmid nanodrop concentration * volume of plasmid precipitated) / 2000. Note the volume of water required is calculated for 2000 ng/µL as this accounts for errors in nanodrop concentration and/or loss of DNA

during precipitation. This often resulted in concentrations of greater than 1000 ng/L. In that case either this was just left as it or the volume of water to be added to achieve 1000 ng/µL was calculated and added.

*When preparing injection mix*: The volumes of plasmids combined at the start of the process were calculated to provide the desired final concentration in a volume of 20 µL. To account for losses during precipitation 17 or 18 µL of 1X injection buffer (5 mM KCl, 0.5 mM $NaPO_4$, pH 7.2) (Lombardo *et al.*, 2009).

## Appendix D-xxix: *E. coli* plasmid transformation and culture

1 - 3 µL ligation mix, 3 µL MegaX DH10B™ T1R Electrocomp™ *E.coli* cells (Invitrogen) and nf$H_2O$ (to a final volume of 20 µL) were combined and introduced into chilled Fisherbrand™ Electroporation Cuvettes Plus™ (Fisher Scientific 15532423). Transformation settings used were 25 µF, 200 Ω, 1.5 mV. Cells were immediately transferred to 1 mL prewarmed LB media and incubated at 37 ˚C for 45 minutes shaking at ~ 300 RPM). 100 µL was then spread on LB agar plates with the appropriate concentration of the required antibiotic (noted in relevant methods sections). The remainder was transferred to a 1.5 mL microcentrifuge tube and centrifuged at 3000 RPM for 5 min. Most of the supernatant was removed leaving just enough to resuspend the bacterial pellet and spread on a second LB agar plate with the required concentration of antibiotic. Both plates were incubated overnight (at least 16 h) at 37˚C. Where colonies were recovered depending on the number either all or a subset of colonies were picked and confirmed to carry the desired plasmid using colony PCR.

Colonies selected for further analysis were inoculated into 5 mL LB media plus the appropriate concentration of antibiotic and incubated overnight (at least 16 h) at 37˚C, shaking at ~ 300 RPM.

When larger concentrations of plasmid were required 50 – 100 mL cultures were set up in the same was with appropriate volumes of antibiotic, inoculated from a 5 mL culture of the desired plasmid.

### Appendix D-xxx: Miniprep of plasmids from *E. coli*

~3 mL of the required cells was pelleted by centrifuging at 13000 RPM for 5 min. The supernatant was removed and if required a second shorter centrifuge step was conducted. The pellet was resuspended in 200 µL Merlin P1 Buffer (Tris Base (50mM) and EDTA (10 mM) adjusted to pH 8). 200 µL of Merlin P2 (NaOH (0.2 M) and SDS (1%)) and then 200 µL of Merlin P3 (Potassium acetate (1.25 M) adjusted to pH 5.5) buffers were added sequentially before centrifuging at 13000 RPM for 1 min. The supernatant was transferred to a clean 1.5 mL eppendorf. 1 mL Merlin P4 (Guanidine hydrochloride (66.9g), Merlin P3 (33.3 mL) and $dH_2O$ (to a total volume of 100 mL), filter sterilised (0.22 µM) before addition of 1.5 g diatomaceous earth) buffer was added and mixed with the supernatant before being added to a syringe attached to a promega miniprep column (which does not contain a DNA binding agent). The plasmid – merlin 4 mix was pushed through the syringe twice before being discarded. The column was washed by passing 2 x 1 mL merlin P5 through the syringe. Plasmid DNA was eluted from the column using 20 – 50 µL prewarmed (60˚C) $nfH_2O$ and the concentration and quality of DNA recovered assessed using a NanoDrop.

### Appendix D-xxxi: Midiprep of plasmids from *E. coli*

50 - 100 mL overnight clonal *E. coli* cultures were processed to purify plasmid DNA following manufacturers instructions for the HiSpeed Plasmid Midi Kit (Qiagen 12643). Plasmid DNA was eluted in TE Buffer. Usually, plasmids were then concentrated using the DNA ethanol precipitation protocol described above.

### Appendix D-xxxii: Sanger sequencing

DNA samples were sent for sequencing at SourceBioscience. Plasmids were supplied at ~ 100 ng/µL. PCR products were supplied at ~ 10 ng/µL. Primers were supplied at 3.2 pMol/µL. Sequences were using Benchling.

## 6.5 APPENDIX E – PUBLISHED PAPERS

jove

# Using the GAL4-UAS System for Functional Genetics in *Anopheles gambiae*

Beth Crawford Poulton[1], Fraser Colman[1], Amalia Anthousi[1,2,3], Linda Grigoraki[1], Adriana Adolfi[1], Amy Lynd[1], Gareth John Lycett[1]

[1] Department of Vector Biology, Liverpool School of Tropical Medicine [2] IMBB FORTH [3] Department of Biology, University of Crete

**Corresponding Authors**

Beth Crawford Poulton
Beth.Poulton@lstmed.ac.uk
Gareth John Lycett
Gareth.Lycett@lstmed.ac.uk

**Citation**

Poulton, B.C., Colman, F., Anthousi, A., Grigoraki, L., Adolfi, A., Lynd, A., Lycett, G.J. Using the GAL4-UAS System for Functional Genetics in *Anopheles gambiae*. *J. Vis. Exp.* (), e62131, doi:10.3791/62131 (2020).

**Date Published**

December 18, 2020

**DOI**

10.3791/62131

**URL**

jove.com/t/62131

**Abstract**

The bipartite GAL4-UAS system is a versatile and powerful tool for functional genetic analysis. The essence of the system is to cross transgenic 'driver' lines that express the yeast transcription factor GAL4 in a tissue specific manner, with transgenic 'responder' lines carrying a candidate gene/RNA interference construct whose expression is controlled by Upstream Activation Sequences (UAS) that bind GAL4. In the ensuing progeny, the gene or silencing construct is thus expressed in a prescribed spatiotemporal manner, enabling the resultant phenotypes to be assayed and gene function inferred. The binary system enables flexibility in experimental approaches to screen phenotypes generated by transgene expression in multiple tissue-specific patterns, even if severe fitness costs are induced. We have adapted this system for *Anopheles gambiae*, the principal malaria vector in Africa.

In this article, we provide some of the common procedures used during GAL4-UAS analysis. We describe the *An. gambiae* GAL4-UAS lines already generated, as well as the cloning of new responder constructs for upregulation and RNAi knockdown. We specify a step by step guide for sexing of mosquito pupae to establish genetic crosses, that also includes screening progeny to follow inheritance of fluorescent gene markers that tag the driver and responder insertions. We also present a protocol for clearing *An. gambiae* embryos to study embryonic development. Finally, we introduce potential adaptions of the method to generate driver lines through CRISPR/Cas9 insertion of GAL4 downstream of target genes.

**Introduction**

The bipartite GAL4-UAS system is the workhorse of functional characterization of genes in the insect model organism *Drosophila melanogaster*[1,2,3]. To use the GAL4-UAS system, transgenic driver lines, expressing the yeast transcription factor GAL4 under control of a regulatory sequence, are crossed with responder lines carrying a gene of




Appendix E-xxxiii: Published First Author Paper - Poulton *et al*, 2021

Contribution – Prepared manuscript, edited, collected images (except embryos), corresponding author, coordinated and participated in filming. Manuscript is published, video footage has been collected but not yet published.

PLOS NEGLECTED TROPICAL DISEASES

RESEARCH ARTICLE

# Automated phenotyping of mosquito larvae enables high-throughput screening for novel larvicides and offers potential for smartphone-based detection of larval insecticide resistance

**Steven D. Buckingham[1☯], Frederick A. Partridge[1☯], Beth C. Poulton[1,2☯], Benjamin S. Miller[3☯], Rachel A. McKendry[3,4], Gareth J. Lycett[2], David B. Sattelle[1*]**

1 UCL Centre for Respiratory Biology, UCL Respiratory, Division of Medicine, University College London, London, United Kingdom, 2 Liverpool School of Tropical Medicine, Liverpool, United Kingdom, 3 London Centre for Nanotechnology, Faculty of Maths & Physical Sciences, University College London, London, United Kingdom, 4 Division of Medicine, University College London, London, United Kingdom

☯ These authors contributed equally to this work.
* d.sattelle@ucl.ac.uk



OPEN ACCESS

**Citation:** Buckingham SD, Partridge FA, Poulton BC, Miller BS, McKendry RA, Lycett GJ, et al. (2021) Automated phenotyping of mosquito larvae enables high-throughput screening for novel larvicides and offers potential for smartphone-based detection of larval insecticide resistance. PLoS Negl Trop Dis 15(6): e0009639. https://doi.org/10.1371/journal.pntd.0009639

**Editor:** Adalgisa Caccone, Yale University, UNITED STATES

**Received:** August 6, 2020

**Accepted:** May 10, 2021

**Published:** June 3, 2021



**Data Availability Statement:** All relevant data are within the manuscript and its Supporting Information files.

**Funding:** BSM and RAM were supported by i-sense EPSRC IRC in Agile Early Warning Sensing Systems for Infectious Diseases and Antimicrobial Resistance (grant number EP/R00529X/1). The funders had no role in study design, data collection

## Abstract

Pyrethroid-impregnated nets have contributed significantly to halving the burden of malaria but resistance threatens their future efficacy and the pipeline of new insecticides is short. Here we report that an invertebrate automated phenotyping platform (INVAPP), combined with the algorithm Paragon, provides a robust system for measuring larval motility in *Anopheles gambiae (and An. coluzzi)* as well as *Aedes aegypti* with the capacity for high-throughput screening for new larvicides. By this means, we reliably quantified both time- and concentration-dependent actions of chemical insecticides faster than using the WHO standard larval assay. We illustrate the effectiveness of the system using an established larvicide (temephos) and demonstrate its capacity for library-scale chemical screening using the Medicines for Malaria Venture (MMV) Pathogen Box library. As a proof-of-principle, this library screen identified a compound, subsequently confirmed to be tolfenpyrad, as an effective larvicide. We have also used the INVAPP / Paragon system to compare responses in larvae derived from WHO classified deltamethrin resistant and sensitive mosquitoes. We show how this approach to monitoring larval response to insecticides can be adapted for use with a smartphone camera application and therefore has potential for further development as a simple portable field-assay with associated real-time, geo-located information to identify hotspots.

## Author summary

We have developed an automated platform for recording the motility of mosquito larvae and applied it to larvae of a mosquito vector of malaria and a mosquito vector of dengue,



Appendix E-xxxiv: Published Co-First Author Paper - Buckingham *et al* 2021

Contribution – WHO larval assay, writing and editing manuscript.

molecules

MDPI

Article

# Actions of camptothecin derivatives on larvae and adults of the arboviral vector *Aedes aegypti*

**Frederick A. Partridge [†], Beth C. Poulton [†], Milly A.I. Lake [†], Rebecca A. Lees [2], Harry-Jack Mann [1], Gareth J. Lycett [2,*] and David B. Sattelle [1,*]**

[1] Centre for Respiratory Biology, UCL Respiratory, Division of Medicine, University College London, London, WC1E 6BT, United Kingdom
[2] Liverpool School of Tropical Medicine, Pembroke Place, Liverpool, L3 5QA, United Kingdom
* Correspondence: d.sattelle@ucl.ac.uk (DBS), gareth.lycett@lstmed.ac.uk (GJL)
† Contributed equally

**Abstract:** Mosquito-borne viruses including dengue, Zika and Chikungunya viruses, and parasites such as malaria and *Onchocerca volvulus* endanger health and economic security around the globe and emerging mosquito-borne pathogens have pandemic potential. However, the rapid spread of insecticide resistance threatens our ability to control mosquito vectors. Larvae of *Aedes aegypti* were screened with the Medicines for Malaria Venture Pandemic Response Box, an open-source compound library, using INVAPP, an invertebrate automated phenotyping platform suited to high-throughput chemical screening of larval motility. We identified rubitecan (a synthetic derivative of camptothecin) as a hit compound that reduced *Ae. aegypti* larval motility. Both rubitecan and camptothecin displayed concentration dependent reduction in larval motility with estimated $BC_{50}$ of 25.5 ± 5.0 µM and 22.3 ± 5.4 µM respectively. We extended our investigation to adult mosquitoes and found that camptothecin increased lethality when delivered in a blood meal to *Ae. aegypti* adults at 100 µM and 10 µM and completely blocked egg laying when fed at 100 µM. Camptothecin and its derivatives are inhibitors of topoisomerase I and have known activity against several agricultural pests and are also approved for the treatment of several cancers. Crucially, they can inhibit Zika virus replication in human cells, so there is potential for dual targeting of both the vector and an important arbovirus that it carries.

**Keywords:** insecticide; mosquito; *Aedes*; camptothecin; vector; rubitecan

Citation: Lastname, F.; Lastname, F.; Lastname, F. Title. *Molecules* **2021**, *26*, x. https://doi.org/10.3390/xxxxx

Academic Editor: Firstname Lastname

Received: date
Accepted: date
Published: date



## 1. Introduction

### 1.1. Vector-borne diseases and pandemics

Humans have had to contend repeatedly with disease epidemics throughout history. Viruses such as Ebola, HIV, SARS-CoV-2 and Zika underscore the vulnerability of the human population to emerging pathogens. Furthermore, changes in our environment and society such as urbanisation, increased travel, and climate change will make epidemics more frequent and harder to control [1]. New and emerging infectious diseases, together with problems of anti-microbial resistance, are a challenge to our limited anti-infective medications and other tools for controlling diseases. To help to address this problem, the Medicines for Malaria Venture has recently launched the Pandemic Response Box, an open-source drug discovery program, where laboratories around the world collaborate by screening a library of structurally diverse compounds selected for potential activity against infective and neglected diseases.

Diseases transmitted by arthropod vectors endanger people in many areas of the globe. These vector-borne pathogens include protozoa, such as *Plasmodium*, *Trypanosoma* and *Leishmania*; nematodes, such as *Onchocerca volvulus*; as well as viruses, such as



Appendix E-xxxv: Co-First Author Paper - Partridge *et al*, 2021

Contribution – All adult assays, writing and editing manuscript.

# 6.6 BIBLIOGRAPHY


Achee, N., Gould, F., Perkins, T., Reiner, R., Morrison, A., Ritchie, S., Gubler, D., Teyssou, R. and Scott, T. (2015) 'A critical assessment of vector control for dengue prevention', *PLoS Neglected Tropical Diseases,* 9(5), pp. e0003655.

Adolfi, A. (2017) *In vivo functional genetic analysis of cytochromes P450 involved in insecticide resistance in the malaria vector Anopheles gambiae.* Ph.D. Doctoral, University of Liverpool, Liverpool [Online] Available at: https://ethos.bl.uk/OrderDetails.do?uin=uk.bl.ethos.733849 (Accessed.

Adolfi, A. and Lycett, G. (2019) 'Opening the toolkit for genetic analysis and control of Anopheles mosquito vectors.', *Europe PMC,* 30, pp. 8-18.

Adolfi, A., Lynd, A., Lycett, G. and James, A. (2021) 'Site-Directed φC31-Mediated Integration and Cassette Exchange in Anopheles Vectors of Malaria', *Journal of Visualized Experiments,* (168).

Adolfi, A., Pondeville, E., Lynd, A., Bourgouin, C. and Lycett, G. (2018) 'Multi-tissue GAL4-mediated gene expression in all Anopheles gambiae life stages using an endogenous polyubiquitin promoter', *Insect Biochemistry and Molecular Biology,* 96, pp. 1-9.

Adolfi, A., Poulton, B., Anthousi, A., Macilwee, S., Ranson, H. and Lycett, G. (2019) 'Functional genetic validation of key genes conferring insecticide resistance in the major African malaria vector, Anopheles gambiae', *Proceedings of the National Academy of Sciences of the United States of America,* 116(51), pp. 25764-25772.

Afrane, Y., Klinkenberg, E., Drechsel, P., Owusu-DK., Garms, R. and Kruppa, T. (2004) 'Does irrigated urban agriculture influence the transmission of malaria in the city of Kumasi, Ghana?', *Acta Tropica,* 89(2), pp. 125-134.

Agossa, F., Aïkpon, R., Azondékon, R., Govoetchan, R., Padonnou, G., Oussou, O., Oké-Agbo, F. and Akogbéto, M. (2014) 'Efficacy of various insecticides recommended for indoor residual spraying: pirimiphos methyl, potential alternative to bendiocarb for pyrethroid resistance management in Benin, West Africa', *Transactions of the Royal Society of Tropical Medicine and Hygiene,* 108(2), pp. 84-91.

Aguas, R., Dorigatti, I., Coudeville, L., Luxemburger, C. and Ferguson, N. (2019) 'Cross-serotype interactions and disease outcome prediction of dengue infections in Vietnam', *Scientific Reports,* 9(1), pp. 1-12.

Ahadji-Dabla, K., Romero-Alvarez, D., Djègbè, I., Amoudji, A., Apétogbo, G., Djouaka, R., Oboussoumi, K., Aawi, A., Atcha-Oubou, T., Peterson, A. and Ketoh, G. (2020) 'Potential Roles of Environmental and Socio-Economic Factors in the Distribution of Insecticide Resistance in Anopheles gambiae sensu lato (Culicidae: Diptera) Across Togo, West Africa', *Journal of Medical Entomology,* 57(4), pp. 1168-1175.

Ahmad, S., Rahi, M., Ranjan, V. and Sharma, A. (2021) 'Mefloquine as a prophylaxis for malaria needs to be revisited', *International Journal for Parasitology - Drugs and Drug resistance,* 17, pp. 23-26.

Ahoua Alou, L., Koffi, A., Adja, M., Tia, E., Kouassi, P., Koné, M. and Chandre, F. (2010) 'Distribution of ace-1R and resistance to carbamates and organophosphates in Anopheles gambiae s.s. populations from Côte d'Ivoire', *Malaria Journal,* 9, pp. 167.

Aiku, A., Yates, A. and Rowland, M. (2006) 'Laboratory evaluation of pyriproxifen treated bednets on mosquito fertility and fecundity. A preliminary study', *West African Journal of Medicine,* 25(1), pp. 22-26.

Aker, W., Hu, X., Wang, P. and Hwang, H. (2008) 'Comparing the relative toxicity of malathion and malaoxon in blue catfish Ictalurus furcatus', *Environmental Toxicology,* 23(4), pp. 548-554.

Akogbeto, M., Padonou, G., Bankole, H., Gazard, D. and Gbedjissi, G. (2011) 'Dramatic decrease in malaria transmission after large-scale indoor residual spraying with bendiocarb in Benin, an area of high resistance of Anopheles gambiae to pyrethroids', *The American Journal of Tropical Medicine and Hygiene,* 85(4), pp. 586-593.

Allossogbe, M., Gnanguenon, V., Yovogan, B., Akinro, B., Anagonou, R., Agossa, F., Houtoukpe, A., Padonou, G. and Akogbeto, M. (2017) 'WHO cone bio-assays of classical and new-generation long-lasting insecticidal nets call for innovative insecticides targeting the knock-down resistance mechanism in Benin', *Malaria Journal,* 16(1), pp. 1-11.

Alout, H., Dabiré, R., Djogbénou, L., Abate, L., Corbel, V., Chandre, F. and Cohuet, A. (2016) 'Interactive cost of Plasmodium infection and insecticide resistance in the malaria vector Anopheles gambiae', *Scientific Reports,* 6(1), pp. 1-11.

Alout, H., Djogbénou, L., Berticat, C., Chandre, F. and Weill, M. (2008) 'Comparison of Anopheles gambiae and Culex pipiens acetycholinesterase 1 biochemical properties', *Comparative Biochemistry and Physiology,* 150(3), pp. 271-277.

Alout, H., Djègbè, I., Chandre, F., Djogbénou, L., Dabiré, R., Corbel, V. and Cohuet, A. (2014) 'Insecticide exposure impacts vector-parasite interactions in insecticide-resistant malaria vectors', *Proceedings Biological Sciences,* 281(1786), pp. 20140389.

Alout, H., Roche, B., Dabire, R. and Cohuet, A. (2017) 'Consequences of insecticide resistance on malaria transmission', *PLoS Pathogens,* 13(9), pp. e1006499.

Andriessen, R., Snetselaar, J., Suer, R., Osinga, A., Deschietere, J., Lyimo, I., Mnyone, L., Brooke, B., Ranson, H., Knols, B. and Farenhorst, M. (2015) 'Electrostatic coating enhances bioavailability of insecticides and breaks pyrethroid resistance in mosquitoes', *Proceedings of the National Academy of Sciences of the United States of America,* 112(39), pp. 12081-12086.

Anopheles gambiae 1000 Genomes Consortium (2017) 'Genetic diversity of the African malaria vector Anopheles gambiae', *Nature,* 552(7683), pp. 96-100.

Antonio-Nkondjio, C., Sandjo, N., Awono-Ambene, P. and Wondji, C. (2018) 'Implementing a larviciding efficacy or effectiveness control intervention against malaria vectors: key parameters for success', *Parasites & Vectors,* 11(1), pp. 1-12.

Araújo, M., Gil, L. H. and e-Silva, A. (2012) 'Larval food quantity affects development time, survival and adult biological traits that influence the vectorial capacity of Anopheles darlingi under laboratory conditions', *Malaria Journal,* 11(1), pp. 1-9.

Arévalo-Cortés, A., Mejia-Jaramillo, A., Granada, Y., Coatsworth, H., Lowenberger, C. and Triana-Chavez, O. (2020) 'The Midgut Microbiota of Colombian Aedes aegypti Populations with Different Levels of Resistance to the Insecticide Lambda-cyhalothrin', *Insects,* 11(9), pp. 584.

Ashley, E. and Poespoprodjo, J. (2020) 'Treatment and prevention of malaria in children', *The Lancet. Child & Adolescent Health,* 4(10), pp. 775-789.

Ashwani, K., MINISTRY OF AGRICULTURE AND FARMERS WELFARE, Department of Agriculture, C.-o.a.F.W. (2016) *DRAFT ORDER - Banning of Pesticides Order, 2016.* New Delhi: Ministry of Agriculture and Farmers Welfare (F. No. 13035/31/2013-PP-I).

Asidi, A., N'Guessan, R., Koffi, A., Curtis, C., Hougard, J., Chandre, F., Corbel, V., Darriet, F., Zaim, M. and Rowland, M. (2005) 'Experimental hut evaluation of bednets treated with an organophosphate (chlorpyrifos-methyl) or a pyrethroid (lambdacyhalothrin) alone and in combination against insecticide-resistant Anopheles gambiae and Culex quinquefasciatus mosquitoes', *Malaria Journal,* 4, pp. 25.

Assogba, B., Alout, H., Koffi, A., Penetier, C., Djogbénou, L., Makoundou, P., Weill, M. and Labbé, P. (2018) 'Adaptive deletion in resistance gene duplications in the malaria vector Anopheles gambiae', *Evolutionary Applications,* 11(8), pp. 1245-1256.

Assogba, B., Djogbénou, L., Milesi, P., Berthomieu, A., Perez, J., Ayala, D., Chandre, F., Makoutodé, M., Labbé, P. and Weill, M. (2015) 'An ace-1 gene duplication resorbs the fitness cost associated with resistance in Anopheles gambiae, the main malaria mosquito', *Scientific Reports,* 5, pp. e14529.

Assogba, B., Djogbénou, L., Saizonou, J., Milesi, P., Djossou, L., Djegbe, I., Oumbouke, W., Chandre, F., Baba-Moussa, L., Weill, M. and Makoutodé, M. (2014) 'Phenotypic effects of concomitant insensitive acetylcholinesterase (ace-1R) and knockdown resistance (kdrR) in Anopheles gambiae : a hindrance for insecticide resistance management for malaria vector control', *Parasites & Vectors,* 7(1), pp. 548.

Assogba, B., Milesi, P., Djogbenou, L., Berthomieu, A., Makoundou, P., Baba-Moussa, L., Fiston-Lavier, A., Belkhir, K., Labbe, P. and Weill, M. (2016) 'The ace-1 Locus Is Amplified in All Resistant Anopheles gambiae Mosquitoes: Fitness Consequences of Homogeneous and Heterogeneous Duplications', *PLoS Biology,* 14(2), pp. e2000618.

Ayres, C., Müller, P., Dyer, N., Wilding, C., Rigden, D. and Donnelly, M. (2011) 'Comparative Genomics of the Anopheline Glutathione S-Transferase Epsilon Cluster', *PLoS ONE,* 6(12), pp. e29237.

Balabanidou, V., Grigoraki, L. and Vontas, J. (2018) 'Insect cuticle: a critical determinant of insecticide resistance', *Current Opinion in Insect Science,* 27, pp. 68-74.

Balaska, S., Fotakis, E. A., Kioulos, I., Grigoraki, L., Mpellou, S., Chaskopoulou, A. and Vontas, J. (2020) 'Bioassay and molecular monitoring of insecticide resistance status in Aedes albopictus populations from Greece, to support evidence-based vector control', *Parasites & Vectors,* 13(1), pp. 1-13.

Bamou, R., Sonhafouo-Chiana, N., Mavridis, K., Tchuinkam, T., Wondji, C., Vontas, J. and Antonio-Nkondjio, C. (2019) 'Status of Insecticide Resistance and Its Mechanisms in Anopheles gambiae and Anopheles coluzzii Populations from Forest Settings in South Cameroon', *Genes,* 10(10), pp. 741.

Bany, A., Dong, M.-Q. and Koelle, M. (2003) 'Genetic and Cellular Basis for Acetylcholine Inhibition of Caenorhabditis elegans Egg-Laying Behavior', *Journal of Neuroscience,* 23(22), pp. 8060-8069.

Barnard, K., Jeanrenaud, A., Brooke, B. and Oliver, S. (2019) 'The contribution of gut bacteria to insecticide resistance and the life histories of the major malaria vector Anopheles arabiensis (Diptera: Culicidae)', *Scientific Reports,* 9(1), pp. 9117.

Barrozo, R., Schilman, P., Minoli, S. and Lazzari, C. (2004) 'Daily Rhythms in Disease-Vector Insects', *Biological Rhythm Research,* 35(1-2), pp. 79-92.

Bass, C., Denholm, I., Williamson, M. and Nauen, R. (2015) 'The global status of insect resistance to neonicotinoid insecticides', *Pesticide Biochemistry and Physiology,* 121, pp. 78-87.

Bass, C. and Jones, C. M. (2016) 'Mosquitoes boost body armor to resist insecticide attack', *PNAS,* 113(33), pp. 9145-9147.

Bass, C., Nikou, D., Vontas, J., Williamson, M. and Field, L. (2010) 'Development of high-throughput real-time PCR assays for the identification of insensitive acetylcholinesterase (ace-1R) in Anopheles gambiae', *Pesticide Biochemistry and Physiology,* 96(2), pp. 80-85.

Bassett, A., Tibbit, C., Ponting, C. and Liu, J. (2013) 'Highly efficient targeted mutagenesis of Drosophila with the CRISPR/Cas9 system', *Cell Reports,* 4(1), pp. 220-228.

Basurko, C., Matheus, S., Hildéral, H., Everhard, S., Restrepo, M., Cuadro-Alvarez, E., Lambert, V., Boukhari, R., Duvernois, J., Favre, A., Nacher, M. and Carles, G. (2018) 'Estimating the Risk of Vertical Transmission of Dengue: A Prospective Study', *The American Journal of Tropical Medicine and Hygiene,* 98(6), pp. 1826-1832.

Bates, P., Lehane, M., Alfaroukh, I., Bucheton, B., Camara, M., Harris, A., Kaba, D., Lumbala, C., Peka, M., Rayaisse, J.-B., Waiswa, C., Solano, P. and Torr, S. (2016) 'Tsetse Control and the Elimination of Gambian Sleeping Sickness', *PLoS Neglected Tropical Diseases,* 10(4), pp. e0004437.

Bell, G., Agnandji, S., Asante, K., Ghansah, A., Kamthunzi, P., Emch, M. and Bailey, J. (2021) 'Impacts of Ecology, Parasite Antigenic Variation, and Human Genetics on RTS,S/AS01e Malaria Vaccine Efficacy', *Current Epidemiology Reports*, pp. 1-10.

Berg, G., Rybakova, D., Fischer, D., Cernava, T., Vergès, M.-C., Charles, T., Chen, X., Cocolin, L., Eversole, K., Corral, G., Kazou, M., Kinkel, L., Lange, L., Lima, N., Loy, A., Macklin, J., Maguin, E., Mauchline, T., McClure, R., Mitter, B., Ryan, M., Sarand, I., Smidt, H., Schelkle, B., Roume, H., Kiran, G. S., Selvin, J., de Souza, R., van Overbeek, L., Singh, B., Wagner, M., Walsh, A., Sessitsch, A. and Schloter, M. (2020) 'Microbiome definition re-visited: old concepts and new challenges', *Microbiome,* 8(1), pp. 1-22.

Bhatt, S., Weiss, D., Cameron, E., Bisanzio, D., Mappin, B., Dalrymple, U., Battle, K., Moyes, C., Henry, A., Eckhoff, P., Wenger, E., Briët, O., Penny, M., Smith, T., Bennett, A., Yukich, J., Eisele, T., Griffin, J., Fergus, C., Lynch, M., Lindgren, F., Cohen, J., Murray, C., Smith, D., Hay, S., Cibulskis, R. and Gething, P. (2015) 'The effect of malaria control on Plasmodium falciparum in Africa between 2000 and 2015', *Nature,* 526(7572), pp. 207-211.

Bigley, W. and Plapp Jr, F. (1962) 'Metabolism of malathion and malaoxon by the mosquito, Culex tarsalis Coq.', *Journal of Insect Physiology,* 8(5), pp. 545-557.

Binka, F., Indome, F. and Smith, T. (1998) 'Impact of spatial distribution of permethrin-impregnated bed nets on child mortality in rural northern Ghana', *The American Journal of Tropical Medicine and Hygiene,* 59(1), pp. 80-85.

Bisset, J., Rodríguez, M., French, L., Severson, D., Gutiérrez, G., Hurtado, D. and Fuentes, I. (2014) 'Insecticide Resistance and Metabolic Mechanisms Involved in Larval and Adult Stages of Aedes aegypti Insecticide-Resistant Reference Strains from Cuba', *Journal of the American Mosquito Control Association,* 30(4), pp. 298-304.

Blus, L. J. (2003) 'Organochlorine Pesticides', in David J. Hoffman, B.A.R., G. Allen Burton, Jr., John Cairns, Jr. (ed.) *Handbook of Ecotoxicology.* 2 ed. Boca Raton: Lewis Publishers, pp. 313-315.

Bosch, J., Colbeth, R., Zirin, J. and Perrimon, N. (2020) 'Gene Knock-Ins in Drosophila Using Homology-Independent Insertion of Universal Donor Plasmids', *Genetics,* 214(1), pp. 75-89.

Brabant, P. and Dobson, S. (2013) 'Methoprene effects on survival and reproductive performance of adult female and male Aedes aegypti', *Journal of the American Mosquito Control Association,* 29(4), pp. 369-375.

Bradley, D. and Warrell, D. (2003) 'Oxford Text Book of Medicine'. Four ed.

Brady, O. and Hay, S. (2020) 'The Global Expansion of Dengue: How Aedes aegypti Mosquitoes Enabled the First Pandemic Arbovirus', *Annual Review of Entomology,* 65, pp. 191-208.

Brand, A. and Perimon, N. (1993) 'Targeted gene expression as a means of altering cell fates and generating dominant phenotypes', *Development,* 118(2), pp. 401-415.

Buckingham, S., Partridge, F., Poulton, B., Miller, B., McKendry, R., Lycett, G. and Sattelle, D. (2021) 'Automated phenotyping of mosquito larvae enables high-throughput screening for novel larvicides and offers potential for smartphone-based detection of larval insecticide resistance', *PLoS Neglected Tropical Diseases,* 15(6), pp. e0008639.

Camara, S., Koffi, A., Ahoua Alou, L., Koffi, K., Kabran, J., Koné, A., Koffi, M., N'Guessan, R. and Pennetier, C. (2018) 'Mapping insecticide resistance in Anopheles gambiae (s.l.) from Côte d'Ivoire', *Parasites & Vectors,* 11(1), pp. 19.

Campbell. BC, Nabel. EM, Murdock. MH, Lao-Peregrin. C, Tsoulfas, P., Blackmore, M., Lee, F., Liston, C., Morishita, H. and Petsko, G. (2020) 'mGreenLantern: a bright monomeric fluorescent

protein with rapid expression and cell filling properties for neuronal imaging', *Proceedings of the National Academy of Sciences of the United States of America,* 117(48), pp. 30710-30721.

Captain-Esoah, M., Kweku Baidoo, P., Frempong, K., Adabie-Gomez, D., Chabi, J., Obuobi, D., Kwame Amlalo, G., Balungnaa Veriegh, F., Donkor, M., Asoala, V., Behene, E., Adjei Boakye, D. and Dadzie, S. (2020) 'Biting Behavior and Molecular Identification of Aedes aegypti (Diptera: Culicidae) Subspecies in Some Selected Recent Yellow Fever Outbreak Communities in Northern Ghana', *Journal of Medical Entomology,* 57(4), pp. 1239-1245.

CDC (2019) *Malaria - About Malaria - Disease*. Available at: https://www.cdc.gov/malaria/about/disease.html (Accessed).

CDC (2020a) *Malaria - About Malaria - Biology*. Available at: https://www.cdc.gov/malaria/about/biology/index.html (Accessed).

CDC (2020b) *Malaria - Malaria Worldwide - How Can Malaria Cases and Deaths Be Reduced? - Larval Control and Other Vector Control Interventions*. Available at: https://www.cdc.gov/malaria/malaria_worldwide/reduction/vector_control.html (Accessed: 27.08.2021).

CDC (2020c) *Mosquitoes - Aerial Spraying*. Available at: https://www.cdc.gov/mosquitoes/mosquito-control/community/aerial-spraying.html (Accessed).

CDC (2021a) *Dengue - Dengue Vaccine*. Available at: https://www.cdc.gov/dengue/prevention/dengue-vaccine.html (Accessed).

CDC (2021b) *Mosquitoes - CDC Bottle Bioassay*: @CDCgov. Available at: https://www.cdc.gov/mosquitoes/mosquito-control/professionals/cdc-bottle-bioassay.html (Accessed).

CDC (2021c) *Yellow Fever - Yellow Fever Vaccine*. Available at: https://www.cdc.gov/yellowfever/vaccine/index.html (Accessed).

Chambers, H., Meek, E. and Chambers, J. (2010a) 'Chemistry of Organophosphorus Insecticides', in Krieger, R. (ed.) *Hayes' Handbook of Pesticide Toxicology.* 3 ed. New York: Academic Press, pp. 1395-1398.

Chambers, J., Meek, E. and Chambers, H. (2010b) 'The Metabolism of Organophosphorus Insecticides', in Krieger, R. (ed.) *Hayes' Handbook of Pesticide Toxicology.* 3 ed. New York: Academic Press, pp. 1399-1407.

Chaverra-Rodriguez, D., Macias, V., Hughes, G., Pujhari, S., Suzuki, Y., Peterson, D., Kim, D., McKeand, S. and Rasgon, J. (2018) 'Targeted delivery of CRISPR-Cas9 ribonucleoprotein into arthropod ovaries for heritable germline gene editing', *Nature Communications,* 9(1), pp. 1-11.

Chen, S., Qin, Q., Zhong, D., Fang, X., He, H., Wang, L., Dong, L., Lin, H., Zhang, M., Cui, L. and Yan, G. (2019) 'Insecticide Resistance Status and Mechanisms of Anopheles Sinensis (Diptera: Culicidae) in Wenzhou, an Important Coastal Port City in China', *Journal of Medical Entomology,* 56(3), pp. 803-810.

Cheung, J., Mahmood, A., Kalathur, R., Liu, L. and Carlier, P. (2018) 'Structure of the G119S Mutant Acetylcholinesterase of the Malaria Vector Anopheles gambiae Reveals Basis of Insecticide Resistance', *Structure,* 26(1), pp. 130-136.

Choi, L., Majambere, S. and Wilson, A. (2019) 'Larviciding to prevent malaria transmission', *Cochrane Database of Systematic Reviews,* (8).

Christensen, K., Harper, B., Luukinen, B., Buhl, K. and Stone, D. (2009) *Chlorpyrifos Technical Fact Sheet*, Oregon State University Extension Services: National Pesticide Information Center.

Cibulskis, R. E., Alonso, P., Aponte, J., Aregawi, M., Barrette, A., Bergeron, L., Fergus, C. A., Knox, T., Lynch, M., Patouillard, E., Schwarte, S., Stewart, S. and Williams, R. (2016) 'Malaria: Global progress 2000 – 2015 and future challenges', *Infectious Diseases of Poverty,* 5(1), pp. 61.

Coats, J. (1990) 'Mechanisms of toxic action and structure-activity relationships for organochlorine and synthetic pyrethroid insecticides', *Environmental Health Perspectives,* 87, pp. 255-62.

Coetzee, M. and Fontenille, D. (2004) 'Advances in the study of Anopheles funestus, a major vector of malaria in Africa', *Insect Biochemistry and Molecular Biology,* 34(7), pp. 599-605.

Collins, E., Vaselli, N., Sylla, M., Beavogui, A., Orsborne, J., Lawrence, G., Wiegand, R., Irish, S., Walker, T. and Messenger, L. (2019) 'The relationship between insecticide resistance, mosquito age and malaria prevalence in Anopheles gambiae s.l. from Guinea', *Scientific Reports,* 9(1), pp. 8846.

Costa, F., Carvalho-Pereira, T., Begon, M., Riley, L. and Childs, J. (2017) 'Zoonotic and Vector-Borne Diseases in Urban Slums: Opportunities for Intervention - ScienceDirect', *Trends in Parasitology,* 33(9), pp. 660-662.

Costa, L. (2015) 'The neurotoxicity of organochlorine and pyrethroid pesticides', in Lotti, M. and Bleecker, M.L. (eds.) *Handbook of Clinical Neurology*: Elsevier, pp. 135-148.

Costa, L., Giordano, G., Guizzetti, M. and Vitalone, A. (2008) 'Neurotoxicity of pesticides: a brief review', *Frontiers in Bioscience,* 13, pp. 1240-1249.

Crawford, J., Clarke, D., Criswell, V., Desnoyer, M., Cornel, D., Deegan, B., Gong, K., Hopkins, K., Howell, P., Hyde, J., Livni, J., Behling, C., Benza, R., Chen, W., Dobson, K., Eldershaw, C., Greeley, D., Han, Y., Hughes, B., Kakani, E., Karbowski, J., Kitchell, A., Lee, E., Lin, T., Liu, J., Lozano, M., MacDonald, W., Mains, J., Metlitz, M., Mitchell, S., Moore, D., Ohm, J., Parkes, K., Porshnikoff, A., Robuck, C., Sheridan, M., Sobecki, R., Smith, P., Stevenson, J., Sullivan, J., Wasson, B., Weakley, A., Wilhelm, M., Won, J., Yasunaga, A., Chan, W., Holeman, J., Snoad, N., Upson, L., Zha, T., Dobson, S., Mulligan, F., Massaro, P. and White, B. (2020) 'Efficient production of male Wolbachia-infected Aedes aegypti mosquitoes enables large-scale suppression of wild populations', *Nature Biotechnology,* 38(4), pp. 482-492.

Daborn, P., Lumb, C., Harrop, T., Blasetti, A., Pasricha, S., Morin, S., Mitchell, S., Donnelly, M., Muller, P. and Batterham, P. (2012) 'Using Drosophila melanogaster to validate metabolism-based insecticide resistance from insect pests', *Insect Biochemistry and Molecular Biology,* 42(12), pp. 918-924.

Dada, N., Lol, J., Benedict, A., López, F., Sheth, M., Dzuris, N., Padilla, N. and Lenhart, A. (2019) 'Pyrethroid Exposure Alters Internal and Cuticle Surface Bacterial Communities in Anopheles Albimanus', *The ISME Journal,* 13(10), pp. 2447-2464.

Dada, N., Sheth, M., Liebman, K., Pinto, J. and Lenhart, A. (2018) 'Whole metagenome sequencing reveals links between mosquito microbiota and insecticide resistance in malaria vectors', *Scientific Reports,* 8(1), pp. 2084.

Dadzie, S., Chabi, J., Asafu-Adjaye, A., Owusu-Akrofi, O., Baffoe-Wilmot, A., Malm, K., Bart-Plange, C., Coleman, S., Appawu, M. and Boakye, D. (2017) 'Evaluation of piperonyl butoxide in enhancing the efficacy of pyrethroid insecticides against resistant Anopheles gambiae s.l. in Ghana', *Malaria Journal,* 16(1), pp. 1-11.

Dattani, M., Prajapati, P. and Raval, D. (2009) 'Impact of Indoor Residual Spray with Synthetic Pyrethroid in Gandhinagar District, Gujarat', *Indian Journal of Community Medicine,* 34(4), pp. 288-92.

David, J., Ismail, H., Chandor-Proust, A. and Paine, M. (2013) 'Role of cytochrome P450s in insecticide resistance: impact on the control of mosquito-borne diseases and use of insecticides on Earth', *Philosophical Transactions of the Royal Society of London,* 368(1612), pp. 20120429.

de Souza, D., Koudou, B., Kelly-Hope, L., Wilson, M., Bockarie, M. and Boakye, D. (2012) 'Diversity and transmission competence in lymphatic filariasis vectors in West Africa, and the implications for accelerated elimination of Anopheles-transmitted filariasis', *Parasites & Vectors,* 5(1), pp. 1-6.

Devine, G., Perea, E., Killeen, G., Stancil, J., Clark, S. and Morrison, A. (2009) 'Using adult mosquitoes to transfer insecticides to Aedes aegypti larval habitats', *Proceedings of the National Academy of Sciences of the United States of America,* 106(28), pp. 11530-11534.

Dewar, A. M. (2016) 'Have Pyrethroid Insecticides Shot the Agricultural Industry in the Foot?', *Outlooks on Pest Management,* 27(3), pp. 98-100.

Diao, F. and White, B. (2012) 'A novel approach for directing transgene expression in Drosophila: T2A-Gal4 in-frame fusion', *Genetics,* 190(3), pp. 1139-1144.

Diarra, R., Traore, M., Junnila, A., Traore, S., Doumbia, S., Revay, E., Kravchenko, V., Schlein, Y., Arheart, K., Gergely, P., Hausmann, A., Beck, R., Xue, R.-D., Prozorov, A., Kone, A., Majambere, S., Vontas, J., Beier, J. and Müller, G. (2021) 'Testing configurations of attractive toxic sugar bait (ATSB) stations in Mali, West Africa, for improving the control of malaria parasite transmission by vector mosquitoes and minimizing their effect on non-target insects', *Malaria Journal,* 20(1), pp. 1-9.

Dillon, R. and Dillon, V. (2004) 'The gut bacteria of insects: nonpathogenic interactions', *Annual Review of Entomology,* 49, pp. 71-92.

Ding, S., Wu, X., Li, G., Han, M., Zhuang, Y. and Xu, T. (2005) 'Efficient transposition of the piggyBac (PB) transposon in mammalian cells and mice', *Cell,* 122(3), pp. 473-483.

Diniz, D., de Melo-Santos, M., Santos, E., Beserra, E., Helvecio, E., de Carvalho-Leandro, D., dos Santos, B., de Menezes Lima, V. and Ayres, C. (2015) 'Fitness cost in field and laboratory Aedes aegypti populations associated with resistance to the insecticide temephos', *Parasites & Vectors,* 8.

Diouf, E., Niang, E., Samb, B., Diagne, C., Diouf, M., Konaté, A., Dia, I., Faye, O. and Konaté, L. (2020) 'Multiple insecticide resistance target sites in adult field strains of An. gambiae (s.l.) from southeastern Senegal', *Parasites & Vectors,* 13(1), pp. 1-10.

Djegbe, I., Agossa, F., Jones, C., Poupardin, R., Cornelie, S., Akogbeto, M., Ranson, H. and Corbel, V. (2014) 'Molecular characterization of DDT resistance in Anopheles gambiae from Benin', *Parasites & Vectors,* 7, pp. 409.

Djogbenou, L., Dabire, R., Diabate, A., Kengne, P., Akogbeto, M., Hougard, J. M. and Chandre, F. (2008) 'Identification and geographic distribution of the ACE-1(R) mutation in the malaria vector Anopheles gambiae in south-western Burkina Faso, West Africa', *American Journal of Tropical Medicine and Hygiene,* 78(2), pp. 298-302.

Djogbénou, L., Assogba, B., Essandoh, J., Constant, E., Makoutodé, M., Akogbéto, M., Donnelly, M. and Weetman, D. (2015) 'Estimation of allele-specific Ace-1 duplication in insecticide-resistant Anopheles mosquitoes from West Africa', *Malaria Journal,* 14, pp. 507.

Djogbénou, L., Chandre, F., Berthomieu, A., Dabiré, R., Koffi, A., Alout, H. and Weill, M. (2008) 'Evidence of introgression of the ace-1(R) mutation and of the ace-1 duplication in West African Anopheles gambiae s. s', *PloS One,* 3(5), pp. e2172.

Djogbénou, L., Labbé, P., Chandre, F., Pasteur, N. and Weill, M. (2009) 'Ace-1 duplication in Anopheles gambiae: a challenge for malaria control', *Malaria Journal,* 8, pp. 70.

Djogbénou, L., Weill, M., Hougard, J., Raymond, M., Akogbéto, M. and Chandre, F. (2007) 'Characterization of insensitive acetylcholinesterase (ace-1R) in Anopheles gambiae (Diptera: Culicidae): resistance levels and dominance', *Journal of Medical Entomology,* 44(5), pp. 805-810.

Djouaka, R., Bakare, A., Coulibaly, O., Akogbeto, M., Ranson, H., Hemingway, J. and Strode, C. (2008) 'Expression of the cytochrome P450s, CYP6P3 and CYP6M2 are significantly elevated in multiple pyrethroid resistant populations of Anopheles gambiae s.s. from Southern Benin and Nigeria', *BMC Genomics,* 9, pp. 538.

Dominguez, A., Lim, W. and Qi, L. (2016) 'Beyond editing: repurposing CRISPR–Cas9 for precision genome regulation and interrogation', *Nature Review Molecular Cell Biology,* 17(1), pp. 5-15.

Dominguez, M. and Schrock, J. (2019) 'Suppression of Yellow Fever', *Salem Press Encyclopedia*.

Dong, K., Du, Y., Rinkevich, F., Nomura, Y., Xu, P., Wang, L., Silver, K. and Zhorov, B. (2014) 'Molecular biology of insect sodium channels and pyrethroid resistance', *Insect Biochemistry and Molecular Biology,* 50, pp. 1-17.

Donnelly, M., Isaacs, A. and Weetman, D. (2016) 'Identification, Validation, and Application of Molecular Diagnostics for Insecticide Resistance in Malaria Vectors', *Trends in Parasitology,* 32(3), pp. 197-206.

Douris, V., Steinbach, D., Panteleri, R., Livadaras, I., Pickett, J., Van Leeuwen, T., Nauen, R. and Vontas, J. (2016) 'Resistance mutation conserved between insects and mites unravels the benzoylurea insecticide mode of action on chitin biosynthesis', *Proceedings of the National Academy of Sciences of the United States of America,* 113(51), pp. 14692-14697.

Downes, G. and Granato, M. (2004) 'Acetylcholinesterase function is dispensable for sensory neurite growth but is critical for neuromuscular synapse stability', *Developmental Biology,* 270(1), pp. 232-245.

Du, M.-H., Yan, Z.-W., Hao, Y.-J., Yan, Z.-T., Si, F.-L., Chen, B. and Qiao, L. (2017) 'Suppression of Laccase 2 severely impairs cuticle tanning and pathogen resistance during the pupal metamorphosis of Anopheles sinensis (Diptera: Culicidae)', *Parasites & Vectors,* 10(1), pp. 1-11.

Du, Y., Nomura, Y., Zhorov, B. and Dong, K. (2016) 'Sodium Channel Mutations and Pyrethroid Resistance in Aedes aegypti', *Insects,* 7(4), pp. 60.

Dusfour, I., Vontas, J., David, J., Weetman, D., Fonseca, D., Corbel, V., Raghavendra, K., Coulibaly, M., Martins, A., Kasai, S. and Chandre, F. (2019) 'Management of insecticide resistance in the major Aedes vectors of arboviruses: Advances and challenges', *PLoS Negl Trop Dis,* 13(10), pp. e0007615.

Edi, C., Djogbenou, L., Jenkins, A., Regna, K., Muskavitch, M., Poupardin, R., Jones, C., Essandoh, J., Ketoh, G., Paine, M., Koudou, B., Donnelly, M., Ranson, H. and Weetman, D. (2014) 'CYP6 P450 enzymes and ACE-1 duplication produce extreme and multiple insecticide resistance in the malaria mosquito Anopheles gambiae', *PLoS Genetics,* 10(3), pp. e1004236.

Elanga-Ndille, E., Nouage, L., Ndo, C., Binyang, A., Assatse, T., Nguiffo-Nguete, D., Djonabaye, D., Irwing, H., Tene-Fossog, B. and Wondji, C. (2019) 'The G119S Acetylcholinesterase ( Ace-1) Target Site Mutation Confers Carbamate Resistance in the Major Malaria Vector Anopheles gambiae From Cameroon: A Challenge for the Coming IRS Implementation', *Genes,* 10(10), pp. 790.

Elliott, M. (1976) 'Properties and applications of pyrethroids', *Environmental Health Perspectives,* 14, pp. 1-13.

Elliott, M. (2006) 'The pyrethroids: Early discovery, recent advances and the future', *Pesticide Science,* 27(4), pp. 337-351.

Engdahl, C., Knutsson, S., Fredriksson, S., Linusson, A., Bucht, G. and Ekström, F. (2015) 'Acetylcholinesterases from the Disease Vectors Aedes aegypti and Anopheles gambiae: Functional Characterization and Comparisons with Vertebrate Orthologues', *PloS One,* 10(10), pp. e0138598.

Epstein, P. (2001a) 'Climate change and emerging infectious diseases', *Microbes and Infection,* 3(9), pp. 747-754.

Epstein, P. R. (2001b) 'West Nile virus and the climate | SpringerLink', *Journal of Urban Health,* 78(2), pp. 367-371.

Essandoh, J., Yawson, A. and Weetman, D. (2013) 'Acetylcholinesterase ( Ace-1 ) target site mutation 119S is strongly diagnostic of carbamate and organophosphate resistance in Anopheles gambiae s.s. and Anopheles coluzzii across southern Ghana', *Malaria Journal,* 12(1), pp. 404.

Evans, T. (2015) 'Considerations for the use of transcriptomics in identifying the 'genes that matter' for environmental adaptation', *The Journal of Experimental Biology,* 218(Pt 12), pp. 1925-1935.

Ewen-Campen, B., Yang-Zhou, D., Fernandes, V., González, D., Liu, L.-P., Tao, R., Ren, X., Sun, J., Hu, Y., Zirin, J., Mohr, S., Ni, J.-Q. and Perrimon, N. (2017) 'Optimized strategy for in vivo Cas9-

activation in Drosophila', *Proceedings of the National Academy of Sciences of the United States of America,* 114(35), pp. 9409-9414.

Fagbohun, I., Idowu, E., Otubanjo, O. and Awolola, T. (2020) 'First report of AChE1 (G119S) mutation and multiple resistance mechanisms in Anopheles gambiae s.s. in Nigeria', *Scientific Reports,* 10(1), pp. 7482.

FAO and WHO (1972) *1971 Evaluations of some pesticide residues in food*, GenevaAGP-1971/M/9/1.).

Faravelli, G., Raimondi, S., Marchese, L., Partridge, F., Soria, C., Mangione, P., Canetti, D., Perni, M., Aprile, F., Zorzoli, I., Di Schiavi, E., Lomas, D., Bellotti, V., Sattelle, D. and Giorgetti, S. (2019) 'C. elegans expressing D76N β 2-microglobulin: a model for in vivo screening of drug candidates targeting amyloidosis', *Scientific Reports,* 9(1), pp. 19960.

Feder, M. and Walser, J. (2005) 'The biological limitations of transcriptomics in elucidating stress and stress responses', *Journal of Evolutionary Biology,* 18(4), pp. 901-910.

Ferguson, N. (2018) 'Challenges and opportunities in controlling mosquito-borne infections', *Nature,* 559(7715), pp. 490-497.

Ferreira-de-Lima, V., Andrade, P., Thomazelli, L., Marrelli, M., Urbinatti, P., Almeida, R. and Lima-Camara, T. (2020) 'Silent circulation of dengue virus in Aedes albopictus (Diptera: Culicidae) resulting from natural vertical transmission', *Scientific Reports,* 10(1), pp. 1-8.

Ffrench-Constant, R. and Bass, C. (2017) 'Does resistance really carry a fitness cost?', *Current Opinion in Insect Science,* 21, pp. 39-46.

Fillinger, U. and Lindsay, S. (2011) 'Larval source management for malaria control in Africa: myths and reality', *Malaria Journal,* 10(1), pp. 1-10.

Findlater, A. and Bogoch, I. (2018) 'Human Mobility and the Global Spread of Infectious Diseases: A Focus on Air Travel', *Trends in Parasitology,* 34(9), pp. 772-783.

Fiorenzano, J., Koehler, P. and Xue, R. (2017) 'Attractive Toxic Sugar Bait (ATSB) For Control of Mosquitoes and Its Impact on Non-Target Organisms: A Review', *International Journal of Environmental Research and Public Health,* 14(4), pp. 398.

Fisher, B., Weiszmann, R., Frise, E., Hammonds, A., Tomancak, P., Beaton, A., Berman, B., Quan, E., Shu, S., Lewis, S., Rubin, G., Barale, C., Laguertas, E., Quinn, J., Ghosh, A., Hartenstein, V., Ashburner, M. and Celniker, S. (2012) *BDGP insitu homepage - Patterns of gene expression in Drosophila embryogenesis* (Accessed: 30.09.2021).

Foster, W. (1995) 'Mosquito sugar feeding and reproductive energetics', *Annual Review of Entomology,* 40, pp. 443-474.

Fotakis, E., Mastrantonio, V., Grigoraki, L., Porretta, D., Puggioli, A., Chaskopoulou, A., Osório, H., Weill, M., Bellini, R., Urbanelli, S. and Vontas, J. (2020) 'Identification and detection of a novel point mutation in the Chitin Synthase gene of Culex pipiens associated with diflubenzuron resistance', *PLoS Neglected Tropical Diseases,* 14(5), pp. e0008284.

Fouet, C., Atkinson, P. and Kamdem, C. (2018) 'Human Interventions: Driving Forces of Mosquito Evolution', *Trends in Parasitology,* 34(2), pp. 127-139.

Fukuto, T. (1990) 'Mechanism of action of organophosphorus and carbamate insecticides', *Environmental Health Perspectives,* 87, pp. 245-254.

Gachelin, G., Garner, P., Ferroni, E., Verhave, J. and Opinel, A. (2018) 'Evidence and strategies for malaria prevention and control: a historical analysis', *Malaria Journal,* 17(1), pp. 1-18.

Galizi, R., Doyle, L., Menichelli, M., Bernardini, F., Deredec, A., Burt, A., Stoddard, B., Windbichler, N. and Crisanti, A. (2014) 'A synthetic sex ratio distortion system for the control of the human malaria mosquito', *Nature Communications,* 5, pp. 3977.

Galizi, R., Hammond, A., Kyrou, K., Taxiarchi, C., Bernardini, F., O'Loughlin, S., Papathanos, P.-A., Nolan, T., Windbichler, N. and Crisanti, A. (2016) 'A CRISPR-Cas9 sex-ratio distortion system for genetic control', *Scientific Reports,* 6(1), pp. 1-5.

George, L., Lenhart, A., Toledo, J., Lazaro, A., Han, W., Velayudhan, R., Runge Ranzinger, S. and Horstick, O. (2015) 'Community-Effectiveness of Temephos for Dengue Vector Control: A Systematic Literature Review', *PLoS Neglected Tropical Diseases,* 9(9), pp. e0004006.

Gervais, J., Luukinen, B., Buhl, K. and Stone, D. (2009) *Malathion Technical Fact Sheet*: National Pesticide Information Center. Available at: http://npic.orst.edu/factsheets/archive/malatech.html.

Gholizadeh, S., Zakeri, S. and Djadid, N. (2013) 'Genotyping Plasmodium vivax isolates infecting Anopheles stephensi, an Asian main malaria vector', *Experimental Parasitology,* 134(1), pp. 48-51.

Gilles, H. and Warrell, D. (2002) 'Essential Malariology'. 4th Edition ed: CRC Press.

Githeko, A., Adungo, N., Karanja, D., Hawley, W., Vulule, J., Seroney, I., Ofulla, A., Atieli, F., Ondijo, S., Genga, I., Odada, P., Situbi, P. and Oloo, J. (1996) 'Some observations on the biting behavior of Anopheles gambiae s.s., Anopheles arabiensis, and Anopheles funestus and their implications for malaria control', *Experimental Parasitology,* 82(3), pp. 306-15.

Gleave, K., Lissenden, N., Chaplin, M., Choi, L. and Ranson, H. (2021) 'Piperonyl butoxide (PBO) combined with pyrethroids in insecticide-treated nets to prevent malaria in Africa', *The Cochrane Database of Systematic Reviews,* 5(5), pp. CD012776.

Global Malaria Programme, WHO (2017) *Conditions for deployment of mosquito nets treated with a pyrethroid and piperonyl butoxide.* Geneva (CC BY-NC-SA 3.0 IGO).

Gnanguenon, V., Azondekon, R., Oke-Agbo, F., Beach, R. and Akogbeto, M. (2014) 'Durability assessment results suggest a serviceable life of two, rather than three, years for the current long-lasting insecticidal (mosquito) net (LLIN) intervention in Benin', *BMC Infectious Diseases,* 14(1), pp. 1-10.

Goindin, D., Delannay, C., Gelasse, A., Ramdini, C., Gaude, T., Faucon, F., David, J.-P., Gustave, J., Vega-Rua, A. and Fouque, F. (2017) 'Levels of insecticide resistance to deltamethrin, malathion, and temephos, and associated mechanisms in Aedes aegypti mosquitoes from the Guadeloupe and Saint Martin islands (French West Indies)', *Infectious Diseases of Poverty,* 6(1), pp. 38.

Gott, R., Kunkel, G., Zobel, E., Lovett, B. and Hawthorne, D. (2017) 'Implicating ABC Transporters in Insecticide Resistance: Research Strategies and a Decision Framework', *Journal of Economic Entomology,* 110(2), pp. 667-677.

Goulson, D. (2013) 'An overview of the environmental risks posed by neonicotinoid insecticides', *Journal of Applied Ecology,* 50(4), pp. 977-987.

Govoetchan, R., Gnanguenon, V., Ogouwalé, E., Oké-Agbo, F., Azondékon, R., Sovi, A., Attolou, R., Badirou, K., Youssouf, R., Ossè, R. and Akogbéto, M. (2014) 'Dry season refugia for anopheline larvae and mapping of the seasonal distribution in mosquito larval habitats in Kandi, northeastern Benin', *Parasites & Vectors,* 7(1), pp. 1-10.

Grancaric, A., Botteri, L. and Ghaffari, P. 'Combating Invasive Mosquitoes by Textiles and Paints', *19th World Textile Conference*, The Crossroads, Ghent, Belgium.

Grau-Bové, X., Lucas, E., Pipini, D., Rippon, E., van 't Hof, A., Constant, E., Dadzie, S., Egyir-Yawson, A., Essandoh, J., Chabi, J., Djogbénou, L., Harding, N., Miles, A., Kwiatkowski, D., Donnelly, M. and Weetman, D. (2021) 'Resistance to pirimiphos-methyl in West African Anopheles is spreading via duplication and introgression of the Ace1 locus', *PLoS Genetics,* 17(1), pp. e1009253.

Greenblatt, H., Guillou, C., Guénard, D., Argaman, A., Botti, S., Badet, B., Thal, C., Silman, I. and Sussman, J. (2004) 'The complex of a bivalent derivative of galanthamine with torpedo acetylcholinesterase displays drastic deformation of the active-site gorge: implications for structure-based drug design', *Journal of the American Chemical Society,* 126(47), pp. 15405-15411.

Grigoraki, L., Balabanidou, V., Meristoudis, C., Miridakis, A., Ranson, H., Swevers, L. and Vontas, J. (2016) 'Functional and immunohistochemical characterization of CCEae3a, a carboxylesterase associated with temephos resistance in the major arbovirus vectors Aedes aegypti and Ae. albopictus', *Insect Biochemistry Molecular Biology,* 74, pp. 61-67.

Grigoraki, L., Cowlishaw, R., Nolan, T., Donnelly, M., Lycett, G. and Ranson, H. (2021) 'CRISPR/Cas9 modified An. gambiae carrying kdr mutation L1014F functionally validate its contribution in insecticide resistance and combined effect with metabolic enzymes', *PLoS Genetics,* 17(7), pp. e1009556.

Grigoraki, L., Grau-Bové, X., Yates, H., Lycett, G. and Ranson, H. (2020) 'Isolation and transcriptomic analysis of Anopheles gambiae oenocytes enables the delineation of hydrocarbon biosynthesis', *eLife,* 9, pp. e58019.

Grigoraki, L., Lagnel, J., Kioulos, I., Kampouraki, A., Morou, E., Labbe, P., Weill, M. and Vontas, J. (2015) 'Transcriptome Profiling and Genetic Study Reveal Amplified Carboxylesterase Genes Implicated in Temephos Resistance, in the Asian Tiger Mosquito Aedes albopictus', *PLoS Neglected Tropical Diseases,* 9(5), pp. e0003771.

Grigoraki, L., Pipini, D., Labbe, P., Chaskopoulou, A., Weill, M. and Vontas, J. (2017a) 'Carboxylesterase gene amplifications associated with insecticide resistance in Aedes albopictus: Geographical distribution and evolutionary origin', *PLoS Neglected Tropical Diseases,* 11(4), pp. e0005533.

Grigoraki, L., Puggioli, A., Mavridis, K., Douris, V., Montanari, M., Bellini, R. and Vontas, J. (2017b) 'Striking diflubenzuron resistance in Culex pipiens , the prime vector of West Nile Virus', *Scientific Reports,* 7(1), pp. 11699.

Grosscurt, A. C. (1978) 'Diflubenzuron: Some aspects of its ovicidal and larvicidal mode of action and an evaluation of its practical possibilities', *Pesticide Science,* 96(5), pp. 373-386.

Gueye, O., Tchouakui, M., Dia, A., Faye, M., Ahmed, A., Wondji, M., Nguiffo, D., Mugenzi, L., Tripet, F., Konaté, L., Diabate, A., Dia, I., Gaye, O., Faye, O., Niang, E. and Wondji, C. (2020) 'Insecticide Resistance Profiling of Anopheles coluzzii and Anopheles gambiae Populations in the Southern Senegal: Role of Target Sites and Metabolic Resistance Mechanisms', *Genes,* 11(12), pp. 1403.

Hakizimana, E., Cyubahiro, B., Rukundo, A., Kabayiza, A., Mutabazi, A., Beach, R., Patel, R., Tongren, J. and Karema, C. (2014) 'Monitoring long-lasting insecticidal net (LLIN) durability to validate net serviceable life assumptions, in Rwanda', *Malaria Journal,* 13(1), pp. 1-8.

Hamid-Adiamoh, M., Nwakanma, D., Assogba, B., Ndiath, M., D'Alessandro, U., Afrane, Y. and Alfred. A-N (2020) 'Biting and resting preferences of malaria vectors in The Gambia', *bioRxiv*.

Hammond, A., Galizi, R., Kyrou, K., Simoni, A., Siniscalchi, C., Katsanos, D., Gribble, M., Baker, D., Marois, E., Russell, S., Burt, A., Windbichler, N., Crisanti, A. and Nolan, T. (2016) 'A CRISPR-Cas9 Gene Drive System Targeting Female Reproduction in the Malaria Mosquito vector Anopheles gambiae', *Nature Biotechnology,* 34(1), pp. 78-83.

Hammond, A., Pollegioni, P., Persampieri, T., North, A., Minuz, R., Trusso, A., Bucci, A., Kyrou, K., Morianou, I., Simoni, A., Nolan, T., Müller, R. and Crisanti, A. (2021) 'Gene-drive suppression of mosquito populations in large cages as a bridge between lab and field', *Nature Communications,* 12(1), pp. 1-9.

Han, Q., Wong, D., Robinson, H., Ding, H., Lam, P., Totrov, M., Carlier, P. and Li, J. (2018) 'Crystal structure of acetylcholinesterase catalytic subunits of the malaria vector Anopheles gambiae', *Insect Science,* 25(4), pp. 721-724.

Han, W., Tian, Y. and Shen, X. (2018) 'Human exposure to neonicotinoid insecticides and the evaluation of their potential toxicity: An overview', *Chemosphere,* 192, pp. 59-65.

Hanboonkunupakarn, B. and White, N. (2020) 'Advances and roadblocks in the treatment of malaria', *British Journal of Clinical Pharmacology*, pp. 1-9.

Harnish, J., Deal, S., Chao, H., Wangler, M. and Yamamoto, S. (2019) 'In Vivo Functional Study of Disease-associated Rare Human Variants Using Drosophila', *Journal of Visualized Experiments,* (150).

Hawley, W., Phillips-Howard, P., ter Kuile, F., Terlouw, D., Vulule, J., Ombok, M., Nahlen, B., Gimnig, J., Kariuki, S., Kolczak, M. and Hightower, A. (2003) 'Community-wide effects of permethrin-treated bed nets on child mortality and malaria morbidity in western Kenya', *The American Journal of Tropical Medicine and Hygiene,* 68(4 Suppl), pp. 121-127.

Hay, S., Guerra, C., Tatem, A., Atkinson, P. and Snow, R. (2005) 'Urbanization, malaria transmission and disease burden in Africa', *Nature Reviews - Microbiology,* 3(1), pp. 81-90.

Helvecio, E., Romão, T., de Carvalho-Leandro, D., de Oliveira, I., Cavalcanti, A., Reimer, L., de Paiva Cavalcanti, M., de Oliveira, A., Paiva, P., Napoleão, T., Wallau, G., de Melo Neto, O., Melo-Santos, M. and Ayres, C. (2020) 'Polymorphisms in GSTE2 is associated with temephos resistance in Aedes aegypti', *Pesticide Biochemistry and Physiology,* 165, pp. 104464.

Hemingway, J., Beaty, B., Rowland, M., Scott, T. and Sharp, B. (2006) 'The Innovative Vector Control Consortium: improved control of mosquito-borne diseases', *Trends in Parasitology,* 22(7), pp. 308-312.

Hemingway, J. and Karunaratne, S. (1998) 'Mosquito carboxylesterases: a review of the molecular biology and biochemistry of a major insecticide resistance mechanism', *Medical and Veterinary Entomology,* 12, pp. 1-12.

Hirata, K. (2016) 'Studies on the mode of action of neurotoxic insecticides', *Journal of Pesticide Science,* 41(3), pp. 87-94.

Hoermann, A., Tapanelli, S., Capriotti, P., Del Corsano, G., Masters, E., Habtewold, T., Christophides, G. and Windbichler, N. (2021) 'Converting endogenous genes of the malaria mosquito into simple non-autonomous gene drives for population replacement', *eLife,* 10, pp. e58791.

Hoffmann, A. (2017) 'Rapid adaptation of invertebrate pests to climatic stress?', *Current Opinion in Insect Science,* 21, pp. 7-13.

Howard, S., Omumbo, J., Nevill, C., Some, E., Donnelly, C. and Snow, R. (2000) 'Evidence for a mass community effect of insecticide-treated bednets on the incidence of malaria on the Kenyan coast', *Transactions of the Royal Society of Tropical Medicine and Hygiene,* 94(4), pp. 357-360.

Ibrahim, S., Ndula, M., Riveron, J., Irving, H. and Wondji, C. (2016) 'The P450 CYP6Z1 confers carbamate/pyrethroid cross-resistance in a major African malaria vector beside a novel carbamate-insensitive N485I acetylcholinesterase-1 mutation', *Molecular Ecology,* 25(14), pp. 3436-3452.

Ingham, V., Anthousi, A., Douris, V., Harding, N., Lycett, G., Morris, M., Vontas, J. and Ranson, H. (2020) 'A Sensory Appendage Protein Protects Malaria Vectors From Pyrethroids', *Nature,* 577(7790), pp. 376-380.

Inácio da Silva, L., Dezordi, F., Paiva, M. and Wallau, G. (2021) 'Systematic Review of Wolbachia Symbiont Detection in Mosquitoes: An Entangled Topic about Methodological Power and True Symbiosis', *Pathogens,* 10(1), pp. 39.

Iovinella, I., Bozza, F., Caputo, B., Della, T. A. and Pelosi, P. (2013) 'Ligand-binding study of Anopheles gambiae chemosensory proteins', *Chemical Senses,* 38(5), pp. 409-419.

Ivics, Z. and Izsvák, Z. (2010) 'The expanding universe of transposon technologies for gene and cell engineering', *Mobile DNA,* 1(1), pp. 1-15.

Jasinskiene, N., Juhn, J. and James, A. (2007) 'Microinjection of A. aegypti Embryos to Obtain Transgenic Mosquitoes', *Journal of Visualized Experiments,* (5), pp. 219.

Jinek, M., Chylinski, K., Fonfara, I., Hauer, M., Doudna, J. and Charpentier, E. (2012) 'A programmable dual-RNA-guided DNA endonuclease in adaptive bacterial immunity', *Science,* 337(6096), pp. 816-821.

Johnson, M., Haupt, L. and Griffiths, L. (2004) 'Locked nucleic acid (LNA) single nucleotide polymorphism (SNP) genotype analysis and validation using real-time PCR', *Nucleic Acids Research,* 32(6), pp. e55.

Kamal, H. and Khater, E. (2010) 'The biological effects of the insect growth regulators; pyriproxyfen and diflubenzuron on the mosquito Aedes aegypti', *Journal of the Egyptian Society of Parasitology,* 40(3), pp. 565-574.

Kanca, O., Zirin, J., Garcia-Marques, J., Knight, S., Yang-Zhou, D., Amador, G., Chung, H., Zuo, Z., Ma, L., He, Y., Lin, W., Fang, Y., Ge, M., Yamamoto, S., Schulze, K., Hu, Y., Spradling, A., Mohr, S., Perrimon, N. and Bellen, H. (2019) 'An efficient CRISPR-based strategy to insert small and large fragments of DNA using short homology arms', *eLife,* 8, pp. e51539.

Kawada, H., Dida, G., Ohashi, K., Kawashima, E., Sonye, G., Njenga, S., Mwandawiro, C. and Minakawa, N. (2014) 'A small-scale field trial of pyriproxyfen-impregnated bed nets against pyrethroid-resistant Anopheles gambiae s.s. in western Kenya', *PloS One,* 9(10), pp. e111195.

Keiser, J., Singer, B. and Utzinger, J. (2005) 'Reducing the burden of malaria in different eco-epidemiological settings with environmental management: a systematic review', *The Lancet. Infectious diseases,* 5(11), pp. 695-708.

Keshtkar, E., Kudsk, P. and Mesgaran, M. (2021) 'Perspective: common errors in dose-response analysis and how to avoid them', *Pest Management Science,* 77(6), pp. 2599-2608.

Keïta, M., Kané, F., Thiero, O., Traoré, B., Zeukeng, F., Sodio, A., Traoré, S., Djouaka, R., Doumbia, S. and Sogoba, N. (2020) 'Acetylcholinesterase (ace-1 R) target site mutation G119S and resistance to carbamates in Anopheles gambiae (sensu lato) populations from Mali', *Parasites & Vectors,* 13(1), pp. 283.

Kilian, A., Byamukama, W., Pigeon, O., Atieli, F., Duchon, S. and Phan, C. (2008) 'Long-term field performance of a polyester-based long-lasting insecticidal mosquito net in rural Uganda', *Malaria Journal,* 7(1), pp. 1-22.

Killeen, G., Fillinger, U., Kiche, I., Gouagna, L. and Knols, B. (2002) 'Eradication of Anopheles gambiae from Brazil: lessons for malaria control in Africa?', *The Lancet - Infectious diseases,* 2(10), pp. 618-627.

Kistler, K., Vosshall, L. and Matthews, B. (2015) 'Genome engineering with CRISPR-Cas9 in the mosquito Aedes aegypti', *Cell Reports,* 11(1), pp. 51-60.

Kitron, U. and Spielman, A. (1989) 'Suppression of transmission of malaria through source reduction: antianopheline measures applied in Israel, the United States, and Italy', *Reviews of Infectious Diseases,* 11(3), pp. 391-406.

Knols, B., Farenhorst, M., Andriessen, R., Snetselaar, J., Suer, R., Osinga, A., Knols, J., Deschietere, J., Ng'habi, K., Lyimo, I., Kessy, S., Mayagaya, V., Sperling, S., Cordel, M., Sternberg, E., Hartmann, P., Mnyone, L., Rose, A. and Thomas, M. (2016) 'Eave tubes for malaria control in Africa: an introduction', *Malaria Journal,* 15(1), pp. 404.

Kokoza, V. and Raikhel, A. (2011) 'Targeted gene expression in the transgenic Aedes aegypti using the binary Gal4-UAS system', *Insect Biochemistry and Molecular Biology,* 41, pp. 637-644.

Kondo, S., Takahashi, T., Yamagata, N., Imanishi, Y., Katow, H., Hiramatsu, S., Lynn, K., Abe, A., Kumaraswamy, A. and Tanimoto, H. (2020) 'Neurochemical Organization of the Drosophila Brain Visualized by Endogenously Tagged Neurotransmitter Receptors', *Cell Reports,* 30(1), pp. 284-297 e5.

Kouamo, M., Ibrahim, S., Hearn, J., Riveron, J., Kusimo, M., Tchouakui, M., Ebai, T., Tchapga, W., Wondji, M., Irving, H., Boudjeko, T., Boyom, F. and Wondji, C. (2021) 'Genome-Wide

Transcriptional Analysis and Functional Validation Linked a Cluster of Epsilon Glutathione S-Transferases with Insecticide Resistance in the Major Malaria Vector Anopheles funestus across Africa', *Genes,* 12(4), pp. 561.

Kouassi, B., Edi, C., Tia, E., Konan, L., Akré, M., Koffi, A., Ouattara, A., Tanoh, A., Zinzindohoue, P., Kouadio, B., Andre, M., Irish, S., Armistead, J., Dengela, D., Cissé, N., Flatley, C. and Chabi, J. (2020) 'Susceptibility of Anopheles gambiae from Côte d'Ivoire to insecticides used on insecticide-treated nets: evaluating the additional entomological impact of piperonyl butoxide and chlorfenapyr', *Malaria Journal,* 19(1), pp. 1-11.

Kraemer, M., Reiner, R., Brady, O., Messina, J., Gilbert, M., Pigott, D., Yi, D., Johnson, K., Earl, L., Marczak, L., Shirude, S., WN., D., Bisanzio, D., Perkins, T., Lai, S., Lu, X., Jones, P., Coelho, G., Carvalho, R., Van Bortel, W., Marsboom, C., Hendrickx, G., Schaffner, F., Moore, C., Nax, H., Bengtsson, L., Wetter, E., Tatem, A., Brownstein, J., Smith, D., Lambrechts, L., Cauchemez, S., Linard, C., Faria, N., Pybus, O., Scott, T., Liu, Q., Yu, H., Wint, G., Hay, S. and Golding, N. (2019) 'Past and future spread of the arbovirus vectors Aedes aegypti and Aedes albopictus', *Nature Microbiology,* 4(5), pp. 854-863.

Kraemer, M., Sinka, M., Duda, K., Mylne, A., Shearer, F., Barker, C., Moore, C., Carvalho, R., Coelho, G., Van Bortel, W., Hendrickx, G., Schaffner, F., Elyazar, I., Teng, H.-J., Brady, O., Messina, J., Pigott, D., Scott, T., Smith, D., Wint, G., Golding, N. and Hay, S. (2015) 'The global distribution of the arbovirus vectors Aedes aegypti and Ae. albopictus', *eLife,* 4, pp. e08347.

Kramer, L. and Ciota, A. (2015) 'Dissecting vectorial capacity for mosquito-borne viruses', *Current Opinion in Virology,* 15, pp. 112-118.

Kreppel, K., Viana, M., Main, B. J., Johnson, P., Govella, N., Lee, Y., Maliti, D., Meza, F., Lanzaro, G. and Ferguson, H. (2020) 'Emergence of behavioural avoidance strategies of malaria vectors in areas of high LLIN coverage in Tanzania', *Scientific Reports,* 10(1), pp. 1-11.

Krzywinska, E., Dennison, N., Lycett, G. and Krzywinski, J. (2016) 'A maleness gene in the malaria mosquito Anopheles gambiae', *Science,* 353(6294), pp. 67-69.

Kyrou, K., Hammond, A., Galizi, R., Kranjc, N., Burt, A., Beaghton, A., Nolan, T. and Crisanti, A. (2018) 'A CRISPR–Cas9 gene drive targeting doublesex causes complete population suppression in caged Anopheles gambiae mosquitoes', *Nature Biotechnology,* 36(11), pp. 1062-1066.

Labun, K., Montague, T., Krause, M., Torres Cleuren, Y., Tjeldnes, H. and Valen, E. (2019) 'CHOPCHOP v3: expanding the CRISPR web toolbox beyond genome editing.', *Nucleic Acids Research*.

Laird, M. (1985) 'New answers to malaria problems through vector control?', *Experientia,* 41(4), pp. 446-456.

Lakshmi, V., Neeraja, M., Subbalaxmi, M., Parida, M., Dash, P., Santhosh, S. and Rao, P. (2008) 'Clinical features and molecular diagnosis of Chikungunya fever from South India', *Clinical Infectious Diseases,* 46(9), pp. 1436-1442.

Lawler, S. (2017) 'Environmental safety review of methoprene and bacterially-derived pesticides commonly used for sustained mosquito control', *Ecotoxicology and Environmental Safety,* 139, pp. 335-343.

Lee, P., Zirin, J., Kanca, O., Lin, W., Schulze, K., Li-Kroeger, D., Tao, R., Devereaux, C., Hu, Y., Chung, V., Fang, Y., He, Y., Pan, H., Ge, M., Zuo, Z., Housden, B., Mohr, S., Yamamoto, S., Levis, R., Spradling, A., Perrimon, N. and Bellen, H. (2018) 'A gene-specific T2A-GAL4 library for Drosophila', *eLife,* 7, pp. e35574.

Lee, R., Choong, C., Goh, B., Ng, L. and Lam-Phua, S. (2014) 'Bioassay and biochemical studies of the status of pirimiphos-methyl and cypermethrin resistance in Aedes (Stegomyia) aegypti and Aedes (Stegomyia) albopictus (Diptera: Culicidae) in Singapore', *Tropical Biomedicine,* 31(4).

Lees, R., Ismail, H., Logan, R., Malone, D., Davies, R., Anthousi, A., Adolfi, A., Lycett, G. and Paine, M. (2020) 'New insecticide screening platforms indicate that Mitochondrial Complex I inhibitors are susceptible to cross-resistance by mosquito P450s that metabolise pyrethroids', *Scientific Reports,* 10(1), pp. 16232.

Lees, R., Praulins, G., Davies, R., Brown, F., Parsons, G., White, A., Ranson, H., Small, G. and Malone, D. (2019) 'A testing cascade to identify repurposed insecticides for next-generation vector control tools: screening a panel of chemistries with novel modes of action against a malaria vector', *Gates Open Research,* 3, pp. 1464.

Lefèvre, T., Gouagna, L.-C., Dabire, K. R., Elguero, E., Fontenille, D., Costantini, C. and Thomas, F. (2009) 'Evolutionary lability of odour-mediated host preference by the malaria vector Anopheles gambiae', *Tropical Medicine and International Health,* 14(2), pp. 228-236.

Li, M., Bui, M., Yang, T., Bowman, C., White, B. and Akbari, O. (2017) 'Germline Cas9 expression yields highly efficient genome engineering in a major worldwide disease vector, Aedes aegypti', *Proceedings of the National Academy of Sciences of the United States of America,* 114(49).

Li, X., Zhao, X., Fang, Y., Jiang, X., Duong, T., Fan, C., Huang, C. and Kain, S. (1998) 'Generation of destabilized green fluorescent protein as a transcription reporter', *The Journal of Biological Chemistry,* 273(52), pp. 34970-34975.

Lindsay, S., Jawara, M., Paine, K., Pinder, M., Walraven, G. and Emerson, P. (2003) 'Changes in house design reduce exposure to malaria mosquitoes', *Tropical Medicine & International Health,* 8(6), pp. 512-517.

Liu, N. (2015) 'Insecticide Resistance in Mosquitoes: Impact, Mechanisms, and Research Directions', *http://dx.doi.org/10.1146/annurev-ento-010814-020828,* 60, pp. 537-559.

Livak, K. (1984) 'Organization and Mapping of a Sequence on the DROSOPHILA MELANOGASTER X and Y Chromosomes That Is Transcribed during Spermatogenesis', *Genetics,* 107(4), pp. 611-634.

Lobo, N., Clayton, J., Fraser, M., Kafatos, F. and Collins, F. (2006) 'High efficiency germ-line transformation of mosquitoes', *Nature Protocols,* 1(3), pp. 1312-1317.

Lombardo, F., Lycett, G., Lanfrancotti, A., Coluzzi, M. and Arcà, B. (2009) 'Analysis of apyrase 5' upstream region validates improved Anopheles gambiae transformation technique', *BMC Research Notes,* 2(1), pp. 1-7.

Lounibos, L. (2003) 'Invasions By Insect Vectors Of Human Disease', *Annual Review of Entomology,* 47, pp. 233-266.

Luc, D., Valérie, N. and Philip, A. (2010) 'Costs of insensitive acetylcholinesterase insecticide resistance for the malaria vector Anopheles gambiae homozygous for the G119S mutation', *Malaria Journal,* 9(1), pp. 1-8.

Lupenza, E., Gasarasi, D. and Minzi, O. (2021) 'Lymphatic filariasis, infection status in Culex quinquefasciatus and Anopheles species after six rounds of mass drug administration in Masasi District, Tanzania', *Infectious Diseases of Poverty,* 10(1), pp. 1-11.

Lycett, G., Amenya, D. and Lynd, A. (2011) 'The Anopheles gambiae alpha-tubulin-1b promoter directs neuronal, testes and developing imaginal tissue specific expression and is a sensitive enhancer detector', *Insect Molecular Biology,* 21(1), pp. 79-88.

Lycett, G., McLaughlin, L., Ranson, H., Hemmingway, J., Kafatos, F., Loukeris, T. and Paine, M. (2006) 'Anopheles gambiae P450 reductase is highly expressed in oenocytes and in vivo knockdown increases permethrin susceptibility', *Insect Molecular Biology,* 15(3), pp. 321-327.

Lynd, A., Balabanidou, V., Grosman, R., Maas, J., Lian, L.-Y., Vontas, J. and Lycett, G. (2019) 'Development of a functional genetic tool for Anopheles gambiae oenocyte characterisation: application to cuticular hydrocarbon synthesis', *bioRxiv*.

Lynd, A. and Lycett, G. (2012) 'Development of the Bi-Partite Gal4-UAS System in the African Malaria Mosquito, Anopheles gambiae', *PLoS ONE,* 7(2), pp. e31552.

Lynd, A. and Lycett, G. J. (2011) 'Optimization of the Gal4-UAS system in an Anopheles gambiae cell line', *Insect Molecular Biology,* 20(5), pp. 599-608.

Marcombe, S., Fustec, B., Cattel, J., Chonephetsarath, S., Thammavong, P., Phommavanh, N., David, J. P., Corbel, V., Sutherland, I., Hertz, J. and Brey, P. (2019) 'Distribution of Insecticide Resistance and Mechanisms Involved in the Arbovirus Vector Aedes Aegypti in Laos and Implication for Vector Control', *PLoS Neglected Tropical Diseases,* 13(12), pp. e0007852.

Marcombe, S., Mathieu, R. B., Pocquet, N., Riaz, M. A., Poupardin, R., Selior, S., Darriet, F., Reynaud, S., Yebakima, A., Corbel, V., David, J. P. and Chandre, F. (2012) 'Insecticide Resistance in the Dengue Vector Aedes aegypti from Martinique: Distribution, Mechanisms and Relations with Environmental Factors', *Plos One,* 7(2), pp. 11.

Martens, P. and Hall, L. (2000) 'Malaria on the move: human population movement and malaria transmission.', *Emerging Infectious Diseases,* 6(2), pp. 103-109.

Martin, C., Curtis, B., Fraser, C. and Sharp, B. (2002) 'The use of a GIS-based malaria information system for malaria research and control in South Africa', *Health & Place,* 8(4), pp. 227-236.

Matowo, N., Tanner, M., Munhenga, G., Mapua, S., Finda, M., Utzinger, J., Ngowi, V. and Okumu, F. (2020) 'Patterns of pesticide usage in agriculture in rural Tanzania call for integrating agricultural and public health practices in managing insecticide-resistance in malaria vectors', *Malaria Journal,* 19(1), pp. 257.

Matthews, B. and Vosshall, L. (2020) 'How to turn an organism into a model organism in 10 'easy' steps', *The Journal of Experimental Biology,* 223(Pt Suppl 1), pp. jeb218198.

Matthews, B., Younger, M. and Vosshall, L. (2019) 'The ion channel ppk301 controls freshwater egg-laying in the mosquito Aedes aegypti', *eLife,* 8, pp. e43963.

Mattson, M. (2008) 'Hormesis Defined', *Ageing Research Reviews,* 7(1), pp. 1-7.

Mbepera, S., Nkwengulila, G., Peter, R., Mausa, E., Mahande, A., Coetzee, M. and Kweka, E. (2017) 'The influence of age on insecticide susceptibility of Anopheles arabiensis during dry and rainy seasons in rice irrigation schemes of Northern Tanzania', *Malaria Journal,* 16(1), pp. 1-9.

McGregor, B. and Connelly, C. (2021) 'A Review of the Control of Aedes aegypti (Diptera: Culicidae) in the Continental United States', *Journal of Medical Entomology,* 58(1), pp. 10-25.

Medjigbodo, A., Djogbenou, L., Koumba, A., Djossou, L., Badolo, A., Adoha, C., Ketoh, G. and Mavoungou, J. (2021) 'Phenotypic Insecticide Resistance in Anopheles gambiae (Diptera: Culicidae): Specific Characterization of Underlying Resistance Mechanisms Still Matters', *Journal of Medical Entomology,* 58(2), pp. 730-738.

Meiwald, A., Clark, E., Kristan, M., Edi, C., Jeffries, C., Pelloquin, B., Irish, S., Walker, T. and Messenger, L. (2020) 'Reduced long-lasting insecticidal net efficacy and pyrethroid insecticide resistance are associated with over-expression of CYP6P4, CYP6P3 and CYP6Z1 in populations of Anopheles coluzzii from South-East Côte d'Ivoire', *The Journal of Infectious Diseases,* jiaa699.

Menze, B., Kouamo, M., Wondji, M., Tchapga, W., Tchoupo, M., Kusimo, M., Mouhamadou, C., Riveron, J. and Wondji, C. (2020) 'An Experimental Hut Evaluation of PBO-Based and Pyrethroid-Only Nets Against the Malaria Vector Anopheles funestus Reveals a Loss of Bed Nets Efficacy Associated With GSTe2 Metabolic Resistance', *Genes,* 11(2), pp. 143.

Mian, L., Dhillon, M. and Dodson, L. (2017) 'Field Evaluation of Pyriproxyfen Against Mosquitoes in Catch Basins in Southern California', *Journal of the American Mosquito Control Association,* 33(2), pp. 145-147.

Milam, C., Farris, J. and Wilhide, J. (2000) 'Evaluating mosquito control pesticides for effect on target and nontarget organisms', *Archives of Environmental Contamination and Toxicology,* 39(3), pp. 324-328.

Millar, N. and Denholm, I. (2007) 'Nicotinic acetylcholine receptors: targets for commercially important insecticides', *Invertebrate Neuroscience,* 7(1), pp. 53-66.

Minard, G., Mavingui, P. and Moro, C. (2013) 'Diversity and function of bacterial microbiota in the mosquito holobiont', *Parasites & Vectors,* 6, pp. 146.

Mitchell, S., Rigden, D., Dowd, A., Lu, F., Wilding, C., Weetman, D., Dadzie, S., Jenkins, A., Regna, K., Boko, P., Djogbenou, L., Muskavitch, M., Ranson, H., Paine, M. J., Mayans, O. and Donnelly, M. (2014) 'Metabolic and target-site mechanisms combine to confer strong DDT resistance in Anopheles gambiae', *PLoS One,* 9(3), pp. e92662.

Mitchell, S., Stevenson, B., Muller, P., Wilding, C., Egyir-Yawson, A., Field, S., Hemingway, J., Paine, M., Ranson, H. and Donnelly, M. (2012) 'Identification and validation of a gene causing cross-resistance between insecticide classes in Anopheles gambiae from Ghana', *Proceedings of the National Academy of Sciences of the United States of America,* 109(16), pp. 6147-6152.

Mohanty, A., Nina, P., Ballav, S., Vernekar, S., Parkar, S., D'souza, M., Zuo, W., Gomes, E., Chery, L., Tuljapurkar, S., Valecha, N., Rathod, P. and Kumar, A. (2018) 'Susceptibility of wild and colonized Anopheles stephensi to Plasmodium vivax infection', *Malaria Journal,* 17(1), pp. 255.

Moller-Jacobs, L., Murdock, C. and Thomas, M. (2014) 'Capacity of mosquitoes to transmit malaria depends on larval environment', *Parasites & Vectors,* 7(1), pp. 1-12.

Montella, I., Martins, A., Viana-Medeiros, P., Lima, J. B., Braga, I. and Valle, D. (2007) 'Insecticide Resistance Mechanisms of Brazilian Aedes aegypti Populations from 2001 to 2004', *American Journal of Tropical Medicine and Hygiene,* 77(3), pp. 467-477.

Moyes, C., Vontas, J., Martins, A., Ng, L., Koou, S., Dusfour, I., Raghavendra, K., Pinto, J., Corbel, V., David, J. and Weetman, D. (2017) 'Contemporary status of insecticide resistance in the major Aedes vectors of arboviruses infecting humans', *PLoS Neglected Tropical Diseases,* 11(7), pp. e0005625.

Muller, P., Warr, E., Stevenson, B., Pignatelli, P., Morgan, J., Steven, A., Yawson, A., Mitchell, S., Ranson, H., Hemingway, J., Paine, M. and Donnelly, M. (2008) 'Field-Caught Permethrin-Resistant Anopheles gambiae Overexpress CYP6P3, a P450 That Metabolises Pyrethroids', *PLoS Genetics,* 4(11), pp. 10.

Muthusamy, R. and Shivakumar, M. (2015) 'Susceptibility status of Aedes aegypti (L.) (Diptera: Culicidae) to temephos from three districts of Tamil Nadu, India', *Journal of Vector Borne Diseases,* 52(2), pp. 159-165.

Muturi, E., Dunlap, C., Smartt, C. and Shin, D. (2021) 'Resistance to permethrin alters the gut microbiota of Aedes aegypti', *Scientific Reports,* 11(1), pp. 1-8.

N'Guessan, R., Boko, P., Odjo, A., Chabi, J., Akogbeto, M. and Rowland, M. (2010) 'Control of pyrethroid and DDT-resistant Anopheles gambiae by application of indoor residual spraying or mosquito nets treated with a long-lasting organophosphate insecticide, chlorpyrifos-methyl', *Malaria Journal,* 9, pp. 44.

N'Guessan, R., Darriet, F., Guillet, P., Carnevale, P., Traore-Lamizana, M., Corbel, V., Koffi, A. and Chandre, F. (2003) 'Resistance to carbosulfan in Anopheles gambiae from Ivory Coast, based on reduced sensitivity of acetylcholinesterase', *Medical and Veterinary Entomology,* 17(1), pp. 19-25.

Nanfack Minkeu, F. and Vernick, K. (2018) 'A Systematic Review of the Natural Virome of Anopheles Mosquitoes', *Viruses,* 10(5), pp. 222.

Niang, E., Konaté, L., Faye, O., Diallo, M. and Dia, I. (2019) 'Vector bionomics and malaria transmission in an area of sympatry of An. arabiensis, An. coluzzii and An. gambiae', *Acta Tropica,* 189, pp. 129-136.

Nkemngo, F., Mugenzi, L., Terence, E., Niang, A., Wondji, M., Tchoupo, M., Nguete, N., Tchapga, W., Irving, H., Ntabi, J., Agonhossou, R., Boussougou-Sambe, T., Akoton, R., Koukouikila-Koussounda, F., Pinilla, Y., Ntoumi, F., Djogbenou, L., Ghogomu, S., Ndo, C., Adegnika, A., Borrmann, S. and Wondji, C. (2020) 'Multiple insecticide resistance and Plasmodium infection in the principal malaria vectors Anopheles funestus and Anopheles gambiae in a forested locality close to the Yaoundé airport, Cameroon', *Wellcome Open Research,* 5, pp. 146.

NobelPrize.org 2021. The Nobel Prize in Chemistry 2020. *In:* Outreach, N.P. (ed.).

Nwane, P., Etang, J., Chouaïbou, M., Toto, J., Koffi, A., Mimpfoundi, R. and Simard, F. (2013) 'Multiple insecticide resistance mechanisms in Anopheles gambiae s.l. populations from Cameroon, Central Africa', *Parasites & Vectors,* 6(1), pp. 1-14.

N'Guessan, R., Corbel, V., Akogbéto, M. and Rowland, M. (2007) 'Reduced Efficacy of Insecticide-treated Nets and Indoor Residual Spraying for Malaria Control in Pyrethroid Resistance Area, Benin', *Emerging Infectious Diseases,* 13(2), pp. 199-206.

O'Brien, R. (1967) *Insecticides action and metabolism.* New York: Academic Press.

Ohashi, K., Nakada, K., Ishiwatari, T., Miyaguchi, J., Shono, Y., Lucas, J. and Mito, N. (2012) 'Efficacy of Pyriproxyfen-Treated Nets in Sterilizing and Shortening the Longevity of Anopheles gambiae (Diptera: Culicidae)', *Journal of Medical Entomology,* 49(5), pp. 1052-1058.

Ohm, J., Baldini, F., Barreaux, P., Lefevre, T., Lynch, P., Suh, E., Whitehead, S. and Thomas, M. (2018) 'Rethinking the extrinsic incubation period of malaria parasites', *Parasites & Vectors,* 11(1), pp. 1-9.

Okech, B., Gouagna, L., Yan, G., Githure, J. and Beier, J. (2007) 'Larval habitats of Anopheles gambiae s.s. (Diptera: Culicidae) influences vector competence to Plasmodium falciparum parasites', *Malaria Journal,* 6(1), pp. 1-7.

Okita, C., Sato, M. and Schroeder, T. (2004) 'Generation of optimized yellow and red fluorescent proteins with distinct subcellular localization', *Short Technical Reports,* 36(3), pp. 418-424.

Oliveira-Ferreira, C., Gaspar, M. and Vasconcelos, M. (2021) 'Neuronal control of suppression, initiation and completion of egg deposition in Drosophila melanogaster', *bioRxiv*.

Omoke, D., Kipsum, M., Otieno, S., Esalimba, E., Sheth, M., Lenhart, A., Njeru, E., Ochomo, E. and Dada, N. (2021) 'Western Kenyan Anopheles gambiae showing intense permethrin resistance harbour distinct microbiota', *Malaria Journal,* 20(1), pp. 77.

Ondiba, I., Oyieke, F., Ong'amo, G., Olumula, M., Nyamongo, I. and Estambale, B. (2018) 'Malaria vector abundance is associated with house structures in Baringo County, Kenya', *PLoS One,* 13(6), pp. e0198970.

Ong, S. and Jaal, Z. (2018) 'Larval Age and Nutrition Affect the Susceptibility of Culex quinquefasciatus (Diptera: Culicidae) to Temephos', *Journal of Insect Science,* 18(2).

Oumbouke, W., Pignatelli, P., Barreaux, A., Tia, I., Koffi, A., Ahoua Alou, L., Sternberg, E., Thomas, M., Weetman, D. and N'Guessan, R. (2020) 'Fine scale spatial investigation of multiple insecticide resistance and underlying target-site and metabolic mechanisms in Anopheles gambiae in central Côte d'Ivoire', *Scientific Reports,* 10(1), pp. 15066.

Owusu, H., Chitnis, N. and Müller, P. (2017) 'Insecticide susceptibility of Anopheles mosquitoes changes in response to variations in the larval environment', *Scientific Reports,* 7(1), pp. 3667.

Owusu, H., Jančáryová, D., Malone, D. and Müller, P. (2015) 'Comparability between insecticide resistance bioassays for mosquito vectors: time to review current methodology?', *Parasites and Vectors,* 8, pp. 357.

Oxborough, R. (2016) 'Trends in US President's Malaria Initiative-funded indoor residual spray coverage and insecticide choice in sub-Saharan Africa (2008–2015): urgent need for affordable, long-lasting insecticides', *Malaria Journal,* 15(1), pp. 1-9.

Padonou, G., Sezonlin, M., Ossé, R., Aizoun, N., Oké-Agbo, F., Oussou, O., Gbédjissi, G. and Akogbéto, M. (2012) 'Impact of three years of large scale Indoor Residual Spraying (IRS) and Insecticide Treated Nets (ITNs) interventions on insecticide resistance in Anopheles gambiae s.l. in Benin', *Parasites & Vectors,* 5, pp. 72.

Paine, M. and Brooke, B. (2016) 'Insecticide Resistance and Its Impact on Vector Control', in Horowitz, A.R. and Ishaaya, I. (eds.) *Advances in Insect Control and Resistance Management*. Cham: Springer International Publishing, pp. 287-312.

Pance, A. (2020) 'Diversify and Conquer: The Vaccine Escapism of Plasmodium falciparum', *Microorganisms,* 8(11).

Papathanos, P., Windbichler, N., Menichelli, M., Burt, A. and Crisanti, A. (2009) 'The vasa regulatory region mediates germline expression and maternal transmission of proteins in the malaria mosquito Anopheles gambiae: a versatile tool for genetic control strategies', *BMC Molecular Biology,* 10(1), pp. 1-13.

Paredes-Esquivel, C., Lenhart, A., del Río, R., Leza, M., Estrugo, M., Chalco, E., Casanova, W. and Miranda, M. (2016) 'The impact of indoor residual spraying of deltamethrin on dengue vector populations in the Peruvian Amazon', *Acta Tropica,* 154, pp. 139-144.

Partridge, F., Brown, A., Buckingham, S., Willis, N., Wynne, G., Forman, R., Else, K., Morrison, A., Matthews, J., Russell, A., Lomas, D. and Sattelle, D. (2018) 'An automated high-throughput system for phenotypic screening of chemical libraries on C. elegans and parasitic nematodes', *International Journal for Parasitology,* 8(1), pp. 8-21.

Partridge, F., Poulton, B., Lake, M., Lees, R., Mann, H., Lycett, G. and Sattelle, D. (2021) 'Actions of camptothecin derivatives on larvae and adults of the arboviral vector Aedes aegypti', *bioRxiv*.

Pasay, C., Arlian, L., Morgan, M., Gunning, R., Rossiter, L., Holt, D., Walton, S., Beckham, S. and McCarthy, J. (2009) 'The effect of insecticide synergists on the response of scabies mites to pyrethroid acaricides', *PLoS Neglected Tropical Diseases,* 3(1), pp. e354.

Pates, H. and Curtis, C. (2005) 'Mosquito behavior and vector control', *Annual Review of Entomology,* 50, pp. 53-70.

Paupy, C., Delatte, H., Bagny, L., Corbel, V. and Fontenille, D. (2009) 'Aedes albopictus, an arbovirus vector: From the darkness to the light', *Microbes and Infection,* 11(14-15), pp. 1177-1185.

Philbert, A., Lyantagaye, S. and Nkwengulila, G. (2019) 'Farmers' pesticide usage practices in the malaria endemic region of North-Western Tanzania: implications to the control of malaria vectors', *BMC Public Health,* 19(1), pp. 1-11.

Piameu, M., Nwane, P., Toussile, W., Mavridis, K., Wipf, N. C., Kouadio, P., Mbakop, L., Mandeng, S., Eyisap Ekoko, W., Toto, J., Ngaffo, K., Etounde, P., Ngantchou, A., Chouaibou, M., Müller, P., Awono-Ambene, P., Vontas, J. and Etang, J. (2021) 'Pyrethroid and Etofenprox Resistance in Anopheles gambiae and Anopheles coluzzii from Vegetable Farms in Yaoundé, Cameroon: Dynamics, Intensity and Molecular Basis', *Molecules,* 26(18), pp. 5543.

Pinkerton, A., Michel, K., O'Brochta, D. and Atkinson, P. (2000) 'Green fluorescent protein as a genetic marker in transgenic Aedes aegypti', *Insect Molecular Biology,* 9(1), pp. 1-10.

Pondeville, E., Puchot, N., Meredith, J., Lynd, A., Vernick, K., Lycett, G., Eggleston, P. and Bourgouin, C. (2014) 'Efficient ΦC31 Integrase-Mediated Site-Specific Germline Transformation of Anopheles Gambiae', *Nature Protocols,* 9(7), pp. 1698-1712.

Pondeville, E., Puchot, N., Parvy, J.-P., Carissimo, G., Poidevin, M., Waterhouse, R., Marois, E. and Bourgouin, C. (2020) 'Hemocyte-targeted gene expression in the female malaria mosquito using the hemolectin promoter from Drosophila', *Insect Biochemistry and Molecular Biology,* 120, pp. 103339.

Poulton, B., Colman, F., Anthousi, A., Grigoraki, L., Adolfi, A., Lynd, A. and Lycett, G. (2021) 'Using the GAL4-UAS System for Functional Genetics in Anopheles gambiae', *Journal of Visualized Experiments,* (170), pp. e62131.

Poupardin, R., Srisukontarat, W., Yunta, C. and Ranson, H. (2014) 'Identification of Carboxylesterase Genes Implicated in Temephos Resistance in the Dengue Vector Aedes aegypti', *PLoS Neglected Tropical Diseases,* 8(3), pp. e2743.

Pronk, I., Speijers, G., Wouters, M. and Ritter, L. (accessed: 2021) *Cypermethrin & alpha-cypermethrin*. International Programme on Chemical Safety (IPCS): WHO. Available at: http://www.inchem.org/documents/jecfa/jecmono/v38je07.htm (Accessed: 2021).

Raghavendra, K., Barik, T., Reddy, B., Sharma, P. and Dash, A. (2011) 'Malaria vector control: from past to future', *Parasitology Research,* 108(4), pp. 757-779.

Rahman, R., Souza, B., Uddin, I., Carrara, L., Brito, L., Costa, M., Mahmood, M., Khan, S., Lima, J. and Martins, A. (2021) 'Insecticide resistance and underlying targets-site and metabolic mechanisms in Aedes aegypti and Aedes albopictus from Lahore, Pakistan', *Scientific Reports,* 11(1), pp. 1-15.

Rahnama-Moghadam, S., Hillis, L. D. and Lange, R. (2015) 'Environmental Toxins and the Heart', in Ramachandran, M. (ed.) *Heart and Toxins*. Boston: Academic Press, pp. 75-132.

Ranson, H., Claudianos, C., Ortelli, F., Abgrall, C., Hemingway, J., Sharakhova, M., Unger, M., Collins, F. and Feyereisen, R. (2002) 'Evolution of supergene families associated with insecticide resistance', *Science,* 298(5591), pp. 179-181.

Ranson, H., Jensen, B., Wang, X., Prapanthadara, L., Hemingway, J. and Collins, F. (2000) 'Genetic mapping of two loci affecting DDT resistance in the malaria vector Anopheles gambiae', *Insect Molecular Biology,* 9(5), pp. 499-507.

Ranson, H. and Lissenden, N. (2016) 'Insecticide Resistance in African Anopheles Mosquitoes: A Worsening Situation that Needs Urgent Action to Maintain Malaria Control', *Trends in Parasitology,* 32(3), pp. 187-196.

Ray, D. (2005) 'Pyrethrins/Pyrethroids', in Wexler, P. (ed.) *Encyclopedia of Toxicology.* Second ed: Elsevier, pp. 574-579.

Reiskind, M. and Lounibos, L. (2009) 'Effects of intraspecific larval competition on adult longevity in the mosquitoes Aedes aegypti and Aedes albopictus', *Medical and Veterinary Entomology,* 23(1), pp. 62-68.

Rezza, G., Chen, R. and Weaver, S. (2017) 'O'nyong-nyong fever: a neglected mosquito-borne viral disease', *Pathogens and Global Health,* 111(6), pp. 271-275.

Riabinina, O., Luginbuhl, D., Marr, E., Liu, S., Wu, M. N., Luo, L. and Potter, C. J. (2015) 'Improved and expanded Q-system reagents for genetic manipulations', *Nature Methods,* 12(3), pp. 219-222.

Riehle, M., Bukhari, T., Gneme, A., Guelbeogo, W., Coulibaly, B., Fofana, A., Pain, A., Bischoff, E., Renaud, F., Beavogui, A., Traore, S., Sagnon, N. and Vernick, K. (2017) 'The Anopheles gambiae 2La chromosome inversion is associated with susceptibility to Plasmodium falciparum in Africa', *eLife,* 6, pp. e25813.

Ringrose, L. (2009) 'Transgenesis in Drosophila Melanogaster', in E, C. (ed.) *Transgenesis Techniques Methods in molecular biology*: Humana Press, pp. 3-19.

Ritz, C., Baty, F., Streibig, J. and Gerhard, D. (2015) 'Dose-Response Analysis Using R', *PLoS ONE,* 10(12), pp. e0146021.

Riveron, J., Ibrahim, S., Mulamba, C., Djouaka, R., Irving, H., Wondji, M., Ishak, I. and Wondji, C. (2017) 'Genome-wide transcription and functional analyses reveal heterogeneous molecular mechanisms driving pyrethroids resistance in the major malaria vector Anopheles funestus across Africa', *Genes Genomes Genetics,* 7(6), pp. 1819-1832.

Riveron, J., Irving, H., Ndula, M., Barnes, K., Ibrahim, S., Paine, M. and Wondji, C. (2013) 'Directionally selected cytochrome P450 alleles are driving the spread of pyrethroid resistance in the major malaria vector Anopheles funestus', *Proceedings of the National Academy of Sciences,* 110(1), pp. 252.

Riveron, J., Yunta, C., Ibrahim, S., Djouaka, R., Irving, H., Menze, B., Ismail, H., Hemingway, J., Ranson, H., Albert, A. and Wondji, C. (2014) 'A single mutation in the GSTe2 gene allows tracking of metabolically based insecticide resistance in a major malaria vector', *Genome Biology,* 15(2).

Rodríguez, M., Bisset, J., de Fernandez, D., Lauzán, L. and Soca, A. (2001) 'Detection of Insecticide Resistance in Aedes aegypti (Diptera: Culicidae) from Cuba and Venezuela', *Journal of Medical Entomology,* 38(5), pp. 623-628.

Rodríguez, M., Bisset, J. A. and Fernández, D. (2007) 'Determination in vivo of the role of esterase and glutathione transferase enzymes in pyrethroid resistance of Aedes aegypti (Diptera: Culicidae)', *Revista Cubana de Medicina Tropical,* 59(3).

Roiz, D., Wilson, A., Scott, T., Fonseca, D., Jourdain, F., Müller, P., Velayudhan, R. and Corbel, V. (2018) 'Integrated Aedes management for the control of Aedes-borne diseases', *PLoS Neglected Tropical Diseases,* 12(12), pp. e0006845.

Ross, P. (2021) 'Designing effective Wolbachia release programs for mosquito and arbovirus control', *Acta Tropica,* 222, pp. 106045.

Rozendaal, J., WHO (1997) *Vector control: Methods for use by individuals and communities.* Geneva.

Rund, S., Labb, L., Benefiel, O. and Duffield, G. (2020) 'Artificial Light at Night Increases Aedes aegypti Mosquito Biting Behavior with Implications for Arboviral Disease Transmission', *The American Journal of Tropical Medicine and Hygiene,* 103(6), pp. 2450-2452.

Samuel, M., Maoz, D., Manrique, P., Ward, T., Runge-Ranzinger, S., Toledo, J., Boyce, R. and Horstick, O. (2017) 'Community effectiveness of indoor spraying as a dengue vector control method: A systematic review', *PLoS Neglected Tropical Diseases,* 11(8), pp. e0005837.

Schmid-Burgk, J., Höning, K., Ebert, T. and Hornung, V. (2016) 'CRISPaint allows modular base-specific gene tagging using a ligase-4-dependent mechanism', *Nature Communications,* 7, pp. 12338.

Schwartz, E. (2012) 'Prophylaxis of Malaria', *Mediterranean Journal of Hematology and Infectious Disease,* 4(1), pp. e2012045.

Scott, M., Hribar, L., Leal, A. and McAllister, J. (2020) 'Characterization of Pyrethroid Resistance Mechanisms in Aedes aegypti from the Florida Keys', *The American Journal of Tropical Medicine and Hygiene,* 104(3), pp. 1111-1122.

Seixas, G., Grigoraki, L., Weetman, D., Vicente, J., Silva, A., Pinto, J., Vontas, J. and Sousa, C. (2017) 'Insecticide resistance is mediated by multiple mechanisms in recently introduced Aedes aegypti from Madeira Island (Portugal)', *PLoS Neglected Tropical Diseases,* 11(7), pp. e0005799.

Sene, N., Mavridis, K., Ndiaye, E., Diane, C., Gaye, A., Ngom, E., Ba, Y., Diallo, D., Vontas, J., Dia, I. and Diallo, M. (2021) 'Insecticide resistance status and mechanisms in Aedes aegypti populations from Senegal', *PLoS Neglected Tropical Diseases,* 15(5), pp. e0009393.

Sereda, B. and Meinhardt, H. (2005) 'Contamination of the Water Environment in Malaria Endemic Areas of KwaZulu-Natal, South Africa, by Agricultural Insecticides', *Bulletin of Environmental Contamination and Toxicology,* 75(3), pp. 530-537.

Service, M. (2012) *Medical Entomology for Students.* Fifth edn. United States of America: Cambridge University Press.

Shankar, S., Tauxe, G., Spikol, E., Li, M., Akbari, O., Giraldo, D. and McMeniman, C. (2020) 'Synergistic Coding of Human Odorants in the Mosquito Brain', *bioRxiv*.

Shousha, A. (1948) 'Species-eradication: The Eradication of Anopheles gambioe from Upper Egypt, 1942-1945', *Bulletin of the World Health Organization,* 1(2), pp. 309-352.

Shretta, R., Liu, J., Cotter, C., Cohen, J., Dolenz, C., Makomva, K., Newby, G., Ménard, D., Phillips, A., Tatarsky, A., Gosling, R. and Feachem, R. (2017) 'Malaria Elimination and Eradication', in Holmes, K.B., S. Bloom, BR. et al (ed.) *Major Infectious Diseases*. Washington DC: The International Bank for Reconstruction and Development / The World Bank.

Shroyer, D. (1990) 'Vertical maintenance of dengue-1 virus in sequential generations of Aedes albopictus', *Journal of the American Mosquito Control Association,* 6(2), pp. 312-314.

Silva, A., Santos, J. and Martins, A. (2014) 'Mutations in the voltage-gated sodium channel gene of anophelines and their association with resistance to pyrethroids - a review', *Parasites & Vectors,* 7, pp. 450.

Singh, S., Pandher, S. and Sharma, R. K., R. (2013) 'Insect growth regulators: practical use, limitations and future', *Journal of Eco-friendly Agriculture,* 8(1), pp. 1-14.

Sinka, M., Bangs, M., Manguin, S., Chareonviriyaphap, T., Patil, A., Temperley, W., Gething, P., Elyazar, I., Kabaria, C., Harbach, R. and Hay, S. (2011) 'The dominant Anopheles vectors of human malaria in the Asia-Pacific region: occurrence data, distribution maps and bionomic précis', *Parasites & Vectors,* 4(4), pp. 89.

Sinka, M., Bangs, M., Manguin, S., Coetzee, M., Mbogo, C., Hemingway, J., Patil, A., Temperley, W., Gething, P., Kabaria, C., Okara, R., Van Boeckel, T., Godfray, H., Harbach, R. and Hay, S. (2010) 'The dominant Anopheles vectors of human malaria in Africa, Europe and the Middle East: occurrence data, distribution maps and bionomic précis', *Parasites & Vectors,* 3(3).

Sinka, M., Bangs, M., Manguin, S., Rubio-Palis, Y., Chareonviriyaphap, T., Coetzee, M., Mbogo, C., Hemingway, J., Patil, A., Temperley, W., Gething, P., Kabaria, C., Burkot, T., Harbach, R. and Hay, S. (2012) 'A global map of dominant malaria vectors', *Parasites and Vectors,* 5, pp. 69.

Smith, L., Kasai, S. and Scott, J. (2016) 'Pyrethroid resistance in Aedes aegypti and Aedes albopictus: Important mosquito vectors of human diseases', *Pesticide biochemistry and physiology,* 133.

Soderlund, D. (2010) 'Toxicology and Mode of Action of Pyrethroid Insecticides', in Krieger, R. (ed.) *Hayes' Handbook of Pesticide Toxicology.* 3 ed. New York: Academic Press, pp. 1665-1686.

Sokhna, C., Ndiath, M. and Rogier, C. (2013) 'The changes in mosquito vector behaviour and the emerging resistance to insecticides will challenge the decline of malaria', *Clinical Microbiology and Infection,* 19(10), pp. 902-907.

Solomon, T., Loha, E., Deressa, W., Balkew, M., Gari, T., Overgaard, H. and Lindtjørn, B. (2018) 'Bed nets used to protect against malaria do not last long in a semi-arid area of Ethiopia: a cohort study', *Malaria Journal,* 17(1), pp. 1-14.

Song, G., Lee, E., Pan, J., Xu, M., Rho, H., Cheng, Y., Whitt, N., Yang, S., Kouznetsova, J., Klumpp-Thomas, C., Michael, S., Moore, C., Yoon, K., Christian, K., Simeonov, A., Huang, W., Xia, M., Huang, R., Lal-Nag, M., Tang, H., Zheng, W., Qian, J., Song, H., Ming, G. and Zhu, H. (2021) 'An Integrated Systems Biology Approach Identifies the Proteasome as A Critical Host Machinery for ZIKV and DENV Replication', *Genomics, Proteomics & Bioinformatics*.

Sougoufara, S., Ottih, E. and Tripet, F. (2020) 'The need for new vector control approaches targeting outdoor biting Anopheline malaria vector communities', *Parasites & Vectors,* 13(1), pp. 295.

South, A. and Hastings, I. M. (2018) 'Insecticide resistance evolution with mixtures and sequences: a model-based explanation', *Malaria Journal,* 17(1), pp. 80.

Sparks, T., Lockwood, J., Byford, R., Graves, J. and Leonard, B. (1989) 'The role of behavior in insecticide resistance', *Pest Management Science,* 26(4), pp. 383-399.

Stanton, M., Kalonde, P., Zembere, K., Hoek Spaans, R. and Jones, C. (2021) 'The application of drones for mosquito larval habitat identification in rural environments: a practical approach for malaria control?', *Malaria Journal,* 20(1), pp. 1-17.

Sternberg, E., Cook, J., Alou, L., Assi, S., Koffi, A., Doudou, D., Aoura, C., Wolie, R., Oumbouke, W., Worrall, E., Kleinschmidt, I., N'Guessan, R., Thomas, M. and . (2021) 'Impact and cost-effectiveness of a lethal house lure against malaria transmission in central Côte d'Ivoire: a two-arm, cluster-randomised controlled trial', *The Lancet,* 397(10276), pp. 805-815.

Stevenson, B., Bibby, J., Pignatelli, P., Muangnoicharoen, S., O'Neill, P., Lian, L. Y., Muller, P., Nikou, D., Steven, A., Hemingway, J., Sutcliffe, M. and Paine, M. (2011) 'Cytochrome P450 6M2 from the malaria vector Anopheles gambiae metabolizes pyrethroids: Sequential metabolism of deltamethrin revealed', *Insect Biochemistry and Molecular Biology,* 41(7), pp. 492-502.

Stica, C., Jeffries, C., Irish, S., Barry, Y., Camara, D., Yansane, I., Kristan, M., Walker, T. and Messenger, L. (2019) 'Characterizing the Molecular and Metabolic Mechanisms of Insecticide Resistance in Anopheles Gambiae in Faranah, Guinea', *Malaria Journal,* 18(1), pp. 244.

Stone, B. F. and Brown, A. (1969) 'Mechanisms of resistance to fenthion in Culex pipiens fatigans Wied*', *Bulletin World Health Organisation,* 40(3), pp. 401-8.

Strode, C., Melo-Santos, M., Magalhaes, T., Araujo, A. and Ayres, C. (2012) 'Expression Profile of Genes during Resistance Reversal in a Temephos Selected Strain of the Dengue Vector, Aedes aegypti', *PLoS ONE,* 7(8), pp. e39439.

Suman, D., Wang, Y., Bilgrami, A. and Gaugler, R. (2013) 'Ovicidal activity of three insect growth regulators against Aedes and Culex mosquitoes', *Acta Tropica,* 128(1), pp. 103-109.

Suman, D., Wang, Y. and Gaugler, R. (2015) 'The Insect Growth Regulator Pyriproxyfen Terminates Egg Diapause in the Asian Tiger Mosquito, Aedes albopictus', *PLoS One,* 10(6), pp. e0130499.

Suppiramaniam, V., Abdel-Rahman, E. A., Buabeid, M. A. and Parameshwaran, K. (2010) 'Ion Channels*', in McQueen, C.A. (ed.) *Comprehensive Toxicology.* 2 ed. Oxford: Elsevier, pp. 129-171.

Syme, T., Fongnikin, A., Todjinou, D., Govoetchan, R., Gbegbo, M., Rowland, M., Akogbeto, M. and Ngufor, C. (2021) 'Which indoor residual spraying insecticide best complements standard pyrethroid long-lasting insecticidal nets for improved control of pyrethroid resistant malaria vectors?', *PLoS One,* 16(1), pp. e0245804.

Szymczak, A., Workman, C., Wang, Y., Vignali, K., Dilioglou, S., Vanin, E. and Vignali, D. (2004) 'Correction of multi-gene deficiency in vivo using a single 'self-cleaving' 2A peptide-based retroviral vector', *Nature Biotechnology,* 22(5), pp. 589-594.

Takken, W., Klowden, M. and Chambers, G. (1998) 'Effect of Body Size on Host Seeking and Blood Meal Utilization in Anopheles gambiae sensu stricto (Diptera: Culicidae): the Disadvantage of Being Small', *Journal of Medical Entomology,* 35(5), pp. 639-645.

Tchicaya, E., Nsanzabana, C., Smith, T., Donzé, J., de Hipsl, M., Tano, Y., Müller, P., Briët, O., Utzinger, J. and Koudou, B. (2014) 'Micro-encapsulated pirimiphos-methyl shows high insecticidal efficacy and long residual activity against pyrethroid-resistant malaria vectors in central Côte d'Ivoire', *Malaria Journal,* 13, pp. 332.

Thany, S. and Tricoire-Leignel, H. (2011) 'Emerging Pharmacological Properties of Cholinergic Synaptic Transmission: Comparison between Mammalian and Insect Synaptic and Extrasynaptic Nicotinic Receptors', *Current Neuropharmacology,* 9(4), pp. 706-714.

Thompson, D., Lehmler, H., Kolpin, D., Hladik, M., Vargo, J., Schilling, K., LeFevre, G., Peeples, T., Poch, M., LaDuca, L., Cwiertny, D. and Field, R. (2020) 'A critical review on the potential impacts of neonicotinoid insecticide use: current knowledge of environmental fate, toxicity, and implications for human health', *Environmental Science - Processes & Impacts,* 22(6), pp. 1315-1346.

Thomsen, E., Koimbu, G., Pulford, J., Jamea-Maiasa, S., Ura, Y., Keven, J., Siba, P., Mueller, I., Hetzel, M. and Reimer, L. (2017) 'Mosquito Behavior Change After Distribution of Bednets Results in Decreased Protection Against Malaria Exposure', *The Journal of Infectious Diseases,* 215(5), pp. 790-797.

Thomson, H., Thomas, S., Sellstrom, E. and Petticrew, M. (2013) 'Housing improvements for health and associated socio-economic outcomes', *The Cochrane Database of Systematic Reviews,* (2), pp. CD008657.

Tizifa, T., Kabaghe, A., McCann, R., BH., v. d., Van Vugt, M. and Phiri, K. (2018) 'Prevention Efforts for Malaria', *Current Tropical Medicine Reports*, pp. 1-10.

Toe, K., Müller, P., Badolo, A., Traore, A., Sagnon, N., Dabiré, R. and Ranson, H. (2018) 'Do bednets including piperonyl butoxide offer additional protection against populations of Anopheles gambiae s.l. that are highly resistant to pyrethroids? An experimental hut evaluation in Burkina Fasov', *Medical and Veterinary Entomology,* 32(4), pp. 407-416.

Tse, E., Korsik, M. and Todd, M. (2019) 'The past, present and future of anti-malarial medicines', *Malaria Journal,* 18(1), pp. 1-21.

Tusting, L., Ippolito, M., Willey, B., Kleinschmidt, I., Dorsey, G., Gosling, R. and Lindsay, S. (2015) 'The evidence for improving housing to reduce malaria: a systematic review and meta-analysis', *Malaria Journal,* 14(1), pp. 1-12.

Tusting, L., Thwing, J., Sinclair, D., Fillinger, U., Gimnig, J., Bonner, K., Bottomley, C. and Lindsay, S. (2013) 'Mosquito larval source management for controlling malaria', *Cochrane Database of Systematic Reviews,* (8).

Utarini, A., Indriani, C., Ahmad, R., Tantowijoyo, W., Arguni, E., Ansari, M., Supriyati, E., Wardana, D., Meitika, Y., Ernesia, I., Nurhayati, I., Prabowo, E., Andari, B., Green, B., Hodgson, L., Cutcher, Z., Rancès, E., Ryan, P., O'Neill, S., Dufault, S., Tanamas, S., Jewell, N., Anders, K. and Simmons, C. (2021) 'Efficacy of Wolbachia-Infected Mosquito Deployments for the Control of Dengue', *The New England journal of medicine,* 384(23), pp. 2177-2186.

Utzinger, J., Tozan, Y. and Singer, B. (2001) 'Efficacy and cost-effectiveness of environmental management for malaria control', *Tropical Medicine and International Health,* 6(9), pp. 677-687.

Vega-Rúa, A., Zouache, K., Girod, R., Failloux, A. and Lourenço-de-Oliveira, R. (2014) 'High level of vector competence of Aedes aegypti and Aedes albopictus from ten American countries as a crucial factor in the spread of Chikungunya virus', *Journal of Virology,* 88(11), pp. 6294-6306.

Velayudhan, R. (2019) *UPDATES: VEM / NTD & STAG 2019*, Geneva: WHO.

Vieira, F. and Rozas, J. (2011) 'Comparative genomics of the odorant-binding and chemosensory protein gene families across the Arthropoda: origin and evolutionary history of the chemosensory system', *Genome Biology and Evolution,* 3, pp. 476-490.

Voice, M., Kaaz, A., Peet, C. and Paine, M. (2012) 'Recombinant cyp6m2 inhibition by insecticides recommended by WHO for indoor residual spraying against malaria vectors', *Drug Metabolism Reviews,* 44(S1), pp. 56-57.

Volohonsky, G., Terenzi, O., Soichot, J., Naujoks, D., Nolan, T., Windbichler, N., Kapps, D., Smidler, A., Vittu, A., Costa, G., Steinert, S., Levashina, E., Blandin, S. and Marois, E. (2015) 'Tools for Anopheles gambiae Transgenesis', *Genes, Genomes, Genetics,* 5(6), pp. 1151-1163.

Vontas, J., Katsavou, E. and Mavridis, K. (2020) 'Cytochrome P450-based metabolic insecticide resistance in Anopheles and Aedes mosquito vectors: Muddying the waters', *Pesticide Biochemistry and Physiology,* 170, pp. 104666.

Wang, Y., Shen, R., Xing, D., Zhao, C., Gao, H., Wu, J., Zhang, N., Zhang, H., Chen, Y., Zhao, T. and Li, C. (2021) 'Metagenome Sequencing Reveals the Midgut Microbiota Makeup of Culex pipiens quinquefasciatus and Its Possible Relationship With Insecticide Resistance', *Frontiers in Microbiology,* 12, pp. 625539.

Wang, Y., Wang, F., Wang, R., Zhao, P. and Xia, Q. (2015) '2A self-cleaving peptide-based multi-gene expression system in the silkworm Bombyx mori', *Scientific Reports,* 5.

Waters, A., Capriotti, P., Gaboriau, D., Papathanos, P. and Windbichler, N. (2018) 'Rationally-engineered reproductive barriers using CRISPR & CRISPRa: an evaluation of the synthetic species concept in Drosophila melanogaster', *Scientific Reports,* 8(1), pp. 1-14.

Weedall, G., Riveron, J., Hearn, J., Irving, H., Kamdem, C., Fouet, C., White, B. and Wondji, C. (2020) 'An Africa-wide genomic evolution of insecticide resistance in the malaria vector Anopheles funestus involves selective sweeps, copy number variations, gene conversion and transposons', *PLoS Genetics,* 16(6), pp. e1008822.

Weetman, D., Mitchell, S., Wilding, C., Birks, D., Yawson, A., Essandoh, J., Mawejje, H., Djogbenou, L., Steen, K., Rippon, E., Clarkson, C., Field, S., Rigden, D. and Donnelly, M. (2015) 'Contemporary evolution of resistance at the major insecticide target site gene Ace-1 by mutation and copy number variation in the malaria mosquito Anopheles gambiae', *Molecular Ecology,* 24(11), pp. 2656-2672.

Weetman, D., Wilding, C., Neafsey, D., Müller, P., Ochomo, E., Isaacs, A., Steen, K., Rippon, E., Morgan, J., Mawejje, H., Rigden, D., Okedi, L. and Donnelly, M. (2018) 'Candidate-gene based GWAS identifies reproducible DNA markers for metabolic pyrethroid resistance from standing genetic variation in East African Anopheles gambiae', *Scientific Reports,* 8(1), pp. 1-12.

Weill, M., Fort, P., Berthomieu, A., Dubois, M., Pasteur, N. and Raymond, M. (2002) 'A novel acetylcholinesterase gene in mosquitoes codes for the insecticide target and is non-homologous to the ace gene in Drosophila', *Proceedings. Biological sciences,* 269(1504), pp. 2007-2016.

Weill, M., Lutfalla, G., Mogensen, K., Chandre, F., Berthomieu, A., Berticat, C., Pasteur, N., Philips, A., Fort, P. and Raymond, M. (2003) 'Insecticide resistance in mosquito vectors', *Nature,* 423(6936), pp. 136-137.

Weill, M., Malcolm, C., Chandre, F., Mogensen, K., Berthomieu, A., Marquine, M. and Raymond, M. (2004) 'The Unique Mutation in ace-1 Giving High Insecticide Resistance Is Easily Detectable in Mosquito Vectors', *Insect Molecular Biology,* 13(1), pp. 1-7.

WHO (2005) *Guidelines for laboratory and field testing of mosquito larvicides*.

WHO, Unit, G.M.P.a.M. (2006a) *Indoor residual spraying : use of indoor residual spraying for scaling up global malaria control and elimination : WHO position statement.* Geneva: World Health Organization (WHO/HTM/MAL/2006.1112 10 p.).

WHO, WHOPES (2006b) *Mosquito Adulticides for Indoor Resisdual Spraying and Treatment of mosquito nets.* Geneva (WHO_CDS_NTD_WHOPES_GCDPP_2006.3).

WHO, WHO, WHO (2009) *Temephos in Drinking-water: Use for Vector Control in Drinking-water Sources and Containers.* Geneva: WHO Press (WHO/HSE/WSH/09.01/1).

WHO, WHOPES (2011) *Guidelines for monitoring the durability of long-lasting insecticidal mosquito nets under operational conditions*: World Health Organization (WHO/HTM/NTD/WHOPES/2011.5).

WHO (2012a) *Handbook for Integrated Vector Management.* Geneva: World Health Organization (9789241502801).

WHO (2012b) *The role of larviciding for malaria control in sub-Saharan Africa: interim position statement*: World Health Organization (WHO/HTM/GMP/2012.06).

WHO (2013) *Larval source management – a supplementary measure for malaria vector control. An operational manual* (9789241505604).

WHO (2015) *Indoor Residual Spraying - An operational manual for indoor residual spraying (IRS) for malaria transmission control and elimination.* Geneva (978 92 4 150894 0).

WHO (2016) *WHO SPECIFICATIONS AND EVALUATIONS FOR PUBLIC HEALTH PESTICIDES PIRIMIPHOS-METHYL*. Available at: https://www.who.int/pq-vector-control/prequalified-lists/PIRIMIPHOS-METHYL.pdf.

WHO, WHOPES (2017) *Report of the twentieth WHOPES working group meeting, WHO/HQ, Geneva, 20–24 March 2017: review of Interceptor G2LN, DawaPlus 3.0 LN, DawaPlus 4.0 LN, SumiLarv 2 MR, Chlorfenapyr 240 SC.* Geneva (CC BY-NC-SA 3.0 IGO).

WHO (2018a) *Fludora Fusion Product Prequalification*. Available at: https://extranet.who.int/pqweb/vector-control-product/fludora-fusion.

WHO, Programme, G.M. (2018b) *Test procedures for insecticide resistance monitoringin malaria vector mosquitoes.* 20 Avenue Appia, 1211 Geneva 27, Switzerland: WHO Press.

WHO (2018c) *WHO recommended insecticides for indoor residual spraying against malaria vectors.* Geneva.

WHO (2018d) *World Malaria Report 2018.* Geneva (Licence: CC BY-NC-SA 3.0 IGO.).

WHO (2019a) *Guidelines for malaria vector control*: World Health Organization (CC BY-NC-SA 3.0 IGO).

WHO (2019b) 'Malaria and related entomological and vector control concepts', *Guidelines for Malaria Vector Control*. Geneva: World Health Organization.

WHO (2019c) *World malaria report*, Geneva: WHOCC BY-NC-SA 3.0 IGO.). Available at: https://www.jci.org/articles/view/135794#B1.

WHO, WHO (2020) *World Malaria Report 2020: 20 years of global progress and challenges* (CC BY-NC-SA 3.0 IGO).

WHO (2021) *Lymphatic Filariasis*. Available at: https://www.who.int/news-room/fact-sheets/detail/lymphatic-filariasis (Accessed: 24.08.2021).

WHO and Global Malaria Programme (2018) *Test procedures for insecticide resistance monitoring in malaria vector mosquitoes.* Geneva: WHO Press.

WHO and UNICEF (2012) *Communication for behavioural impact (COMBI): A toolkit for behavioural and social communication in outbreak response.* Luxembourg (WHO/HSE/GCR/2012.13).

WHO, UNICEF, UNDP, World Bank and WHO Special Programme for Research Training in Tropical Diseases (2017) *Global vector control response 2017-2030.* Geneva: World Health Organization.

Williams, J., Flood, L., Praulins, G., Ingham, V., Morgan, J., Lees, R. and Ranson, H. (2019) 'Characterisation of Anopheles strains used for laboratory screening of new vector control products', *Parasites & Vectors,* 12(1), pp. 1-14.

Wilson, A., Courtenay, O., Kelly-Hope, L., Scott, T., Takken, W., Torr, S. and Lindsay, S. (2020) 'The importance of vector control for the control and elimination of vector-borne diseases', *PLoS Neglected Tropical Diseases,* 14(1), pp. e0007831.

Wilson, M., Coates, C. and George, A. (2007) 'PiggyBac transposon-mediated gene transfer in human cells', *Molecular Therapy : The Journal of the American Society of Gene Therapy,* 15(1), pp. 139-145.

Winokur, O., Main, B., Nicholson, J. and Barker, C. (2020) 'Impact of temperature on the extrinsic incubation period of Zika virus in Aedes aegypti', *PLOS Neglected Tropical Diseases,* 14(3), pp. e0008047.

Wolff, G. and Riffell, J. (2018) 'Olfaction, experience and neural mechanisms underlying mosquito host preference', *Journal of Experimental Biology,* 221(4), pp. jeb157131.

Wolford, R. and Schaefer, T. (2021) 'Zika Virus', *StatPearls Publishing*.

Wong, D., Li, J., Chen, Q., Han, Q., Mutunga, J., Wysinski, A., Anderson, T., Ding, H., Carpenetti, T., Verma, A., Islam, R., Paulson, S., Lam, P., Totrov, M., Bloomquist, J. and Carlier, P. (2012) 'Select small core structure carbamates exhibit high contact toxicity to "carbamate-resistant" strain malaria mosquitoes, Anopheles gambiae (Akron)', *PloS One,* 7(10), pp. e46712.

Wood, T. and Goulson, D. (2017) 'The environmental risks of neonicotinoid pesticides: a review of the evidence post 2013', *Environmental Science and Pollution Research,* 24(21), pp. 17285-17325.

Worrall, E. and Fillinger, U. (2011) 'Large-scale use of mosquito larval source management for malaria control in Africa: a cost analysis', *Malaria Journal,* 10(1), pp. 1-21.

Wu, Y., Parthasarathy, R., Bai, H. and Palli, S. (2006) 'Mechanisms of midgut remodeling: juvenile hormone analog methoprene blocks midgut metamorphosis by modulating ecdysone action', *Mechanisms of Development,* 123(7), pp. 530-547.

Yewhalaw, D., Wassie, F., Steurbaut, W., Spanoghe, P., Bortel, W., Denis, L., Tessema, D., Getachew, Y., Coosemand, M., Duchateau, L. and Speybroeck, N. (2011) 'Multiple Insecticide Resistance: An Impediment to Insecticide-Based Malaria Vector Control Program', *PLoS ONE,* 6(1), pp. e16066.

Yunta, C., Hemmings, K., Stevenson, B., Koekemoer, L., Matambo, T., Pignatelli, P., Voice, M., Nasz, S. and Paine, M. (2019) 'Cross-resistance profiles of malaria mosquito P450s associated with pyrethroid resistance against WHO insecticides', *Pesticide Biochemistry and Physiology,* 161, pp. 61-67.

Yunta. C, Grisales, N., Nász, S., Hemmings, K., Pignatelli, P., Voice, M., Ranson, H. and Paine, M. (2016) 'Pyriproxyfen Is Metabolized by P450s Associated With Pyrethroid Resistance in An. Gambiae', *Insect Biochemistry and Molecular Biology,* 78, pp. 50-57.

Zalucki, M. and Furlong, M. (2017) 'Behavior as a mechanism of insecticide resistance: evaluation of the evidence', *Current Opinion in Insect Science,* 21, pp. 19-25.

Zhao, P., Wang, Y. and Jiang, H. (2013) 'Biochemical properties, expression profiles, and tissue localization of orthologous acetylcholinesterase-2 in the mosquito, Anopheles gambiae', *Insect Biochemistry and Molecular Biology,* 43(3), pp. 260-267.

Zhao, Z., Tian, D. and McBride, C. (2021) 'Development of a pan-neuronal genetic driver in Aedes aegypti mosquitoes', *Cell Reports Methods,* 1(3), pp. 100042.

Zoh, D., Ahoua, A., Toure, M., Pennetier, C., Camara, S., Traore, D., Koffi, A., Adja, A., Yapi, A. and Chandre, F. (2018) 'The current insecticide resistance status of Anopheles gambiae (s.l.) (Culicidae) in rural and urban areas of Bouaké, Côte d'Ivoire', *Parasites & Vectors,* 11(1), pp. 1-12.